2013

COPLANAR PCB-INDUCED INFLAMMATION AND DIETARY INTERVENTIONS

Katryn Elizabeth Eske
University of Kentucky, katryn_eske@yahoo.com

STUDENT AGREEMENT:

I represent that my thesis or dissertation and abstract are my original work. Proper attribution has been given to all outside sources. I understand that I am solely responsible for obtaining any needed copyright permissions. I have obtained and attached hereto needed written permission statements(s) from the owner(s) of each third-party copyrighted matter to be included in my work, allowing electronic distribution (if such use is not permitted by the fair use doctrine).

I hereby grant to The University of Kentucky and its agents the non-exclusive license to archive and make accessible my work in whole or in part in all forms of media, now or hereafter known. I agree that the document mentioned above may be made available immediately for worldwide access unless a preapproved embargo applies.

I retain all other ownership rights to the copyright of my work. I also retain the right to use in future works (such as articles or books) all or part of my work. I understand that I am free to register the copyright to my work.

REVIEW, APPROVAL AND ACCEPTANCE

The document mentioned above has been reviewed and accepted by the student's advisor, on behalf of the advisory committee, and by the Director of Graduate Studies (DGS), on behalf of the program; we verify that this is the final, approved version of the student's dissertation including all changes required by the advisory committee. The undersigned agree to abide by the statements above.

Katryn Elizabeth Eske, Student

Dr. Bernhard Hennig, Major Professor

Dr. Howard Glauert, Director of Graduate Studies

COPLANAR PCB-INDUCED INFLAMMATION AND DIETARY INTERVENTIONS

DISSERTATION

A dissertation submitted in partial fulfillment of the requirements for the degree of Doctor of Philosophy in the College of Medicine at the University of Kentucky.

By

Katryn Elizabeth Eske

Lexington, Kentucky

Chair: Dr. Shuxia Wang, Professor of Nutritional Sciences

Lexington, Kentucky

2013

ABSTRACT OF DISSERTATION

COPLANAR PCB-INDUCED INFLAMMATION AND DIETARY INTERVENTIONS

Diseases, such as cardiovascular disease (CVD), are linked to chronic low levels of inflammation. This inflamed state is the product of risk factors including exposure to environmental pollutants, such as polychlorinated biphenyls (PCBs), which are correlated with increased risk for CVD and diabetes. In response to this health risk, our research addresses the mechanisms by which coplanar PCBs elicit an inflammatory response and the mitigation of PCB-induced inflammation through dietary intervention using docosahexaenoic acid (DHA), an omega-3 lipid.

Investigators from the University of Kentucky Engineering Department are developing remediation technologies that detoxify PCBs through dechlorination. We studied the cellular toxicity of coplanar PCB 77 remediation products in primary vascular endothelial cells. The dechlorination products elicited different toxicological responses, which were less than the parent compound and contributed to the overall inflammatory response. The presence of PCB 77 at any concentration was sufficient to promote an inflammatory response, which was attenuated with complete dechlorination.

PCB 77 is a good model for coplanar PCB-induced toxicity, but in environmental and human samples, coplanar PCB 126 is detected more frequently. Using different doses of PCB 126, we determined that acute exposure to 5 μmol PCB 126/kg mouse was sufficient to produce an inflammatory response without inducing a toxic wasting phenotype. PCB-induced inflammation was attenuated *in vitro* by DHA-derived neuroprostanes. Applying this information, we fed mice a DHA-enriched diet and exposed them to PCB 126. Liver and adipose lipid profiles confirm an increase in omega-3 fatty acid composition and DHA metabolites, and changes in gene expression indicate a heightened anti-oxidant response in the presence of PCB-induced inflammation. These data provide an overview of the *in vivo* response to a PCB-induced inflammation after DHA dietary feeding.

We have demonstrated that PCB-induced endothelial dysfunction is propagated through lipid domains called caveolae. Caveolae are also signaling domains for toll-like receptor 4 (TLR4), and receptor for lipopolysaccharide (LPS). Similar to PCBs, TLR4 signaling is inhibited by DHA. We compared the caveolae-associated signaling response after exposure to coplanar PCB 126 or LPS. The domain localization of caveolae was altered by both PCB 126 and LPS. Our study determined that PCB 126-induced inflammation was not inhibited by a TLR4-specific inhibitor, but caveolae-based signaling was critical to both PCB 126- and LPS-induced inflammation.

Environmental pollutants, such as coplanar PCBs, are risk factors in the development of chronic diseases. Here we investigate possible signaling pathways associated with environmental toxicity and apply potential dietary interventions with omega-3 lipids.

KEYWORDS: Polychlorinated biphenyls (PCBs); endothelial cells; inflammation; docosahexaenoic acid (DHA); caveolae

Katryn Elizabeth Eske

09/18/13

COPLANAR PCB-INDUCED INFLAMMATION AND DIETARY INTERVENTIONS

By

Katryn Elizabeth Eske

Dr. Bernhard Hennig
Director of Dissertation

Dr. Howard Glauert
Director of Graduate Studies

11-1-13

Acknowledgements

To the amazing community of people that has surrounded me throughout my career as a Ph.D. student, my sincerest thanks. I would like to thank my mentor, Dr. Bernie Hennig, for recognizing a passion in me for nutrition and toxicology and extending a kind invitation to become part of his laboratory. Thank you for challenging me to step out and be adventurous with my science. For the many opportunities to network and broaden my scientific perspective, I am very grateful. You have given me the opportunity to grow in more ways than I can attest.

To my other committee members, thank you for your service. Dr. Cassis, thank you for setting an example for other women scientists to follow; your practical and creative insights have been an encouragement and a help throughout this process. To Dr. Morris, thank you for extending your support and expertise to my pre-doctoral grant writing efforts. To both you and your Small Molecule Mass Spectrometry Core Laboratory, thank you for the expertise and training that you have shared. Dr. Pearson, thank you for your straight forward advice and consistent support; you have helped make a career in science seem attainable. To my outside examiner, Dr. Porter, thank you for your availability and enthusiasm.

For the many individuals both in Dr. Hennig's laboratory and other laboratories that have offered their invaluable time and expertise, your support has made this experience possible. My fellow labmates, Maggie Murphy, Brad Newsome, and Michael Petriello, you have provided endless support as colleagues and friends. Dr. Sung Gu Han, your training and expertise have been an invaluable asset to me; thank you for your patience. To Manjula Sunkara, your tireless efforts have deepened the insights of my research; thank you for the training and friendship that you have extended me during my time here. The laboratory of Dr. Allen Daugherty has contributed to my training on many

levels; specifically, thank you Deb, Deborah, and Jess for your help with everything from animal handling techniques to FPLC. I would also like to thank the undergraduate students who have contributed their efforts and who have shown me the beauty and value of the mentorship experience. Thank you, Christopher R. Barton[1]and Alex N. Palumbo[1], for your contributions to the preliminary work on the dechlorination paper (chapter two). Thank you to Rebecca Brock[1] for your efforts to perfect the sucrose gradient protocol (chapter five); I am confident that you will make a brilliant scientist.

To the people of my church community who have prayed with me and encouraged me through every step of this process, I could not have accomplished this without your support. My family, you have always supported and encouraged me. I would not be here without you. To my Lord and Savior Jesus Christ, who has taught me that perseverance develops character and character hope, thank you for giving me peace through the storm.

[1] Undergraduate ARRA Summer Research student.

Table of Contents

List of Tables

List of Figures

Chapter One: Introduction

1.1 Environmental pollution – PCB

The unprecedented boom in chemical manufacturing had produced a legacy of chemical wastes and byproducts that flowed into streams and piled up in landfills. Scientists and the public began to awaken to the horror of a polluted world. Rachel Carson, a leader in the environmental movement, raised public awareness through her book *Silent Spring*; she writes,

> "The most alarming of all man's assaults upon the environment is the contamination of air, earth, rivers, and sea with dangerous and even lethal materials. This pollution is for the most part irrecoverable; the chain of evil it initiates not only in the world that must support life but in living tissues is for the most part irreversible[1]."

In response to the public outcry and mounting scientific evidence about environmental and human health effects, Congress passed a series of environmental legislation, and the President established the Environmental Protection Agency (EPA)[2]. Within this legislation, certain environmental pollutants were banned from manufacturing including polychlorinated biphenyls (PCBs). PCBs like many other contaminants from that era are distinguished by their stable chemical structure which includes a biphenyl and many configurations of chlorine substitutions that account for up to 209 possible congeners[3] (Figure 1.1). Produced in mixtures, called Aroclors, PCBs were widely marketed and used in applications in which their stability and low electrical conductivity were prized; these applications included dielectric fluid in capacitors and light ballasts and building materials such as paint and sealants[4].

The two major classes of PCBs are defined by the stereochemistry of the biphenyl bond (Figure 1.1)[3, 5]. The coplanar PCBs do not contain *ortho*-substitutions and exhibit dioxin-like properties. The presence of coplanar PCBs in human and animal tissues are orders of magnitude lower than other congeners, but as a class of compounds they exhibit greater potential for toxicity, especially PCB 126[6, 7]. They are dioxin-like and bind the aryl hydrocarbon receptor (AhR) which activates cytochrome P450 (CYP) metabolizing enzymes, the expression of which are associated with increased cellular oxidative stress and inflammation[8]. Chlorine substitutions in the *ortho*- position cause steric hindrance for noncoplanar PCBs, which have different biological activity than the coplanar PCBs. Noncoplanar PCBs have an affinity for the constitutive androstane receptor (CAR)[9], which activates CYP metabolizing enzymes, and are known to disrupt Ca^{2+} signaling in

the brain through the ryanodine receptors[3, 10]. In addition, noncoplanar PCBs have been associated with certain metabolic disorders. For example, PCB 153 is a noncoplanar PCB that is present in high levels in human serum; it is associated with increased risk for nonalcoholic fatty liver disease and Type 2 diabetes[11, 12]. Congeners which are mono-*ortho*-substituted, such as PCB 118, have reduced AhR activity and have molecular similarities to noncoplanar PCBs[3, 5, 13]. Our research has demonstrated that in comparison to noncoplanar PCBs, coplanar PCBs and mixed inducers promote oxidative stress and decrease endothelial barrier function, which is critical to inflammatory process that causes endothelial dysfunction and promotes the vascular inflammation that leads to atherosclerosis[14]. We have also demonstrated that certain nutrients either promote or inhibit coplanar PCB-induced endothelial cell dysfunction. For example, the omega-6 fatty acid linoleic acid promotes coplanar PCB-induced inflammation, but when the ratio of omega-3 to omega-6 fatty acids is increased, the omega-3 fatty acids protect against PCB-induced oxidative stress and nuclear factor kappa B (NFκB) activation[15, 16]. As a result, the work in our laboratory has focused on the dioxin-like, coplanar PCBs.

Pollutant toxicity is compared using toxic equivalency factors (TEFs) which designate a toxicity value based on a comparison to the toxicity of 2,3,7,8-tetrachlorodibenzo-*p*-dioxin (TCDD, dioxin). For PCBs, only coplanar PCBs (non-ortho substituted) exhibit dioxin-like qualities and are ligands had arylhydrocarbon receptor (AhR). The major congeners in this class are PCB 77, PCB 126, and PCB 169 with TEFs in humans of 0.0001, 0.1 and 0.01, respectively[17]. In addition, PCB 170 and PCB 180 have ethoxyresorufin-O-deethylase (EROD) activity that is sufficient for a TEF equivalency to be assigned. Based on the median TEF values of PCB 105, PCB 118, and PCB 156, the TEF for mono-ortho PCBs, containing one ortho substitution or a mixed congener, is 0.00003[18]. Together, TEFs can be combined to develop toxic equivalents (TEQ) that may be applied when assessing limits in food sources, sediments, waterways, etc. However, the TEFs are based primarily on studies of oral exposure, which is often the source of exposure for both animals and humans[18]. As such, human exposure risk and risk attenuation continue to be primary concerns in environmental health research.

PCB distribution in the body

The concept of persistence and biomagnification in humans and animals is based on the ability of adipose tissue to act as a storage facility for persistent organic pollutants (POPs)[19, 20]. The degree of lipophilicity for a particular toxicant is determined by a $\log_{10}$

value of >6.0 for the solubility ratio of octanol to water[21]. POPs that exceed the 6.0 lipophilicity threshold are soluble in dietary fat sources and are absorbed in the intestinal lumen with triacylglycerols into the lymphatic circulation[22]. After entry into the lymphatic system, they are incorporated into chylomicrons which transport the toxicants to other tissues including the primary storage depot, the adipose. PCBs display a range of affinities and distribute among LDL, HDL, and albumin fractions[23, 24]. Fortunately, the body has a mechanism for reducing its burden of PCBs and other POPs by utilizing enterohepatic circulation[21]. Through this cycle, POPs may be returned to circulation in the blood, be acquired by the liver which packages them with bile for excretion into the intestine. Once in the intestine, the pollutants will either be reabsorbed with the bile salts or be excreted in the feces. Through a similar pattern of circulation, POPs are also incorporated into mother's breast milk, which serves as one of the first and most concentrated exposures for humans[25, 26]. The circulation of these compounds is not an innocuous process, and PCBs or other compounds are able to interact with the tissues that are exposed during circulation including the vascular endothelium and the liver. PCBs and other dioxin-like compounds are associated with a wide range of human health outcomes, the mechanisms of which are still being explored. The immune, hepatic, neural, endocrine, vascular and reproductive systems are all affected in by PCB exposure[27-29].

Molecular interactions of coplanar PCBs with target receptors

As dioxin-like compounds, coplanar PCBs are ligands for the AhR. The transcription factor, AhR, is a member of the PER-ARNT-SIM (PAS) superfamily that has a helix-loop-helix structure. This highly conserved protein requires ligand binding for activity and is a cellular sensor that has a critical function in development, especially of the liver and vascular systems, circadian rhythms, hypoxia, hormonal signaling, inflammation and other biological processes[30]. The AhR and its chaperone proteins including two HSP90 units reside in the cytosol until ligand binding which causes the release of one HSP90 and translocation into the nucleus where AhR dimerizes with ARNT (AhR nuclear translocator), releases the second HSP90, binds to a xenobiotic response element (XRE, also called the dioxin response element, DRE) and facilitates transcription[29]. The transcriptional changes directed by XRE binding facilitate cellular responses to environmental stimuli; however, when these signals are prolonged by strong ligand affinity, such as is the case of AhR binding with TCDD, disease processes are activated. AhR activity promotes expression of Phase I and Phase II metabolism and anti-oxidant

response enzymes, such as the Phase I enzyme cytochrome P450 1A1 (CYP1A1)[31, 32]. Ligands of the AhR require a degree of hydrophobicity, e.g. be lipophilic in nature, and exhibit certain electronegative and hydrogen bonding properties, and as follows, this includes a varied set of xenobiotic, endogenous and dietary compounds[33]. The xenobiotic ligands that meet the physical requirements of the AhR binding pocket represent a large number of environmental pollutants examples of which include the following: PCBs, dioxins, naphthalenes and PAHs (polycyclic aromatic hydrocarbons), such as benzo[a]pyrene. An equally extensive list of possible endogenous ligands have also been identified for the AhR; these include the following: indigoids (indigo and indirubin), 2-(1′H-indole-3′-carbonyl)-thiazole-4-carboxylic acid methyl ester (ITE), equilenin (equine estrogen), metabolites of arachidonic acid, of heme and of tryptophan. From food sources, derivatives of indole-3-carbinol, found in cruciferous vegetables, and flavonoids, such as quercetin are potential ligands. The diversity of AhR ligands has led scientists to appreciate a number of functional roles for this transcription factor. Through endogenous ligand activation, the AhR is responsible for a number of developmental and cellular processes including cardiovascular, immune and neuronal systems[34]; for example, AhR deficient mice have incomplete liver vascularization[33]. Dietary polyphenols, like flavonoids, have been linked to the protective anti-oxidant response and initiate binding to alternative XRE binding sites. In contrast, xenobiotics, such as PCBs, hijack the endogenous functions of the AhR to produce an inflammatory response[34]. The AhR-induced inflammatory response is linked to the upregulation of detoxifying enzymes, such as CYP1A1, and cross-talk with the nuclear nuclear factor (erythroid-derived 2)-like 2 (Nrf2) mediated anti-oxidant response[35].

The AhR induces CYP1A1 expression in response to coplanar PCBs and other ligands[36, 37]. CYP1A1 activity includes the hydroxylation or epoxidation of the offending xenobiotic. When the reaction is unsuccessful and the enzyme “slips” or becomes uncoupled, a superoxide ion is released into the cell rather than being added to the compound[38]. Xenobiotics, such as PCBs, are not well metabolized, and their interaction with Phase I enzymes, like CYP1A1, leads to a greater release of reactive oxygen species (ROS), which significantly shift the redox balance of the cell[39]. Nrf2 regulated anti-oxidant enzymes, such as glutathione-S-transferase (GST) and NAD(P)H:quinine oxidoreductase (NQO1), serve to mitigate the increase in ROS, but when the oxidant capacity has been exceeded the cell initiates NFκB and other redox sensitive

transcription factors to produce a heightened inflammatory cascade[40, 41]. NFκB promotes the transcription of the chemokine monocyte chemoattractant protein 1 (MCP-1)[42, 43], also called CCL2, and vascular cell adhesion molecule 1 (VCAM1)[44, 45], which are key markers of endothelial cell dysfunction and the initiation of macrophage recruitment. The cytochrome P450 enzymes are part of Phase I metabolism during which the substrates are attacked at the site of a good leaving group which is replaced by hydroxyl, epoxide or carboxyl functional groups [46, 47]. This conversion is the first step in the transformation of the liphophilic molecule into a water soluble substrate that can be excreted through the kidneys. Phase II metabolizing enzymes that are upregulated through AhR activation include glutathione transferases, UDP-glucuronyltransferases and sulfotransferases[48], which utilize the nucleophilic functional group to add a water soluble moiety such as a glucuronic acid, amino acid (glutathione, GSH) or sulfuric acid[47]. CYP metabolism of PCBs results in epoxide and hydroxylated products that are processed by the Phase II enzymes to generate all these metabolites[3].

1.2 PCBs and predisposition to inflammatory response

Endothelial dysfunction

As sensitive modulators of vascular homeostasis, endothelial cells both respond to the changing climate within the blood and regulate the vascular environment[49]. For the average American, this "climate" includes the following: dietary factors such as high levels of fatty acids, sodium, and glucose; lifestyle factors such as minimal physical activity; and exposure environmental pollutants from food, air, and built environments[50, 51]. The endothelium responds to each of these factors by modulating the physiological environment including vasorelaxation through endothelial nitric oxide synthase (eNOS) signaling or inflammation through cytokine and adhesion molecule expression[52, 53]. The endothelial inflammatory response culminates in a change in function termed endothelial dysfunction in which cytokines like the chemokine monocyte chemoattractant protein-1 (MCP-1) are secreted to recruit macrophages that are captured via adhesion molecules like VCAM1, and decreases in cell:cell junction integrity allow the macrophages to penetrate the endothelial cell barrier[42, 54, 55]. Once in the intimal space, macrophages promote the inflammatory state by producing cytokines and through phagocytosis of ox-LDL, which together promote formation of foam cells that accumulate to form plaques.

Inflammation and disease risk

Inflammation is a characteristic held in common by a variety of diseases including lupus, rheumatoid arthritis, Crohn disease, ulcerative colitis, dermatomyositis and polymyositis[56]. The majority of these disorders can increase a patient's risk for myocardial infarction or coronary artery disease related events when compared to control or the general population; for this analysis, only disorders associated with inflammatory bowel disease did not increase vascular disease risk[56]. The heightened inflammatory state increased lipoprotein oxidation and unresolved inflammation promoting the observed effect on cardiovascular outcomes. The pro-inflammatory cytokines, tumor necrosis factor alpha (TNFα) and interleukin-6 (IL-6) are risk factors for cardiovascular diseases and are increased in rheumatoid arthritis (RA) patients; further, coronary calcification is greater in RA patients with longer disease histories, which is associated with increased cardiovascular disease prevalence in this patient population[57]. Interestingly, many chronic inflammatory disease states are characterized by a dysregulated immune response in the epithelial and mesenchymal cell structures of the affected organ; in the case of atherosclerosis, the endothelium is activated by bacterial components, lipoproteins or other stimuli which induce vascular cell adhesion molecule 1 (VCAM1) expression and the recruitment of immune cells that perpetuate the interstitial inflammatory response[58]. Coplanar PCBs and other environmental pollutants are potential activators of vascular inflammation.

PCBs as a risk factor in diseases of inflammation

Low grade inflammation is associated with many of chronic disorders including cardiovascular diseases, diabetes, metabolic syndrome and obesity. Tissue inflammation in the vascular system, adipose, and liver are all indicators and risk factors for the development of disease. PCBs have been associated with the development of multiple inflammation-associated medical conditions. For example, diabetes and metabolic syndrome are increased relative to PCB levels in both the general population and in communities with increased PCB exposure[59-61]. In particular, a survey of the Japanese population indicated that PCB 126 was a key toxicant associated with the increased prevalence of metabolic syndrome[61]. In a study of the 2003-2004 NHANES data, elevated serum alanine aminotransferase (ALT), a biomarker associated with non-alcoholic fatty liver disease (NAFLD) and other liver diseases, was increased in association with heavy metal and PCB exposure[62], and NAFLD was increased in mice exposed to PCBs[11]. Toxicant induced liver diseases, which include toxicant-associated

fatty liver disease and toxicant-associated steatohepatitis, are associated with exposure to industrial chemicals including vinyl chloride and PCBs[63]. Further, cardiovascular disease risk was increased in an elderly population independent of lipid levels and other cardiovascular disease risk factors[64], and in rats, PCB 126 was associated with heightened cardiovascular disease risk resulting from changes in cholesterol, blood pressure and heart weight[65]. Industrial workers with high levels of PCB exposure have significantly increased levels of cardiovascular disease-related death[66]. These data support of the role of PCBs in the propagation of inflammatory diseases.

PCBs, as lipophilic compounds, accumulate in the adipose and are recirculated through the body by enterohepatic circulation, a process which exposes both the vascular system and the liver to these toxicants. Given this environment, PCBs induce a stress response that promotes chronic, low grade inflammation and thus predispose the vasculature, specifically the endothelium, to heightened response to lifestyle and pathogenic stressors, like bacterial lipopolysaccharide (LPS)[67]. A recent study of the Framingham heart study cohort has concluded that the traditional risk factors are insufficient to explain the level of inflammation observed in the study[68]; this would suggest that genetic factors and environmental factors like PCBs could be the "unobserved" risk factors. Vascular biomarkers like soluble VCAM1 provide a critical observational link between metabolic syndrome and insulin resistance and the development of CVD and diabetes[69]. Studies have suggested that certain PCBs contribute to the development of metabolic syndromes like Type II Diabetes and atherosclerosis[64, 70-72]. Coplanar PCBs initiate an inflammatory signaling cascade that increases oxidative stress and promotes endothelial dysfunction in vascular endothelial cells[73]. To better understand the inflammatory potential of PCBs, chapter two assesses endothelial cell response to PCB 77 and PCB 77 remediation products which are the byproducts of PCB 77 dechlorination. To establish a dosing model and further our understanding of environmentally persistent coplanar PCBs, chapter three determines which of five increasing concentration of PCB 126 are effective in producing a moderate inflammatory response without causing toxic wasting syndrome. Using the dosing model developed in chapter three, we were able to test nutritional interventions of PCB 126-induced inflammation in chapter four.

1.3 Nutrition and inflammation

Fatty acids and inflammation

A fatty acid is a long carbon chain with four to twenty-four carbons that is capped by a methyl group containing the omega carbon and a carboxyl group[74]. There are multiple structural classes of fatty acids that are defined by the number and location of double bonds within the carbon chain and include saturated, monounsaturated, polyunsaturated, and trans fatty acids. Diets high in saturated fat have been associated with cardiovascular disease and are known to promote inflammation[75, 76]. Saturated fatty acids, which are not essential for a complete human diet, are long carbon chains that are fully substituted with hydrogen atoms and do not contain double bonds; examples include palmitate, laurate, myristate and stearate, which are found in red meat and dairy[74]. The amount of saturated fat consumed determines the inflammatory effects. In a study in mice, mice consuming 12% saturated fat, which is equivalent to the average American diet, had greater adipose inflammation and macrophage activity than mice fed diets with 6% and 24% saturated fat[77]. One of the mechanism by which saturated fatty acids cause inflammation is through the toll-like receptors (TLRs)[76], including TLR4 which has increased expression in atherosclerotic lesions[78]. Saturated fatty acids modulate gene expression and increase TLR expression which increases sensitivity to inflammatory stimuli, such as lipopolysaccharide (LPS)[79]. In the Nurses' Health Study, women who consumed 5% more saturated fat compared to those who consumed 5% more carbohydrate were 17% more likely to have a cardiac event[80]. Replacing dietary saturated fatty acids with polyunsaturated fatty acids reduces the number of coronary events[81]. Unlike saturated fatty acids, polyunsaturated fats (PUFA), e.g. omega-3 and omega-6 fatty acids, have two or more double bonds with the first double bond at the third or sixth carbon, respectively. PUFA are essential to the human diet[74], yet differences exist between the omega-3 and omega-6 inflammatory potential.

Omega-3 and omega-6 fatty acids and inflammation

The ratio of omega-3/omega-6 fatty acids influences metabolism of fatty acid substrates and the generation of inflammatory mediators. For example, the elongation of the parent omega-3 fatty acid α-linolenic acid to the longer chain docosahexaenoic acid (DHA) molecules can be inhibited by competition with high levels of the omega-6 linoleic acid for the same desaturase enzymes[82]. Linoleic acid is elongated to form arachidonic acid, which is the primary substrate for prostaglandin, leukotriene and thromboxane formation; higher substrate availability increases the baseline levels of these inflammatory

eicosanoids[82]. Long-chain omega-3 fatty acids, eicosapentanoic acid (EPA) and DHA are also metabolized by cyclooxygenases (COX) and lipoxygenases.(LOX) to form eicosanoid and docosanoid metabolites, which are either less inflammatory than their omega-6 derived counterparts or have anti-inflammatory properties[83, 84] (Figure 1.2[85-88]). Arachidonic acid is a major component of the plasma membrane and is the precursor of prostaglandin E2 (PGE_2) and leukotriene B4 (LTB4); diets containing omega-3 fatty acid rich-flaxseed oil or fish oil competitively reduced the production of arachidonic acid-derived eicosanoids and other inflammatory cytokines[89]. F_2-isoprostanes (F_2-IsoPs), which are similar in structure to the COX-derived prostaglandins, are formed by non-enzymatic peroxidation of arachidonate and are an indication of oxidative stress[90]. Elevated levels of F_2-IsoPs are associated with chronic disease states including atherosclerosis, hypercholesterolemia, diabetes, obesity, Alzheimer's, pulmonary disorders, and allergen-aggravated asthma[90]. All of these disorders are associated with elevated levels of inflammation and oxidative stress.

Different fatty acids modulate PCB-induced inflammation. In a feeding study using LDL-$R^{-/-}$ (low-density lipoprotein receptor deficient) mice, we observed VCAM1 tissue expression in the endothelium of mice fed omega-6-rich corn oil, and PCB treatment promoted more extensive VCAM1 expression extending to the smooth muscle portions of the vessel wall[91]. In contrast, dietary feeding of monounsaturated-rich olive oil did not promote vascular inflammation, and though PCBs induced inflammation in olive oil fed mice, the high oleic acid diet supported compensatory metabolic changes in the livers of PCB-treated mice. *In vitro* work using primary vascular endothelial cells enabled us to modulate PCB-induced inflammation by changing the omega-3/omega-6 fatty acid ratio. Increasing levels of α-linolenic acid (omega-3) to linoleic acid (omega-6) reduced VCAM1 and COX-2 mRNA and protein expression and attenuated PGE_2 production. With the same model, we demonstrated that oxidized DHA-derived A_4/J_4-neuroprostanes reduced coplanar PCB-induced oxidative stress, NFκB activation, and MCP-1 protein and mRNA expression[92]. When compared, DHA-derived neuroprostanes were more effective at attenuating PCB-induced inflammation than those derived from EPA. From these data, we concluded that future *in vivo* nutritional intervention studies, as presented in chapter four, would use a DHA-enriched diet.

Omega-3 fatty acids and implications in inflammation resolution

Fish oil presents the richest source of DHA and EPA, and the precursor fatty acid, α-linolenic acid, is available from multiple plant sources including walnuts, flax seed, and canola oil[74]. A human trial comparing the effect of DHA-EPA, α-linolenic acid (ALA), DHA-EPA/ALA combination or placebo treatment on major cardiovascular events found that ALA was most beneficial to women and that the DHA-EPA treatment was most beneficial to patients with a diabetic comorbidity[93]. A meta-analysis of eleven studies that provided DHA/EPA supplementation for one year or longer determined that supplementation significantly reduced the risk of sudden cardiac death and all-cause mortality for high risk patients and reduced the risk of nonfatal cardiovascular events in patients with moderate risk[94]. In culture, omega-6 fatty acid-exposed endothelial cells had more monocyte adhesion, a pre-cursor to atherosclerotic plaque formation, than those treated with omega-3 fatty acids; these changes were attributed to an alteration in the function of COX-2[95]. Omega-3 fatty acids alter inflammatory response through many potential mechanisms including (a) modification of the membrane through disruption of lipid rafts, (b) propagation of bioactive metabolites, and/or (c) alteration of nuclear transcription factor signaling[96]. Omega-3 enriched diet disrupts the microenvironment of caveolae lipid domains in colonocytes initiating changes in signaling by displacing caveolin-1 (Cav-1) and other raft specific signaling molecules[97]. Endothelial cells treated with DHA have similar disruption in lipid raft composition that displaces the Cav-1 protein and releases endothelial nitric oxide (eNOS), which is critical to vascular homeostasis[98]. In a model of allergic lung inflammation, omega-3 fatty acid supplementation reduced arachidonic acid-derived F_2-isoprostane production presumably through displacement of arachidonic acid and competition for COX and LOX enzymes[99]. E-series and D-series resolvins are derived from EPA and DHA, respectively. Research into the functional roles of resolvins and other EPA- and DHA-derived metabolites demonstrate changes to leukocyte response including the inhibition of dendritic cell and T-cell maturation and activation, reduction of leukocyte chemotaxis, and changes in the cytokine response by immune cells[100-102]. Understanding the molecular signaling pathways by which omega-3 fatty acid-derived metabolites promote these actions is an area of active research. Peroxisome proliferator-activated receptors (PPARs) are of particular interest. An increase in PPARγ activity is associated improved outcomes in many inflammatory disease states; unfortunately, rosiglitazone, pioglitazone and other PPARγ agonists have undesirable side effects[103]. Oxidized-DHA metabolites are possible ligands of PPARγ

Chapter One: Introduction

1.1 Environmental pollution – PCB

The unprecedented boom in chemical manufacturing had produced a legacy of chemical wastes and byproducts that flowed into streams and piled up in landfills. Scientists and the public began to awaken to the horror of a polluted world. Rachel Carson, a leader in the environmental movement, raised public awareness through her book *Silent Spring*; she writes,

> "The most alarming of all man's assaults upon the environment is the contamination of air, earth, rivers, and sea with dangerous and even lethal materials. This pollution is for the most part irrecoverable; the chain of evil it initiates not only in the world that must support life but in living tissues is for the most part irreversible[1]."

In response to the public outcry and mounting scientific evidence about environmental and human health effects, Congress passed a series of environmental legislation, and the President established the Environmental Protection Agency (EPA)[2]. Within this legislation, certain environmental pollutants were banned from manufacturing including polychlorinated biphenyls (PCBs). PCBs like many other contaminants from that era are distinguished by their stable chemical structure which includes a biphenyl and many configurations of chlorine substitutions that account for up to 209 possible congeners[3] (Figure 1.1). Produced in mixtures, called Aroclors, PCBs were widely marketed and used in applications in which their stability and low electrical conductivity were prized; these applications included dielectric fluid in capacitors and light ballasts and building materials such as paint and sealants[4].

The two major classes of PCBs are defined by the stereochemistry of the biphenyl bond (Figure 1.1)[3, 5]. The coplanar PCBs do not contain *ortho*-substitutions and exhibit dioxin-like properties. The presence of coplanar PCBs in human and animal tissues are orders of magnitude lower than other congeners, but as a class of compounds they exhibit greater potential for toxicity, especially PCB 126[6, 7]. They are dioxin-like and bind the aryl hydrocarbon receptor (AhR) which activates cytochrome P450 (CYP) metabolizing enzymes, the expression of which are associated with increased cellular oxidative stress and inflammation[8]. Chlorine substitutions in the *ortho*- position cause steric hindrance for noncoplanar PCBs, which have different biological activity than the coplanar PCBs. Noncoplanar PCBs have an affinity for the constitutive androstane receptor (CAR)[9], which activates CYP metabolizing enzymes, and are known to disrupt Ca^{2+} signaling in

the brain through the ryanodine receptors[3, 10]. In addition, noncoplanar PCBs have been associated with certain metabolic disorders. For example, PCB 153 is a noncoplanar PCB that is present in high levels in human serum; it is associated with increased risk for nonalcoholic fatty liver disease and Type 2 diabetes[11, 12]. Congeners which are mono-*ortho*-substituted, such as PCB 118, have reduced AhR activity and have molecular similarities to noncoplanar PCBs[3, 5, 13]. Our research has demonstrated that in comparison to noncoplanar PCBs, coplanar PCBs and mixed inducers promote oxidative stress and decrease endothelial barrier function, which is critical to inflammatory process that causes endothelial dysfunction and promotes the vascular inflammation that leads to atherosclerosis[14]. We have also demonstrated that certain nutrients either promote or inhibit coplanar PCB-induced endothelial cell dysfunction. For example, the omega-6 fatty acid linoleic acid promotes coplanar PCB-induced inflammation, but when the ratio of omega-3 to omega-6 fatty acids is increased, the omega-3 fatty acids protect against PCB-induced oxidative stress and nuclear factor kappa B (NFκB) activation[15, 16]. As a result, the work in our laboratory has focused on the dioxin-like, coplanar PCBs.

Pollutant toxicity is compared using toxic equivalency factors (TEFs) which designate a toxicity value based on a comparison to the toxicity of 2,3,7,8-tetrachlorodibenzo-*p*-dioxin (TCDD, dioxin). For PCBs, only coplanar PCBs (non-ortho substituted) exhibit dioxin-like qualities and are ligands had arylhydrocarbon receptor (AhR). The major congeners in this class are PCB 77, PCB 126, and PCB 169 with TEFs in humans of 0.0001, 0.1 and 0.01, respectively[17]. In addition, PCB 170 and PCB 180 have ethoxyresorufin-O-deethylase (EROD) activity that is sufficient for a TEF equivalency to be assigned. Based on the median TEF values of PCB 105, PCB 118, and PCB 156, the TEF for mono-ortho PCBs, containing one ortho substitution or a mixed congener, is 0.00003[18]. Together, TEFs can be combined to develop toxic equivalents (TEQ) that may be applied when assessing limits in food sources, sediments, waterways, etc. However, the TEFs are based primarily on studies of oral exposure, which is often the source of exposure for both animals and humans[18]. As such, human exposure risk and risk attenuation continue to be primary concerns in environmental health research.

PCB distribution in the body

The concept of persistence and biomagnification in humans and animals is based on the ability of adipose tissue to act as a storage facility for persistent organic pollutants (POPs)[19, 20]. The degree of lipophilicity for a particular toxicant is determined by a $\log_{10}$

value of >6.0 for the solubility ratio of octanol to water[21]. POPs that exceed the 6.0 lipophilicity threshold are soluble in dietary fat sources and are absorbed in the intestinal lumen with triacylglycerols into the lymphatic circulation[22]. After entry into the lymphatic system, they are incorporated into chylomicrons which transport the toxicants to other tissues including the primary storage depot, the adipose. PCBs display a range of affinities and distribute among LDL, HDL, and albumin fractions[23, 24]. Fortunately, the body has a mechanism for reducing its burden of PCBs and other POPs by utilizing enterohepatic circulation[21]. Through this cycle, POPs may be returned to circulation in the blood, be acquired by the liver which packages them with bile for excretion into the intestine. Once in the intestine, the pollutants will either be reabsorbed with the bile salts or be excreted in the feces. Through a similar pattern of circulation, POPs are also incorporated into mother's breast milk, which serves as one of the first and most concentrated exposures for humans[25, 26]. The circulation of these compounds is not an innocuous process, and PCBs or other compounds are able to interact with the tissues that are exposed during circulation including the vascular endothelium and the liver. PCBs and other dioxin-like compounds are associated with a wide range of human health outcomes, the mechanisms of which are still being explored. The immune, hepatic, neural, endocrine, vascular and reproductive systems are all affected in by PCB exposure[27-29].

Molecular interactions of coplanar PCBs with target receptors

As dioxin-like compounds, coplanar PCBs are ligands for the AhR. The transcription factor, AhR, is a member of the PER-ARNT-SIM (PAS) superfamily that has a helix-loop-helix structure. This highly conserved protein requires ligand binding for activity and is a cellular sensor that has a critical function in development, especially of the liver and vascular systems, circadian rhythms, hypoxia, hormonal signaling, inflammation and other biological processes[30]. The AhR and its chaperone proteins including two HSP90 units reside in the cytosol until ligand binding which causes the release of one HSP90 and translocation into the nucleus where AhR dimerizes with ARNT (AhR nuclear translocator), releases the second HSP90, binds to a xenobiotic response element (XRE, also called the dioxin response element, DRE) and facilitates transcription[29]. The transcriptional changes directed by XRE binding facilitate cellular responses to environmental stimuli; however, when these signals are prolonged by strong ligand affinity, such as is the case of AhR binding with TCDD, disease processes are activated. AhR activity promotes expression of Phase I and Phase II metabolism and anti-oxidant

response enzymes, such as the Phase I enzyme cytochrome P450 1A1 (CYP1A1)[31, 32]. Ligands of the AhR require a degree of hydrophobicity, e.g. be lipophilic in nature, and exhibit certain electronegative and hydrogen bonding properties, and as follows, this includes a varied set of xenobiotic, endogenous and dietary compounds[33]. The xenobiotic ligands that meet the physical requirements of the AhR binding pocket represent a large number of environmental pollutants examples of which include the following: PCBs, dioxins, naphthalenes and PAHs (polycyclic aromatic hydrocarbons), such as benzo[a]pyrene. An equally extensive list of possible endogenous ligands have also been identified for the AhR; these include the following: indigoids (indigo and indirubin), 2-(1′H-indole-3′-carbonyl)-thiazole-4-carboxylic acid methyl ester (ITE), equilenin (equine estrogen), metabolites of arachidonic acid, of heme and of tryptophan. From food sources, derivatives of indole-3-carbinol, found in cruciferous vegetables, and flavonoids, such as quercetin are potential ligands. The diversity of AhR ligands has led scientists to appreciate a number of functional roles for this transcription factor. Through endogenous ligand activation, the AhR is responsible for a number of developmental and cellular processes including cardiovascular, immune and neuronal systems[34]; for example, AhR deficient mice have incomplete liver vascularization[33]. Dietary polyphenols, like flavonoids, have been linked to the protective anti-oxidant response and initiate binding to alternative XRE binding sites. In contrast, xenobiotics, such as PCBs, hijack the endogenous functions of the AhR to produce an inflammatory response[34]. The AhR-induced inflammatory response is linked to the upregulation of detoxifying enzymes, such as CYP1A1, and cross-talk with the nuclear nuclear factor (erythroid-derived 2)-like 2 (Nrf2) mediated anti-oxidant response[35].

The AhR induces CYP1A1 expression in response to coplanar PCBs and other ligands[36, 37]. CYP1A1 activity includes the hydroxylation or epoxidation of the offending xenobiotic. When the reaction is unsuccessful and the enzyme “slips” or becomes uncoupled, a superoxide ion is released into the cell rather than being added to the compound[38]. Xenobiotics, such as PCBs, are not well metabolized, and their interaction with Phase I enzymes, like CYP1A1, leads to a greater release of reactive oxygen species (ROS), which significantly shift the redox balance of the cell[39]. Nrf2 regulated anti-oxidant enzymes, such as glutathione-S-transferase (GST) and NAD(P)H:quinine oxidoreductase (NQO1), serve to mitigate the increase in ROS, but when the oxidant capacity has been exceeded the cell initiates NFκB and other redox sensitive

transcription factors to produce a heightened inflammatory cascade[40, 41]. NFκB promotes the transcription of the chemokine monocyte chemoattractant protein 1 (MCP-1)[42, 43], also called CCL2, and vascular cell adhesion molecule 1 (VCAM1)[44, 45], which are key markers of endothelial cell dysfunction and the initiation of macrophage recruitment. The cytochrome P450 enzymes are part of Phase I metabolism during which the substrates are attacked at the site of a good leaving group which is replaced by hydroxyl, epoxide or carboxyl functional groups [46, 47]. This conversion is the first step in the transformation of the liphophilic molecule into a water soluble substrate that can be excreted through the kidneys. Phase II metabolizing enzymes that are upregulated through AhR activation include glutathione transferases, UDP-glucuronyltransferases and sulfotransferases[48], which utilize the nucleophilic functional group to add a water soluble moiety such as a glucuronic acid, amino acid (glutathione, GSH) or sulfuric acid[47]. CYP metabolism of PCBs results in epoxide and hydroxylated products that are processed by the Phase II enzymes to generate all these metabolites[3].

1.2 PCBs and predisposition to inflammatory response

Endothelial dysfunction

As sensitive modulators of vascular homeostasis, endothelial cells both respond to the changing climate within the blood and regulate the vascular environment[49]. For the average American, this "climate" includes the following: dietary factors such as high levels of fatty acids, sodium, and glucose; lifestyle factors such as minimal physical activity; and exposure environmental pollutants from food, air, and built environments[50, 51]. The endothelium responds to each of these factors by modulating the physiological environment including vasorelaxation through endothelial nitric oxide synthase (eNOS) signaling or inflammation through cytokine and adhesion molecule expression[52, 53]. The endothelial inflammatory response culminates in a change in function termed endothelial dysfunction in which cytokines like the chemokine monocyte chemoattractant protein-1 (MCP-1) are secreted to recruit macrophages that are captured via adhesion molecules like VCAM1, and decreases in cell:cell junction integrity allow the macrophages to penetrate the endothelial cell barrier[42, 54, 55]. Once in the intimal space, macrophages promote the inflammatory state by producing cytokines and through phagocytosis of ox-LDL, which together promote formation of foam cells that accumulate to form plaques.

Inflammation and disease risk

Inflammation is a characteristic held in common by a variety of diseases including lupus, rheumatoid arthritis, Crohn disease, ulcerative colitis, dermatomyositis and polymyositis[56]. The majority of these disorders can increase a patient's risk for myocardial infarction or coronary artery disease related events when compared to control or the general population; for this analysis, only disorders associated with inflammatory bowel disease did not increase vascular disease risk[56]. The heightened inflammatory state increased lipoprotein oxidation and unresolved inflammation promoting the observed effect on cardiovascular outcomes. The pro-inflammatory cytokines, tumor necrosis factor alpha (TNFα) and interleukin-6 (IL-6) are risk factors for cardiovascular diseases and are increased in rheumatoid arthritis (RA) patients; further, coronary calcification is greater in RA patients with longer disease histories, which is associated with increased cardiovascular disease prevalence in this patient population[57]. Interestingly, many chronic inflammatory disease states are characterized by a dysregulated immune response in the epithelial and mesenchymal cell structures of the affected organ; in the case of atherosclerosis, the endothelium is activated by bacterial components, lipoproteins or other stimuli which induce vascular cell adhesion molecule 1 (VCAM1) expression and the recruitment of immune cells that perpetuate the interstitial inflammatory response[58]. Coplanar PCBs and other environmental pollutants are potential activators of vascular inflammation.

PCBs as a risk factor in diseases of inflammation

Low grade inflammation is associated with many of chronic disorders including cardiovascular diseases, diabetes, metabolic syndrome and obesity. Tissue inflammation in the vascular system, adipose, and liver are all indicators and risk factors for the development of disease. PCBs have been associated with the development of multiple inflammation-associated medical conditions. For example, diabetes and metabolic syndrome are increased relative to PCB levels in both the general population and in communities with increased PCB exposure[59-61]. In particular, a survey of the Japanese population indicated that PCB 126 was a key toxicant associated with the increased prevalence of metabolic syndrome[61]. In a study of the 2003-2004 NHANES data, elevated serum alanine aminotransferase (ALT), a biomarker associated with non-alcoholic fatty liver disease (NAFLD) and other liver diseases, was increased in association with heavy metal and PCB exposure[62], and NAFLD was increased in mice exposed to PCBs[11]. Toxicant induced liver diseases, which include toxicant-associated

fatty liver disease and toxicant-associated steatohepatitis, are associated with exposure to industrial chemicals including vinyl chloride and PCBs[63]. Further, cardiovascular disease risk was increased in an elderly population independent of lipid levels and other cardiovascular disease risk factors[64], and in rats, PCB 126 was associated with heightened cardiovascular disease risk resulting from changes in cholesterol, blood pressure and heart weight[65]. Industrial workers with high levels of PCB exposure have significantly increased levels of cardiovascular disease-related death[66]. These data support of the role of PCBs in the propagation of inflammatory diseases.

PCBs, as lipophilic compounds, accumulate in the adipose and are recirculated through the body by enterohepatic circulation, a process which exposes both the vascular system and the liver to these toxicants. Given this environment, PCBs induce a stress response that promotes chronic, low grade inflammation and thus predispose the vasculature, specifically the endothelium, to heightened response to lifestyle and pathogenic stressors, like bacterial lipopolysaccharide (LPS)[67]. A recent study of the Framingham heart study cohort has concluded that the traditional risk factors are insufficient to explain the level of inflammation observed in the study[68]; this would suggest that genetic factors and environmental factors like PCBs could be the "unobserved" risk factors. Vascular biomarkers like soluble VCAM1 provide a critical observational link between metabolic syndrome and insulin resistance and the development of CVD and diabetes[69]. Studies have suggested that certain PCBs contribute to the development of metabolic syndromes like Type II Diabetes and atherosclerosis[64, 70-72]. Coplanar PCBs initiate an inflammatory signaling cascade that increases oxidative stress and promotes endothelial dysfunction in vascular endothelial cells[73]. To better understand the inflammatory potential of PCBs, chapter two assesses endothelial cell response to PCB 77 and PCB 77 remediation products which are the byproducts of PCB 77 dechlorination. To establish a dosing model and further our understanding of environmentally persistent coplanar PCBs, chapter three determines which of five increasing concentration of PCB 126 are effective in producing a moderate inflammatory response without causing toxic wasting syndrome. Using the dosing model developed in chapter three, we were able to test nutritional interventions of PCB 126-induced inflammation in chapter four.

1.3 Nutrition and inflammation

Fatty acids and inflammation

A fatty acid is a long carbon chain with four to twenty-four carbons that is capped by a methyl group containing the omega carbon and a carboxyl group[74]. There are multiple structural classes of fatty acids that are defined by the number and location of double bonds within the carbon chain and include saturated, monounsaturated, polyunsaturated, and trans fatty acids. Diets high in saturated fat have been associated with cardiovascular disease and are known to promote inflammation[75, 76]. Saturated fatty acids, which are not essential for a complete human diet, are long carbon chains that are fully substituted with hydrogen atoms and do not contain double bonds; examples include palmitate, laurate, myristate and stearate, which are found in red meat and dairy[74]. The amount of saturated fat consumed determines the inflammatory effects. In a study in mice, mice consuming 12% saturated fat, which is equivalent to the average American diet, had greater adipose inflammation and macrophage activity than mice fed diets with 6% and 24% saturated fat[77]. One of the mechanism by which saturated fatty acids cause inflammation is through the toll-like receptors (TLRs)[76], including TLR4 which has increased expression in atherosclerotic lesions[78]. Saturated fatty acids modulate gene expression and increase TLR expression which increases sensitivity to inflammatory stimuli, such as lipopolysaccharide (LPS)[79]. In the Nurses' Health Study, women who consumed 5% more saturated fat compared to those who consumed 5% more carbohydrate were 17% more likely to have a cardiac event[80]. Replacing dietary saturated fatty acids with polyunsaturated fatty acids reduces the number of coronary events[81]. Unlike saturated fatty acids, polyunsaturated fats (PUFA), e.g. omega-3 and omega-6 fatty acids, have two or more double bonds with the first double bond at the third or sixth carbon, respectively. PUFA are essential to the human diet[74], yet differences exist between the omega-3 and omega-6 inflammatory potential.

Omega-3 and omega-6 fatty acids and inflammation

The ratio of omega-3/omega-6 fatty acids influences metabolism of fatty acid substrates and the generation of inflammatory mediators. For example, the elongation of the parent omega-3 fatty acid α-linolenic acid to the longer chain docosahexaenoic acid (DHA) molecules can be inhibited by competition with high levels of the omega-6 linoleic acid for the same desaturase enzymes[82]. Linoleic acid is elongated to form arachidonic acid, which is the primary substrate for prostaglandin, leukotriene and thromboxane formation; higher substrate availability increases the baseline levels of these inflammatory

eicosanoids[82]. Long-chain omega-3 fatty acids, eicosapentanoic acid (EPA) and DHA are also metabolized by cyclooxygenases (COX) and lipoxygenases.(LOX) to form eicosanoid and docosanoid metabolites, which are either less inflammatory than their omega-6 derived counterparts or have anti-inflammatory properties[83, 84] (Figure 1.2[85-88]). Arachidonic acid is a major component of the plasma membrane and is the precursor of prostaglandin E2 (PGE_2) and leukotriene B4 (LTB4); diets containing omega-3 fatty acid rich-flaxseed oil or fish oil competitively reduced the production of arachidonic acid-derived eicosanoids and other inflammatory cytokines[89]. F_2-isoprostanes (F_2-IsoPs), which are similar in structure to the COX-derived prostaglandins, are formed by non-enzymatic peroxidation of arachidonate and are an indication of oxidative stress[90]. Elevated levels of F_2-IsoPs are associated with chronic disease states including atherosclerosis, hypercholesterolemia, diabetes, obesity, Alzheimer's, pulmonary disorders, and allergen-aggravated asthma[90]. All of these disorders are associated with elevated levels of inflammation and oxidative stress.

Different fatty acids modulate PCB-induced inflammation. In a feeding study using LDL-$R^{-/-}$ (low-density lipoprotein receptor deficient) mice, we observed VCAM1 tissue expression in the endothelium of mice fed omega-6-rich corn oil, and PCB treatment promoted more extensive VCAM1 expression extending to the smooth muscle portions of the vessel wall[91]. In contrast, dietary feeding of monounsaturated-rich olive oil did not promote vascular inflammation, and though PCBs induced inflammation in olive oil fed mice, the high oleic acid diet supported compensatory metabolic changes in the livers of PCB-treated mice. *In vitro* work using primary vascular endothelial cells enabled us to modulate PCB-induced inflammation by changing the omega-3/omega-6 fatty acid ratio. Increasing levels of α-linolenic acid (omega-3) to linoleic acid (omega-6) reduced VCAM1 and COX-2 mRNA and protein expression and attenuated PGE_2 production. With the same model, we demonstrated that oxidized DHA-derived A_4/J_4-neuroprostanes reduced coplanar PCB-induced oxidative stress, NFκB activation, and MCP-1 protein and mRNA expression[92]. When compared, DHA-derived neuroprostanes were more effective at attenuating PCB-induced inflammation than those derived from EPA. From these data, we concluded that future *in vivo* nutritional intervention studies, as presented in chapter four, would use a DHA-enriched diet.

Omega-3 fatty acids and implications in inflammation resolution

Fish oil presents the richest source of DHA and EPA, and the precursor fatty acid, α-linolenic acid, is available from multiple plant sources including walnuts, flax seed, and canola oil[74]. A human trial comparing the effect of DHA-EPA, α-linolenic acid (ALA), DHA-EPA/ALA combination or placebo treatment on major cardiovascular events found that ALA was most beneficial to women and that the DHA-EPA treatment was most beneficial to patients with a diabetic comorbidity[93]. A meta-analysis of eleven studies that provided DHA/EPA supplementation for one year or longer determined that supplementation significantly reduced the risk of sudden cardiac death and all-cause mortality for high risk patients and reduced the risk of nonfatal cardiovascular events in patients with moderate risk[94]. In culture, omega-6 fatty acid-exposed endothelial cells had more monocyte adhesion, a pre-cursor to atherosclerotic plaque formation, than those treated with omega-3 fatty acids; these changes were attributed to an alteration in the function of COX-2[95]. Omega-3 fatty acids alter inflammatory response through many potential mechanisms including (a) modification of the membrane through disruption of lipid rafts, (b) propagation of bioactive metabolites, and/or (c) alteration of nuclear transcription factor signaling[96]. Omega-3 enriched diet disrupts the microenvironment of caveolae lipid domains in colonocytes initiating changes in signaling by displacing caveolin-1 (Cav-1) and other raft specific signaling molecules[97]. Endothelial cells treated with DHA have similar disruption in lipid raft composition that displaces the Cav-1 protein and releases endothelial nitric oxide (eNOS), which is critical to vascular homeostasis[98]. In a model of allergic lung inflammation, omega-3 fatty acid supplementation reduced arachidonic acid-derived F_2-isoprostane production presumably through displacement of arachidonic acid and competition for COX and LOX enzymes[99]. E-series and D-series resolvins are derived from EPA and DHA, respectively. Research into the functional roles of resolvins and other EPA- and DHA-derived metabolites demonstrate changes to leukocyte response including the inhibition of dendritic cell and T-cell maturation and activation, reduction of leukocyte chemotaxis, and changes in the cytokine response by immune cells[100-102]. Understanding the molecular signaling pathways by which omega-3 fatty acid-derived metabolites promote these actions is an area of active research. Peroxisome proliferator-activated receptors (PPARs) are of particular interest. An increase in PPARγ activity is associated improved outcomes in many inflammatory disease states; unfortunately, rosiglitazone, pioglitazone and other PPARγ agonists have undesirable side effects[103]. Oxidized-DHA metabolites are possible ligands of PPARγ

Chapter One: Introduction

1.1 Environmental pollution – PCB

The unprecedented boom in chemical manufacturing had produced a legacy of chemical wastes and byproducts that flowed into streams and piled up in landfills. Scientists and the public began to awaken to the horror of a polluted world. Rachel Carson, a leader in the environmental movement, raised public awareness through her book *Silent Spring*; she writes,

> "The most alarming of all man's assaults upon the environment is the contamination of air, earth, rivers, and sea with dangerous and even lethal materials. This pollution is for the most part irrecoverable; the chain of evil it initiates not only in the world that must support life but in living tissues is for the most part irreversible[1]."

In response to the public outcry and mounting scientific evidence about environmental and human health effects, Congress passed a series of environmental legislation, and the President established the Environmental Protection Agency (EPA)[2]. Within this legislation, certain environmental pollutants were banned from manufacturing including polychlorinated biphenyls (PCBs). PCBs like many other contaminants from that era are distinguished by their stable chemical structure which includes a biphenyl and many configurations of chlorine substitutions that account for up to 209 possible congeners[3] (Figure 1.1). Produced in mixtures, called Aroclors, PCBs were widely marketed and used in applications in which their stability and low electrical conductivity were prized; these applications included dielectric fluid in capacitors and light ballasts and building materials such as paint and sealants[4].

The two major classes of PCBs are defined by the stereochemistry of the biphenyl bond (Figure 1.1)[3, 5]. The coplanar PCBs do not contain *ortho*-substitutions and exhibit dioxin-like properties. The presence of coplanar PCBs in human and animal tissues are orders of magnitude lower than other congeners, but as a class of compounds they exhibit greater potential for toxicity, especially PCB 126[6, 7]. They are dioxin-like and bind the aryl hydrocarbon receptor (AhR) which activates cytochrome P450 (CYP) metabolizing enzymes, the expression of which are associated with increased cellular oxidative stress and inflammation[8]. Chlorine substitutions in the *ortho*- position cause steric hindrance for noncoplanar PCBs, which have different biological activity than the coplanar PCBs. Noncoplanar PCBs have an affinity for the constitutive androstane receptor (CAR)[9], which activates CYP metabolizing enzymes, and are known to disrupt Ca^{2+} signaling in

the brain through the ryanodine receptors[3, 10]. In addition, noncoplanar PCBs have been associated with certain metabolic disorders. For example, PCB 153 is a noncoplanar PCB that is present in high levels in human serum; it is associated with increased risk for nonalcoholic fatty liver disease and Type 2 diabetes[11, 12]. Congeners which are mono-*ortho*-substituted, such as PCB 118, have reduced AhR activity and have molecular similarities to noncoplanar PCBs[3, 5, 13]. Our research has demonstrated that in comparison to noncoplanar PCBs, coplanar PCBs and mixed inducers promote oxidative stress and decrease endothelial barrier function, which is critical to inflammatory process that causes endothelial dysfunction and promotes the vascular inflammation that leads to atherosclerosis[14]. We have also demonstrated that certain nutrients either promote or inhibit coplanar PCB-induced endothelial cell dysfunction. For example, the omega-6 fatty acid linoleic acid promotes coplanar PCB-induced inflammation, but when the ratio of omega-3 to omega-6 fatty acids is increased, the omega-3 fatty acids protect against PCB-induced oxidative stress and nuclear factor kappa B (NFκB) activation[15, 16]. As a result, the work in our laboratory has focused on the dioxin-like, coplanar PCBs.

Pollutant toxicity is compared using toxic equivalency factors (TEFs) which designate a toxicity value based on a comparison to the toxicity of 2,3,7,8-tetrachlorodibenzo-*p*-dioxin (TCDD, dioxin). For PCBs, only coplanar PCBs (non-ortho substituted) exhibit dioxin-like qualities and are ligands had arylhydrocarbon receptor (AhR). The major congeners in this class are PCB 77, PCB 126, and PCB 169 with TEFs in humans of 0.0001, 0.1 and 0.01, respectively[17]. In addition, PCB 170 and PCB 180 have ethoxyresorufin-O-deethylase (EROD) activity that is sufficient for a TEF equivalency to be assigned. Based on the median TEF values of PCB 105, PCB 118, and PCB 156, the TEF for mono-ortho PCBs, containing one ortho substitution or a mixed congener, is 0.00003[18]. Together, TEFs can be combined to develop toxic equivalents (TEQ) that may be applied when assessing limits in food sources, sediments, waterways, etc. However, the TEFs are based primarily on studies of oral exposure, which is often the source of exposure for both animals and humans[18]. As such, human exposure risk and risk attenuation continue to be primary concerns in environmental health research.

PCB distribution in the body

The concept of persistence and biomagnification in humans and animals is based on the ability of adipose tissue to act as a storage facility for persistent organic pollutants (POPs)[19, 20]. The degree of lipophilicity for a particular toxicant is determined by a $\log_{10}$

value of >6.0 for the solubility ratio of octanol to water[21]. POPs that exceed the 6.0 lipophilicity threshold are soluble in dietary fat sources and are absorbed in the intestinal lumen with triacylglycerols into the lymphatic circulation[22]. After entry into the lymphatic system, they are incorporated into chylomicrons which transport the toxicants to other tissues including the primary storage depot, the adipose. PCBs display a range of affinities and distribute among LDL, HDL, and albumin fractions[23, 24]. Fortunately, the body has a mechanism for reducing its burden of PCBs and other POPs by utilizing enterohepatic circulation[21]. Through this cycle, POPs may be returned to circulation in the blood, be acquired by the liver which packages them with bile for excretion into the intestine. Once in the intestine, the pollutants will either be reabsorbed with the bile salts or be excreted in the feces. Through a similar pattern of circulation, POPs are also incorporated into mother's breast milk, which serves as one of the first and most concentrated exposures for humans[25, 26]. The circulation of these compounds is not an innocuous process, and PCBs or other compounds are able to interact with the tissues that are exposed during circulation including the vascular endothelium and the liver. PCBs and other dioxin-like compounds are associated with a wide range of human health outcomes, the mechanisms of which are still being explored. The immune, hepatic, neural, endocrine, vascular and reproductive systems are all affected in by PCB exposure[27-29].

Molecular interactions of coplanar PCBs with target receptors

As dioxin-like compounds, coplanar PCBs are ligands for the AhR. The transcription factor, AhR, is a member of the PER-ARNT-SIM (PAS) superfamily that has a helix-loop-helix structure. This highly conserved protein requires ligand binding for activity and is a cellular sensor that has a critical function in development, especially of the liver and vascular systems, circadian rhythms, hypoxia, hormonal signaling, inflammation and other biological processes[30]. The AhR and its chaperone proteins including two HSP90 units reside in the cytosol until ligand binding which causes the release of one HSP90 and translocation into the nucleus where AhR dimerizes with ARNT (AhR nuclear translocator), releases the second HSP90, binds to a xenobiotic response element (XRE, also called the dioxin response element, DRE) and facilitates transcription[29]. The transcriptional changes directed by XRE binding facilitate cellular responses to environmental stimuli; however, when these signals are prolonged by strong ligand affinity, such as is the case of AhR binding with TCDD, disease processes are activated. AhR activity promotes expression of Phase I and Phase II metabolism and anti-oxidant

response enzymes, such as the Phase I enzyme cytochrome P450 1A1 (CYP1A1)[31, 32]. Ligands of the AhR require a degree of hydrophobicity, e.g. be lipophilic in nature, and exhibit certain electronegative and hydrogen bonding properties, and as follows, this includes a varied set of xenobiotic, endogenous and dietary compounds[33]. The xenobiotic ligands that meet the physical requirements of the AhR binding pocket represent a large number of environmental pollutants examples of which include the following: PCBs, dioxins, naphthalenes and PAHs (polycyclic aromatic hydrocarbons), such as benzo[a]pyrene. An equally extensive list of possible endogenous ligands have also been identified for the AhR; these include the following: indigoids (indigo and indirubin), 2-(1′H-indole-3′-carbonyl)-thiazole-4-carboxylic acid methyl ester (ITE), equilenin (equine estrogen), metabolites of arachidonic acid, of heme and of tryptophan. From food sources, derivatives of indole-3-carbinol, found in cruciferous vegetables, and flavonoids, such as quercetin are potential ligands. The diversity of AhR ligands has led scientists to appreciate a number of functional roles for this transcription factor. Through endogenous ligand activation, the AhR is responsible for a number of developmental and cellular processes including cardiovascular, immune and neuronal systems[34]; for example, AhR deficient mice have incomplete liver vascularization[33]. Dietary polyphenols, like flavonoids, have been linked to the protective anti-oxidant response and initiate binding to alternative XRE binding sites. In contrast, xenobiotics, such as PCBs, hijack the endogenous functions of the AhR to produce an inflammatory response[34]. The AhR-induced inflammatory response is linked to the upregulation of detoxifying enzymes, such as CYP1A1, and cross-talk with the nuclear nuclear factor (erythroid-derived 2)-like 2 (Nrf2) mediated anti-oxidant response[35].

The AhR induces CYP1A1 expression in response to coplanar PCBs and other ligands[36, 37]. CYP1A1 activity includes the hydroxylation or epoxidation of the offending xenobiotic. When the reaction is unsuccessful and the enzyme “slips” or becomes uncoupled, a superoxide ion is released into the cell rather than being added to the compound[38]. Xenobiotics, such as PCBs, are not well metabolized, and their interaction with Phase I enzymes, like CYP1A1, leads to a greater release of reactive oxygen species (ROS), which significantly shift the redox balance of the cell[39]. Nrf2 regulated anti-oxidant enzymes, such as glutathione-S-transferase (GST) and NAD(P)H:quinine oxidoreductase (NQO1), serve to mitigate the increase in ROS, but when the oxidant capacity has been exceeded the cell initiates NFκB and other redox sensitive

transcription factors to produce a heightened inflammatory cascade[40, 41]. NFκB promotes the transcription of the chemokine monocyte chemoattractant protein 1 (MCP-1)[42, 43], also called CCL2, and vascular cell adhesion molecule 1 (VCAM1)[44, 45], which are key markers of endothelial cell dysfunction and the initiation of macrophage recruitment. The cytochrome P450 enzymes are part of Phase I metabolism during which the substrates are attacked at the site of a good leaving group which is replaced by hydroxyl, epoxide or carboxyl functional groups [46, 47]. This conversion is the first step in the transformation of the liphophilic molecule into a water soluble substrate that can be excreted through the kidneys. Phase II metabolizing enzymes that are upregulated through AhR activation include glutathione transferases, UDP-glucuronyltransferases and sulfotransferases[48], which utilize the nucleophilic functional group to add a water soluble moiety such as a glucuronic acid, amino acid (glutathione, GSH) or sulfuric acid[47]. CYP metabolism of PCBs results in epoxide and hydroxylated products that are processed by the Phase II enzymes to generate all these metabolites[3].

1.2 PCBs and predisposition to inflammatory response

Endothelial dysfunction

As sensitive modulators of vascular homeostasis, endothelial cells both respond to the changing climate within the blood and regulate the vascular environment[49]. For the average American, this "climate" includes the following: dietary factors such as high levels of fatty acids, sodium, and glucose; lifestyle factors such as minimal physical activity; and exposure environmental pollutants from food, air, and built environments[50, 51]. The endothelium responds to each of these factors by modulating the physiological environment including vasorelaxation through endothelial nitric oxide synthase (eNOS) signaling or inflammation through cytokine and adhesion molecule expression[52, 53]. The endothelial inflammatory response culminates in a change in function termed endothelial dysfunction in which cytokines like the chemokine monocyte chemoattractant protein-1 (MCP-1) are secreted to recruit macrophages that are captured via adhesion molecules like VCAM1, and decreases in cell:cell junction integrity allow the macrophages to penetrate the endothelial cell barrier[42, 54, 55]. Once in the intimal space, macrophages promote the inflammatory state by producing cytokines and through phagocytosis of ox-LDL, which together promote formation of foam cells that accumulate to form plaques.

Inflammation and disease risk

Inflammation is a characteristic held in common by a variety of diseases including lupus, rheumatoid arthritis, Crohn disease, ulcerative colitis, dermatomyositis and polymyositis[56]. The majority of these disorders can increase a patient's risk for myocardial infarction or coronary artery disease related events when compared to control or the general population; for this analysis, only disorders associated with inflammatory bowel disease did not increase vascular disease risk[56]. The heightened inflammatory state increased lipoprotein oxidation and unresolved inflammation promoting the observed effect on cardiovascular outcomes. The pro-inflammatory cytokines, tumor necrosis factor alpha (TNFα) and interleukin-6 (IL-6) are risk factors for cardiovascular diseases and are increased in rheumatoid arthritis (RA) patients; further, coronary calcification is greater in RA patients with longer disease histories, which is associated with increased cardiovascular disease prevalence in this patient population[57]. Interestingly, many chronic inflammatory disease states are characterized by a dysregulated immune response in the epithelial and mesenchymal cell structures of the affected organ; in the case of atherosclerosis, the endothelium is activated by bacterial components, lipoproteins or other stimuli which induce vascular cell adhesion molecule 1 (VCAM1) expression and the recruitment of immune cells that perpetuate the interstitial inflammatory response[58]. Coplanar PCBs and other environmental pollutants are potential activators of vascular inflammation.

PCBs as a risk factor in diseases of inflammation

Low grade inflammation is associated with many of chronic disorders including cardiovascular diseases, diabetes, metabolic syndrome and obesity. Tissue inflammation in the vascular system, adipose, and liver are all indicators and risk factors for the development of disease. PCBs have been associated with the development of multiple inflammation-associated medical conditions. For example, diabetes and metabolic syndrome are increased relative to PCB levels in both the general population and in communities with increased PCB exposure[59-61]. In particular, a survey of the Japanese population indicated that PCB 126 was a key toxicant associated with the increased prevalence of metabolic syndrome[61]. In a study of the 2003-2004 NHANES data, elevated serum alanine aminotransferase (ALT), a biomarker associated with non-alcoholic fatty liver disease (NAFLD) and other liver diseases, was increased in association with heavy metal and PCB exposure[62], and NAFLD was increased in mice exposed to PCBs[11]. Toxicant induced liver diseases, which include toxicant-associated

fatty liver disease and toxicant-associated steatohepatitis, are associated with exposure to industrial chemicals including vinyl chloride and PCBs[63]. Further, cardiovascular disease risk was increased in an elderly population independent of lipid levels and other cardiovascular disease risk factors[64], and in rats, PCB 126 was associated with heightened cardiovascular disease risk resulting from changes in cholesterol, blood pressure and heart weight[65]. Industrial workers with high levels of PCB exposure have significantly increased levels of cardiovascular disease-related death[66]. These data support of the role of PCBs in the propagation of inflammatory diseases.

PCBs, as lipophilic compounds, accumulate in the adipose and are recirculated through the body by enterohepatic circulation, a process which exposes both the vascular system and the liver to these toxicants. Given this environment, PCBs induce a stress response that promotes chronic, low grade inflammation and thus predispose the vasculature, specifically the endothelium, to heightened response to lifestyle and pathogenic stressors, like bacterial lipopolysaccharide (LPS)[67]. A recent study of the Framingham heart study cohort has concluded that the traditional risk factors are insufficient to explain the level of inflammation observed in the study[68]; this would suggest that genetic factors and environmental factors like PCBs could be the "unobserved" risk factors. Vascular biomarkers like soluble VCAM1 provide a critical observational link between metabolic syndrome and insulin resistance and the development of CVD and diabetes[69]. Studies have suggested that certain PCBs contribute to the development of metabolic syndromes like Type II Diabetes and atherosclerosis[64, 70-72]. Coplanar PCBs initiate an inflammatory signaling cascade that increases oxidative stress and promotes endothelial dysfunction in vascular endothelial cells[73]. To better understand the inflammatory potential of PCBs, chapter two assesses endothelial cell response to PCB 77 and PCB 77 remediation products which are the byproducts of PCB 77 dechlorination. To establish a dosing model and further our understanding of environmentally persistent coplanar PCBs, chapter three determines which of five increasing concentration of PCB 126 are effective in producing a moderate inflammatory response without causing toxic wasting syndrome. Using the dosing model developed in chapter three, we were able to test nutritional interventions of PCB 126-induced inflammation in chapter four.

1.3 Nutrition and inflammation

Fatty acids and inflammation

A fatty acid is a long carbon chain with four to twenty-four carbons that is capped by a methyl group containing the omega carbon and a carboxyl group[74]. There are multiple structural classes of fatty acids that are defined by the number and location of double bonds within the carbon chain and include saturated, monounsaturated, polyunsaturated, and trans fatty acids. Diets high in saturated fat have been associated with cardiovascular disease and are known to promote inflammation[75, 76]. Saturated fatty acids, which are not essential for a complete human diet, are long carbon chains that are fully substituted with hydrogen atoms and do not contain double bonds; examples include palmitate, laurate, myristate and stearate, which are found in red meat and dairy[74]. The amount of saturated fat consumed determines the inflammatory effects. In a study in mice, mice consuming 12% saturated fat, which is equivalent to the average American diet, had greater adipose inflammation and macrophage activity than mice fed diets with 6% and 24% saturated fat[77]. One of the mechanism by which saturated fatty acids cause inflammation is through the toll-like receptors (TLRs)[76], including TLR4 which has increased expression in atherosclerotic lesions[78]. Saturated fatty acids modulate gene expression and increase TLR expression which increases sensitivity to inflammatory stimuli, such as lipopolysaccharide (LPS)[79]. In the Nurses' Health Study, women who consumed 5% more saturated fat compared to those who consumed 5% more carbohydrate were 17% more likely to have a cardiac event[80]. Replacing dietary saturated fatty acids with polyunsaturated fatty acids reduces the number of coronary events[81]. Unlike saturated fatty acids, polyunsaturated fats (PUFA), e.g. omega-3 and omega-6 fatty acids, have two or more double bonds with the first double bond at the third or sixth carbon, respectively. PUFA are essential to the human diet[74], yet differences exist between the omega-3 and omega-6 inflammatory potential.

Omega-3 and omega-6 fatty acids and inflammation

The ratio of omega-3/omega-6 fatty acids influences metabolism of fatty acid substrates and the generation of inflammatory mediators. For example, the elongation of the parent omega-3 fatty acid α-linolenic acid to the longer chain docosahexaenoic acid (DHA) molecules can be inhibited by competition with high levels of the omega-6 linoleic acid for the same desaturase enzymes[82]. Linoleic acid is elongated to form arachidonic acid, which is the primary substrate for prostaglandin, leukotriene and thromboxane formation; higher substrate availability increases the baseline levels of these inflammatory

eicosanoids[82]. Long-chain omega-3 fatty acids, eicosapentanoic acid (EPA) and DHA are also metabolized by cyclooxygenases (COX) and lipoxygenases.(LOX) to form eicosanoid and docosanoid metabolites, which are either less inflammatory than their omega-6 derived counterparts or have anti-inflammatory properties[83, 84] (Figure 1.2[85-88]). Arachidonic acid is a major component of the plasma membrane and is the precursor of prostaglandin E2 (PGE_2) and leukotriene B4 (LTB4); diets containing omega-3 fatty acid rich-flaxseed oil or fish oil competitively reduced the production of arachidonic acid-derived eicosanoids and other inflammatory cytokines[89]. F_2-isoprostanes (F_2-IsoPs), which are similar in structure to the COX-derived prostaglandins, are formed by non-enzymatic peroxidation of arachidonate and are an indication of oxidative stress[90]. Elevated levels of F_2-IsoPs are associated with chronic disease states including atherosclerosis, hypercholesterolemia, diabetes, obesity, Alzheimer's, pulmonary disorders, and allergen-aggravated asthma[90]. All of these disorders are associated with elevated levels of inflammation and oxidative stress.

Different fatty acids modulate PCB-induced inflammation. In a feeding study using LDL-$R^{-/-}$ (low-density lipoprotein receptor deficient) mice, we observed VCAM1 tissue expression in the endothelium of mice fed omega-6-rich corn oil, and PCB treatment promoted more extensive VCAM1 expression extending to the smooth muscle portions of the vessel wall[91]. In contrast, dietary feeding of monounsaturated-rich olive oil did not promote vascular inflammation, and though PCBs induced inflammation in olive oil fed mice, the high oleic acid diet supported compensatory metabolic changes in the livers of PCB-treated mice. *In vitro* work using primary vascular endothelial cells enabled us to modulate PCB-induced inflammation by changing the omega-3/omega-6 fatty acid ratio. Increasing levels of α-linolenic acid (omega-3) to linoleic acid (omega-6) reduced VCAM1 and COX-2 mRNA and protein expression and attenuated PGE_2 production. With the same model, we demonstrated that oxidized DHA-derived A_4/J_4-neuroprostanes reduced coplanar PCB-induced oxidative stress, NFκB activation, and MCP-1 protein and mRNA expression[92]. When compared, DHA-derived neuroprostanes were more effective at attenuating PCB-induced inflammation than those derived from EPA. From these data, we concluded that future *in vivo* nutritional intervention studies, as presented in chapter four, would use a DHA-enriched diet.

Omega-3 fatty acids and implications in inflammation resolution

Fish oil presents the richest source of DHA and EPA, and the precursor fatty acid, α-linolenic acid, is available from multiple plant sources including walnuts, flax seed, and canola oil[74]. A human trial comparing the effect of DHA-EPA, α-linolenic acid (ALA), DHA-EPA/ALA combination or placebo treatment on major cardiovascular events found that ALA was most beneficial to women and that the DHA-EPA treatment was most beneficial to patients with a diabetic comorbidity[93]. A meta-analysis of eleven studies that provided DHA/EPA supplementation for one year or longer determined that supplementation significantly reduced the risk of sudden cardiac death and all-cause mortality for high risk patients and reduced the risk of nonfatal cardiovascular events in patients with moderate risk[94]. In culture, omega-6 fatty acid-exposed endothelial cells had more monocyte adhesion, a pre-cursor to atherosclerotic plaque formation, than those treated with omega-3 fatty acids; these changes were attributed to an alteration in the function of COX-2[95]. Omega-3 fatty acids alter inflammatory response through many potential mechanisms including (a) modification of the membrane through disruption of lipid rafts, (b) propagation of bioactive metabolites, and/or (c) alteration of nuclear transcription factor signaling[96]. Omega-3 enriched diet disrupts the microenvironment of caveolae lipid domains in colonocytes initiating changes in signaling by displacing caveolin-1 (Cav-1) and other raft specific signaling molecules[97]. Endothelial cells treated with DHA have similar disruption in lipid raft composition that displaces the Cav-1 protein and releases endothelial nitric oxide (eNOS), which is critical to vascular homeostasis[98]. In a model of allergic lung inflammation, omega-3 fatty acid supplementation reduced arachidonic acid-derived F_2-isoprostane production presumably through displacement of arachidonic acid and competition for COX and LOX enzymes[99]. E-series and D-series resolvins are derived from EPA and DHA, respectively. Research into the functional roles of resolvins and other EPA- and DHA-derived metabolites demonstrate changes to leukocyte response including the inhibition of dendritic cell and T-cell maturation and activation, reduction of leukocyte chemotaxis, and changes in the cytokine response by immune cells[100-102]. Understanding the molecular signaling pathways by which omega-3 fatty acid-derived metabolites promote these actions is an area of active research. Peroxisome proliferator-activated receptors (PPARs) are of particular interest. An increase in PPARγ activity is associated improved outcomes in many inflammatory disease states; unfortunately, rosiglitazone, pioglitazone and other PPARγ agonists have undesirable side effects[103]. Oxidized-DHA metabolites are possible ligands of PPARγ

with natural metabolism pathways that would limit potential side effects[103]. Others have demonstrated an Nrf2-dependent anti-oxidant effect in adipocytes following EPA and DHA treatment[104]. Our work suggests that caveolae are critical to PCB-induced inflammation making lipid rafts a target for omega-3 fatty acid nutritional intervention[105], and our study of oxidized DHA neuroprostane metabolites indicates molecular modulation of Nrf2 signaling[92]. Thus, omega-3 fatty acid-derived protection is most likely an integration of multiple mechanisms. We recognize that the inflammatory signaling of TLR4 is sensitive to DHA modulation of caveolae-based signaling molecules[106, 107]. In chapter five, we propose TLR4 as a model caveolae-based signaling pathway that could be developed for future study of omega-3 nutritional intervention of PCB-induced inflammation.

1.4 Targets for nutritional modulation of inflammation

Caveolae – the interface of innate immunity and nutritional intervention

Lipid or membrane rafts are 10-200 nm structures that are typified by sphingolipid and cholesterol enrichment and are characterized dynamic protein interactions as these domains play a critical though often transient role in protein scaffolding and signaling[108]. Caveolae are some of the larger raft structures included in this classification. The major structural proteins are the caveolins. Caveolin-1 (Cav-1) and caveolin-2 (Cav-2) are ubiquitously expressed and are particularly enriched in endothelial cells and adipocytes[109]. Muscle specific caveolin-3 (Cav-3) is structurally similar to Cav-1, and both Cav-1 and Cav-3 are critical to caveolae formation in their respective tissues whereas Cav-2 is not essential for the formation of the raft structure[110]. Caveolae play a crucial role in cellular and tissue nutrition having the ability to capture and endocytose albumin and fatty acids[111, 112]. Fatty acid binding by Cav-1 facilitates fatty acid distribution within cellular membranes as Cav-1 migrates between the plasma membrane and the Golgi apparatus[24], which makes Cav-1 a likely modulator of lipophilic environmental pollutant trafficking. Further, caveolae provide a signaling hub, in which endogenous molecules, like fatty acids, and xenobiotics, such as PCBs, may modulate the cellular response, which make them of particular interest in the study of lipophilic environmental pollutants and nutrients[105].

The development of Cav-1/ApoE double knockout (KO) mice substantiated the role of caveolae in vascular disease in part by altering protein expression of CD36 and VCAM1 in the plasma membrane[113]. In addition, Cav-1 deficient mice are more resistant to LPS

challenge with reduced mortality from 90% to 30%[114]. LPS is the primary ligand of TLR4, which initiates an inflammatory signaling cascade[115]. TLR4 signaling requires dimerization of the TLR4 monomer and membrane translocation to lipid rich domains, such as caveolae, in the plasma membrane[116, 117]. Cholesterol and saturated fat enrichment promote TLR4 trafficking to Cav-1-rich membrane fractions[76, 118]. TLR activity is inhibited by omega-3 fatty acids including the inflammatory response modulated by TLR4, TLR2/1 and TLR2/6[106, 119], and this inhibition has been attributed to disruption of TLR4 activated COX-2 expression and mitigation of ROS[107, 120, 121]. Nrf2 regulates anti-oxidant enzyme expression that is critical to cell survival; this includes hemeoxygenase 1 (HO-1), an anti-oxidant enzyme that interacts with caveolae[122]. Interestingly, in LPS stimulated cells, carbon monoxide CO production by HO-1 inhibits NADPH oxidase generated ROS and alters the Cav-1/TLR4 interaction to prevent myeloid differentiation primary response 88 (MyD88) scaffolding with TLR4[121, 123]. Similarly, DHA inhibits TLR4 dimerization and trafficking into lipid rafts by altering the raft microdomain composition and inhibiting NADPH oxidase ROS production[107]. It is clear that caveolae provide a critical structural interface for membrane signaling and protein scaffolding[108], and Cav-1 is also integral to both PCB-induced inflammation and modulation of inflammation.

Coplanar PCB induction of the AhR-mediated inflammatory response including up-regulation of CYP1A1, MCP1, and VCAM1 expression require the presence of Cav-1[124-126]. Further Cav-1 is a key regulator of nutritional interventions including both fatty acids and flavonoids. For example, we have demonstrated that α-linolenic acid, an omega-3 fatty acid, reduces Cav-1 expression and overall inflammatory response to TNFα stimulation[127]. Similarily, quercetin, a flavanol found in fruit and vegetables, decreases PCB-mediated CYP1A1 expression by reducing the levels of phosphorylated Cav-1[128]. Epigallocatechin gallate (EGCG), a green tea catechin, accumulates in the caveolae rich cellular fractions, displaces Cav-1, promotes Nrf2-dependent anti-oxidant gene expression, and reduces the NFκB-mediated inflammatory response[129, 130]. EGCG and α-linolenic acid both attenuate the linoleic acid and PCB-induced inflammatory response[16, 130, 131]. Caveolae are critical mediators of both pro- and anti-inflammatory stimuli and present an ideal platform in which to study the interface of innate immune and toxicant-induced inflammatory signaling as a potential target for nutritional modulation.

1.5 Summary

The major aim of this dissertation is to better understand the molecular consequences of coplanar PCB-induced inflammation and examine omega-3 fatty acids as potential nutritional modulators of environmental toxicant-induced inflammation. From the environmental to the molecular level, the human body is a staging ground for the many environmental factors that we encounter. Whether the stimuli are PCBs or remediation mixtures, the nuances of the physiological response include oxidative stress and the induction of inflammatory cytokines. We propose that omega-3 fatty acids are protective dietary components against inflammation. Thus, the activation of anti-oxidant enzymes and the fine tuning of the immunological response by fatty acid metabolites are fields ready for continued investigation.

The following dissertation provides a discussion which begins with an environmental problem, tests a nutritional intervention using omega-3 fatty acids, and explores a mechanistic target for studies of nutritional interventions (Figure 1.3):

In chapter two, endothelial cell culture provides an *in vitro* model for the study of the inflammatory response to coplanar PCBs, such as PCB 77. Remediation products of PCB 77 were used to demonstrate the sensitivity of the biological response to low levels of the parent compound and its dechlorination products. As long as remediation technologies such as the dechlorination process that was assessed in chapter two are not a hundred percent efficient, there will be a continued risk of human exposures and disease outcomes associated with PCBs and other environmental pollutants.

In response, we need to develop means of attenuating health risks using lifestyle changes such as diet/nutrition and exercise. The subsequent chapters develop a toxicant exposure model and test a nutritional intervention. In chapter three, we characterize the use of PCB 126 as a model toxicant and define the toxicological response to acute exposure in C57BL/6 mice. After defining the PCB 126 exposure level in chapter three, we assess *in vivo* the role of the omega-3 fatty acid, DHA, in the modulation of the PCB 126-induced inflammatory response in chapter four.

In chapter five, we complement the *in vivo* work by investigating *in vitro* mechanisms of the toxicant inflammatory responses. Others have shown that omega-3 fatty acids attenuate LPS stimulated inflammation; thus, LPS was used as a positive control. The

research in this chapter was focused on caveolae-based signaling in the response to PCB 126 and LPS-induced inflammation, which could broaden our ability to apply fatty acids as a nutritional intervention. Together these studies provide insight into the regulation of coplanar PCB-induced inflammation and possible protection by omega-3 lipids.

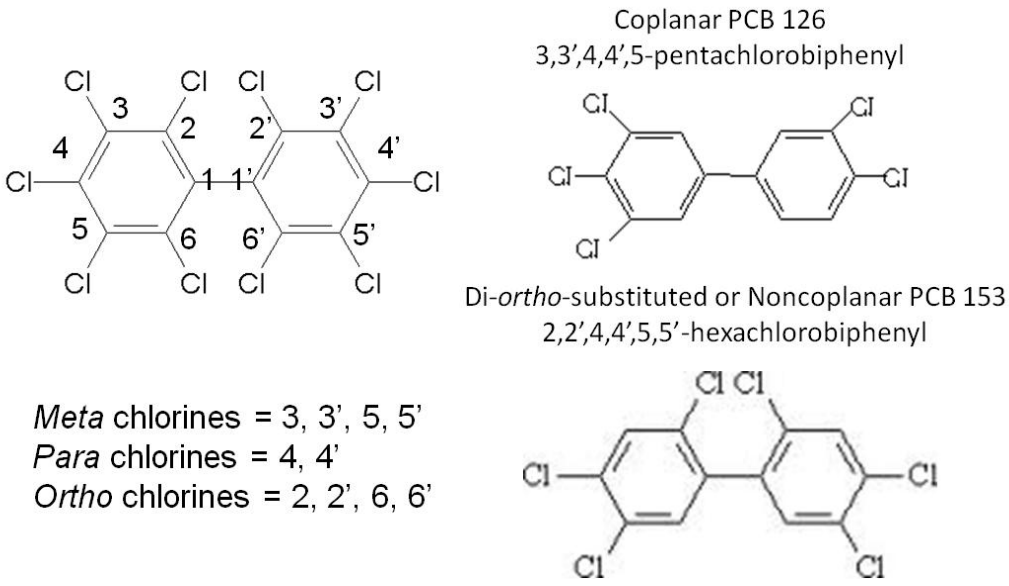

Figure 1.1 Polychlorinated biphenyl (PCB) structure, nomenclature and classifications. PCBs consist of chlorine-substituted biphenyl rings. The chemical name of each PCB congener includes the position and number of the chlorine substituted carbons. The two major classifications of PCBs include the coplanar PCBs, which do not have *ortho*- substitutions, and the noncoplanar or *ortho*-substituted congeners. For example, PCB 126 is a coplanar PCB named 3,3',4,4',5-pentachlorobiphenyl. The *ortho*-substituted PCB 153 is noncoplanar and is named 2,2',4,4',5,5'-hexachlorobiphenyl.

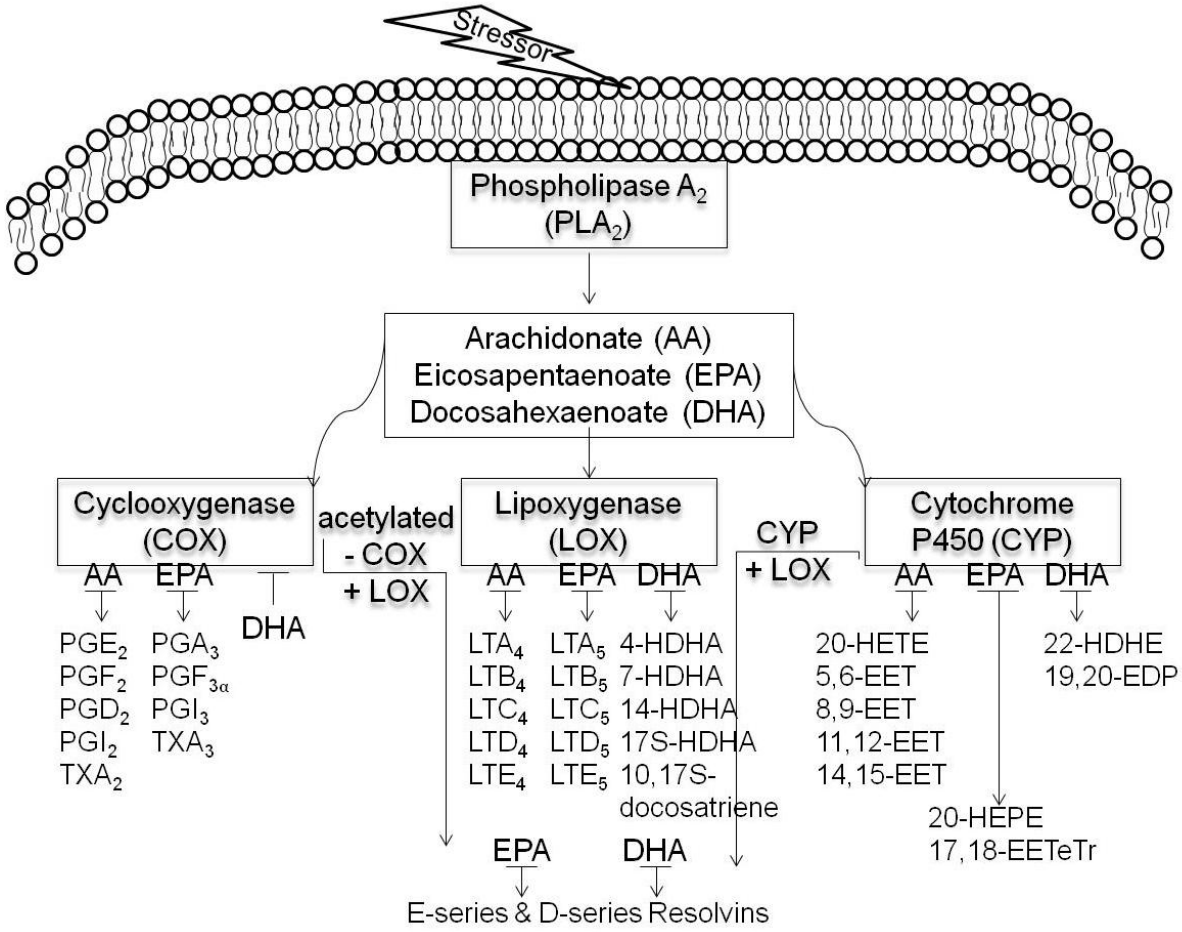

Figure 1.2 Summary of the eicosanoid and docosanoid metabolites formed following stressed-induced phospholipase A_2 fatty acid release. The arachidonic acid (AA)-derived metabolites contribute to inflammation and oxidative stress while eicosapentaenoic acid (EPA)-derived metabolites exhibit either moderately inflammatory effects or anti-inflammatory effects. Docosahexaenoic acid (DHA) metabolites are anti-inflammatory and pro-resolving. The metabolite class names are as follows: prostaglandin (PG), thromboxane (TX), leukotriene (LT), hydroxydocosahexaenoic acid (HDHA), hydroperoxy eicosatetraenoic acids (HPETE), hydroxyeicosatetraenoic acid (HETE), hydroxyeicosapentaenoic acid (HEPE), epoxyeicosatrienoic acids (EET), epoxyeicosatetraenoic acid (EETeTr), epoxydocosapentaenoic acid (EDP), hydroxydocosahexaenoic acid (HDHE).

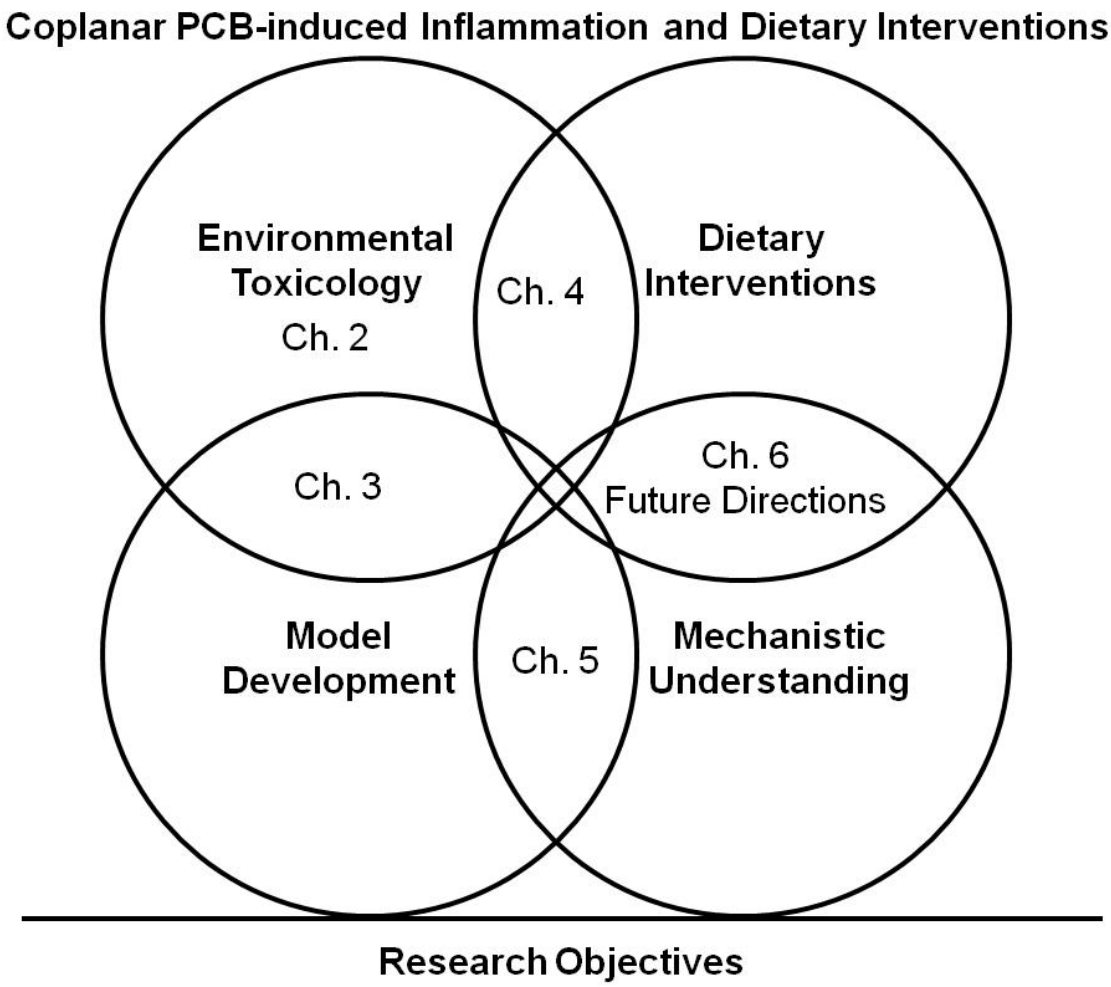

Figure 1.3 Overview of dissertation objectives and placement of chapters within these goals.

Chapter Two: PCB 77 dechlorination products modulate pro-inflammatory events in vascular endothelial cells

Springer and *Environmental Science and Pollution Research International*, DOI 10.1007/s11356-013-1591-3, 2013, PCB 77 dechlorination products modulate pro-inflammatory events in vascular endothelial cells, Eske K, Newsome B, Han SG, Murphy M, Bhattacharyya D, Hennig B is given to the publication in which the material was originally published; with kind permission from Springer Science and Business Media.

2.1 Synopsis

Persistent organic pollutants such as polychlorinated biphenyls (PCBs) are associated with detrimental health outcomes including cardiovascular diseases. Remediation of these compounds is a critical component of environmental policy. Although remediation efforts aim to completely remove toxicants, little is known about the effects of potential remediation byproducts. We previously published that Fe/Pd nanoparticles effectively dechlorinate PCB 77 to biphenyl, thus eliminating PCB-induced endothelial dysfunction using primary vascular endothelial cells. Herein, we analyzed the toxic effects of PCB congener mixtures (representative mixtures of commercial PCBs based on previous dechlorination data) produced at multiple time points during the dechlorination of PCB 77 to biphenyl. Compared to pure PCB 77, exposing endothelial cells to lower chlorinated PCB byproducts led to improved cellular viability, decreased superoxide production, and decreased nuclear factor kappa B (NFκB) activation based on duration of remediation. Presence of the parent compound, PCB 77, led to significant increases in mRNA and protein inflammatory marker expression. These data implicate that PCB dechlorination reduces biological toxicity to vascular endothelial cells.

2.2 Introduction

Polychlorinated biphenyls (PCBs) are a class of organic pollutants that were used heavily as dielectric fluids in industrial and electrical applications until evidence surfaced linking PCBs to cancer and cardiovascular disease. Remediation efforts for these highly persistent pollutants have proven difficult, expensive and slow. Our laboratories have developed new fast, low-cost techniques that employ Pd/Fe nanoparticles for reductive PCB dechlorination, which systematically dechlorinate higher congener PCBs to biphenyl, with lower chlorinated congeners produced as byproducts prior to complete degradation. The goal of this work is to better understand the toxicological effects of these byproducts and to further validate the importance of PCB dechlorination for reducing cardiovascular risk factors and for improving overall public health.

Even though PCB production has been banned in the US since the late 1970s, PCBs remain concentrated in many waterways and Superfund sites, as well as in electrical devices such as transformers and light ballasts. Additionally, recent research has indicated that a variety of PCB congeners are still being generated as industrial byproducts from pigment production and certain paper manufacturing [132, 133]. PCBs exhibit unique properties, such as high environmental persistence and resistance to metabolism in organisms, which lead to difficulties for remediation. Additionally, the costs associated with large-scale clean-up and removal of these and other chemical pollutants is great, and thus the development of more efficient, cost effective technologies continues to be important. Current remediation techniques rely on expensive dredging followed by incineration or bioremediation techniques. Although PCBs can be degraded through some natural processes such as bacterial degradation [134, 135] and photolysis [136-138], these processes are prohibitively slow for remediation of larger scale contaminations. Our research group recently developed a Pd/Fe nanoparticle system that catalyzes the dechlorination of PCBs to form biphenyl in order to address this need for low cost, high throughput chlorinated aromatic degradation ([139, 140]. During chlorinated aromatic degradation, hydrogen ions are used to displace chlorine on biphenyl rings in stages, resulting in the production of lower chlorinated PCB congeners prior to complete degradation to biphenyl. It is generally believed that less-chlorinated congeners are more water soluble, more volatile, and more likely to biodegrade further [141]. In a previous study, we compared the biological activity of the parent compound (PCB 77) with the dechlorination end product (biphenyl), and found that complete dechlorination markedly reduced the pro-inflammatory activity of PCB 77 [140].

Many environmental contaminants, and especially persistent organic pollutants, are risk factors for cardiovascular diseases such as atherosclerosis because they can initiate or exacerbate the underlying disease by altering gene expression patterns and subsequent vascular inflammation [142, 143]. Because the endothelium is in immediate contact with the blood, endothelial cells are particularly susceptible to the effect of environmental contaminants. The lining of blood vessels is protected by the endothelium, and endothelial cells play an active role in physiological processes such as regulation of vessel tone, blood coagulation, and vascular permeability. In turn, endothelial cell

activation or dysfunction is a critical marker of the pathology of cardiovascular diseases such as atherosclerosis.

Activated endothelial cells produce chemokines such as monocyte chemoattractant protein 1 (MCP-1) and inflammatory cytokines, which attract monocytes from the blood stream to the site of injury. Part of the resulting inflammatory process includes the endothelial cell expression of adhesion molecules, like vascular adhesion molecule 1 (VCAM1), which allow the monocytes to attach to the endothelial layer and infiltrate this barrier into the intimal space. We have demonstrated previously that coplanar PCBs (e.g., PCB 77) can induce DNA-binding activity of the oxidative stress-sensitive transcription factor nuclear factor kappa B (NFκB) and expression of VCAM1, which is dependent on functional aryl hydrocarbon receptor (AhR) activity [73]. Recently, we have reported the mechanisms of PCB 77-mediated upregulation of MCP-1 [125].

Little is known about vascular toxicity of PCBs, and especially about the toxicity of dechlorination or remediation products. There is a clear need to evaluate products of remediation (e.g., dechlorination products) for biological activity in mammalian systems [144]. It is important to know to what degree remediation processes of persistent organic pollutants have to occur before toxicity and any vascular injury becomes negligible. Thus, the present study was designed to test the effects of PCB 77 dechlorination products on pro-inflammatory parameters in a vascular endothelial cell model system. Data from this study suggest that the presence of the parent compound (e.g., PCB 77) is necessary for maximal endothelial cell dysfunction and inflammation. These data also suggest that dechlorination is a successful method for decreasing biological toxicity, with overall toxicity linked to the level of degradation of the parent compound. Herein, dechlorination is demonstrated to be an effective platform for addressing public health concerns associated with these persistent chlorinated pollutants.

2.3 Materials and Methods

Biphenyl, 3-chlorobiphenyl (PCB 2), 4-chlorobiphenyl (PCB 3), 3,3'-dichlorobiphenyl (PCB 11), 3,4-dichlorobiphenyl (PCB 12), 3,4'-dichlorobiphenyl (PCB 13), 4,4'-dichlorobiphenyl (PCB 15), 3, 3',4-trichlorobiphenyl (PCB 35), 3,4,4'-trichlorobiphenyl (PCB 37) and 3, 3', 4, 4'-tetrachlorobiphenyl (PCB 77) were purchased from AccuStandard, Inc. (New Haven, CT). Experiments that included hazardous materials such as PCBs were performed in accordance with institutional and federal guidelines

(11). All cell culture reagents, including ProLong Gold antifade reagent with 4',6-diamidino-2-phenylindole (DAPI), were purchased from Life Technologies (Carlsbad, CA). All other chemicals were purchased from Sigma-Aldrich Corporation (St. Louis, MO), unless otherwise specified.

Description of PCB 77 dechlorination treatment mixtures

Treatment mixtures were based on the composition of PCB 77 and its dechlorination products at 0, 10, 24, and 48 hours of remediation as derived from GC-MS data comparing the reductive efficiencies of 0.1 mg mL^{-1} 400 nm Pd/Fe nanotubes and 1 mg mL^{-1} Pd/Fe nanoparticles [139, 140]. Dechlorination product compositions were determined from these data (Table 2.1); treatments from each stage of the dechlorination are described as percent by weight and as molarity. Stocks of individual PCB commercial congeners were solubilized in fresh dimethyl sulfoxide (DMSO) at a concentration of 10 mM. Treatment mixtures were developed to delineate between the effects of the parent compound and dechlorination products including treatments representing product mixtures without PCB 77 (mixtures 4 and 6), treatments representing only the concentration of PCB 77 at a particular stage of dechlorination (mixtures 9 and 10), and a treatment representing the 24 h dechlorination products with the higher PCB 77 concentration found following 10 h dechlorination (mixture 7), to emphasize the role of PCB 77 in overall toxicity (Table 2). Stock treatment mixtures were prepared in DMSO at a 5 mM total concentration and diluted 1:1000 in cell culture medium for 5 μM final cell culture treatments. PCB mixtures were kindly composed by Bradley Newsome.

Cell culture

Primary endothelial cells (ECs) were isolated from porcine pulmonary arteries as described previously [145]. Cell culture media consisted of medium 199 (M199) containing 10% fetal bovine serum (FBS). At 70-80% confluence, cells were incubated overnight with treatment media (M199 with 1% FBS), followed by exposure to PCB 77 or respective treatment mixtures for 24 h. Treatment mixtures were added to cell culture at a final concentration of 5 μM, which represented a maximum concentration of 0.1% v/v DMSO/media (see Tables 1 and 2 for PCB treatment concentrations). Cell viability was tested in the presence of dechlorination products using the Vybrant MTT Cell Proliferation Assay Kit (Invitrogen, Eugene, OR) according to manufacturer guidelines and was kindly performed by Bradley Newsome.

Assessment of superoxide ($O_2^{\cdot-}$) levels

Superoxide levels were assessed as recently reported [92]. Cells were grown to confluence in 4-chamber culture slides (BD Biosciences, Bedford, MA). After 4 h exposure to PCB treatments (5 μM total concentrations; Table 1), the cells were rinsed 2x with Krebs-Ringer buffer (KRB) and incubated with 5 μM dihydroethidium (DHE) or KRB (blank) at 37°C for 30 min. Cells were rinsed with KRB, fixed with 10% buffered formalin, and washed with PBS. Slides were mounted with ProLong Gold antifade reagent with DAPI for nuclei staining. Slides were evaluated with an Olympus BX61W1 fluorescence microscope. Mean fluorescence intensity was quantified using ImageJ 1.42q (NIH, Bethesda, MD).

Assessment of NFκB activation

Nuclear extracts were prepared from endothelial cells cultured as described above in 10 cm dishes and treated with PCB 77 or dechlorination mixtures for 4 h. The nuclear extraction was performed as described previously [146]. EMSA (electrophoretic mobility shift assay) of nuclear factor kappa B (NFκB) binding was kindly performed by Dr. Seong-Su Han of the University of Iowa College of Medicine using the DNA-protein binding detection kit (Gibco-BRL, Grand Island, NY) with radio-labeled oligonucleotides [130, 147].

Measurement of CYP1A1, MCP-1 or VCAM1 mRNA

CYP1A1, MCP-1 and VCAM1 mRNA expression was assessed using real-time PCR (RT-PCR), as described previously [125, 126]. Briefly, mRNA was isolated using TRIzol Reagent (Life Technologies, Carlsbad, CA) and quantified using a SmartSpec Plus Spectrophotometer (BIO-RAD, Philadelphia, PA). cDNA was then generated using Promega AMV reverse transcriptase (Fisher Scientific, Waltham, MA) and RT-PCR was performed using Power SYBR Green PCR Master Mix (Life Technologies, Carlsbad, CA) and the following porcine primer sequences: β-actin sense 5′-TCA TCA CCA TCG GCA ACG-3′ and antisense, 5′-TTC CTG ATG TCC ACG TCG-3′; CYP1A1 sense 5’- TGG AGA GGC AAG AGT AGT TGG-3’and anti-sense 5’-GGC ACA ACG GAG TAG CTC ATA-3’; MCP-1 sense 5′-CGG CTG ATG AGC TAC AGA AGA GT-3′and antisense, 5′-GCT TGG GTT CTG CAC AGA TCT-3′; and VCAM1 sense 5′-TGG AAA GAC ATG GCT GCC TAT-3′ and antisense, 5′-ACA CCA CCC CAG TCA CCA TAT-3′. Assays were run using the Applied Biosystems 7300 Real time PCR System (Life Technologies, Carlsbad, CA) using absolute quantification. The raw data were quantified using a

standard curve and analyzed with a manual C_T threshold of 0.200. Sample data were normalized to individual β-actin values.

Measurement of CYP1A1, MCP-1 and VCAM1 protein

CYP1A1 and VCAM1 protein levels were assessed by Western blotting, as described previously [140]. After semi-dry transfer, nitrocellulose membranes were incubated for 2 h in blocking buffer (5% non-fat milk in Tris-buffered saline containing 0.05% Tween 20). Rabbit polyclonal CYP1A1 (H-70) and VCAM1 (C-19)-R (Santa Cruz Biotechnology, Inc., Santa Cruz, CA) primary antibodies were diluted 1:1000 in blocking buffer and incubated overnight at 4 °C, and the secondary antibody was diluted 1:4000. β-actin primary and secondary antibodies were diluted 1:10,000 [125]. MCP-1 protein levels were measured in cell culture media diluted 1:7 using an OptEIA Human MCP-1 ELISA Kit (BD Biosciences, San Diego, CA) according to manufacturer guidelines.

Statistical analysis

Values are reported as means ± SEM obtained from a representative sample set of a minimum of three independent experiments, unless otherwise stated. Comparisons were made by one-way analysis of variance (ANOVA) with Tukeys test for post-hoc analysis, using SigmaPlot 12.0 software (Systat Software, San Jose, CA). Statistical probability of $p_{value} < 0.05$ was considered significant. Different statistical marker letters indicate statistical differences.

2.4 Results

Dechlorination alters cellular oxidative stress and viability

PCB-induced cellular dysfunction is characterized by increased oxidative stress and subsequent activation of inflammatory pathways including NFκB. The uncoupling of CYP1A1 leads to the generation of reactive oxygen species (ROS), such as superoxide. Endothelial cell monolayers were exposed to representative dechlorination product mixtures (Table 2.1) for 4 h before ROS were visualized with DHE fluorescence (Figure 2.1a). Strong staining was observed in cells exposed to 0 h (pure PCB 77) and 10 h dechlorination products, whereas mixtures representing longer periods of dechlorination showed decreased superoxide production. When DHE fluorescence was quantified and normalized to DAPI nuclear staining, fluorescence from initial dechlorination mixtures (0 and 10 h of dechlorination) indicated higher ROS production which decreased to control levels with further dechlorination (differences between groups approached significance, p=0.052; See Figure 2.1b). A similar trend was observed with regard to viability, where

no changes were observed in cells treated with PCB vehicle (DMSO) and the 48 h dechlorination product, although cell viability was decreased in 0 h (parent compound, PCB 77), 10 h and 24 h dechlorination product treatments to 69±1%, 61±3%, 87±2% of control, respectively.

NFκB activation is attenuated by dechlorination

Data from an NFκB EMSA showed that cells treated for 4 h with the dechlorination products exhibited a prominent increase in NFκB activation when treated with the 0 h product, or pure PCB 77. Intermediate activation by the 10 and 24 h products was observed; NFκB:DNA binding for these treatments was significantly decreased compared to exposure to the 0 h product but remained increased relative to the vehicle control and biphenyl (48 h product; see Figure 2.2). Biphenyl was consistently within control expression levels for superoxide fluorescence, viability, and NFκB:DNA binding. The 10 and 24 h dechlorination products were increased from control but did not exhibit a consistent linear change from parent PCB 77, 0 h of dechlorination, expression levels. We, therefore, tested a series of treatment mixtures to delineate between the effects of the dechlorination products and the residual PCB 77.

Dechlorination products alter CYP1A1, MCP-1 and VCAM1 mRNA expression

CYP1A1, VCAM1 and MCP-1 levels were assessed in mRNA using treatment groups 1-10 (Figure 2.3, Table 2.2). CYP1A1 expression is a sensitive marker of coplanar PCB-mediated cellular activation and toxicity. Thus, significant response from all treatments containing PCB 77 was expected (Figure 2.3a). Indeed, all treatments that contained pure or some PCB 77 (treatments 2, 3, 5, 7, 9 and 10) exhibited almost maximal CYP1A1 expression. There was no difference in CYP1A1 expression among the pure PCB 77 (treatment 2) and both 10 h (treatment 3) and 24 h (treatment 5) dechlorination mixtures. Interestingly, when 10 h and 24 h dechlorination treatments lacked PCB 77 (treatments 4 and 6, respectively), induction of CYP1A1 was reduced linearly. Both MCP-1 and VCAM1 mRNA expression patterns (Figures 2.3b and 2.3c, respectively) followed approximately the CYP1A1 treatment patterns, suggesting some correlation between CYP1A1 induction and inflammatory markers in these dechlorination experiments. As with CYP1A1 expression, MCP-1 and VCAM1 expression exhibited a linear decrease to control levels when treated with mixtures representing 10, 24 and 48 h dechlorination products without PCB 77 (treatments 4, 6 and 8), indicating that any

byproduct contribution to the inflammatory response was eliminated by further dechlorination. Total dechlorination to biphenyl (48 h product) showed no statistical difference from control, indicating that it was relatively benign in our EC model. The presence of residual parent PCB dominated the inflammatory response in product mixtures, but mRNA expression levels of PCB 77 alone were moderately attenuated at the lower concentrations.

Degree of dechlorination affects CYP1A1, MCP-1 and VCAM1 protein expression

Endothelial cells were treated with the dechlorination mixtures mentioned above (Table 2.2) in order to determine the effects of PCB 77 dechlorination on endothelial cell inflammatory response expressed in protein markers (Figure 2.4). Treatments containing the parent compound showed strong correlations in both mRNA and protein. Similar to the mRNA expression levels, CYP1A1 protein levels were highest for treatments containing PCB 77 (Figure 2.4a). However, treatments that did not contain PCB 77 showed a marked decrease in CYP1A1 and MCP-1 protein expression, correlated to the degree of dechlorination. Significant increases in MCP-1 expression were observed with the 0 h product (PCB 77, treatment 2) and, to a lesser degree, with dechlorination products containing decreasing concentrations of PCB 77 (treatments 3, 5, and 8). VCAM1 protein expression of dechlorination product mixtures without PCB 77 (treatments 4 and 6) and biphenyl (treatment 8) were not significantly different from control. The presence of PCB 77 in all treatment groups corresponded to significant increases in VCAM1 protein expression above control levels. These data suggest a complicated interplay between inflammatory parameters in response to PCB 77 dechlorination product exposure. Nevertheless, the presence of PCB 77 in the individual treatments markedly induced vascular inflammation.

2.5 Discussion

PCBs are man-made chemicals that were used in hundreds of industrial and commercial applications [148] and are byproducts of certain industries today [133]. Even though their mass production has been banned, PCBs are chemically stable, persistent environmental toxicants that can cause harmful health effects. Remediation or detoxification of contaminated sites is difficult and expensive, and it is not clear to what extent these remediation processes have to occur before their disease potential is mitigated. The present study was designed to test the hypothesis that dechlorination of coplanar PCB 77 diminishes its pro-inflammatory potential in vascular endothelial cells.

This is an important issue because PCBs can damage vascular tissues and thus contribute to cardiovascular diseases such as atherosclerosis. In fact, a recent study reported increased hospitalization rates for acute myocardial infarction and diabetes mellitus in populations residing near areas contaminated with persistent organic pollutants [149, 150]. Furthermore, the administration of PCB 77 to male apolipoprotein E (ApoE) -/- mice has been shown to promote atherosclerosis [151].

The lining of blood vessels is protected by the endothelium, and endothelial cells play an active role in physiological processes such as regulation of vessel tone, blood coagulation, and vascular permeability. Dysfunction of endothelial cells is a critical underlying cause of the initiation of cardiovascular diseases such as atherosclerosis. Coplanar PCBs are initiators of endothelial dysfunction and exert their toxicity through binding to the AhR. AhR target genes, including CYP1A1, are considered a source of oxidative stress in endothelial cells and subsequent vascular dysfunction [152, 153]. We confirmed in the present study the oxidative stress potential of coplanar PCBs. In fact, CYP1A1 induction was maximal in cells exposed to pure PCB 77 and remained elevated in all dechlorination mixtures that contained PCB 77, independent of its relative concentration. When residual amounts of PCB 77 were excluded from the dechlorination mixtures, CYP1A1 induction was markedly reduced, suggesting that the presence of the parent coplanar PCB is necessary for maximal CYP1A1 expression. Furthermore, we have previously shown that coplanar PCBs 77, 126 and 169 increased expression of the CYP1A1 gene, oxidative stress (DCF fluorescence), and the DNA-binding activity of NF-κB [73]. In the current study, oxidative stress and DNA-binding of NF-κB decreased with increasing dechlorination. In fact, when PCB 77 was completely dechlorinated to biphenyl, oxidative stress and NF-κB levels approached control levels. This suggests that effective dechlorination should be as complete as possible to avoid oxidative stress-mediated tissue toxicity.

Oxidative stress-induced transcription factors such as NF-κB, which regulate inflammatory cytokine and adhesion molecule production, play critical roles in the induction of inflammatory responses and subsequent atherosclerotic lesion formation. We have demonstrated previously that coplanar PCBs can cause endothelial cell dysfunction as determined by inflammatory markers, such as expression of inflammatory cytokines and adhesion molecules, i.e. MCP-1 and VCAM1, respectively [91, 125, 154]. In our

analysis of the dechlorination product mixtures, we found that inflammatory patterns of MCP-1 and VCAM1 were similar to CYP1A1 patterns induced by pure PCB 77 and the dechlorination mixtures that contained residual PCB 77, suggesting that the parent compound is necessary for an endothelial inflammatory response. The 10 h dechlorination byproducts also induced an MCP-1 and VCAM1 response that was alleviated by further dechlorination. Again, as was found with CYP1A1, total dechlorination to biphenyl did not induce MCP-1 and VCAM1 inflammatory parameters in our endothelial cell model system.

The dechlorination process decreased the parent PCB 77 but contributed to various lower-chlorinated PCBs. Furthermore, the ratio and proportion of these lower-chlorinated PCBs changes with degree of dechlorination. Even though their level of interaction with the AhR is not well characterized, lower-chlorinated PCBs may contribute to cellular dysfunction. PCB cogeners with substitutions in both *para* positions (4,4') are reported to exhibit a level of AhR activity; this includes PCBs 15 and 37 in addition to the parent compound PCB 77[5]. For example, PCB 15, which was found in relatively high concentrations in the dechlorination mixtures, can contribute to liver carcinogenesis [155]. PCB 11, another common PCB in our dechlorination mixtures, recently has been discovered in relatively large amounts in commercial paint pigments [133]. Furthermore, other lower chlorinated PCBs generated during dechlorination have been shown to be metabolically activated by electrophilic quinoid species, which can bind to DNA, including PCBs 2, 3, 12 and 15[156-158]. Our data suggest that the temporary formation of lower chlorinated PCBs during dechlorination can contribute in part to induction of inflammatory parameters.

In addition, the lipophilic nature of PCBs enables them to perturb membrane structures. We have evidence that membrane domains like caveolae are critically involved in endothelial inflammation induced by exposure to PCBs. For example, PCB 77 can accumulate in caveolae-rich fractions of endothelial cells [124], and upregulation of endothelial MCP-1 by PCB 77 is caveolin-1-dependent [125]. Evidence from our laboratory implicates caveolae as a regulatory platform involved in endothelial activation and inflammation by environmental contaminants (Figure 2.5). As a regulatory platform, caveolae facilitate the interaction of PCBs with the AhR, which in turn promotes the upregulation of CYP1A1, a phase I detoxifying enzyme. CYP1A1 metabolism of coplanar

PCBs, like PCB 77, is inefficient, leading to protein uncoupling and release of superoxide, which promotes the formation of reactive oxygen species (ROS) in the cell [38]. The cell responds to this change in redox status by activating the transcription factor NFκB, which regulates enzymes and inflammatory parameters associated with endothelial dysfunction and cell injury such as MCP1 and VCAM1 [159]. Further studies are needed to understand whether caveolae have differential selectivity for various PCB species such as those present in dechlorination mixtures and to determine if the interaction of these congeners with caveolae has potential to induce endothelial cell dysfunction.

In summary, our study provides evidence that dechlorination of highly chlorinated PCBs is beneficial for protecting the vasculature from oxidative stress-induced inflammation and subsequent pathologies like atherosclerosis. Highly chlorinated PCBs are persistent and cytotoxic and a significant risk factor to endothelial injury and associated vasculature pathologies. The pro-inflammatory potential of the dechlorination mixtures that we observed appears to depend largely on the presence of the parent compound (e.g., PCB 77). Clearly, cytotoxicity decreased relative to degree of dechlorination, and the final dechlorination product, biphenyl, was nontoxic in our endothelial cell model system. More studies are needed to understand threshold concentrations of dechlorination mixtures that are required to prevent or mitigate compromised health associated with exposure to environmentally toxic chlorinated biphenyls.

2.6 Acknowledgements

This work was supported by National Institutes of Health/National Institute of Environmental Health Sciences grant P42ES007380, American Recovery and Reinvestment Act (ARRA) funds (3P42ES007380-13S1), and with funds from the University of Kentucky Agricultural Experiment Station. We would like to thank Christopher R. Barton[2] and Alex N. Palumbo[2] for their contributions to the preliminary work on this project. Thanks also to Dr. Seong-Su Han for his work with the NFκB binding assay. A special thanks to Michael Petriello for his editorial assistance.

[2] Undergraduate ARRA Summer Research student.

Table 2.1 Treatment mixtures representing PCB 77 dechlorination byproducts at various time points during dechlorination.

Mixture Components	DMSO (Vehicle)	0 hour (5 µM PCB 77) wt% (µM)	10 hour (5 µM Dechlor. product) wt% (µM)	24 hour (5 µM Dechlor. product) wt% (µM)	48 hour (5 µM Biphenyl) wt% (µM)
PCB 77		100% (5)	20% (0.7)	7% (0.2)	0%
PCB 37		0%	4% (0.2)	2% (0.1)	0%
PCB 35		0%	4% (0.2)	2% (0.1)	0%
PCB 15		0%	11% (0.5)	9% (0.4)	0%
PCB 13		0%	8% (0.3)	7% (0.3)	0%
PCB 12		0%	8% (0.3)	7% (0.3)	0%
PCB 11		0%	11% (0.5)	9% (0.4)	0%
PCB 03		0%	3% (0.1)	3% (0.1)	0%
PCB 02		0%	3% (0.1)	3% (0.1)	0%
Biphenyl		0%	30% (1.9)	50% (3.1)	100% (5)
Total		100% (5)	100% (5)	100% (5)	100% (5)

Table 2.2 Original and modified treatment conditions based on PCB 77 dechlorination byproducts.

Mixture Components	1 DMSO [a] (0.1 % v/v Vehicle)	2 0 h[a] [μM (ppm)]	3 10 h[a] [μM (ppm)]	4 10 h without PCB 77[b] [μM (ppm)]	5 24 h[a] [μM (ppm)]	6 24 h without PCB 77[b] [μM (ppm)]	7 24 h with addition of 10 h PCB 77[c] [μM (ppm)]	8 48 h[a] [μM (ppm)]	9 10 h Concentration of PCB 77 [d] [μM (ppm)]	10 24 h Concentration of PCB 77[d] [μM (ppm)]
PCB 77	—	5 (1.46)	0.7 (0.200)	—	0.2 (0.064)	—	0.7 (0.200)	—	0.7 (0.200)	0.2 (0.064)
PCB 37	—	—	0.2 (0.042)	0.2 (0.042)	0.1 (0.020)	0.1 (0.020)	0.1 (0.020)	—	—	—
PCB 35	—	—	0.2 (0.042)	0.2 (0.042)	0.1 (0.020)	0.1 (0.020)	0.1 (0.020)	—	—	—
PCB 15	—	—	0.5 (0.110)	0.5 (0.110)	0.4 (0.090)	0.4 (0.090)	0.4 (0.090)	—	—	—
PCB 13	—	—	0.3 (0.076)	0.3 (0.076)	0.3 (0.070)	0.3 (0.070)	0.3 (0.070)	—	—	—
PCB 12	—	—	0.3 (0.076)	0.3 (0.076)	0.3 (0.070)	0.3 (0.070)	0.3 (0.070)	—	—	—
PCB 11	—	—	0.5 (0.110)	0.5 (0.110)	0.4 (0.090)	0.4 (0.090)	0.4 (0.090)	—	—	—
PCB 03	—	—	0.1 (0.028)	0.1 (0.028)	0.1 (0.024)	0.1 (0.024)	0.1 (0.024)	—	—	—
PCB 02	—	—	0.1 (0.028)	0.1 (0.028)	0.1 (0.024)	0.1 (0.024)	0.1 (0.024)	—	—	—
Biphenyl	—	—	1.9 (0.300)	1.9 (0.300)	3.1 (0.480)	3.1 (0.480)	3.1 (0.480)	5 (0.771)	—	—
Total Concentration	—	5 (1.46)	5 (1.01)	4.3 (0.810)	5 (0.954)	4.8 (0.890)	5.5 (1.09)	5 (0.771)	0.7 (0.200)	0.2 (0.064)

Concentrations listed represent final PCB concentrations in cell culture media.

[a] Treatment compositions representing different products at various points in the dechlorination process (see also Table 1).

[b] Treatment compositions representing dechlorination products at 10 and 24 h of dechlorination without the parent compound, PCB 77.

[c] Treatment composition representing the dechlorination products of 24 h dechlorination with the increased concentration of PCB 77 present at 10 h of dechlorination.

[d] Treatment composition representing the concentrations of PCB 77 present at 10 and 24 h of dechlorination.

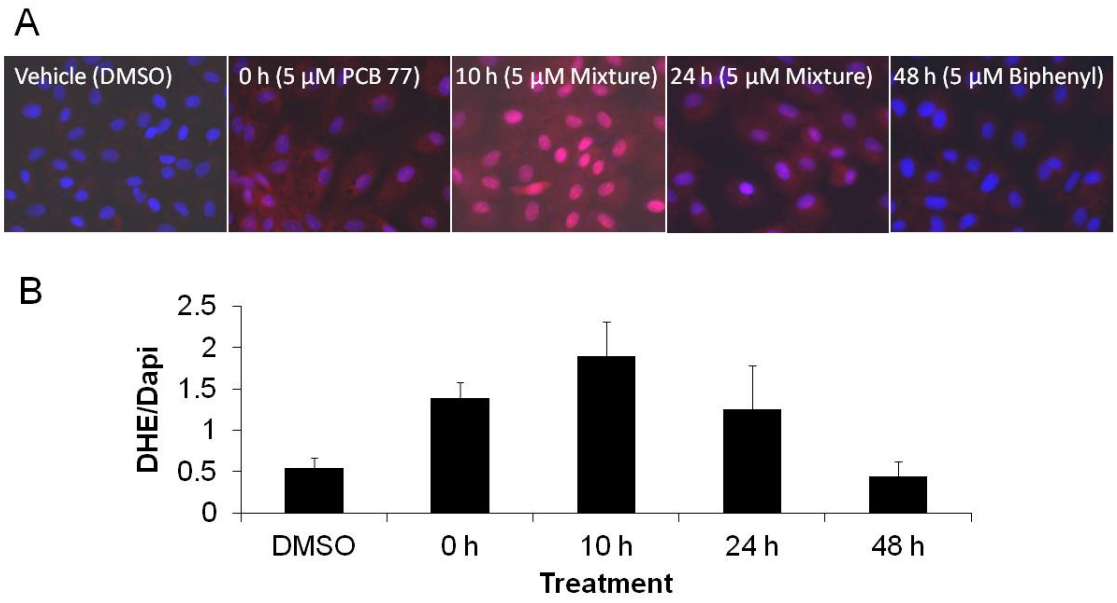

Figure 2.1 Dechlorination of PCB 77 alters cellular oxidative stress. Cells grown on chamber slides were treated with DMSO (vehicle control) or dechlorination products with a total concentration of 5 µM total concentrations and were incubated for 4 h. Cells were then treated with N,N'-(1,2-dihydroxyethylene) bisacrylamide, (DHE, in red) for superoxide detection. Slides were fixed with DAPI (in blue) for nuclear staining, (a) fluorescent images were recorded at 40X and (b) DHE fluorescence was quantified and normalized to DAPI.

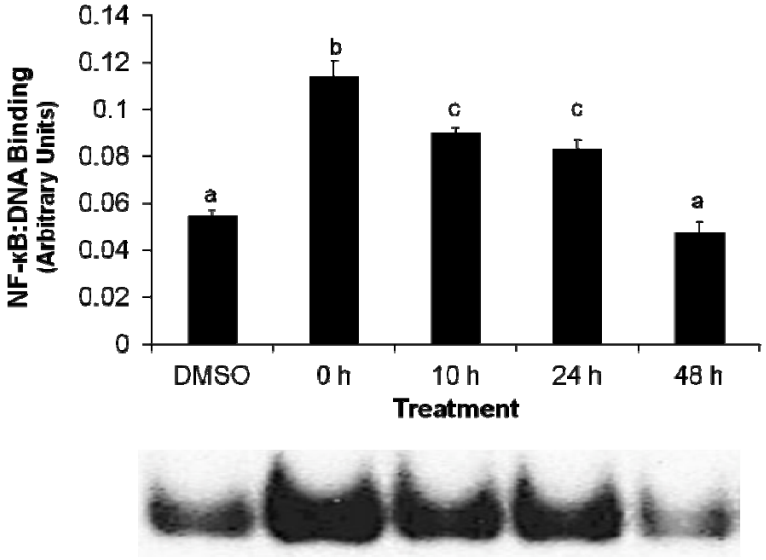

Figure 2.2 Dechlorination of PCB 77 attenuates NFκB activation. Cells were treated with vehicle control (DMSO), 0 h (PCB 77, 5 μM) 10 h, 24 h and 48 h dechlorination mixtures (5 μM), and incubated for 4 h. Both PCB 77 and dechlorination products (10 and 24 h product treatments) significantly increased DNA binding of NFκB over DMSO and biphenyl (48 h treatment). Results are given as mean ± SEM. Different statistical marker letters represent significant differences among treatment groups (determined by $p_{value} \leq 0.05$).

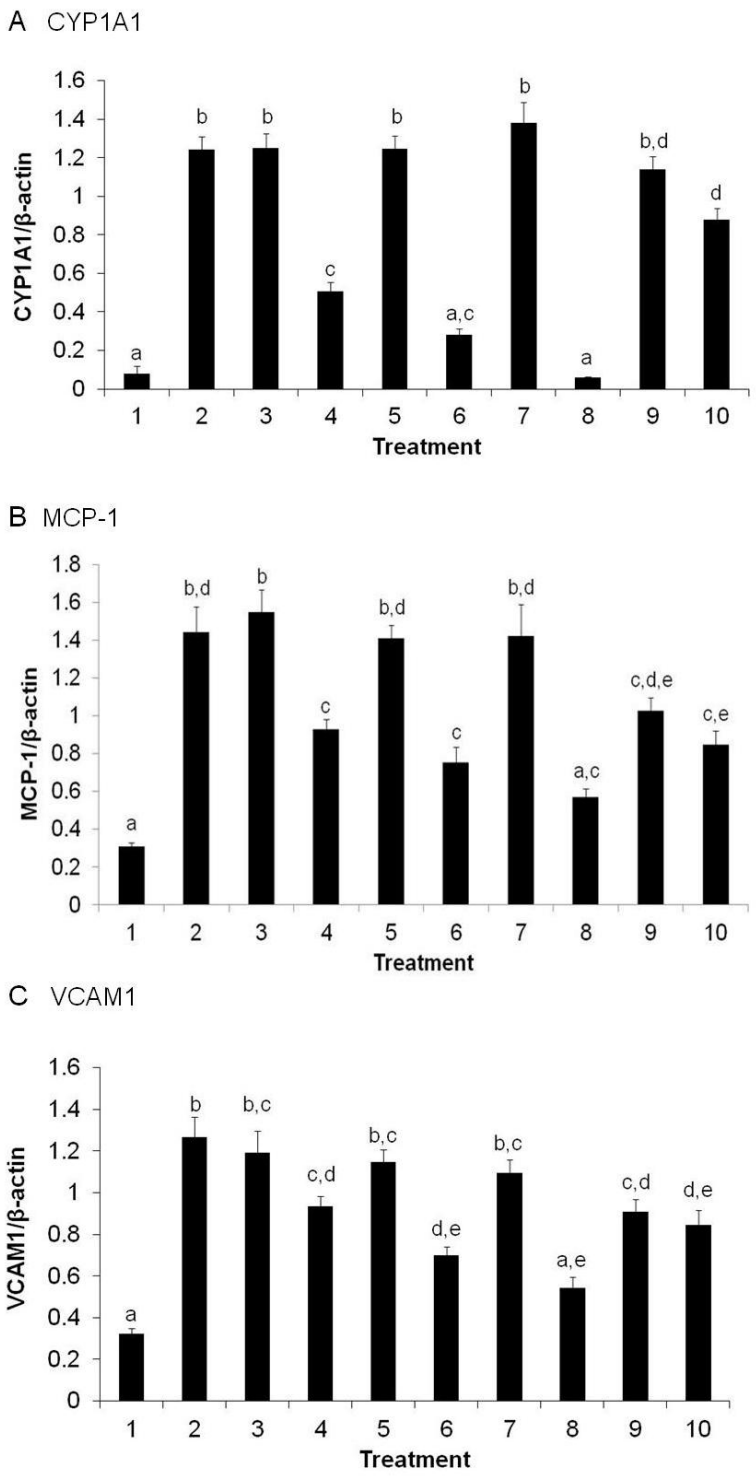
A CYP1A1
CYP1A1/β-actin
1.6
1.4
1.2
1
0.8
0.6
0.4
0.2
0
a
b
b
c
b
a,c
b
a
b,d
d
1 2 3 4 5 6 7 8 9 10
Treatment
B MCP-1
MCP-1/β-actin
1.8
1.6
1.4
1.2
1
0.8
0.6
0.4
0.2
0
a
b,d
b
c
b,d
c
b,d
a,c
c,d,e
c,e
1 2 3 4 5 6 7 8 9 10
Treatment
C VCAM1
VCAM1/β-actin
1.6
1.4
1.2
1
0.8
0.6
0.4
0.2
0
a
b
b,c
c,d
b,c
d,e
b,c
a,e
c,d
d,e
1 2 3 4 5 6 7 8 9 10
Treatment

Figure 2.3

Figure 2.3 Dechlorination products alter CYP1A1 (A), MCP-1 (B) and VCAM1 (C) mRNA expression. The presence of PCB 77 significantly upregulated mRNA inflammatory markers in ECs; inflammation decreased with further dechlorination of the parent compound. Please see Table 2.2 for detailed treatment descriptions. The vehicle, DMSO (treatment 1), was applied at 0.1% v/v for all treatments. Treatments representing the dechlorination products at 0 h (treatment 2), 10 h (treatment 3), 24 h (treatment 5), and 48 h (treatment 8) are the same as those tested previously for NFκB, superoxide production and viability. Treatments 4 and 6 excluded PCB 77 while maintaining the representative concentrations of the dechlorination products found at 10 h and 24 h, respectively. In contrast, treatments 9 and 10 contained only PCB 77 at the concentrations found in the 10 h and 24 h mixtures, respectively. Treatment 7 consisted of the 24 h dechlorination mixture with the level of PCB 77 found in the 10 h mixture. Different statistical marker letters represent significant differences among treatment groups (determined by $P_{value} \leq 0.05$ using one-way ANOVA with Tukey's post hoc). For example, in CYP1A1, treatment 2 (statistical marker "b") is significantly different from treatment 1 ("a") and treatment 4 ("c").

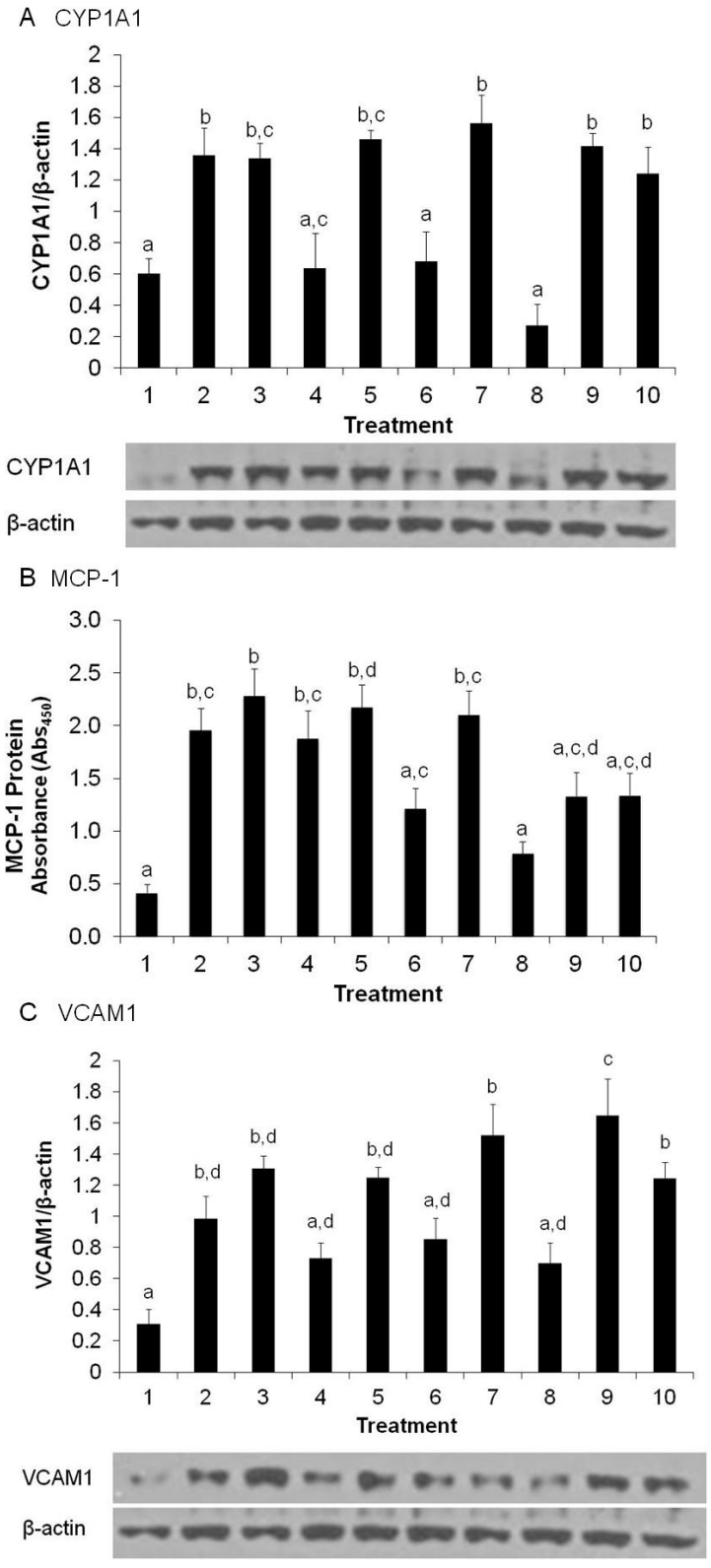
A CYP1A1
CYP1A1/β-actin
Treatment
CYP1A1
β-actin
B MCP-1
MCP-1 Protein Absorbance (Abs450)
Treatment
C VCAM1
VCAM1/β-actin
Treatment
VCAM1
β-actin

Figure 2.4

Figure 2.4 Dechlorination mixtures alter CYP1A1 (A), MCP-1 (B) and VCAM1 (C) protein expression. The presence of PCB 77 significantly upregulated protein inflammatory markers in ECs; inflammation decreased with further dechlorination of the parent compound. Treatments are the same as described in Figure 3 (please see Table 2.2 for detailed treatment descriptions). Statistical differences among treatment groups (determined by $p_{value} \leq 0.05$) are represented by marker letters, as stated previously.

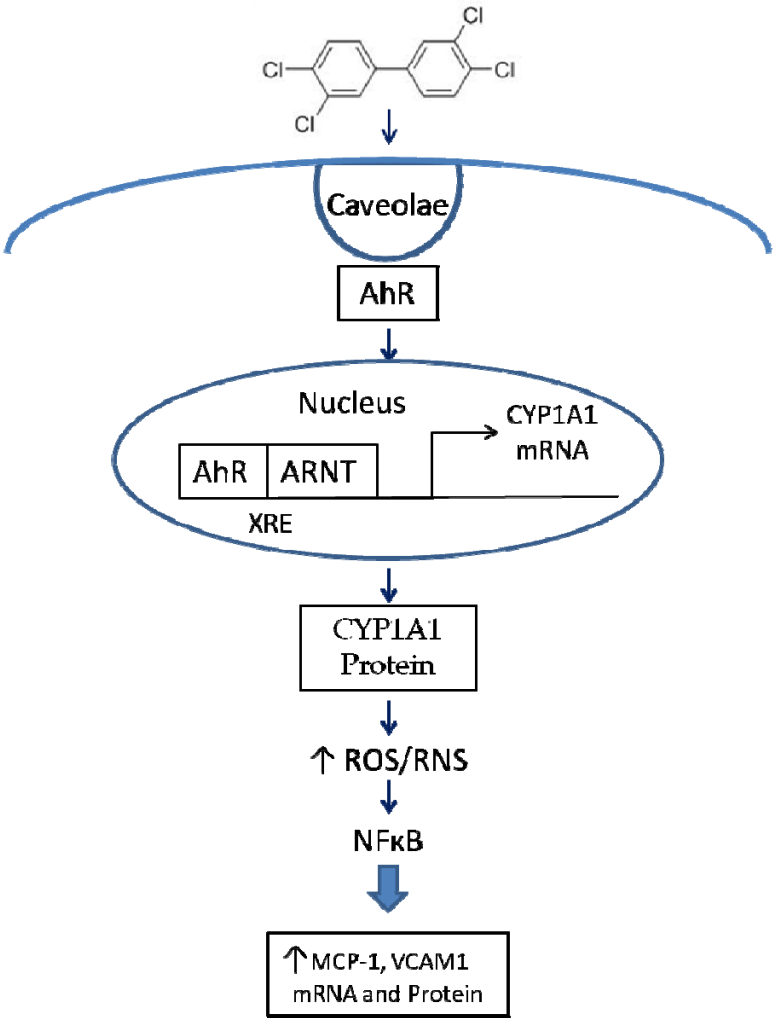

Figure 2.5 PCB 77 increases ROS production and downstream cellular dysfunction. PCB 77 interacts with caveolae in the plasma membrane, is endocytosed into the cell, and interacts with the AhR and its chaperone ARNT (aryl hydrocarbon receptor nuclear translocater), leading to nuclear translocation, XRE (xenobiotic response element) binding and CYP1A1 upregulation. CYP1A1 protein uncoupling occurs during PCB 77 metabolism and leads to an increase in cellular ROS. NFκB is activated in response to the change in cellular redox status and translocates to the nucleus where it acts as a transcription factor to upregulate adhesion molecules and cytokines.

Chapter Three: Assessment of toxicological and inflammatory endpoints following acute exposure to increasing concentrations of PCB 126

3.1 Synopsis

Polychlorinated biphenyls (PCBs) are persistent organic pollutants. The dioxin-like coplanar PCBs, such as PCB 77 and PCB 126, interact with the aryl hydrocarbon receptor (AhR), and previous work has demonstrated that coplanar PCBs initiate endothelial dysfunction which leads to inflammation, that can lead to diseases such as atherosclerosis. Many of these animal studies utilized PCB 77; however, use of PCB 126, a coplanar PCB with a higher affinity for the AhR, has not been well characterized. In order to determine the appropriate dose of PCB 126 in mice, a concentration range was selected including 0.0, 0.5, 5.0, 50, and 150 μmol/kg, also expressed as 0.0, 0.16, 1.63, 16.3, and 49.0 mg/kg (ppm). Each group of C57BL/6 mice was gavaged twice with the same concentration of PCB126 within a seven day period. After this acute exposure, the mice were sacrificed and assessed for toxicological and inflammatory endpoints of PCB 126 exposure. The goal of this study was to identify PCB 126 concentrations which do not lead to wasting syndrome. Mice receiving the highest doses (50 and 150 μmol/kg) of PCB 126 exhibited a significant decrease in body weight, indicative of broad toxicity. The lowest concentrations of 0.0 and 0.5 μmol/kg did not contribute to weight loss or changes in inflammatory markers. All mice which received PCB 126 had significant increases in cytochrome P4501A1 (CYP1A1) mRNA expression, while those mice which received 5.0 μmol/kg of PCB 126 had significant increases in liver to body weight ratio and the inflammatory marker monocyte chemoattractant protein-1 (MCP- 1). Exposure to 5.0 μmol/kg PCB 126 did not contribute to weight loss. These data indicate that a concentration of 5.0 μmol/kg PCB 126 may be used to study inflammation in C57BL/6 mice without causing overt toxicity.

3.2 Introduction

General Overview

Persistent organic pollutants (POPs) present a chronic disease risk and are linked to a range of vascular, neurological, and teratogenic outcomes[65, 160-163]. Our work with coplanar PCBs addresses both dioxin-like toxicity and the toxicity of PCBs as a class of compounds. We have demonstrated the role of PCB 77 in inducing vascular inflammation, modulating molecular aspects of vascular tone and responding to nutritional interventions[73, 92, 164, 165]. The literature suggests that PCB 77 is metabolized,

and methodology to detect the hydroxylated products confirms the generation of these metabolites which has led us and other researchers to question the persistent nature of PCB 77[166]. Clearly, PCB 77 has been an effective tool for the study dioxin-like inflammation and general knowledge of coplanar PCB activity, but PCB 126 presents a more useful model for the study of POPs because of its persistence and resistance to metabolism.

Chemical problem

Co-planar PCBs are model toxicants, but each PCB congener evokes a unique biological response. PCB 77, for example, contains an open meta and two open ortho positions on each phenol which facilitate metabolism by Phase I metabolizing enzymes, such as CYP1A1, which form epoxides and cause hydroxyl substitution. In contrast, PCB 126 contains only one open meta position making it less vulnerable to electrophilic substitution and, therefore, more resistant to metabolism and more environmentally persistent, a characteristic which better represents the nature of PCBs as a class of compounds. When compared to dioxin, PCB 77 has a TEF of 0.0005 in contrast to the more toxic PCB 126 with a TEF of 0.1[167]. Though both compounds are AhR ligands, the theoretical potential of PCB 126 to induce oxidative stress and cellular damage is much greater.

PCB 126 in health and disease

The National Toxicology Program (NTP) comparative study of PCB 126 and 2,3,7,8-Tetrachlorodibenzo-p-dioxin (TCDD) concluded that vascular disease was a critical risk factor following exposure to dioxin-like compounds[168]. The liver, as a highly vascularized organ that is critically involved in toxicant metabolism, is also affected by exposure to coplanar PCBs including PCB 126[169]. NHANES data suggests a statistical link between elevated amino L transferase (ALT) and aspartate aminotransferase (AST) levels and plasma levels of persistent organic pollutants, such as coplanar PCBs[62].

Hypothesis and Rationale

We hypothesize that acute exposure to high doses of PCB 126 will cause wasting syndrome and that low to median doses will induce inflammation and associated toxicological endpoints without wasting symptoms. To establish the use of PCB 126 as a model toxicant, we utilized a dose-response study that assessed basic toxicity and inflammatory endpoints including PCB tissue distribution, liver to body weight ratio

changes, and mRNA levels of inflammatory markers, such as CYP1A1 and MCP-1, in liver.

3.3 Methods

Reagents and Materials

PCB 126 was obtained from AccuStandard (New Haven, CT). The Jackson Laboratory provided the C57BL/6 mice (Bar Harbor, MN). Tocopherol-stripped safflower oil (vehicle) was obtained from Dyets (Bethlehem, PA). Reverse transcriptase reagents were purchased from Fisher Scientific (Waltham, MA). Western blotting reagents were obtained from BioExpress (Kaysville, UT). Reagents used for mRNA isolation and qPCR were purchased from Life Technologies (Grand Island, NY).

Animal Care

Male C57BL/6 mice were housed and handled according to a protocol approved by the University of Kentucky IACUC. After acclimation, animals were treated with an initial dose of 0.0, 0.5, 5.0, 50, or 150 µmol/kg PCB 126 in safflower oil (vehicle, Table 3.1) on Day 1 and received a second gavage of the same dose on Day 7. Animals were sacrificed 24 hours after the final dose and tissues were collected for analysis. For the dose response study, C57BL/6 mice were maintained on standard chow.

PCB 126 Tissue Analysis

Analysis of tissues for PCB 126 was kindly performed by the lab of Dr. Yinan Wei in the University of Kentucky Department of Chemistry[70]. Frozen tissue samples, including liver, adipose, lung, muscle, and kidney, and sera were weighed and processed with an internal standard (100 µL 0.35 ng/µL PCB 166 in isooctane). Samples were combined with diatomaceous earth and extracted with hexane. The dry hexane extract was combined with 10 µL of 0.1 ng/µL PCB 209, internal standard. Analysis was performed using GC/MS with the Agilent 6890N GC, G2913A auto sampler, and 5975 MS detector (Agilent Technologies, Santa Clara, CA) using an HP-5MS 5% phenyl methyl siloxane column (30 m length, 0.25 mm internal diameter, 0.25 µm film thickness). Retention times were used to identify standards and PCB 126. Internal standard values were used to calculate recovery efficiency, and tissue amounts were normalized to sample weight for µg of PCB 126/g of tissue.

Alanine Aminotransferase (ALT) ELISA

Serum was collected by cardiac puncture, incubated on ice to allow clotting and centrifuged for 15 min at 12,000 rpm and 4°C. Serum was collected and stored at -80°C.

Mouse alanine aminotransferase (ALT) ELISA kit (TSZ ELISA, Framingham, MA) was used to measure serum ALT levels. Serum was diluted 1:5 in assay Sample Solution, and the ELISA was performed according to manufacturer's instructions. Sample absorbances were measured at 450 nm using a SpectraMax M2 spectrophotometer (Molecular Devices, Sunnyvale, CA), and sample values were calculated from the standard curve using the SoftMax Pro 4.8 software (Molecular Devices, Sunnyvale, CA).

Western Blot

Protein was collected from liver tissue homogenates, was quantified using the Bradford method, and run on 10% SDS-PAGE gels. Bax was detected using primary antibody from Cell Signaling[170].

Real time – PCR

RNA was isolated from homogenized liver tissues using the TRIzol® method. Isolated mRNA was resuspended in RN/DNAse free water and quantified using UV-vis spectroscopy at 260 nM. cDNA was made using Promega AMV reverse transcriptase. CYP1A1, MCP-1, IL-6, VCAM1, HO-1, NQO1 and β-actin were analyzed with using SYBR® Green reagent and assessed using the qPCR on the 7300 Real Time PCR Systems (Life Technologies, Grand Island, NY) [125, 126].

Statistical Analysis

Comparisons between treatments were made by one-way analysis of variance followed by Tukey's post-hoc test. Statistical probability of $P<0.05$ was considered significant. Statistical tests were performed using SigmaPlot©12.0.

3.4 Results

Gross Physiological Changes

PCB 126 was distributed throughout the animal, but as was consistent with current literature, liver and adipose were the primary storage depots (Table 3.2). A very low level of PCB was detected in animals that did not receive PCB 126 treatment, which is consistent with the ubiquitous nature of PCB environmental contamination. As expected, this baseline level of PCB 126 was found predominantly in adipose.

Significant changes in body weight following toxicant exposure are associated with toxic wasting syndrome. The total body weights of animals receiving 0.0, 0.5 or 5.0 μmol/kg PCB 126 were not changed due to treatment. The higher concentrations of PCB 126, 50 and 150 μmol/kg, caused significant decreases in total body weight when compared to

vehicle treated animals (Table 3.3, Figure 3.1). Interestingly, the liver to body weight ratio, another indicator of toxicant exposure, was only significantly changed in the 5.0 μmol/kg treatment when compared to both the 0.0 and 0.5 μmol/kg treatment groups (Figure 3.2). The liver to body weight ratios of the 50 and 150 μmol/kg PCB 126 treated mice were not different from vehicle and low dose treated animals. This unexpected result led us to investigate Bcl-2-associated X protein (Bax) a key marker of apoptosis and liver damage[171]. Bax protein expression was low in the 0.0, 0.5, and 5.0 μmol/kg PCB 126 treated animals; in contrast significant increases were observed in 50 and 150 μmol/kg treated animals, an indicator of liver cell apoptosis (Figure 3.3). Interestingly, when the serum samples were assessed by alanine aminotransferase (ALT) ELISA, an indicator of liver damage, no significant increases were detected (Figure 3.4). Further analysis was performed on liver mRNA to assess the PCB 126-induced inflammatory response.

Markers of AhR activation and inflammatory response

CYP1A1 expression is a hallmark of AhR activation. As expected, all mice exposed to PCB 126 had increased CYP1A1 mRNA expression regardless of treatment concentration (Figure 3.5a). MCP-1, a down-stream target of CYP1A1 mediated oxidative stress and NFκB activation, was significantly increased only in the mRNA of 5 μmol/kg treated mice when compared to both the 0.0 and 0.5 μmol/kg groups (Figure 3.5b). IL-6 expression was similar to MCP-1 with a significant increase in the 5.0 μmol/kg group over all other treatment groups (Figure 3.5c). Interestingly, VCAM1 expression in the 50 and 150 μmol/kg groups was highly increased compared to 0.0 μmol/kg and the lower PCB 126 doses. This observation correlates with the indications of cell death. Using the macrophage marker F4/80, the presence of macrophages was assessed and correlated with the increase in VCAM1 expression reaching significance in the 150 μmol/kg treatment group (Figure 3.6). In response to the cellular stress associated with these inflammatory markers, the anti-oxidant response, as indicated by hemeoxygenase 1 (HO-1) and NADPH:quinone oxidoreductase 1 (NQO1) enzyme mRNA, was significantly increased with the highest doses of PCB 126 (Figure 3.7). NQO1 was increased in the 5 μmol/kg group relative to the 0.0 and 0.5 μmol/kg doses but was significantly lower than the highest doses. Together these data suggest that 5.0 μmol/kg was sufficient to produce moderate inflammation.

3.5 Discussion

Differences exist between model species and their response to PCBs and other environmental toxicants[172], and the literature does not provide sufficient mouse data to determine an inflammatory but not overtly toxic dose of PCB 126. For this reason, we performed this dose-response assessment in C57BL/6 mice. The National Toxicology Program (NTP) assessment of PCB 126 in rats corroborates our tissue distributions data[173]. They and other investigators found the liver and the adipose to be the primary depots for PCB 126 deposition. In our animals, the higher doses of PCB 126 resulted in an increase in the percentage of PCB distributed to the adipose (Table 3.2). During a study which included a 22-day observation period, liver levels of PCB 126 were reported to remain stable[174]. These findings indicate that the PCB tissue levels are in keeping with dose and duration of exposure. As is consistent with our results in mice, peripheral tissues, i.e. lung, and serum contained detectable but much lower levels of PCB 126[173]. When compared to TCDD, PCB 126 has greater tissue retention[175]. The PCB 126 tissue retention levels in our mice were dose dependent with 150 μmol/kg mice having estimated total body levels (μg) correlating to dose amount. The lower PCB 126 doses did not correlate as well implicating metabolism and excretion through feces[174, 176]. Concentrations of 50 μmol/kg PCB 126 and above induced wasting in C57BL/6 mice, which is associated with metabolic and hormonal changes that affect the metabolism of glucose and decrease appetite[177, 178]. A change in liver to body weight ratio was observed in mice receiving two doses of 5 μmol/kg PCB 126. The hepatic response to toxicants promotes an increase in liver fatty acid and protein content, which is supported by both the increase in liver weight and gene expression[179].

All treatment doses of PCB 126 upregulated Phase I enzyme CYP1A1. Previous work from our laboratory has established CYP1A1 as a key response enzyme to PCB 77-induced inflammation via critical interaction between AhR and Cav-1[124]. CYP1A1 is responsible for the oxidative stress induced by PCB 126 and other aromatic hydrocarbons which cause the release of hydroxyl radicals and uncoupling of the enzyme[38]. In response to the cellular stress, multiple indicators of inflammation were increased. The liver mRNA expression of the chemokine MCP-1 and the cytokine IL-6 were increased in the 5 μmol/kg PCB 126 exposure group. IL-6 is an acute phase cytokine that stimulates protein synthesis and promotes tissue healing and is expressed by hepatocytes, leukocytes, and endothelial cells[180, 181]. Mice deficient in IL-6 were unable to induce normal protein synthesis in response to turpentine tissue damage or

Gram-positive bacterial infection, though systemic response to LPS stimulation was near normal[182]. The role of IL-6 in protein synthesis and tissue healing supports the observation that 5 μmol/kg treated mice had higher liver to body weight ratios. Some literature indicates that AhR agonists moderate the IL-6 response[183, 184], which provides a limited explanation for the low induction of IL-6 in higher PCB 126 doses. In vascular disease, IL-6 is a marker of plaque instability[185] and has been noted as a common risk factor associated with low-grade inflammation and CVD risk[186]. Similarly, VCAM1 is a common marker for vascular disease that is critical to lesion formation and the recruitment of monocytes to regions of tissue damage and endothelial dysfunction[44, 45, 69]. Coplanar PCBs promote VCAM1 expression and endothelial dysfunction[126], as is supported by the increase in VCAM1 in the 50 and 150 μmol/kg PCB 126 treatment groups. PCB 126-induced VCAM1 expression in the 50 and 150 μmol/kg treatment groups indicates a dose and tissue-dependent effect that promotes macrophage accumulation with the highest exposure. Further the oxidative stress resulting from the 50 and 150 μmol/kg exposure levels were sufficient to induce HO-1 and NQO1 expression, which is associated with the cellular ant-oxidant response. Oxidative stress induces Nrf2 regulated anti-oxidant genes[187, 188]. This critical protective response is positively regulated by lifestyle factors such as diet through phytochemicals including flavonoids found in green tea, fruit and vegetables and through long-chain omega-3 polyunsaturated fatty acids including docosahexaenoic acid (DHA)[189, 190]. Our *in vitro* work with epigallocatechin 3-gallate (EGCG), a green tea catechin, and oxidized DHA neuroprostanes has implicated Nrf2 as a critical protective mechanism in response to coplanar PCB-induced oxidative stress[92, 129, 130]. The protective nature of these dietary factors warrants further exploration *in vivo*.

Previous work assessing different concentrations of PCB 126 have reported similar dose-dependent expression patterns of CYP and anti-oxidant response genes[175, 191]. PCB 126 exhibits a lower TEQ than TCDD, which induces more genes and exhibits greater toxicity[18]. However, low levels of exposure and the persistent nature of PCB 126 is sufficient to alter the inflammatory and metabolic homeostasis, which promotes the development of atherosclerosis and other diseases associated with inflammation[192]. Together these changes indicate that acute exposure to 5 μmol PCB 126/kg body weight is sufficient to produce a moderate inflammatory response without overt toxicity and could be utilized for experimental designs that include, for example, nutritional modulation of PCB 126-induced metabolic insults.

Table 3.1 Treatment doses shown in µmol/kg and mg/kg (ppm). Mice were treated via oral gavage. Each group of mice (n=6) received two doses of PCB 126 in tocopherol stripped safflower oil (vehicle, Dyets®) at the respective concentrations.

PCB 126 Treatments	
µmol/kg	mg/kg
0.00	0.00
0.50	0.16
5.00	1.63
50.0	16.3
150	49.0

Table 3.2 PCB 126 tissue concentration and distributions represented by dose. Each group of mice received two doses of PCB 126 at the respective concentrations. Total average tissue concentration is represented in µg of PCB 126 per g of tissue and is the summation of the tissue averages from each group as a representation of body burden. The distribution of PCB 126 within the representative tissues was calculated as a percentage of the total for the respective concentrations.

Group (µmol/kg)	Total Average Recovery (µg/g tissue)	Percentage of Total PCB 126 by Treatment and Tissue (average µg PCB 126/g tissue)					
		Serum	Liver	Adipose	Muscle	Kidney	Lung
0.00	1.03	0.00 (0.00)	27.0 (0.28)	69.4 (0.71)	0.00 (0.00)	3.65 (0.04)	0.00 (0.00)
0.50	31.4	0.00 (0.00)	37.9 (11.9)	4.28 (1.34)	56.7 (17.8)	0.82 (0.26)	0.27 (0.08)
5.00	143	0.07 (0.09)	55.7 (79.9)	15.0 (21.6)	25.6 (36.7)	2.84 (4.08)	0.80 (1.15)
50.0	937	0.18 (1.67)	29.0 (272)	54.5 (510)	7.24 (67.8)	7.09 (66.4)	2.00 (18.8)
150	2148	0.40 (8.67)	22.0 (473)	56.0 (1200)	11.9 (256)	5.57 (119)	4.07 (87.4)

Table 3.3 Body weight was decreased by treatment with high-doses of PCB 126. Average pre- and post-treatment whole body weights were calculated. The changes in body weight were calculated and were compared to vehicle treated animals (0.0 µmol/kg).

PCB126 Dose (µmol/kg)	PCB126 Dose in ppm (mg/kg)	Average Pre-treament Weight (g)	Average Post-treatment Weight (g)	Average Change in Weight (g)	Standard Deviation	SEM	P value
0.00	0.00	23.00	24.13	1.15	1.13	0.128	-
0.50	0.16	23.58	24.73	1.13	0.62	0.251	1.000
5.00	1.63	22.97	23.62	0.65	0.82	0.334	0.897
50.0	16.3	23.92	22.37	-1.55	1.71	0.700	<0.001
150	49.0	23.97	22.00	-1.97	0.55	0.226	<0.001

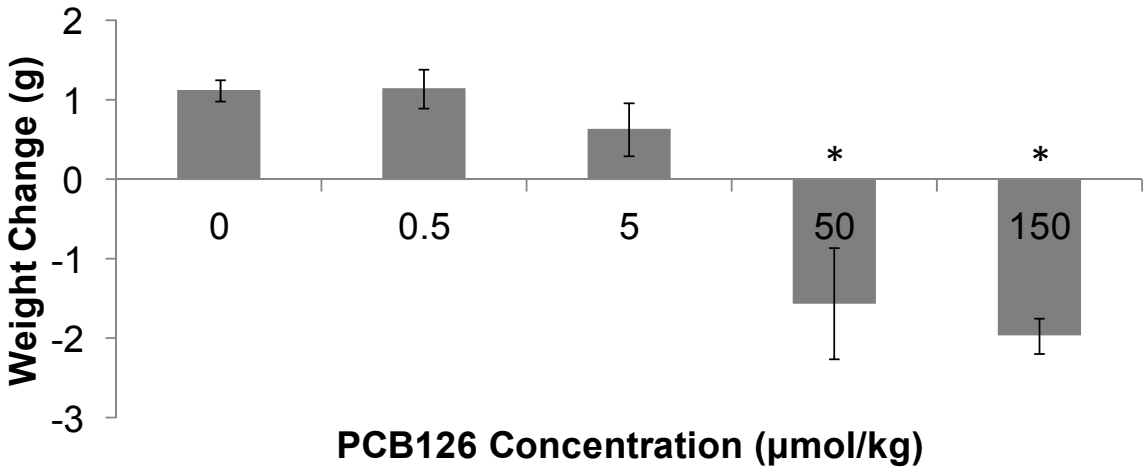

Figure 3.1 PCB 126 treatment causes a decrease in body weight at higher concentrations. Mice were orally gavaged twice with PCB 126. Weights were recorded before and after treatment with PCB 126. The average weight change is expressed as a positive or negative change from baseline weight. Results are the mean ± SEM, n=6. Significantly different compared with 0.0 µmol/kg at *P < 0.001. (See also Table 3.3)

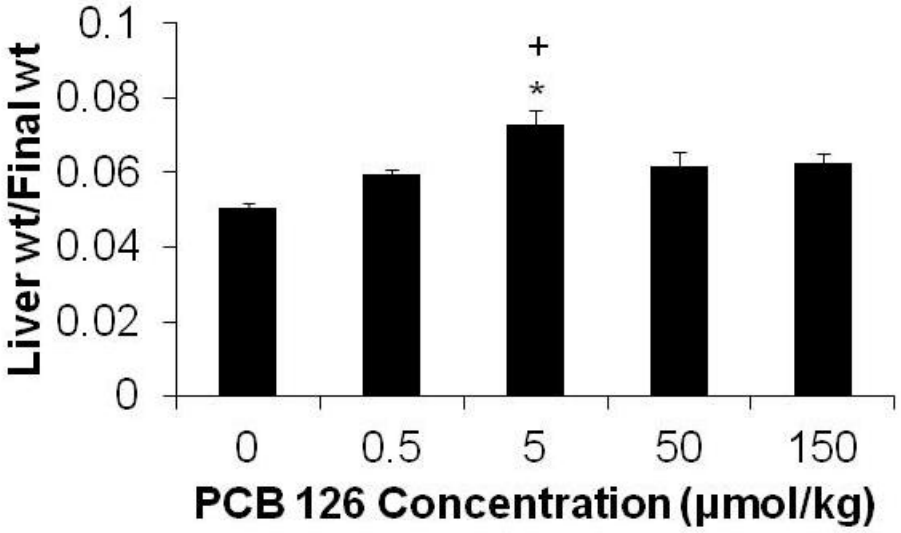

Figure 3.2 PCB 126 treatment at 5 µmol PCB 126/kg mouse causes a significant increase in liver wet weight compared to body weight. Liver weights were recorded after sacrifice and set over the final body weight to determine the ratio. Results are the mean ± SEM, n=6. Significantly different compared with 0.0 µmol/kg at * $P<0.001$ and compared with 0.5 µmol/kg at $^{+}$ $P < 0.05$.

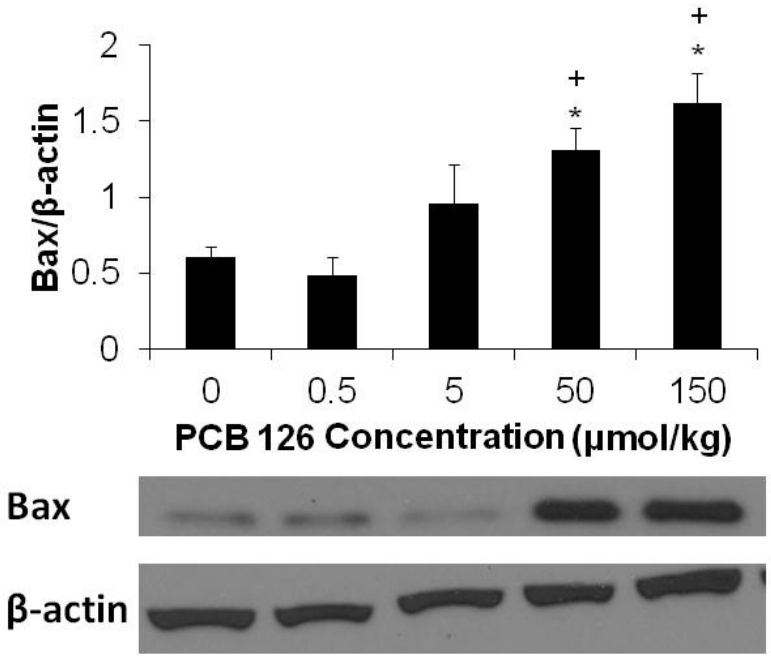

Figure 3.3 PCB 126 induced dose-dependent increases in Bax protein expression. Bax results are the mean ± SEM, n=6. Significantly different compared with 0.0 µmol/kg at *P<0.05 and 0.5 µmol/kg at $^{+}$ P<0.05.

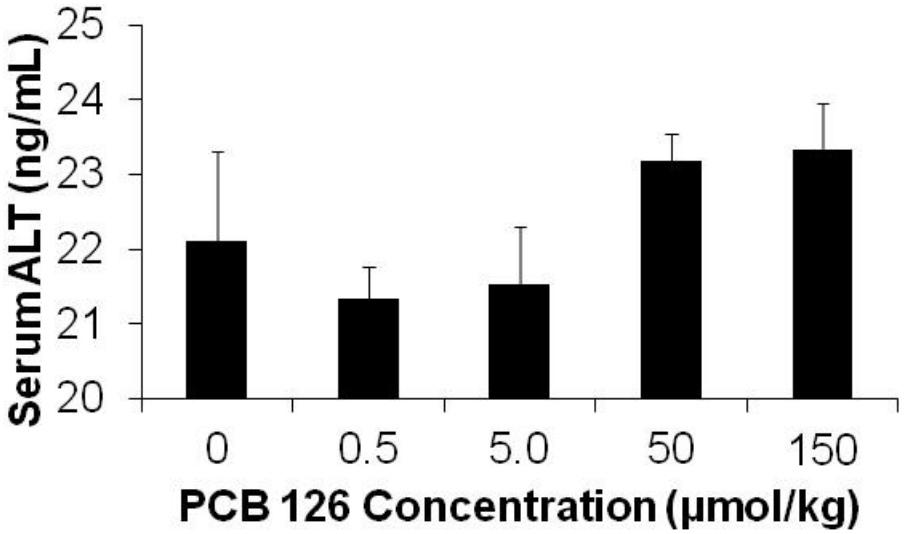

Figure 3.4 PCB 126 did not significantly increase the serum ALT levels. Alanine aminotransferase (ALT) results are the mean ± SEM $P<0.05$, n=6.

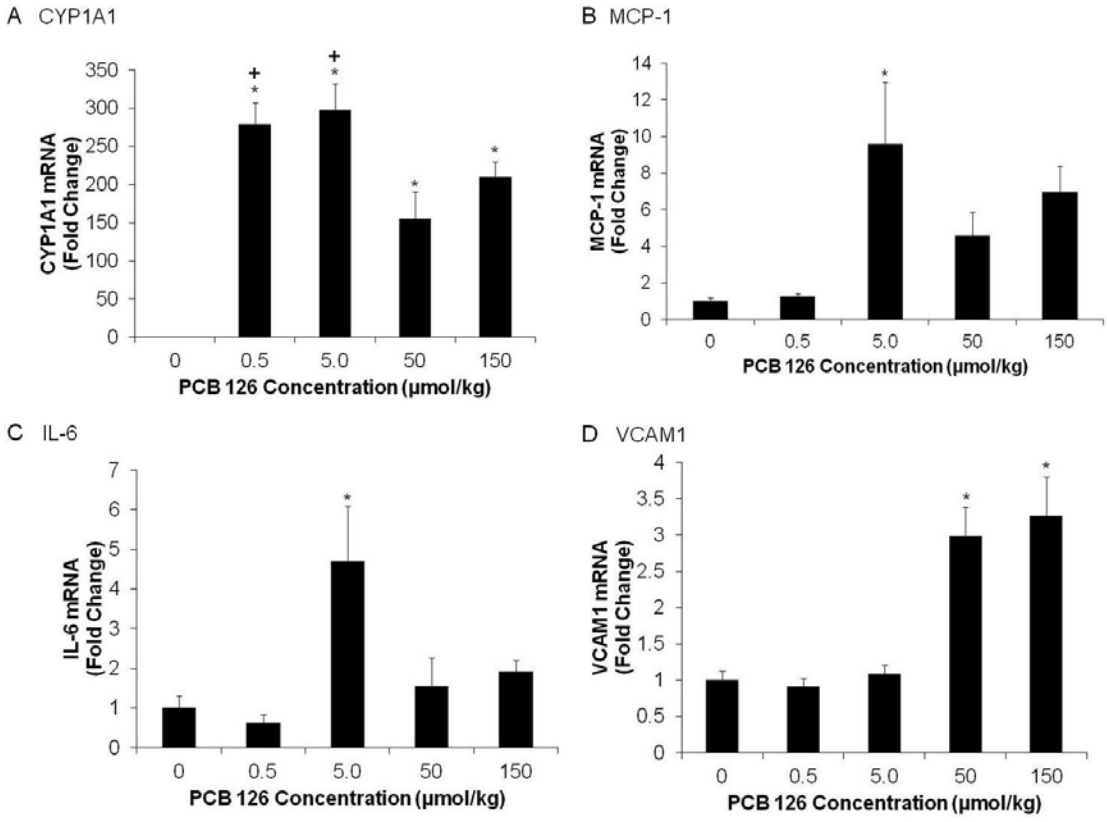

Figure 3.5 Expression of inflammatory markers increased following PCB 126 exposure. (A) CYP1A1 mRNA results are significantly different compared with 0.0 µmol/kg (Oil) at * P<0.005 and significantly different from 50 µmol/kg $^{+}$ P < 0.02. (B) For MCP-1, the 5.0 µmol/kg group was significantly different from 0.0 and 0.5 µmol/kg treatments at * P<0.02. (C) VCAM-1 expression was significantly increased in the 50 and 150 µmol/kg treatments P≤0.001. (D) 5.0 µmol/kg PCB 126 treatment caused a significant increase in IL-6 expression, * P<0.05.

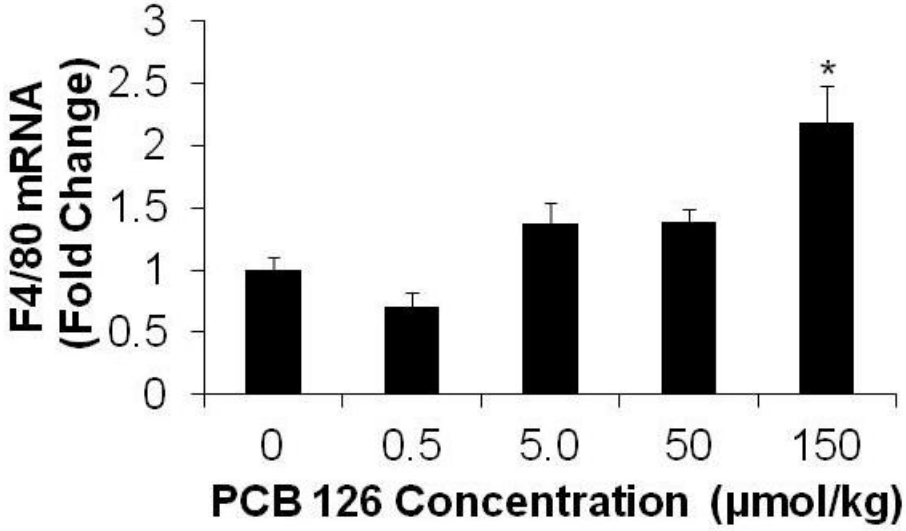

Figure 3.6 The highest dose, 150 µmol PCB 126/kg mouse, initiated infiltration of macrophages after acute exposure. F4/80 mRNA expression was significantly increased in the 150 µmol/kg treatment group, * P<0.03.

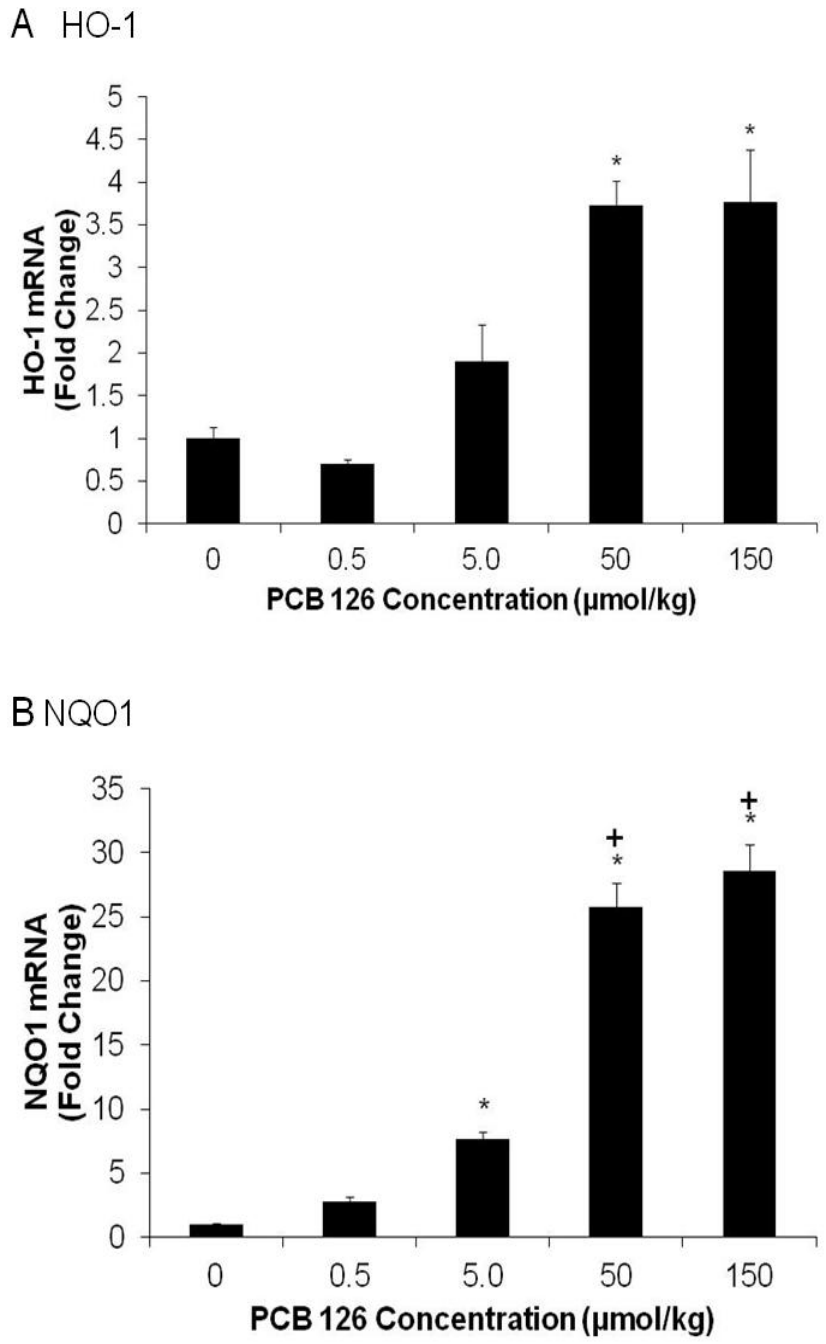

Figure 3.7 Anti-oxidant enzyme mRNA expression increased with higher concentrations of PCB 126. (A) HO-1 expression was significantly increased in the 50 and 150 µmol/kg treatments, * P≤0.007. (B) NQO1 mRNA increased significantly over vehicle (0.0 µmol/kg) and 0.5 µmol/kg at * P<0.05. The 5.0 µmol/kg expression level was significantly less than 50 and 150 µmol/kg levels, $^{+}$ P < 0.001.

Chapter Four: DHA feeding modulates the inflammatory profile of C57BL/6 mice exposed to coplanar PCB 126

4.1 Synopsis

Consumption of fish oil is associated with improved coronary health outcomes, but the mechanism of protection is not fully understood. Environmental stressors, such as polychlorinated biphenyls (PCBs), contribute to the development of cardiovascular diseases like atherosclerosis. We study the protective benefits of nutrients such as the polyunsaturated omega-3 fatty acids found in fish oil in reducing the inflammatory response to PCBs. Higher consumption of fatty fish or fish oil supplementation has been associated with improved cardiac outcomes in high-risk patients[193, 194]. To further our understanding of the mechanism by which the omega-3 fatty acid, docosahexaenoic acid (DHA), is protective, we fed C57BL/6 mice diets enriched in DHA (3% DHA/22% safflower oil in % kcal) or a safflower control diet for four weeks before administration of the coplanar PCB 126 via oral gavage at week five. DHA feeding moderately attenuated serum expression of pro-inflammatory cytokines following PCB 126 gavage. CYP1A1 mRNA expression was reduced in DHA-fed/PCB 126-treated mice. CYP1A1 activity promotes oxidative stress, yet 8-iso-prostaglandin 2 alpha (8-iso-$PGF_{2\alpha}$), a measure of tissue oxidative stress, was not changed by PCB 126. DHA monohydroxy lipoxygenase (LOX) metabolites were increased with DHA-enriched diet and compensatory decreases in omega-6 fatty acids and metabolites were observed. In DHA-fed mice, peroxisome proliferator-activated receptor gamma (PPARγ), a positive co-activator of Nrf2, had increased mRNA expression which indicate priming of the anti-oxidant response even in the absence of oxidative stress. Nuclear factor (erythroid-derived 2)-like 2 (Nrf2) mRNA was increased following DHA/PCB 126 treatment. Real time- PCR analysis revealed increased expression levels of Nrf2 activated anti-oxidant enzymes NAD(P)H dehydrogenase (quinone 1) (NQO1) and hemeoxygenase 1 (HO-1) in PCB treated mice on a DHA diet. Liver samples were analyzed by microarray to examine the interactive effects of PCBs and DHA and identify potential pathways for future investigation. Together these data suggest that DHA promotes an anti-oxidant response in mice exposed to environmental pollutants such as PCBs.

4.2 Introduction

Inflammation is a key characteristic of many disorders including atherosclerosis, Type 2 diabetes mellitus and obesity[58, 195, 196]. Patients who suffer from a chronic inflammatory

disease state, such rheumatoid arthritis and diabetes, have an accelerated risk for vascular disease development[56, 57, 197]. Inflammation is a response to a range of stimuli which includes the oxidative stress caused by environmental pollutants and is linked by the nuclear factor kappa B (NFκB) signaling pathway which drives the expression of an array of genes including cytokines and adhesion molecules[198]. Coplanar PCBs, such as PCB 77 and PCB 126, initiate an oxidative stress response in the vascular endothelium, which disrupts barrier function and promotes the expression of adhesion molecules like vascular cell adhesion molecule 1 (VCAM1) and chemokines such as monocyte chemoattractant protein 1 (MCP-1)[14, 125, 126]. The inflammatory response that is initiated by coplanar PCBs is sensitive to fatty acid exposure. For example, the omega-6 fatty acid linoleic acid promotes endothelial inflammation[199, 200], and increasing the ratio of omega-3 fatty acids attenuates this response[16]. Further, oxidized docosahexaenoic acid (DHA) neuroprostanes promote an anti-oxidant response to coplanar PCB-induced inflammation through activation of the nuclear factor (erythroid-derived 2)-like 2 (Nrf2) pathway[92]. Others have reported that the disruption of lipid rafts, called caveolae, by DHA prevents an oxidative stress response by displacing lipid raft-based signaling proteins[201]. Omega-3 fatty acids, especially those found in fish oil, are of interest in the treatment of inflammation based diseases, such as atherosclerosis.

Fish oil supplementation has been a subject of much study as epidemiological data reveal lower rates of heart disease in populations such as the Japanese who have diets high in omega-3 fatty acids[202]. Many clinical trials have tested fish oil supplementation in cardiac patients, and some have concluded that supplementation following a cardiac event reduces secondary events[94, 193]. A Finnish study compared the effects of fish consumption and exposure to pollutants on low-grade inflammation and indicators of vascular and metabolic health; insulin sensitivity was decreased in association with pollutant exposure while high omega-3 consumption was associated with lower serum interleukin-6 (IL-6), a marker of inflammation[203]. Though not conclusive, higher fish intake in the presence of higher pollutant exposure produced a null effect on plaque formation, indicating a compensatory effect[203]. The long-chain omega-3 fatty acids, such as EPA and DHA which are found in fish oil, are reported to be more efficacious than α-linolenic acid in the prevention of primary and secondary cardiac events[194].

The beneficial nature of long-chain, omega-3 fatty acids may be due in part to the generation of oxidized and enzymatically derived metabolites. Our observations of

oxidized-DHA A_4/J_4-neuroprostane support their role in the anti-oxidant response[92]. The research of the Morrow laboratory has demonstrated neuroprostane-derived protection from the LPS-induced NFκB signaling response and that oxidized long-chain omega-3 fatty acids disrupt the Kelch-like ECH-associated protein 1 (Keap1) inhibition of Nrf2[204, 205]. Further, their laboratory has detected the presence of oxidized long-chain fatty acids *in vivo* in brain, cerebrospinal fluid and small amounts in plasma[204, 206]. The enzymatically derived long-chain, omega-3 fatty acid metabolites include the resolvins and protectins, which promote macrophage clearance of the inflammatory polymorphonuclear neutrophils (PMNs), which is a critical step in the resolution of local inflammation[207, 208]. Protectins and resolvins are the products of lipoxygenase (LOX) and cycloxygenase (COX) metabolism of EPA and DHA, and the activity of these enzymes is part of the response to the inflammatory states associated with allergies, obesity, diabetes and cardiovascular disease[102]. In epithelial cells, resolvin E1 promotes the expression of CD55, which disrupts neutrophil interaction with intercellular adhesion molecule 1 (ICAM1) and reduces transepithelial migration[209]. Human aortic endothelial cells (HAECs) activated by TNF-α and exposed to protectin D1 expressed lower levels of the inflammatory cytokines MCP-1 and interleukin 8 (IL-8)[208]. Taken together, a diet enriched in long-chain, omega-3 fatty acids provides substrate for the generation of these metabolites which have great potential as protective mediators that intervene in the development of the inflammatory pathology associated with disease states such as atherosclerosis. In addition, the metabolic actions of long-chain omega-3 fatty acids, such as DHA, promote an anti-oxidant response that is critical in the presence of oxidative stress caused by coplanar PCBs and other inflammatory stimuli.

Hypothesis and Rationale

We hypothesize that long-chain omega-3 fatty acids can be protective by modulating the inflammatory profile in mice following exposure to coplanar PCB 126. The protective nature of omega-3 fatty acids common in fish oil was tested in mice supplemented with dietary DHA and exposed to PCB 126. To characterize the role of DHA in response to PCB 126-induced inflammation in C57BL/6 mice, we monitored changes in body composition and metabolic endpoints, measured fatty acid incorporation into animal tissues, and reviewed the shift in cytokine expression, DHA metabolite levels, and anti-oxidant enzyme expression following PCB 126 challenge. We anticipate that the inflammatory environment will be shifted toward a pro-resolving phenotype.

4.3 Methods

Reagents and Materials

PCB 126 was obtained from AccuStandard (New Haven, CT). The Jackson Laboratory provided the C57BL/6 mice (Bar Harbor, MN). Tocopherol-stripped safflower oil (vehicle) and specialized diet were obtained from Dyets (Bethlehem, PA). Reverse transcriptase reagents were purchased from Fisher Scientific (Waltham, MA). Western blotting reagents were obtained from BioExpress (Kaysville, UT). Reagents used for mRNA isolation and qPCR were purchased from Life Technologies (Grand Island, NY).

Animal Work

Male C57BL/6 mice were housed and handled according to a protocol approved by the University of Kentucky IACUC. A summary of the experimental design is provided in Table 4.1. After acclimation, baseline body compositions were assessed by ECHO MRI, and animals were trained in the Techniplast cages from which were taken baseline urine, feces, and food consumption data. Following the baseline measurements, animals were fed a semi-purified safflower oil control diet (25%kcal fat, Table 4.2) or a DHA-enriched diet for 4 weeks (3%kcalDHA/22%kcal safflower, Table 4.2)[99, 210-212]. Body composition was assessed by ECHO MRI at the end of the third week and after the first gavage. During the fourth week, animals were individually housed in the Techniplast cages and underwent a glucose tolerance test (GTT). During the final week, animals were gavaged on the first and seventh day with 5.0 µmol/kg of PCB 126. Following the initial gavage, the animals were assessed by Techniplast cage observation, GTT, and ECHO MRI. The final gavage was performed 24 h before the animals were sacrificed. Liver and adipose were collected and divided between storage in RNALater for mRNA extraction or flash frozen in liquid nitrogen. All tissues were stored at -80°C. Serum was collected by cardiac puncture, kept on ice, centrifuged to separate serum from red blood cells, aliquoted and stored at -80°C. Unless otherwise stated, all animals from a group were used in the analysis, n= 9 or 10.

The ECHO MRI for body composition analysis was available through the support of the Center of Obesity and Cardiovascular Disease (COCVD) Center for Biomedical Research Excellence (COBRE) grant from the National Institute of General Medical Sciences (8 P20 GM103527-05) of the National Institutes of Health. Techniplast solo mouse metabolic cages were used to collect urine and feces and monitor individual food consumption. Mice were placed in individual metabolic cages with free access to water

and food for 24 h. Animals and diet were weighed before and after placement into the cage, and the mice were returned to their normal social housing environment.

For the glucose tolerance test (GTT), animals were fasted for 6 h. Blood was collected from the tail vein by use of a 0.5 inch 27 gauge sterile needle and measured using a glucometer to record fasting blood glucose levels. Mice were intraperitoneally (i.p.) injected with 20% sterile glucose solution (2 g dextrose in 10 mL of 0.9% saline solution) at 2 mg glucose/g body weight. For example, a 20 g mouse would receive 200 µL of 20% glucose solution. Blood glucose levels were measured by glucometer at 15, 30, 60, and 120 minutes after glucose i.p. injection.

Real Time - PCR

Messenger RNA (mRNA) was isolated from homogenized liver tissues using the Trizol® method. Isolated mRNA was resuspended in RNA/DNAse free water and quantified using UV-vis spectroscopy at 260 nM. Complementary DNA (cDNA) was made using Promega AMV Reverse Transcriptase (Madison, WI) and followed a modified Promega protocol. For cDNA synthesis, 1 µg of mRNA per 10 µL reaction volume was used. Water volume was adjusted for volume of 1 µg mRNA to a total of 4.95 µl/10 µL reaction volume, and mRNA was heat denatured at 70°C for 10 min. Reverse transcription was run using the following thermocycler protocol: 25°C for 10 min, 42°C for 60 min, 95°C for 5 min and 4°C hold. RT-PCR was performed using SYBR® Green reagent and run on the 7300 Real Time PCR System (Life Technologies, Grand Island, NY)[126]. Primer sequences are found in Table 4.3.

Measurements in Serum

Alanine Aminotransferase (ALT) ELISA

Serum was collected by cardiac puncture, incubated on ice and centrifuged for 15 min at 12,000 rpm and 4°C. Serum was collected and stored at -80°C. Mouse alanine aminotransferase (ALT) ELISA kit (TSZ ELISA, Framingham, MA) was used to measure serum ALT levels. Serum was diluted 1:5 in assay Sample Solution, and the ELISA was performed according to manufacturer's instructions. Sample absorbances were measured at 450 nm using a SpectraMax M2 spectrophotometer (Molecular Devices, Sunnyvale, CA), and sample values were calculated from the standard curve using the SoftMax Pro 4.8 software (Molecular Devices, Sunnyvale, CA).

Total Serum Cholesterol and Fast Protein Liquid Chromatography (FPLC) Analysis

Total serum cholesterol was measured using the Wako Cholesterol E colorimetric assay (Wako Chemicals USA, Inc., #439-17501, Richmond, VA) and serum samples were diluted 1:25 in H_2O (n = 4 or 5). Fast Protein Liquid Chromatography (FPLC) was performed in collaboration with the laboratory of Dr. Allen Daugherty, University of Kentucky, using the Bio-Rad Biological DuoFlow System with BioFrac Fraction Collector and a Superose 6 10/300GL Column (GE Healthcare, #17-5172-01)[213]. Serum samples (n= 4 or 5) were eluted with a 1.0 mM EDTA/0.15 M NaCl/0.02% wt/vol Azide buffer solution and a total of thirty-two fractions were collected in Fraction Collection Tubes in a 96-well rack (BioRad, #233-9390). Fractions were stored at 4°C for less than a week and analyzed for cholesterol content using the Wako Cholesterol E colorimetric assay. Area under the curves (AUCs) and elution times were assessed using PeakFit software (Systat Software, Inc., San Jose, CA). The Center parameter was used as a proxy for elution time and lipoprotein fractions were classified using the following parameters: 0-15 were VLDL, 16-20 were LDL/IDL, and 21-28 were HDL. C57BL/6 mice are normolipidemic mice[214].

Serum Cytokine Measurements

Serum cytokines were analyzed using a mouse cytokine/chemokine 16X custom multiplex assay from Millipore (Milliplex MAP Kit, Billerica, MA) and run on a Bioplex 200 system from Biorad (Hercules, CA). Frozen serum aliquots were selected from each group (n=5) and diluted 1:1 in Assay Buffer. Standards and reagents were prepared

according to manufacturer's directions, and the assay was performed as stated in the manufacture's protocol.

Lipid, DHA Metabolite and Isoprostane Extraction

Lipids, DHA metabolites and isoprostanes were assessed in collaboration with the laboratory of Dr. Morris, University of Kentucky using a Shimadzu UFLC coupled with an ABI 4000-Qtrap hybrid linearion trap triple quadrupole MS.

Tissue Lipid Extraction

Frozen liver and adipose (20-30 mg, n= 9 or 10) was homogenized in 1 mL of methanol using 4 mm stainless steel ball bearings and a Geno/Grinder homogenizer (SPEX SamplePrep, Metuchen, NJ). Homogenized samples were transferred to 8 mL borosilicate glass tubes with Teflon cap, and 1 mL of MeOH was added to the homogenate. The following were added to each tube in sequence: 1 mL chloroform, 500 µL of 0.1 M HCL, 50 µL of 1 µM C_{17} internal standard. Samples were vortexed for 5 min and were stored at 4°C for a minimum of 1 hr. After incubation, 1 mL of chloroform and 1.3 mL of 0.1 M HCl was added to separate the phases. The samples were vortexed for 5 min and centrifuged for 10 min at 4000 rpm. The lower phase was transferred to 4 mL screw cap vials with a Pasteur pipette. Care was taken to avoid the upper phase and the protein interface. Using N_2 in a N_2-evaporation system, the lower phase was evaporated to dryness. Each sample was resuspended in 100 µL of methanol which was split for the respective experiments: 10 µL for phosphate assay and 90 µL for derivitization and further processing. Samples were evaporated to dryness and stored at -20°C. Samples were resuspended in 100 µL of methanol for liver and for adipose 100 µL methanol:chloroform 1:1, loaded to autosampler vials and run on the LC/MS according to protocols described previously[215]. Samples were normalized to C_{17} and phosphate.

DHA Metabolite and Isoprostane Extraction

For solid phase extraction, approximately 30 mg of liver or adipose tissue (n= 9 or 10) was ground in 1 mL of 0.5% acetic acid in ethyl acetate:methanol (5:1 v/v). Each sample received 100 µL 10 µM isoprostane standards and 50 µL 1 µM DHA/EPA standards, were vortexed to mix, and were centrifuged for 10 min at room temperature and 2500 *x g*. Supernatants were transferred to a glass tube and dried under nitrogen. Dried samples were reconstituted in 200 µL of methanol, vortexed, diluted in 3 mL of 0.5% acetic acid and vortexed. Solid phase extraction columns (Supelco Supel Select HLB

SPE, 60 mg/3 mL SPE tube, #54182-U, Sigma Aldrich, St. Louis, MO) were preconditioned with 3 mL of methanol and 3 mL of 0.5% acetic acid. The samples were applied to the columns and washed with 3 mL of 0.5% acetic acid and 3 mL of 0.5% acetic acid with 20% methanol. Columns were dried for 5 min and samples were eluted into glass vials with 3 mL of methanol. Samples were dried under nitrogen and stored at -20°C. Samples were resuspended in 100 µL of methanol, loaded to autosampler vials and run on the LC/MS according to protocols described previously[216-218]. Samples were normalized to internal standard and/or tissue weight.

Microarray

Microarray was performed in conjunction with University of Kentucky Microarray Core Facility using Affymetrix Genechip Mouse Exon 1.0 ST Arrays (Affymetrix Genechips, Santa Clara, CA). Liver mRNA was isolated from tissues frozen in RNALater via the TRIzol® method. RNA integrity number (RIN) values were measured in isolated mRNA samples. Samples from 3 mice were pooled and applied to one microarray chip with a total of 3 chips per treatment group representing nine total samples.

Statistical analyses

Comparisons of data were made by two-way analysis of variance (ANOVA) followed by Tukey's post-hoc testing using SigmaPlot 12.0 software (Systat Software, Inc., San Jose, CA). Due to the nature of our study, animals which did not receive DHA-enriched diet or did not receive PCB 126 treatment did not necessarily express detectible levels of DHA metabolites, inflammatory cytokines, etc. For this reason, certain data sets contained zero values that proved problematic for statistical assumptions associated with normality and variance made by parametric tests and variance for non-parametric tests. For example, the data associated with the DHA metabolite 14-HDHA failed both normality and variance tests because the safflower/vehicle group did not have detectable levels of this metabolite (Supplemental Figure 4.1a). In contrast, 4-HDHA was produced by all groups and failed to reject the statistical assumption tests (Supplemental Figure 4.1b). In observing the data for 14-HDHA, the levels of 14-DHDA are increased for DHA-fed mice, and sufficient differences beteen the groups are present for both parametric and non-parametric analyses detected overall differences between diets. For the parametric two-way ANOVA, the overall difference between diets had $p<0.001$ with statistically significant differences between diets in the vehicle treatments ($p<0.001$) and

PCB treatments (p= 0.029). Following consultation with the University of Kentucky Department of Statistics, it was determined that the parametric two-way ANOVA was the most appropriate method for determining the statistical differences for these data. Statistical probability of $p<0.05$ was considered significant.

Microarray data were analyzed in collaboration with the University of Kentucky, Department of Statistics**.** Affymetrix MAS 5 was used to normalization the chip expression levels and to determine probe set expression measurements. For quality control, distributions of gene expression for each chip and correlations between chips were confirmed. Each probe set was fit to a 2 × 2 ANOVA model, and changes in gene expression were determined using overall significance of the model with a significant difference of $p \leq 0.01$. Increases and decreases in expression between treatment group pairs were determined by t-tests. The resulting gene list was sorted for overall significance and upregulated or downregulated gene expression between the safflower/PCB 126 treated and the DHA/PCB 126 treated groups. Supplemental data was generated by sorting for significant difference ($p \leq 0.01$) in the safflower-fed groups.

4.4 Results

Food consumption and body composition

Following baseline measurements, animals were placed on safflower control diet and DHA-enriched diet. Assessment of food consumption during 24 h isolation in the Techniplast cages at weeks four and five did not reveal statistical differences between diet or treatment (Figure 4.1). Animals fed diet enriched in DHA had significant increases in DHA and eicosapentaenoic acid (EPA) free fatty acid levels in both adipose and liver (Figure 4.2) but not in the serum of our DHA-fed animals. Arachidonic acid (AA) free fatty acid levels were decreased in DHA-fed animals compared to safflower-fed animals. PCB treatment significantly decreased tissue free fatty acid content AA levels in adipose (Figure 4.2a) and EPA levels in liver (Figure 4.2b). In addition, body weights were not different between groups prior to PCB gavage (Figure 4.3). Following treatment with 5 μmol PCB 126/kg body weight, PCB 126 treated mice weighed significantly more than vehicle treated mice (Figure 4.3, Figure 4.4). The PCB 126 treated mice had diet independent increases in lean mass, but fat mass was not changed between groups (Figure 4.4). We attributed this increase in lean mass in part to the PCB 126-induced increase in liver weight to body weight ratio (Figure 4.5). The increase in liver size

demonstrated a clear response to the environmental toxicant; however, serum ALT levels were not increased by PCB 126 treatment (Figure 4.6). We concluded from this that there was no significant liver damage or cell death following this acute exposure to PCB 126.

Metabolic assessment

In order to gain a complete overview of the diet and toxicant interaction, we assessed basic metabolic parameters including glucose tolerance and serum cholesterol with lipoprotein profiles. Prior to treatment with PCB 126, glucose challenge did not result in significant changes in glucose clearance (Figure 4.7a&b). However, following a single gavage with 5 µmol/ kg of PCB 126, mice on a DHA-enriched diet had a significantly lower area under the curve (AUC) response to glucose challenge than both controls and safflower/PCB 126-treated mice (Figure4.7d). During the glucose tolerance test (GTT), DHA/PCB 126-treated animals had significantly lower glucose levels by 60 min, and at 120 min, mice receiving PCB 126 had significantly lower glucose levels than dietary controls (Figure 4.7c). Similarly, total serum cholesterol was decreased in PCB 126-treated mice (Figure 4.8). DHA-enriched diet produced an overall decrease in the serum cholesterol levels (Figure 4.8). The FPLC data revealed major changes in the high density lipoprotein (HDL) fraction with overall cholesterol decreases in response to dietary DHA and PCB 126 treatment (Figure 4.9). The safflower/PCB 126 treated animals had lower very low density lipoprotein (VLDL) cholesterol compared to safflower/control mice (Figure 4.9b). Similarly, all the VLDL, low density lipoprotein/intermediate density lipoprotein (LDL/IDL), and HDL fractions of the DHA/PCB 126 treated animals had lower levels of cholesterol compared to the DHA/control treated animals. Liver metabolic function was clearly affected by the presence of both dietary DHA and coplanar PCB 126. To assess the inflammatory and anti-oxidant response, we tested serum and liver for changes in markers of inflammation and oxidative stress.

Markers of inflammation and oxidative stress

Serum levels of sixteen cytokines were measured using the Milleplex MAP Kit for mouse cytokines and chemokines. Ten of the sixteen cytokines had detectable protein levels and were assessed for differences (Figure 4.10). Granulocyte colony-stimulating factor (G-CSF) and IL-6 were significantly increased only in the safflower/PCB 126 treated animals (Figure 4.10a&c). MCP-1 and MIG, mitokine induced by gamma-interferon or

CXCL9, were increased by PCB 126 in both diets (Figure 4.10f&h). Interleukin-12 (p70) (IL-12 p70) demonstrated an interactive effect between diet and treatment (Figure 4.10d). The safflower/PCB 126 treated group was significantly increased; in comparison, the DHA/PCB 126 treated group was significantly decreased. The other cytokines were not significantly affected by diet or PCB 126 treatment including interleukin-1 alpha (IL-1α), keratinocyte chemoattrant (KC), macrophage colony-stimulating factor (M-CSF), macrophage inflammatory protein 1 alpha (MIP-1α) and macrophage inflammatory protein 1 beta (MIP-1β) (Figure 4.12b,e,g,i,&j, respectively). The cytokine protein expression changes implicate a moderate inflammatory response to PCB 126 treatment with a slightly higher response in safflower fed animals. With an exception for IL-12 expression, dietary DHA did not alter the cytokine profile to the extent that we had hypothesized. The lack of significant data from the other cytokines may be attributed in part to the high variability between animals in each group. There was moderate attenuation of the PCB 126-induced serum cytokine levels in mice fed a DHA-enriched diet when compared to the overall response of safflower/PCB 126 treated mice.

The liver is the primary site for toxicant metabolism and excretion. We expected a strong inflammatory response given the metabolic changes that we observed in glucose tolerance and lipoprotein cholesterol levels. Cytochrome P450 1A1 (CYP1A1) is an important Phase I metabolizing enzyme that responds to aryl hydrocarbon receptor (AhR) induction by PCB 126 and other dioxin-like molecules[124]. CYP1A1 mRNA expression was significantly increased above dietary controls, but DHA-fed animals had lower CYP1A1 expression than their safflower-fed counterparts (Figure 4.11a). In contrast to the serum protein expression (Figure 4.10c), IL-6 had a significant mRNA increase only in the DHA/PCB 126-treated animals (Figure 4.11b). MCP-1 mRNA was increase following PCB treatment in both diets which is similar to the protein expression levels (Figures 4.11c and 4.10f, respectively); however, the fold change in the DHA/PCB 126-treated animals was greater that the safflower/PCB 126-treated animals. In contrast, VCAM1 expression was not affected by either diet or treatment with PCB 126 (Figure 4.11d). The overall expression patterns in Figure 4.11 resemble the moderate inflammatory profile of 5 μmol PCB 126/kg body weight that was observed in chapter three (Figure 3.5). Given the decrease in CYP1A1 mRNA expression in DHA-fed mice, we had expected to observe compensatory decreases in the inflammatory profile.

CYP1A1 is prone to enzyme uncoupling during the metabolism of coplanar PCBs; the consequence of the unsuccessful reaction is the release of superoxide which increases cellular oxidative stress[38, 39, 73]. 8-iso-prostaglandin 2 alpha (8-iso-$PGF_{2\alpha}$) is an arachidonic acid metabolite that serves as an *in vivo* marker of oxidative stress[219-221]. When measured in adipose and liver, PCB 126 did not induce significant increases in the relative levels of 8-iso-$PGF_{2\alpha}$, but in the DHA/PCB 126 treated animals, there was a significant decrease in adipose levels compared to DHA diet control (Figure 4.12). The only change in the 8-iso-$PGF_{2\alpha}$ levels implicated a baseline decrease in oxidative stress for animals exposed to both DHA and PCB 126.

DHA Metabolism Products

The literature indicates that metabolites of DHA, such as the protectins, promote the resolution of an inflammatory state[222]. Adipose and liver tissues were assessed for the presence of hydroxydocosahexaenoic acid (HDHA) lipoxygenanse (LOX) derived metabolites (see also Figure 1.2). Tissue levels of DHA and EPA were verified in these sample preparations with significant diet-dependent increases in both fatty acids (Figure 4.13a and 4.14a). The levels of DHA and EPA were significantly decreased in adipose following treatment with PCB 126 (Figure 4.13a); a similar trend was observed in the liver (Figure 4.14a). 5-LOX generates leukotriene E_4, an arachidonic acid metabolite and DHA-derived 4-HDHA and 7-HDHA[222-224]. The generation of these metabolites in both adipose and liver was not altered by either diet or PCB treatment (Figure 4.13b and 4.14b, respectively). Tissue levels of 12-LOX and 15-LOX HDHA metabolites were significantly increased in response to administration of dietary DHA but not PCB 126 (Figures 4.13c and 4.14c). In particular, 14-HDHA is the monohydroxy marker from the 12-LOX pathway that generates maresin 1[222]. Protectin D1 (PD1) biosynthesis is indicated by the presence of 17-hydroxyl-docosa-4Z,7Z,10Z,13Z,15E,19Z-hexaenoic acid (17-HDHA)[207], and 17S-HDHA is the product of DHA metabolism by 15-lipoxygenase (15-LOX)[102]. In comparison to the overall trend observed in the DHA-lipoxygenase metabolites, the 15-LOX products derived from the omega-6 fatty acid linoleic acid, 9-HODE and 13-HODE, were increased significantly only in the safflower/PCB 126 groups [225], and there was a significant difference in metabolite levels between diets (Figure 4.13d and 4.14d). The implication is that there is a compensatory shift from omega-6 to omega-3 fatty acid substrate following consumption of a DHA-enriched diet.

Anti-oxidant response

We would expect a minimal anti-oxidant response to PCB 126 given the unchanged oxidative stress levels of 8-iso-$PGF_{2\alpha}$ following treatment (Figure 4.12). Interestingly, the anti-oxidant profile would suggest that the underlying anti-oxidant phenotype is changed by dietary DHA. The anti-inflammatory arachidonic acid metabolite, 15-deoxy-$\Delta^{12,14}$-PGJ_2 with an m/z of 315.2 to 217.1, was significantly increased only in the DHA-fed control group (Figure 4.15a). 15-deoxy-$\Delta^{12,14}$-PGJ_2 is the dehydration product of cyclooxygenase derived PGD_2 and an activator of PPAR and Nrf2 [226, 227]. PPAR gamma isoform 2 (PPARγ2) also had increased expression in the DHA control group (Figure 4.15b), which was attributed to the heightened levels of 15-deoxy-$\Delta^{12,14}$-PGJ_2[228]. In contrast, exposure to PCB 126 significantly reduced the level of 15-deoxy-$\Delta^{12,14}$-PGJ_2 and PPARγ2 to levels equivalent to the safflower-fed groups (Figure 4.15a&b). Nrf2, the nuclear transcription factor that regulates anti-oxidant response, was increased in mRNA of animals exposed to PCB 126 (Figure 4.15c). Further, the Nrf2 regulatory element Keap1 had reduced expression in the DHA-fed/PCB 126 treated animals (Figure 4.15d). In response to the changes in Nrf2 and Keap1, the anti-oxidant genes HO-1 and NQO1 were both significantly increased following PCB 126 exposure, but the DHA/PCB 126 group had higher NQO1 expression than the safflower/PCB 126 group (Figure 4.15e&f). Together, these data indicate that the presence of dietary DHA sensitizes the anti-oxidant response by dampening Nrf2 regulation to promote a heightened anti-oxidant response to moderate inflammation induced by PCB 126.

Microarray overview

Of the 35,000 probes assessed by the Agilent mouse chip, 624 probes had a significant interaction between PCB 126 treatment and dietary feeding, $p_{value} \leq 0.01$. Of these genes, 495 have known functions and were sorted for increased or decreased expression between the safflower/PCB 126 treated and the DHA/PCB 126 treated groups. The resulting genes sets were applied to the DAVID© software system and were sorted for Kyoto Encyclopedia of Genes and Genomes (KEGG) pathway interactions[229]. The major metabolic pathways that were down-regulated in animals fed a DHA-enriched diet and exposed to PCB 126 when compared to the safflower/PCB 126 group include the glycine, serine, threonine metabolism pathway, the terpenoid backbone biosynthesis pathway, the proteasome pathway, and the porphyrin and chlorypyll metabolism pathway (Table 4.4). These are indicators that the cell modified the rate of enzyme

metabolism to modulate the xenobiotic response which includes Phase I and II enzymes and the anti-oxidant response enzymes. The gene expression of control animals, e.g. safflower fed animals with or without 5 μmol/kg PCB 126 treatment, were compared; genes associated with biosynthesis of fatty acids and steroid hormones, insulin signaling, PPAR (peroxisome proliferator-activated receptor) signaling, and drug metabolism were down-regulated (Supplemental Table 4.1) Major upregulated pathways in the DHA/PCB 126 group include several pathways related to the cytotoxic response including cytokine/chemokine receptor interactions, chemokine and calcium signaling pathways, and adhesion molecule expression (Table 4.5). Increased expression was detected for genes associated with hematopoietic cell lineages and melanoma. For the direct comparison of safflower oil-fed animals with or without PCB 126 treatment, expression of genes associated with xenobiotic metabolism, energy metabolism, and certain cancers were increased by PCB 126 treatment (Supplemental Table 4.2).

4.5 Discussion

Others have demonstrated the incorporation of omega-3 fatty acids into tissues after only three weeks of feeding and have observed relative decreases in arachidonic acid with increased dietary DHA or EPA, which are similar to our observations[230]. The DHA-enriched algal oil, derived from *Crypthecodinium cohnii* , a microalga, that was used in our diet carried the fatty acids primarily in triglyceride form[231]. The DHASCO product contains minor constituents (5%) which are not triglycerides; these include tocopherols and other phenolic compounds, which promote the stability of the DHASCO product in various light and oxidizing conditions[232]. In addition, fish bioaccummulate PCBs, which makes fish oil a potential source of pollutant exposure[233]. This is not a concern for the microalgal oil. In a 72 h study of omega-3 fatty acid incorporation in plasma phospholipids, natural oils had the highest incorporation level followed by re-esterified triglycerides < ethyl esters[234]. The highest omega-3 plasma levels were achieved at 24 hr post-supplementation and no differences were observed between EPA and DHA incorporation. In a study comparing healthy young and elderly subjects who consumed a meal containing ^{13}C-DHA, the total omega-3 lipid profile increased at 24 h, but the triglyceride and free fatty acid profiles for ^{13}C-DHA peaked at 4 h[235]. These data along with our observations indicate that long chain, omega-3 fatty acids have relatively short half-lives in plasma compared to tissues. The DHASCO product in our diet contained

negligible levels of EPA, <0.03% of the fat content, yet EPA tissue levels were increased following DHA feeding (Figure 4.2). Liver peroxisomes retroconvert DHA to EPA[236]. Retroconversion of DHA to EPA was observed at an average rate of 9.4% in human subjects receiving DHA supplementation for six weeks[237]. These findings were confirmed in a study of post-menopausal women, and interestingly, those who received hormone replacement therapy had lower rates of retroconversion, which was attributed to possible estrogen-mediated changes in both peroxisomal and mitochondrial β-oxidation[238]. As discussed in chapter three, coplanar PCB 126 toxicity mediates an increase in liver protein content[179], which is supported both by our observations of total and lean body mass increases resulting in significant increases in liver to body weight ratio (Figures 4.3-4.5). Further, as in chapter three, we did not detect toxicant-induced increases in serum ALT levels (Figure 4.6).

The metabolic changes observed in this study present some interesting points for discussion. Our glucose tolerance data is in keeping with other reports of heightened insulin sensitivity in obese mice fed omega-3 fatty acids[239] (Figure 4.7). Both PCBs and obesity promote a certain level of inflammatory stress[240]. DHA metabolites have been studied for their similar binding potentials to thiazolidinediones and may promote insulin sensitization through PPAR activation[103, 241]. Interestingly, changes to insulin sensitivity are only observed following the stress of PCB treatment indicating the formation of unidentified DHA oxidation products that activate PPAR[103, 242]. In addition, IL-6 is a critical mediator in adiponectin induced insulin sensitivity[243]. IL-6 mRNA levels were significantly increased in the DHA/PCB 126 treatment group in which heightened sensitivity was observed (Figure 4.11b). Cholesterol levels are affected by both the presence of PCB 126 and DHA diet. In contrast to our data, significant increases in total and HDL cholesterol have been reported in rats[65]. In a PCB 126 dosing study, also in rats, investigators observed both increases in cholesterol and decreases in serum glucose levels following exposure to 0.1 ppm PCB 126 for thirteen weeks[244]. These studies used different exposure routes and dosing models but assessed the outcome of chronic PCB 126 exposure as opposed to the acute nature of this study. We previously reported that a high fat, omega-6 fatty acid-enriched diet increased genes involved in triglyceride synthesis, fatty acid metabolism and cholesterol catabolism which was reversed following coplanar PCB 77 exposure in C57BL/6 mice[245]. The contribution of dietary DHA to the observed reduction in cholesterol is supported by studies that

suggest that dietary omega-3 fatty acids are suppressors of sterol-regulatory element-binding proteins (SREBPs) and 3-hydroxy-3-methylglutaryl-Coenzyme A reductase (HMGCR), which are both critical to cholesterol production[246, 247] (Figures 4.8 and 4.9).

Interestingly, the cytokine expression pattern reveals moderate attenuation by DHA diet (Figure 4.10). Of the ten cytokines, five were significantly increased in the safflower/PCB 126 group when compared to diet control. In contrast, only two, MCP-1 and MIG, were significantly increased in the DHA/PCB 126 group compared to DHA diet control. Our data demonstrates increased MCP-1 expression in both the cytokine assay and mRNA (Figure 4.10f and 4.11c). This observation contrasts with our *in vitro* findings in which PCB 77-induced MCP-1 expression is attenuated by oxidized DHA neuroprostanes[92]. Other groups have demonstrated similar findings with DHA or EPA[248] and oxidized EPA[249] in which NFκB activation of MCP-1 expression was mitigated in a PPARγ- or PPARα -dependent manner, respectively. The omega-3 oxidation products have been implicated in PPAR activation[63], and our findings indicate increases in enzymatically produced DHA metabolites in the plasma or liver which suggest an environment where oxidized metabolites may be formed. IL-12 (p70) was the only cytokine in which the DHA/PCB 126 group levels were significantly less than the safflower/PCB 126 group levels (Figure 4.10d). IL-12 stimulates interferon gamma (INF-γ) secretion by natural killer and T helper cells and facilitates the transition from the innate immune response to the adaptive immune response[250]. In dendritic cells, DHA inhibits NFκB-induced expression of IL-12 by activating PPARγ[100]. In protein, IL-6 was increased only in the safflower/PCB 126 treatment group (Figure 4.10c); in contrast, the DHA/PCB 126 group had increased in IL-6 mRNA expression (Figure 4.11b). Data from a study of allergic lung inflammation reported heterogeneity within the inflammatory endpoints as well. Following ovalbumin challenge, they observed that EPA and DHA-fed mice produced high IL-5 and IL-13 levels while suppressing F_2-isoprostanes[99].

The formation of LTE_4, 4-HDHA and 7-HDHA metabolites were not altered by either DHA-enriched diet or PCB 126, which implicates minimal activity of 5-LOX in both liver and adipose (Figures 4.13b and 4.14b). Phospholipids that contain DHA have been reported to inhibit 5-LOX activity[251]. As a result, we would have expected altered metabolite generation in DHA-fed animals. Others have found that the omega-3 to omega-6 ratio and the total amount of dietary fat alter the leukotriene levels[252]. High fat diet (20% fat) alone reduces leukotriene levels, and animals fed a high fat diet require a

high ratio of omega-3 to omega-6 fatty acids to observe a decrease in inflammation-induced LTE_4 levels[252]. We have reported that the ratio of omega-3 to omega-6 fatty acids influences the inflammatory response to coplanar PCB-induced inflammation[16]. Together these data suggest that at 25% kcal the fat content in our diet was sufficient to alter leukotriene and other eicosanoid levels and the 3% kcal DHA enrichment was not robust enough to mitigate the inflammatory response to PCB 126. We did not observe overall changes in eicosanoid metabolites as demonstrated by the 8-iso-$PGF_{2\alpha}$ data, a phenomena which is supported by the insight that a high fat diet suppress the eicosanoid levels and a low omega-3 to omega-6 ratio with high fat diet is inefficacious in altering the inflammatory response Figure 4.12). Despite the impact of this observation on our findings, 3% kcal from DHA altered tissue fatty acid content and was sufficient for DHA monohydroxy metabolite formation (Figures 4.2, 4.13 and 4.14).

The omega-6 metabolites 9-HODE, 13-HODE and 15-deoxy-$\Delta^{12,14}$-PGJ_2 are endogenous PPARγ ligands and as such contribute to PPAR-activated vascular remodeling, vasoprotection and anti-inflammatory potential[253] (figures 4.13d, 4.13d and 4.15a). 15-deoxy-$\Delta^{12,14}$-PGJ_2 promotes Nrf2 activation by binding to the intervening region of Keap1and facilitating the release of Nrf2[227]. Similarly, the oxidized DHA and EPA products have potential as nuclear receptor activators of both Nrf2 and PPAR[92, 249]. Resolvin E1 is also a potent PPARγ inducer[102, 239]. Our DHA control mRNA data supports increased expression of PPARγ2 (Figure 4.15b), and the changes in glucose clearance in the DHA/PCB 126 treated mice support PPARγ activity[102, 239, 246]. PPARγ has had a controversial role in the field of DHA metabolite activity. Some have demonstrated that the oxidized DHA neuroprostanes exhibited anti-oxidant properties independent of the PPARs[204]. In contrast, the structural compatibility and the PPARγ transactivation potency of DHA oxidation products have been reported[103]. Our research supports the role of PPARs in the attenuation of PCB-induced inflammation[254, 255]. DHA metabolite interaction with Nrf2 has not been well characterized. In the DHA/PCB 126 treated group, we observe a trend toward increased anti-oxidant response due to reduced Keap1 expression and heighted NQO1 expression, which cannot be correlated to an increase in the oxidative stress marker, 8-iso-$PGF_{2\alpha}$ (Figures 4.15 and 4.12, respectively). Others have demonstrated *in vitro* with 3T3-L1 cells that EPA and DHA are protective against hydrogen peroxide-derived oxidative stress through Nrf2-dependent anti-oxidant gene expression, an effect which is attenuated by Nrf2

silencing[104]. Of interest to us, the promoter regions of Nrf2 and PPARγ contain the alternate's binding elements[256]. By extension, the heightened levels of PPARγ2 prior to PCB exposure would prime the hepatocytes for increased Nrf2 expression after PCB challenge (Figure 4.15).

The microarray data support the idea that the enzymatic response is selectively regulated to sustain xenobiotic clearance and anti-oxidant enzyme activity when comparing safflower/PCB 126 and DHA/PCB 126 treatment groups. For example, porphyrins are intermediates in heme biosynthesis, and the genes included in this pathway, such as hydroxymethylbilane synthase (HMBS, also known as porphobilinogen deaminase) are essential to heme formation and the production of oxidative stress inducing cytochrome P450's[257]. The attenuated level of CYP1A1 is supported by the suppression of the porphyrin metabolism pathway (Figure 4.11a). Further, it is not surprising that proteasome pathway genes are decreased to regulate xenobiotic response. Oxidative stress conditions modify the efficacy of specific proteasomal activities which ensures the resolution of inflammation through inhibition of the NFκB response and the support of the anti-oxidant response through sustained Keap1 degradation (Figure 4.15c&d)[258]. The reduced expression of proteasome regulated genes supports the observed increase in liver protein content[259, 260]. In addition, the inhibition of proteasomes has been attributed to a decrease in cholesterol[261]. Similarly, products of the terpenoid backbone biosynthesis pathway feed into cholesterol biosynthesis, which is reduced in this model[262]. The suppression of these two pathways supports a mechanism that explains the reduction in total and specifically HDL cholesterol levels (Figures 4.8&4.9, respectively). The KEGG pathways associated with increased gene expression in the safflower/PCB 126 and DHA/PCB 126 treatment groups (Table 4.5) indicate subtle changes in the inflammatory response including higher expression of cytokine receptors and adhesion molecules including VCAM1 expression, which was unchanged in the mRNA. For comparison, we assessed changes in the safflower diet response following PCB 126 exposure.

Animals fed the safflower oil control diet and exposed to 5 µmol/kg PCB 126 exhibited dysregulation of a variety of metabolic processes (Supplemental Tables 4.1 and 4.2). For example, the microarray indicates suppression of acyl-CoA synthetase 1 (ACSL1) in control diet, PCB 126-treated animals (Supplemental Table 4.1). ACSL1 is associated with the PPAR signaling pathway and plays a role in both fatty acid efflux and insulin-

mediated glucose uptake[263], which supports the changes indicated by the microarray in the insulin signaling pathway and links the PPAR family with metabolic homeostasis[264]. Treatmen with PCB 126 decreases in the expression of certain CYP enzymes including constitutively expressed CYP3A25[265]. On the other hand, PCB 126 activation of the AhR induces the CYP1 family, including CYP1A1 and CYP1B1 (Supplemental Table 4.2). Upregulated genes from the safflower diet groups indicates expression changes in KEGG pathways associated with colorectal, pancreatic, and small cell lung cancer. Sustained activation of the AhR induces gene expression that potentiates the induction of cancer[266]. In a two-year chronic exposure study conducted by the National Toxicology Program (NTP), rats exposed to PCB 126 developed cancerous lesions[173]. Further, AhR activation promotes increased expression of Phase II metabolizing enzymes including glutathionine S- transferases and UDP- glucuronosyltransferases[35]. The gene expression changes in safflower-fed mice acutely exposed to PCB 126 are sufficient to disrupt a variety of cellular processes and initiate an inflammatory response.

Omega-3 fatty acids may modulate the cellular response through several mechanisms including changing the membrane signaling capacity by alterations in the membrane structure, antagonizing signaling through key receptors, or activating critical cellular response mechanisms[96]. The data presented here demonstrate a shift in the inflammatory response and implicate activation of key anti-oxidant pathways which may be linked to the generation of DHA metabolites (Figure 4.16). Long-chain, omega-3 fatty acids also selectively alter the composition of membrane lipid rafts, by which they may reduce the pro-inflammatory potential of toxicants, such as coplanar PCBs[267, 268]. In chapter five, we will explore this third aspect of the inflammatory pathway by studying the activation of lipid raft-based signaling molecules.

Table 4.1 Experimental design.

WEEK	1	2	3	4	5	6
Diet [a]		■	■	■	■	■
Oral Gavage [b]					■	■
Glucose Tolerence Test [c]				■	■	
Blood Collection [d]						■
Techniplast Cage Observation	■			■	■	
ECHO MRI	■		■			■
Takedown						■

[a] Animals maintained on control diet 25% kcal from fat (safflower oil) or DHA diet 3% DHA/22% Safflower oil diet (% kcal)

[b] Oral gavage of 5.0 µmol/kg PCB 126 or safflower oil, vehicle control

[c] Intraperitoneal injection of 2 mg/g 20% glucose solution

[d] Cardiac puncture at takedown

Table 4.2 Control and DHA-enriched diet compositions. Semi-purified diets were manufactured by Dyets (Bethlehem, PA). Dietary compositions represent the composition for one kilogram of diet. The DHASCO product was generously provided by Martek Biosciences Corporation (Columbia, MD). The diets were matched for kilocalorie composition.

Diet		Safflower		DHA	
Ingredient	kcal/g	g/kg	kcal/kg	g/kg	kcal/kg
Casein	3.58	200	716	200	716
L-Cystine	4	3	12	3	12
Sucrose	4	100	400	100	400
Cornstarch	3.6	355.58	1280.1	355.6	1280.1
Dyetrose	3.8	132	501.6	132	501.6
Safflower Oil	9	110.4	993.6	77.28	695.52
DHASCO (40% DHA)*	9	-	-	33.12	298.08
t-Butylhydroquinone	0	0.022	0	0.022	0
Cellulose	0	50	0	50	0
Mineral Mix #210025	0.88	35	30.8	35	30.8
Vitamin Mix # 310025	3.87	10	38.7	10	38.7
Choline Bitartrate	0	2.5	0	2.5	0
Cholesterol	0	1.5	0	1.5	0
		1000	3972.8	1000	3972.8

* Supplied by Martek Biosciences Corporation

Table 4.3 Relative Real Time-PCR sequences.

Gene name	Forward primer 5'-3'	Reverse primer 5'-3'
Endogenous Control		
β-actin	TGTCCACCTTCCAGCAGATGT	GCTCAGTAACAGTCCGCCTAGAA
Inflammatory response markers		
CYP1A1	TGGAGCTTCCCCGATCCT	CATACATGGAAGGCATGATCTAGGT
IL-6	AGAAGCAGTGGCTAAGGACCAA	ACGCACTAGGTTTGCCGAGTA
MCP-1	GCAGTTAACGCCCCACTCA	CCTACTCATTGGGATCATCTTGCT
VCAM1	TCCCAGGACTCAGAATGACTTCA	AAACCCAGAGCCAGGGAAA
Antioxidant response markers		
HO-1	CAGCCCCACCAAGTTCAAAC	GGCGGTCTTAGCCTCTTCTGT
Keap1	CCCATACCCCATCCCAGACT	GACTGGGATGCCTTGTAAAGGA
NQO1	GGCATCCAGTCCTCCATCAA	GTTAGTCCCTCGGCCATTGTT
Nrf2	GAGTCGCTTGCCCTGGATATC	TCATGGCTGCCTCCAGAGAA
PPARγ2	TTCGCTGATGCACTGCCTAT	TTCGCTGATGCACTGCCTAT

Table 4.4 Genes down-regulated by 5 µmol/kg PCB 126 treatment and DHA feeding affect multiple metabolic pathways. Of the approximately 35,000 gene transcripts, 624 were significantly affected by the interaction of PCB treatment and diet and were further sorted by a decrease of DHA/PCB 126 expression in comparison to safflower/PCB 126 expression. Analysis of 232 down-regulated gene transcripts was generated using the DAVID© software system, which assessed the genes for activity in shared metabolic pathways. ($p_{value} \leq 0.01$)

Category	Term	Count	%	PValue	Genes	List Total	Pop Hits	Pop Total	Fold Enrichment	Bonferroni	Benjamini	FDR
KEGG_PATHWAY	mmu00260:Glycine, serine and threonine metabolism	4	1.754	0.012	GCAT, SARDH, AGXT, GLDC	87	32	5738	8.244	0.702	0.702	12.373
KEGG_PATHWAY	mmu00900:Terpenoid backbone biosynthesis	3	1.316	0.018	LOC674674, LOC637711, GM5873, FDPS, GM3571, MVK, GM8163, LOC634846, PMVK	87	14	5738	14.133	0.843	0.604	18.298
KEGG_PATHWAY	mmu03050:Proteasome	4	1.754	0.033	PSMF1, PSMC3, PSMD3, PSMD4	87	47	5738	5.613	0.967	0.679	31.060
KEGG_PATHWAY	mmu00860:Porphyrin and chlorophyll metabolism	3	1.316	0.074	HMBS, UROD, MMAB	87	30	5738	6.595	1.000	0.858	57.384

Table 4.5 Genes up-regulated by 5 µmol/kg PCB 126 treatment and DHA feeding affect multiple metabolic pathways. Of the approximately 35,000 gene transcripts, 624 were significantly affected by the interaction of PCB treatment and diet and were further sorted by an increase of DHA/PCB 126 expression in comparison to safflower/PCB 126 expression. Analysis of 263 up-regulated gene transcripts was generated using the DAVID© software system, which assessed the genes for activity in shared metabolic pathways.

Category	Term	Count	%	PValue	Genes	List Total	Pop Hits	Pop Total	Fold Enrichment	Bonferroni	Benjamini	FDR
KEGG_PATHWAY	mmu04060:Cytokine-cytokine receptor interaction	9	3.846	0.013	LOC100048875, CXCR4, LOC100047704, TGFBR1, CCR2, CX3CR1, EDA2R, CXCR2, HGF, IL15, PDGFD	75	244	5738	2.822	0.699	0.699	13.085
KEGG_PATHWAY	mmu04514:Cell adhesion molecules (CAMs)	7	2.991	0.014	VCAM1, PTPRC, CADM1, CD80, SELL, NRXN1, JAM2	75	154	5738	3.478	0.734	0.484	14.329
KEGG_PATHWAY	mmu05218:Melanoma	4	1.709	0.063	PIK3CG, MITF, HGF, PDGFD	75	71	5738	4.310	0.998	0.870	51.099
KEGG_PATHWAY	mmu04062:Chemokine signaling pathway	6	2.564	0.085	PIK3CG, LOC100048875, CXCR4, LOC100047704, CCR2, CX3CR1, GNG2, CXCR2	75	182	5738	2.522	1.000	0.875	62.176
KEGG_PATHWAY	mmu04640:Hematopoietic cell lineage	4	1.709	0.094	CD3G, CD33, ITGA1, CD24A	75	84	5738	3.643	1.000	0.843	66.012
KEGG_PATHWAY	mmu04020:Calcium signaling pathway	6	2.564	0.099	ATP2B1, SLC8A1, SLC25A4, CYSLTR1, CYSLTR2, PTAFR	75	191	5738	2.403	1.000	0.805	68.218

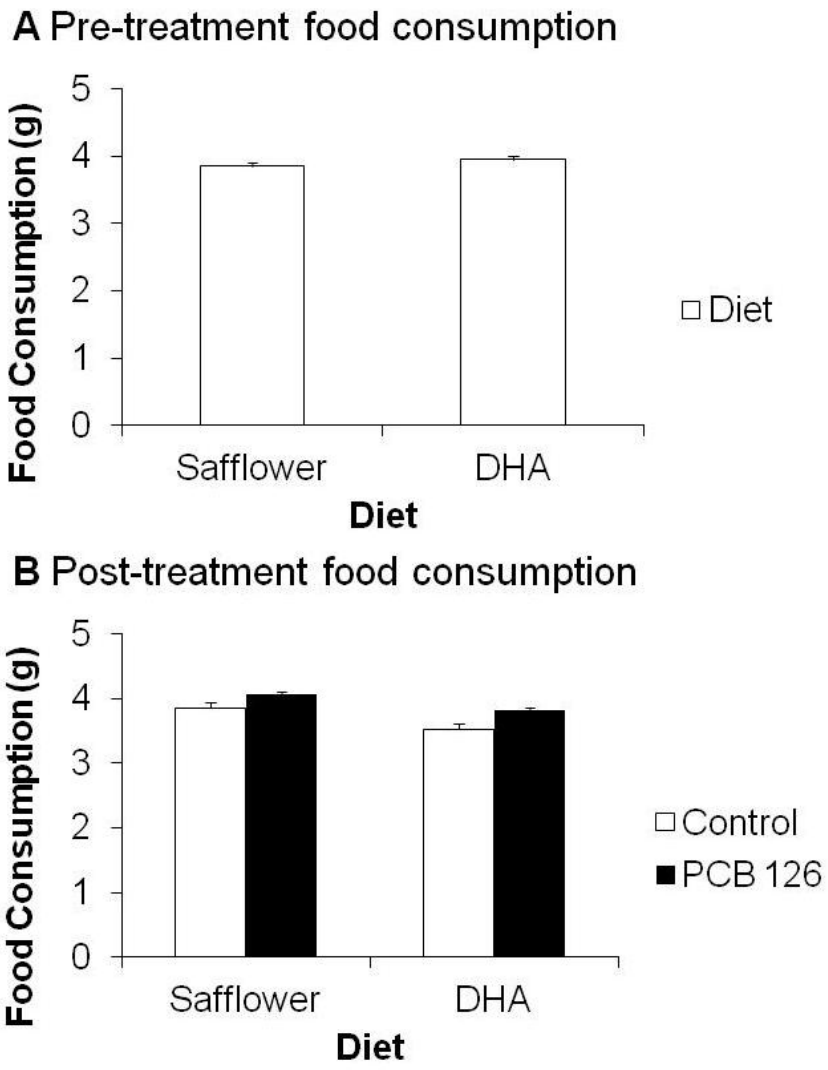

Figure 4.1 Neither diet nor PCB 126 treatment caused significant differences in food consumption. (A) Pre-treatment food consumption averages based on animals individually housed in urine/feces collection cages for 24 hr, and (B) food consumption following initial gavage with 5 μmol PCB 126/kg body weight from animals housed in urine/feces collection cages.

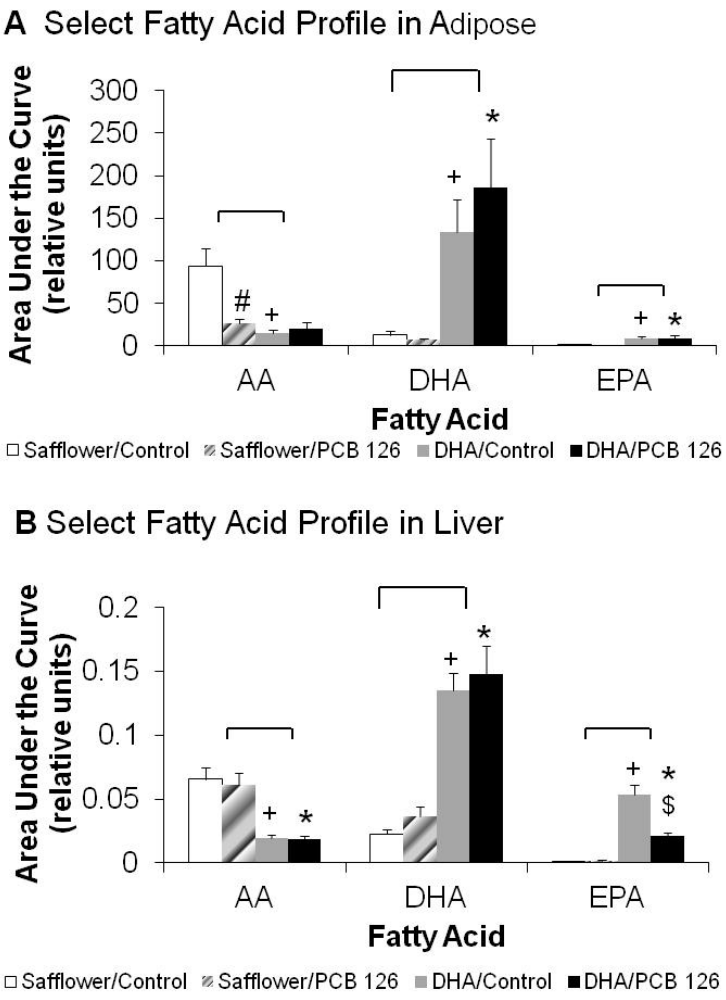

Figure 4.2 DHA-enriched dietary feeding promotes accumulation of DHA and EPA in both (A) adipose and (B) liver tissues. Both tissues have a significant overall increase in free fatty acids between diets for EPA and DHA and an overall significant decrease in arachidonic acid (AA). There is an overall effect of PCB 126 treatment on adipose AA fatty acid levels and liver EPA fatty acid levels. A difference was detected between safflower/PCB 126 and DHA/PCB 126 treatments * p_{value} <0.05, and a difference was detected between safflower/saline and DHA/saline treatments, $^{+}$ p_{value} < 0.05. Significant differences between DHA/saline and DHA/PCB 126 are represented by $^{\$}$ p_{value}<0.05. Significant differences between safflower/saline and safflower/PCB 126 are represented by $^{\#}$ p_{value}<0.05. Overall difference between dietary feeding is represented by a bar.

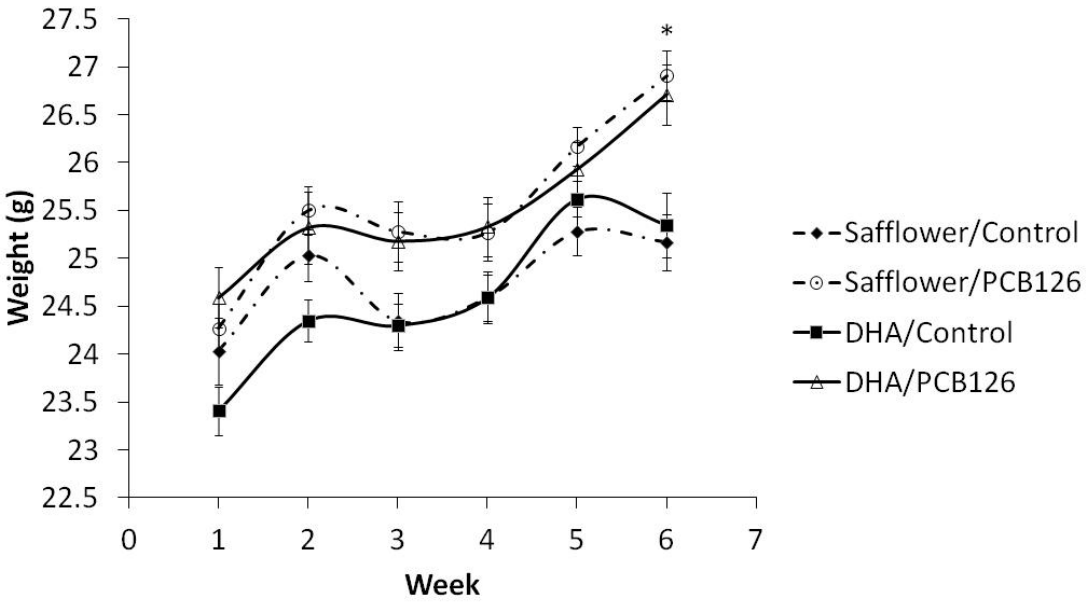

Figure 4.3 Body weights were affected by treatment but not by diet. Control safflower oil diet is represented by black circles and a dashed line, and control safflower oil diet with PCB 126 treatment is represented by open circles with a dashed line. DHA diet only is represented by black squares and a solid line, and DHA-fed, PCB 126 treated animals are represented by open triangles and a solid line. Significant differences in body weight were observed following treatment with PCB 126 regardless of diet, *p_{value} <0.05 significantly different from treatment controls of both diets.

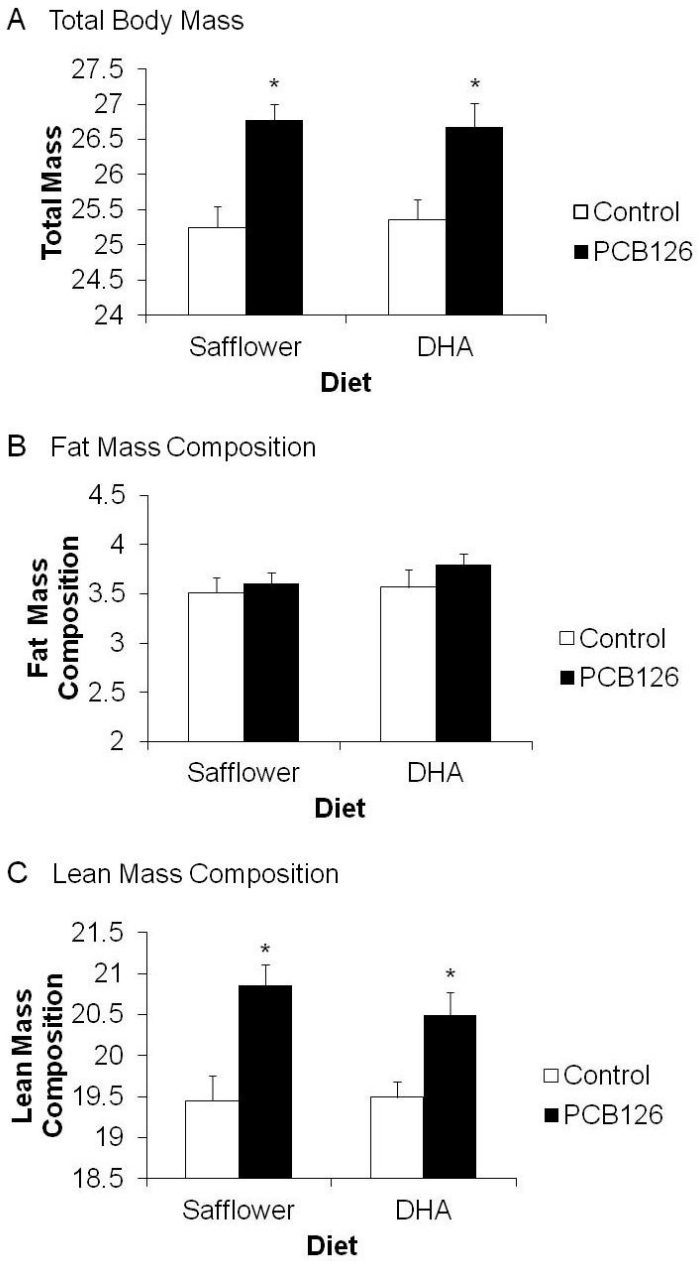

Figure 4.4 Body compositions were affected by PCB 126 treatment but not by diet. (A) Total body mass was significantly increased following PCB 126 treatment. (B) Fat composition was not affected by PCB 126 treatment. (C) Lean body composition was significantly increased in the groups receiving PCB 126 treatment. Significantly difference found when compared to their respective treatment controls, $^{*}p_{value} < 0.05$.

Figure 4.5 Liver weight to body weight ratio is increased with PCB 126 treatment. Liver weight divided by total body weight in the PCB 126 treated animals was significantly increased when compared to their respective treatment controls, *p_{value} <0.05.

Figure 4.6 PCB 126 did not significantly increase the serum ALT levels. Alanine aminotransferase (ALT) results are the mean + SEM p_{value} <0.05, n=5.

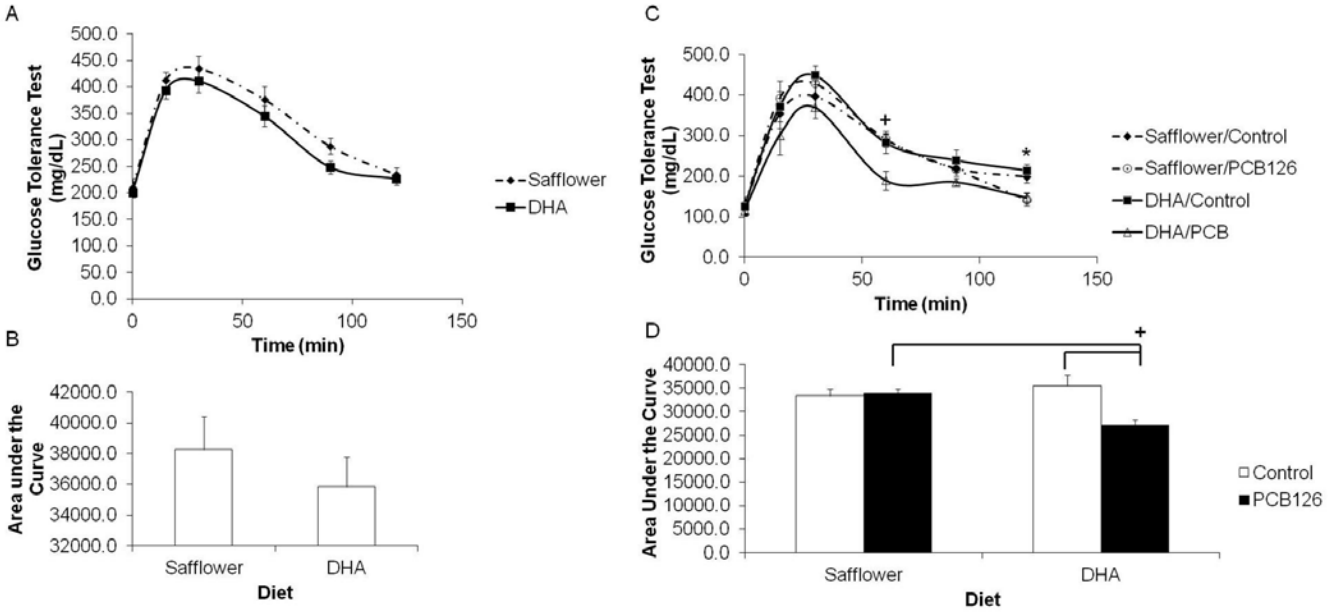

Figure 4.7 DHA-fed, PCB 126 treated mice have a heightened response to glucose challenge. Control safflower oil diet is represented by black circles and a dashed line in (A) and (C), and control safflower oil diet with PCB 126 treatment is represented by open circles with a dashed line in (C). DHA diet only is represented by black squares and a solid line in (A) and (C), and DHA-fed, PCB 126 treated animals are represented by open triangles and a solid line in (C). (A) and (B) represent the oral glucose tolerance test (GTT) at week 4 (before PCB 126 treatment) with respective area under the curve (AUC) in arbitrary units. (C) and (D) represent the GTT and respective AUC post 5 µmol PCB 126/kg body weight gavage in week 5. In (C) the post-treatment GTT, the DHA-fed, PCB 126 treated animals had significantly lower blood glucose levels at 60 min than all other treatments, $^{+}$ $p_{value}<0.05$. Blood glucose levels at 120 min were significantly decreased in the groups receiving PCB 126 treatment compared to their respective treatment controls, $*p_{value}<0.05$. The DHA-fed, PCB 126 treated animals (D) had a significantly lower AUC when compared to all other treatment groups, $^{+}$ $p_{value}<0.05$.

Figure 4.8 Treatment with PCB 126 decreases total serum cholesterol. Total serum cholesterol (mg/dL) in the PCB 126 treated animals was significantly decreased when compared to their respective treatment controls, * p_{value} <0.001, and an overall difference was detected between diets, $^{+}$ p_{value} = 0.032, with DHA/control being significantly less than Safflower/control, $^{\#}$ p_{value} = 0.01, n = 4 or 5.

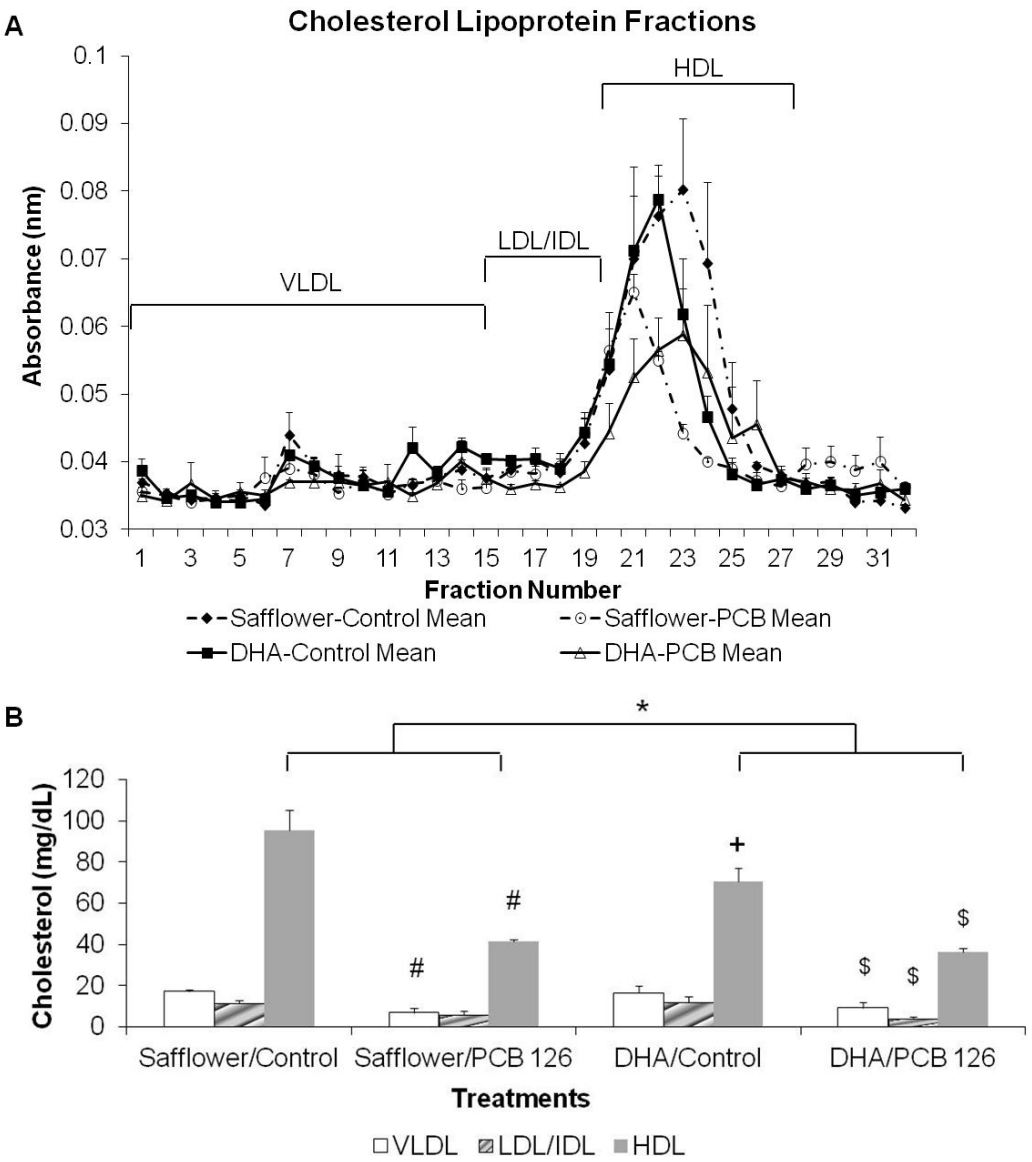

Figure 4.9 Acute exposure to PCB 126 reduces lipoprotein cholesterol content in C57BL/6 mice. (A) Average FPLC chromatograms representing cholesterol distribution within the lipoprotein fraction for normolipodemic C57BL/6 mice. (B) Significant overall differences were observed between PCB 126-treated and control animals. Differences between safflower/control and safflower/PCB 126 treatment were designated by $^{\#}$ $p_{value}<0.05$. Differences between in DHA/control and DHA/PCB 126 were designated by $^{\$}$ $p_{value}<0.05$. HDL was significantly decreased when comparing safflower/control and DHA/control, + p_{value} <0.05, and an overall difference was detected between diets in the HDL lipoprotein fraction, * $p_{value}< 0.05$, n = 4 or 5.

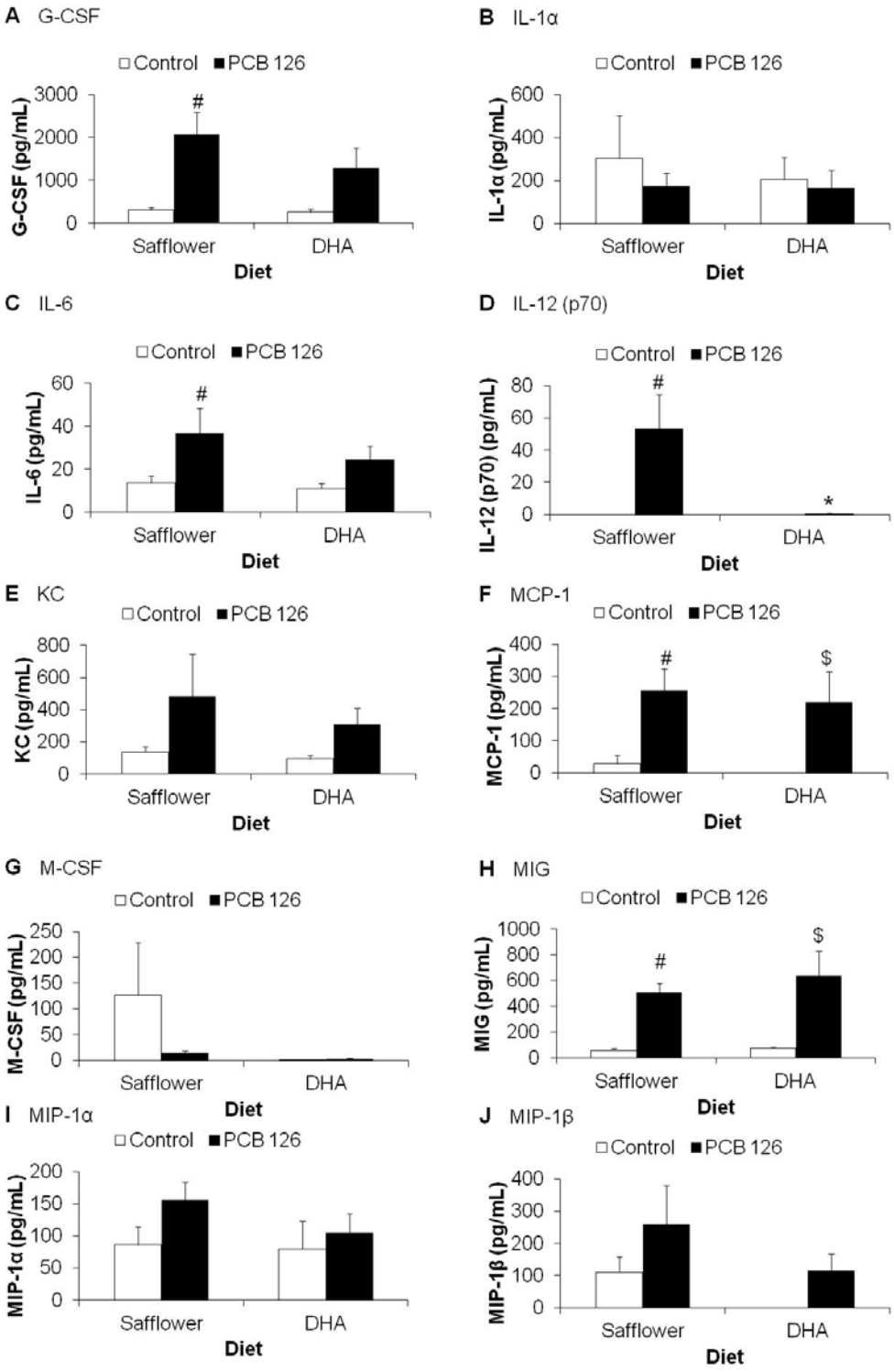
A G-CSF
Control PCB 126
G-CSF (pg/mL)
3000
2000
1000
0
#
Safflower
DHA
Diet
B IL-1α
Control PCB 126
IL-1α (pg/mL)
600
400
200
0
Safflower
DHA
Diet
C IL-6
Control PCB 126
IL-6 (pg/mL)
60
40
20
0
#
Safflower
DHA
Diet
D IL-12 (p70)
Control PCB 126
IL-12 (p70) (pg/mL)
80
60
40
20
0
#
*
Safflower
DHA
Diet
E KC
Control PCB 126
KC (pg/mL)
800
600
400
200
0
Safflower
DHA
Diet
F MCP-1
Control PCB 126
MCP-1 (pg/mL)
400
300
200
100
0
#
$
Safflower
DHA
Diet
G M-CSF
Control PCB 126
M-CSF (pg/mL)
250
200
150
100
50
0
Safflower
DHA
Diet
H MIG
Control PCB 126
MIG (pg/mL)
1000
800
600
400
200
0
#
$
Safflower
DHA
Diet
I MIP-1α
Control PCB 126
MIP-1α (pg/mL)
200
150
100
50
0
Safflower
DHA
Diet
J MIP-1β
Control PCB 126
MIP-1β (pg/mL)
400
300
200
100
0
Safflower
DHA
Diet

Figure 4.10

Figure 4.10 Treatment with PCB 126 induces cytokine expression in serum with a trend toward increased expression in safflower fed mice. Overall differences between PCB 126 and vehicle treatment were found for (A) G-CSF, (C) IL-6, (F) MCP-1, and (H) MIG. (A) G-CSF and (C) IL-6 were significantly increased only in the safflower/PCB 126 treated group. (D) IL-12 (p70) had an interactive effect between diet and treatment with significant differences between safflower/PCB 126 and both safflower/vehicle and DHA/PCB 126. (F) MCP-1 and (H) MIG were significantly increased for both PCB treated groups when compared to their respective dietary controls. There were no significant differences in cytokine expression for (B) IL-1α, (E) KC, (G) M-CSF, (I) MIP-1α, and (J) MIP-1β. Significant differences between safflower/saline and safflower/PCB 126 are represented by $^{\#}$ $p_{value}<0.05$. Differences detected between safflower/PCB 126 and DHA/PCB 126 treatments are represented by * p_{value} <0.05, and significant differences between DHA/saline and DHA/PCB 126 are represented by $^{\$}$ $p_{value}<0.05$, n=5.

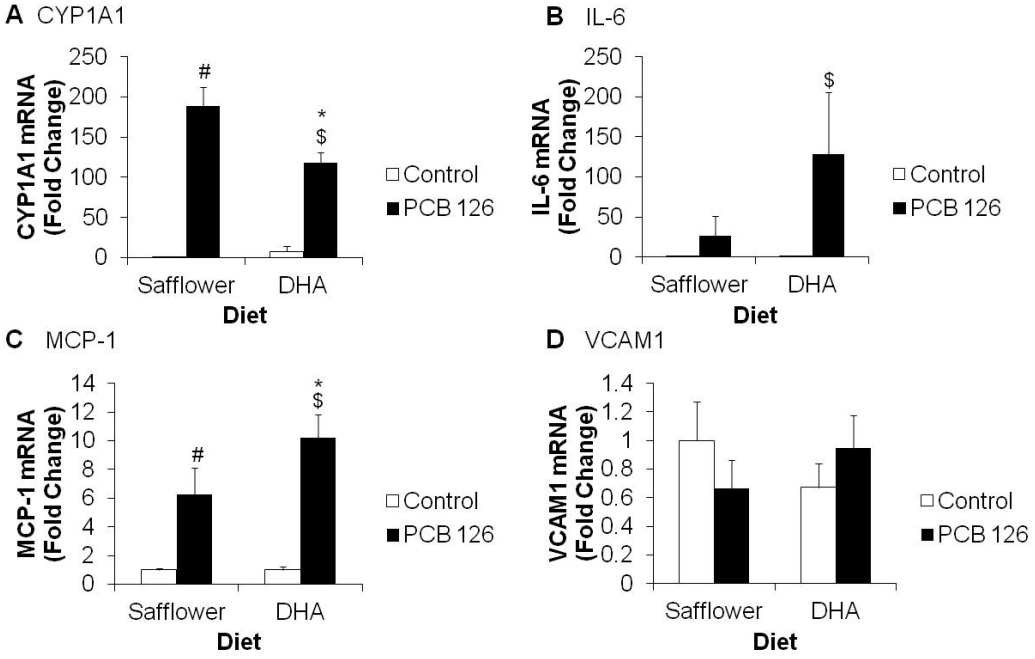

Figure 4.11 PCB 126 promotes an inflammatory response in acutely exposed mice. Overall differences between PCB 126 and vehicle treatment were found for (A) CYP1A1, (B) IL-6 and (C) MCP-1. (A) CYP1A1 had overall differences between diets with reduced expression in the DHA-fed/PCB 126-treated animals. PCB 126 significantly increased CYP1A1 expression over the control treated animals. (B) IL-6 had increased expression for DHA/PCB 126- treated mice in comparison to the untreated controls. PCB 126 signficantly increased (C) MCP-1 expression over controls, and DHA/PCB 126-treated animals had higher MCP-1 expression than the safflower/PCB 126 treated group. There were no significant differences in (D) VCAM1 expression for treatment or diet. Significant differences between safflower/saline and safflower/PCB 126 are represented by $^{\#}$ $p_{value}<0.05$. Differences detected between safflower/PCB 126 and DHA/PCB 126 treatments are represented by * p_{value} <0.05, and significant differences between DHA/saline and DHA/PCB 126 are represented by $^{\$}$ $p_{value}<0.05$.

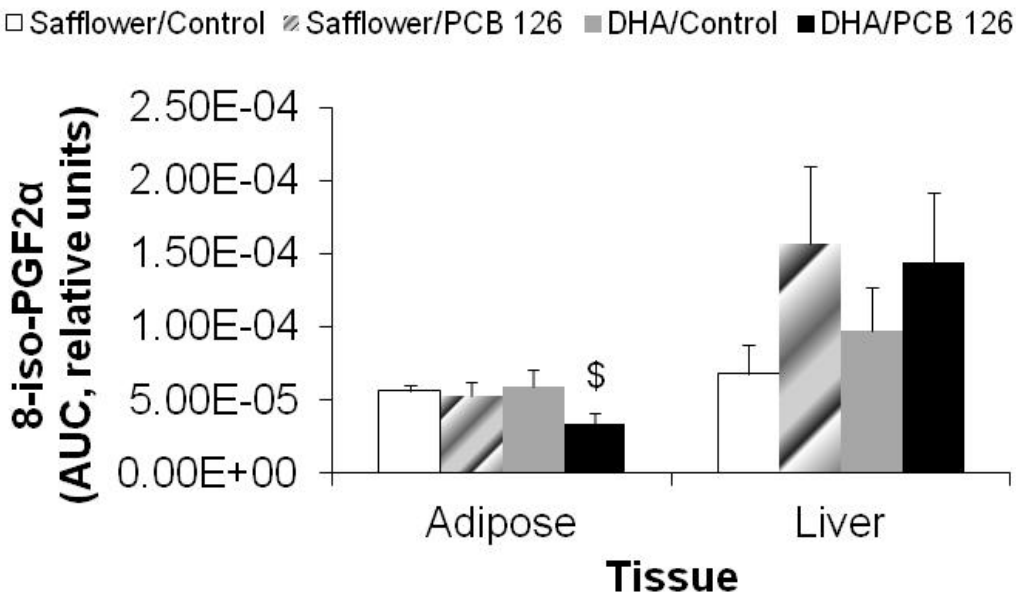

Figure 4.12 Oxidative stress is not increased in the adipose and liver of mice acutely exposed to PCB 126. 8-iso-prostaglandin F2 alpha (8-iso-PGF2α) is a marker of oxidative stress, and neither adipose nor liver tissues contained significant increases of 8-iso-PGF2α following PCB 126 exposure. DHA-fed mice had lower levels following PCB 126 exposure. Significant differences between DHA/saline and DHA/PCB 126 are represented by $^{\$}$ $p_{value}<0.05$.

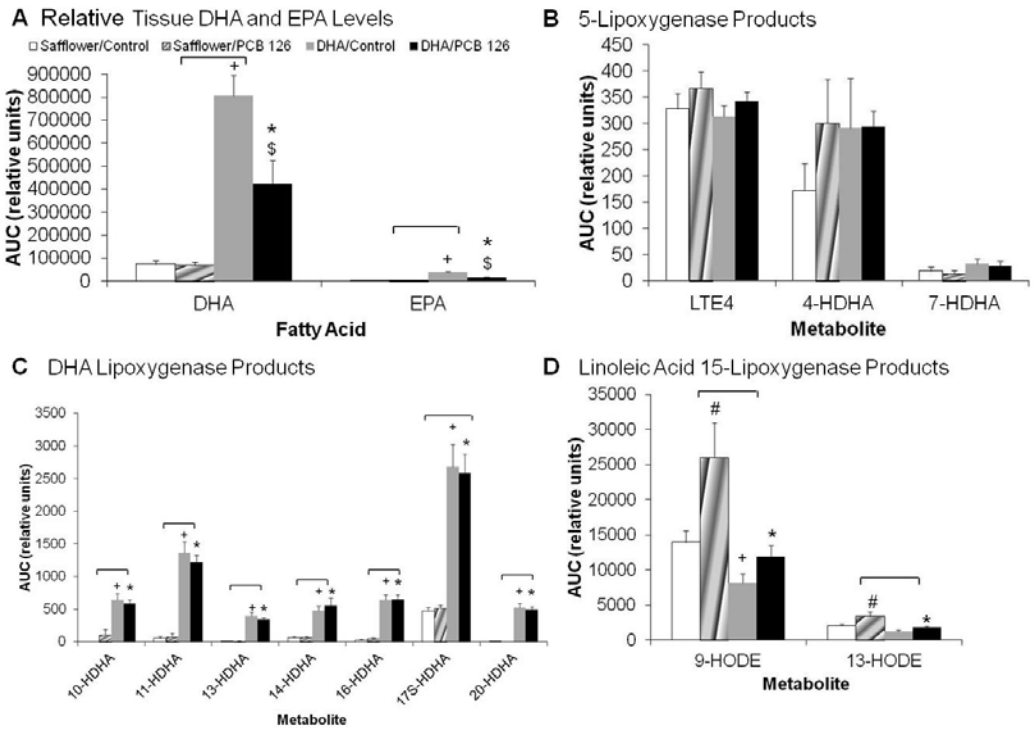

Figure 4.13 Treatment with PCB 126 promotes DHA metabolite formation in the adipose of DHA fed mice. For DHA and EPA, there is an interactive effect between diet and treatment with a significant decrease in the DHA/PCB 126 treated group. LTE_4, 4-HDHA and 7-HDHA have no significant differences. For 9-HODE and 13-HODE, there are overall difference between diets and treatments with an increase in the safflower/PCB 126 treatment group. For 10-HDHA, 11-HDHA, 13-HDHA, 14-HDHA, 16-HDHA, 17S-HDHA and 20-HDHA, there were overall differences between diets. Samples were normalized to tissue weight. A difference was detected between safflower/PCB 126 and DHA/PCB 126 treatments * p_{value} <0.05, and a difference was detected between safflower/saline and DHA/saline treatments, $^{+}$ p_{value} < 0.05. Significant differences between DHA/saline and DHA/PCB 126 are represented by $^{\$}$ p_{value}<0.05. Significant differences between safflower/saline and safflower/PCB 126 are represented by $^{\#}$ p_{value}<0.05. Overall difference between dietary feeding is represented by a bar.

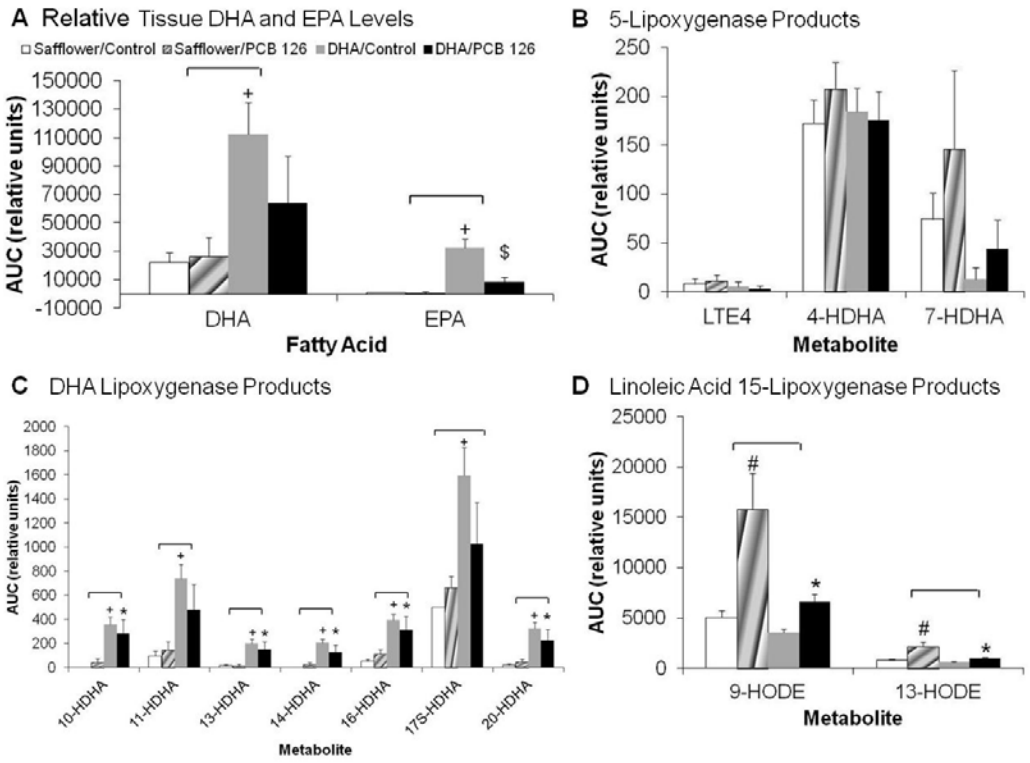

Figure 4.14 Treatment with PCB 126 promotes DHA metabolite formation in the livers of DHA fed mice. For DHA, there is a significant overall increase between diets. For EPA, there is an interactive effect between diet and treatment with a significant decrease in the DHA/PCB 126 treated group. LTE_4, 4-HDHA and 7-HDHA have no significant differences. For 10-HDHA, 11-HDHA, 13-HDHA, 14-HDHA, 16-HDHA, 17S-HDHA and 20-HDHA, there were overall differences between diets. For 9-HODE, there is almost an interactive effect with an overall difference between diets and an increase in the safflower/PCB 126 treatment group. 13-HODE had an interactive effect between diet and treatment. Samples were normalized to tissue weight. A difference was detected between safflower/PCB 126 and DHA/PCB 126 treatments * p_{value} <0.05, and a difference was detected between safflower/saline and DHA/saline treatments, $^{+}$ p_{value} < 0.05. Significant differences between DHA/saline and DHA/PCB 126 are represented by $^{\$}$ p_{value}<0.05. Significant differences between safflower/saline and safflower/PCB 126 are represented by $^{\#}$ p_{value}<0.05. Overall difference between dietary feeding is represented by a bar.

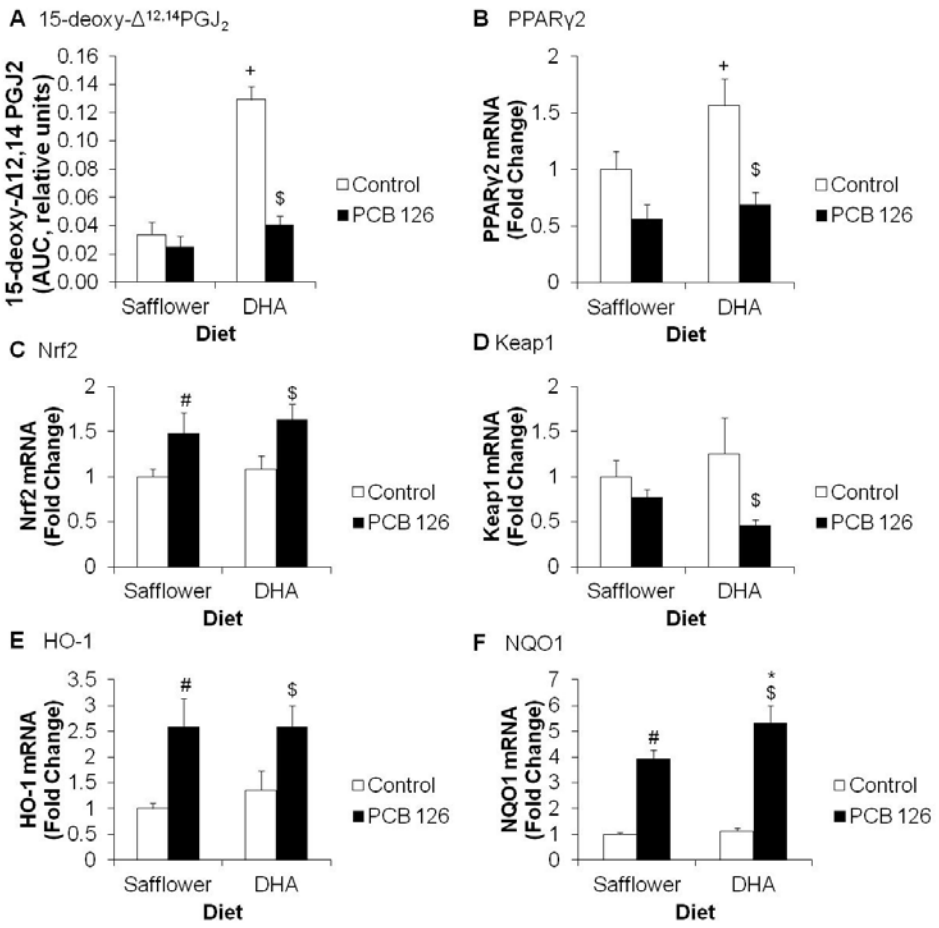

Figure 4.15 DHA-feeding promotes the formation of anti-inflammatory 15-deoxy-$\Delta^{12,14}PGJ_2$ and anti-oxidant gene expression in response to PCB 126-induced inflammation. Overall differences between PCB 126 and vehicle treatment and diet were found for (A) arachidonic acid metabolite 15-deoxy-$\Delta^{12,14}PGJ_2$ and (B) PPARγ2, though PCB 126 treatment reduces this response. Overall differences between PCB 126 and vehicle treatment were found for (C) Nrf2, (D) Keap1, (E) HO-1, and (F) NQO1. (D) Keap1 mRNA expression is significantly decreased in the DHA/PCB 126 group when compared to control. (F) NQO1 is significantly increased in the DHA/PCB 126 treated group above both control and safflower/PCB 126 treated animals. Differences detected between safflower/control and DHA/control treatments are represented by $^{+}$ p_{value} <0.05, and significant differences between DHA/saline and DHA/PCB 126 are represented by $^{\$}$ p_{value}<0.05. Significant differences between safflower/saline and safflower/PCB 126 are represented by $^{\#}$ p_{value}<0.05.

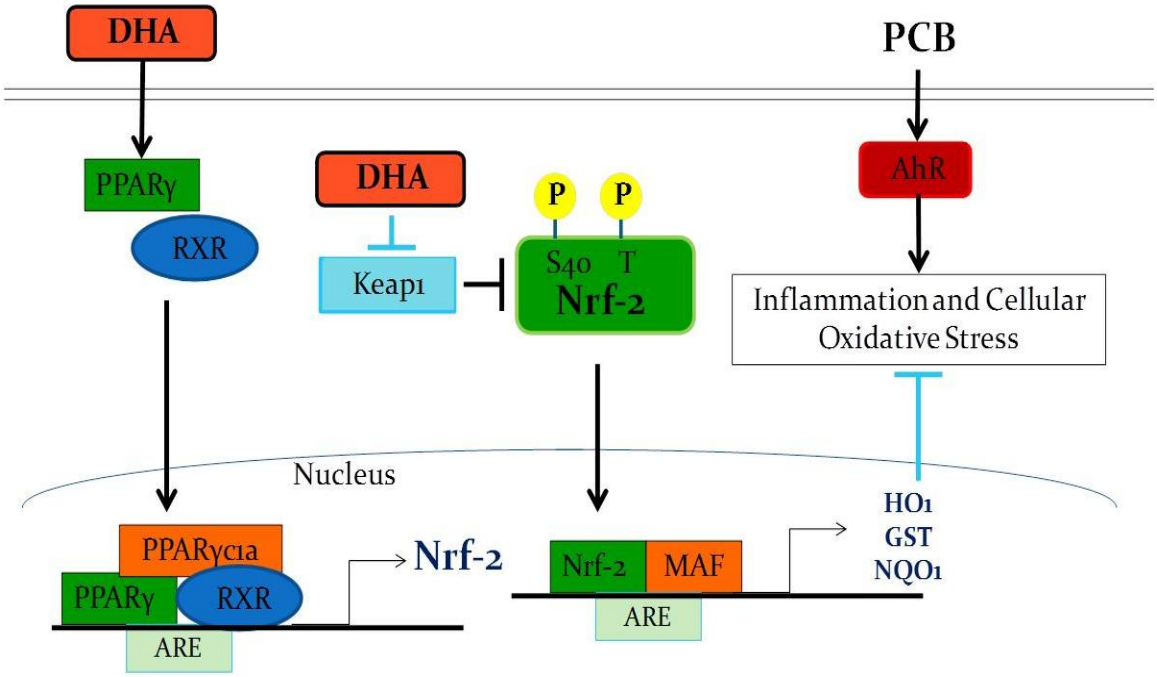

Figure 4.16 DHA and DHA metabolites positively regulate anti-inflammatory signaling pathways. The cell utilizes DHA to activate anti-oxidant enzyme systems through increased activity of the nuclear transcription factors, PPARγ and Nrf-2. PCB 126 binding with the AhR promotes an inflammatory response which is mitigated by increased anti-oxidant enzyme expression.

Supplemental Table 4.1 Genes down-regulated by 5 µmol/kg PCB 126 treatment affect multiple metabolic pathways. Analysis of 102 down-regulated gene transcripts was generated using the DAVID© software system, which assessed the genes for activity in shared metabolic pathways.

Category	Term	Count	%	PValue	Genes	List Total	Pop Hits	Pop Total	Fold Enrichment	Bonferroni	Benjamini	FDR
KEGG_PATHWAY	mmu00983:Drug metabolism	6	2.39	0.001	TYMP, CYP3A25, CYP3A41A, CYP3A59, DPYD, ES31, TK1	102	48	5738	7.032	0.135	0.135	1.587
KEGG_PATHWAY	mmu00140:Steroid hormone biosynthesis	5	1.992	0.008	HSD3B2, CYP3A25, CYP3A41A, HSD3B5, CYP3A59, SRD5A1	102	45	5738	6.251	0.544	0.325	8.289
KEGG_PATHWAY	mmu01040:Biosynthesis of unsaturated fatty acids	4	1.594	0.011	SCD3, FADS1, ELOVL2, ACAA1B	102	27	5738	8.334	0.686	0.320	12.0
KEGG_PATHWAY	mmu03320:PPAR signaling pathway	6	2.39	0.012	SCD3, ACSL1, SORBS1, FABP2, ACAA1B, SCP2	102	79	5738	4.273	0.714	0.269	12.89
KEGG_PATHWAY	mmu00910:Nitrogen metabolism	3	1.195	0.061	CAR14, HAL, CPS1	102	23	5738	7.338	0.998	0.720	50.38
KEGG_PATHWAY	mmu04910:Insulin signaling pathway	6	2.39	0.095	SREBF1, SORBS1, GCK, PYGL, PKLR, GYS2	102	138	5738	2.446	1.000	0.815	67.16

Supplemental Table 4.2 Genes up-regulated by 5 µmol/kg PCB 126 treatment affect multiple metabolic pathways.

Analysis of 160 up- regulated gene transcripts was generated using the DAVID© software system, which assessed the genes for activity in shared metabolic pathways.

Category	Term	Count	%	PValue	Genes	List Total	Pop Hits	Pop Total	Fold Enrichment	Bonferroni	Benjamini	FDR
KEGG_PATHWAY	mmu00982:Drug metabolism	13	3.621	7.81E-07	GSTA1, GSTA2, CYP1A2, ALDH3B1, GSTM7, GSTM1, GSTM2, GSTM3, UGT1A9, GSTM4, FMO2, AOX1, FMO3	160	75	5738	6.22	0.000	0.000	0.001
KEGG_PATHWAY	mmu00980:Metabolism of xenobiotics by cytochrome P450	12	3.343	1.51E-06	GSTM1, GSTA1, GSTA2, GSTM2, UGT1A9, GSTM3, GSTM4, CYP1B1, CYP1A1, CYP1A2, ALDH3B1, GSTM7	160	66	5738	6.52	0.000	0.000	0.002
KEGG_PATHWAY	mmu00480:Glutathione metabolism	10	2.786	1.02E-05	GSTM1, GSS, GSTA1, GSTA2, GSTM2, GSR, GSTM3, GSTM4, PGD, GSTM7	160	52	5738	6.90	0.002	0.001	0.012
KEGG_PATHWAY	mmu00230:Purine metabolism	12	3.343	0.004	XDH, FHIT, NME2, ITPA, POLE2, ATIC, NME1, PKM2, ENTPD5, POLR3A, POLR2D, ENTPD2	160	157	5738	2.74	0.459	0.142	4.694
KEGG_PATHWAY	mmu00240:Pyrimidine metabolism	9	2.507	0.005	UMPS, NME2, ITPA, POLE2, UPRT, NME1, ENTPD5, POLR3A, POLR2D	160	96	5738	3.36	0.528	0.139	5.708
KEGG_PATHWAY	mmu04110:Cell cycle	9	2.507	0.025	CCND1, TGFB3, BUB1, CDC23, MCM2, MCM3, MYC, MCM5, TGFB2	160	128	5738	2.52	0.980	0.478	26.312
KEGG_PATHWAY	mmu05222:Small cell lung cancer	7	1.95	0.030	FHIT, CCND1, RXRG, PIK3R3, TRAF5, MYC, TRAF3	160	85	5738	2.95	0.990	0.484	30.450
KEGG_PATHWAY	mmu05210:Colorectal cancer	7	1.95	0.031	CCND1, RAC3, TGFB3, PIK3R3, MYC, FZD7, TGFB2	160	86	5738	2.92	0.992	0.457	31.753
KEGG_PATHWAY	mmu00140:Steroid hormone biosynthesis	5	1.393	0.035	UGT1A9, CYP1B1, CYP1A1, HSD17B2, COMT1	160	45	5738	3.98	0.996	0.455	34.809
KEGG_PATHWAY	mmu03010:Ribosome	7	1.95	0.036	RPSA, RPS28, RPL13, RPLP0, RPLP1, RPLP2, UBB	160	89	5738	2.82	0.996	0.432	35.774
KEGG_PATHWAY	mmu00010:Glycolysis / Gluconeogenesis	6	1.671	0.039	AKR1A4, HK3, PKM2, FBP1, PGAM1, ALDH3B1	160	68	5738	3.16	0.998	0.429	38.277
KEGG_PATHWAY	mmu03050:Proteasome	5	1.393	0.040	PSMF1, PSMC3, PSMD4, PSMB8, PSMB9	160	47	5738	3.82	0.998	0.408	38.883
KEGG_PATHWAY	mmu00983:Drug metabolism	5	1.393	0.043	XDH, UMPS, UGT1A9, ITPA, 2210023G05RIK	160	48	5738	3.74	0.999	0.404	40.946
KEGG_PATHWAY	mmu05212:Pancreatic cancer	6	1.671	0.049	CCND1, RAC3, TGFB3, STAT1, PIK3R3, TGFB2	160	72	5738	2.99	1.000	0.420	44.930
KEGG_PATHWAY	mmu03030:DNA replication	4	1.114	0.072	POLE2, MCM2, MCM3, MCM5	160	35	5738	4.10	1.000	0.532	58.976
KEGG_PATHWAY	mmu00040:Pentose and glucuronate interconversions	3	0.836	0.079	UGT1A9, AKR1B3, UGDH	160	17	5738	6.33	1.000	0.545	62.737
KEGG_PATHWAY	mmu00051:Fructose and mannose metabolism	4	1.114	0.082	AKR1B3, HK3, FBP1, PMM1	160	37	5738	3.88	1.000	0.536	64.029
KEGG_PATHWAY	mmu00350:Tyrosine metabolism	4	1.114	0.092	AOX1, WBSCR22, COMT1, ALDH3B1	160	39	5738	3.68	1.000	0.562	68.746
KEGG_PATHWAY	mmu00380:Tryptophan metabolism	4	1.114	0.098	CYP1B1, CYP1A1, AOX1, CYP1A2	160	40	5738	3.59	1.000	0.564	70.965

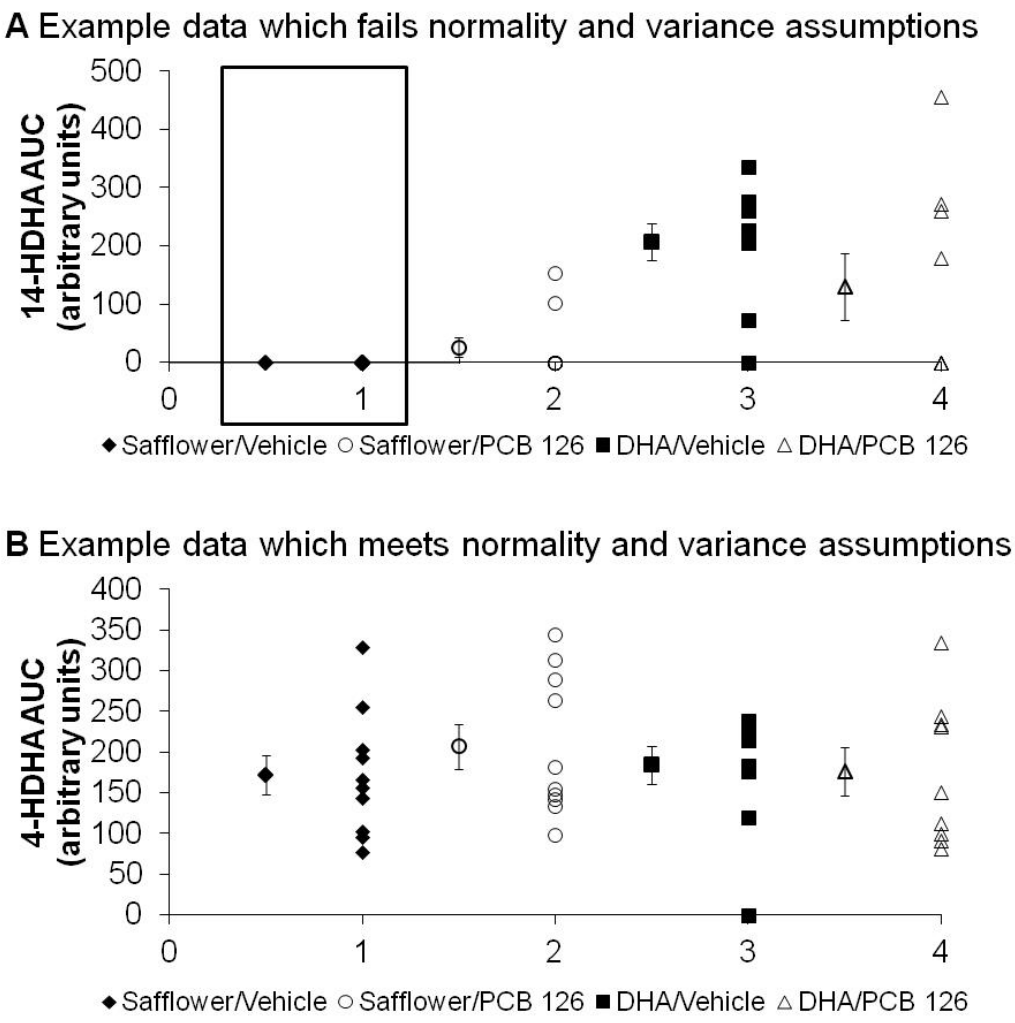

Supplemental Figure 4.1 Data containing zero numbers do not meet all the assumptions of parametric and non-parametric tests. (A) 14-HDHA is not formed in safflower-fed, vehicle treated mice and the zero values are incompatible with assumptions of normality and equal variance. In contrast, 4-HDHA (B) is a metabolite found in all mice, and thus, the presence of non-zero data values satisfies both the normality and variance assumptions. Data are represented as averages ± SEM or as scatter plots of individual data points.

Chapter Five: Mechanisms of PCB-induced Inflammation

5.1 Synopsis

Inflammation has been identified as a critical risk factor for a host of diseases including cardiovascular diseases (CVDs) such as atherosclerosis[58]. One of the many contributors to endothelial dysfunction and CVDs are environmental pollutants, e.g., polychlorinated biphenyls (PCBs), a class of persistent organic pollutants. Our laboratory has explored the role of coplanar PCBs in endothelial dysfunction and atherosclerosis. PCBs, and especially coplanar PCBs, induce inflammation by interaction with lipid rafts called caveolae that promote signaling through the aryl hydrocarbon receptor (AhR). Lipid rafts are also essential for toll-like receptor 4 (TLR4) signaling, an innate immune receptor associated with inflammation and atherosclerosis. Both TLR4 and PCBs induce inflammation through NFκB signaling pathways. There is limited evidence to suggest that environmental toxins interact with TLR4 or its associated proteins to induce inflammatory signaling. Thus, the potential interaction of PCBs with TLR4 to induce endothelial dysfunction is not well understood. We investigated the interaction of coplanar PCB 126 with caveolae based TLR4 signaling to induce NFκB inflammatory targets and subsequent initiation of endothelial dysfunction.

5.2 Introduction

General Overview

Environmental toxicants, such as polychlorinated biphenyls (PCBs), promote the low-grade inflammation that contributes to the development of a host of diseases including diabetes and cardiovascular disease (CVD)[59, 143, 160, 269]. Our laboratory's work with the vascular endothelium promotes the understanding of the molecular mechanisms by which coplanar PCBs induce inflammation and promote endothelial dysfunction[270]. These changes in the vascular homeostasis create an ideal environment for the development of atherosclerotic plaques[151]. PCBs initiate endothelial inflammation through interaction with caveolae, a form of lipid rafts which harbor receptors and signaling domains[126]. Caveolae also host innate immune receptors including Toll-like receptor 4 (TLR4), which is the receptor of bacterial lipopolysaccharide (LPS), and is linked to the development of CVD[78]. Evidence suggests that environmental stimuli interact with TLR4 to promote an inflammatory response. Here we investigated PCB 126 interaction with TLR4.

PCBs, CVD and Inflammation

National Health and Nutrition Examination Survey (NHANES) and a study in elderly patients revealed that circulating levels of PCBs are significantly associated with hypertension[271] and atherosclerosis[64], respectively. Further, angiotensin II-infused apolipoprotein E–deficient mice exposed to coplanar PCBs developed more extensive atherosclerotic lesions[151]. The endothelium is a critical component of inflammation and disease progression in atherosclerosis. Our studies using primary endothelial cells (ECs) have demonstrated that silencing or deficiency of caveolin-1 (Cav-1), a major structural and signaling protein of caveolae, decreases PCB–mediated extracellular signal-regulated kinase-1/2 (ERK1/2) phosphorylation leading to a reduction in associated vascular cell adhesion molecule-1 (VCAM-1) expression and monocyte adhesion[126]. PCB-mediated endothelial dysfunction has classically been attributed to AhR activation and subsequent upregulation of cytochrome P4501A1 (CYP1A1) and other xenobiotic metabolizing proteins[124]. CYP1A1 causes an increase of reactive oxygen and nitrogen species (ROS/RNS) which promote cellular damage and NFκB activation[73, 152]. The classical model of AhR-induced inflammation has not explained other interactions of coplanar PCBs with membrane based domains; our work with caveolae addresses this question.

Caveolae and Molecular Signaling

Caveolae are a specific sub-class of lipid rafts that form sphingolipid and cholesterol rich invaginations on the plasma membrane, and cholesterol depletion or buoyancy separation have been classical methodologies for defining and studying these domains[272]. Caveolin-1 (Cav-1) is the major structural protein located within the rafts of endothelial cells, and is required for caveolae formation[270]. Caveolae have been identified as critical components in vascular homeostasis and tone[272], and our work with PCBs and endothelial nitric oxide synthase (eNOS) have clearly demonstrated the role that caveolae play in mediating environmental pollutant-induced changes on vascular homeostasis[164]. Caveolae are involved in intracellular trafficking in which the endocytosis of caveolae is followed by merging to endosomes[273-276]. PCBs appear to exacerbate caveolae endocytosis[124]. Caveolar endocytosis may act as mitigating response to

negative stimuli helping the cell to "sort" and develop a specific response[277], and caveolae are critical to the signaling of the innate immune response.

TLR4 and Associated Signaling Outcomes

Lipid rafts are complex signaling domains that play host to a variety of receptors and associated scaffolding proteins including TLR4 and Cav-1. TLR4 signaling requires dimerization and migration to lipid domains from which downstream activation of NFκB occurs[107, 117]. It has been proposed that TLR4 scaffolding in caveolae stimulates endocytosis of caveolae which is essential for the induction of down-stream inflammatory signaling[278]. Activation of TLR4 promotes signaling through an array of pathways. The "classical" signaling pathways include signaling through MyD88 scaffolding pathway to IRAK/TRAF6/TAK1 pathway to induce both NFκB and MAP-kinase family signaling[279]. A second MyD88-dependent signaling pathway utilizes the TIRAP/Mal adapter proteins, which also lead to NFκB signaling, and both the MyD88-dependent pathways are associated with "early" phase NFκB signaling[280]. Alternative and complimentary to the MyD88-dependent pathway is the TRIF-dependent signaling pathway[281]. MyD88-independent TRIF associates with TLR4 via the TRAM adaptor molecule which initiates TRAF3/IRF3 for interferon activation and TRAF6 for NFκB-induced chemokine and cytokine expression, RIP1/caspase 8-dependent induction of apoptosis and RIP3-activated ROS-dependent necrosis[282]. Together these TLR4 initiated signaling pathways induce a range of inflammatory responses.

The nuances of the innate immune response continue to unfold as investigators report changing specificity depending on chaperone molecules, adaptor protein recruitment, and a host of other modifications that dictate the type of cellular response given to a particular ligand. The following studies explore the concept of toxicant interaction with TLR4; these interactions may be facilitated by chaperone proteins such as lipopolysaccharide binding protein (LBP) and CD14. In a study of macrophages stimulated with LPS to induce TLR4, cells demonstrated a hyperactive cytokine response when challenged with environmental toxicants[283]. In a lung inflammation model, cigarette smoke-induced inflammatory cytokine production and neutrophil infiltration were attenuated in knockout (KO) mice for TLR4 and interleukin-1 receptor 1 (IL-1R1)[284]. (Cigarette smoke contains polycyclic aromatic hydrocarbons (PAHs) which like PCBs are AhR ligands.) Inflammation in astroglial cells, which was caused by low

concentrations of ethanol, was attributed to the caveolae-dependent endocytosis of IL1-R1/TLR4 and activation of associated downstream pathways[278]. Finally, a recent study demonstrated that PCBs modified intestinal and blood brain barrier function through activation of TLR4[67]. Together these studies indicate that TLR4 plays a critical role in environmental pollutant-induced inflammation.

Hypothesis and Rationale

We hypothesize that PCB 126-induced inflammation is mediated through caveolae-based TLR4 signaling. A growing body of literature has associated TLR4 with atherosclerotic development[285-289]. For example, a study examining human Stage VI lesions found that the endothelium and macrophages (MΦ) had increased expression of TLR4 and p65, a subunit of NFκB [78]. Coplanar PCBs, also, contribute to endothelial dysfunction and vascular inflammation. Evidence suggests that both sources of inflammation may be sensitive to nutritional modulation, and the proposed mechanism would provide a platform with which to test potential nutritional interventions. The hypothesis proposed here seeks to clarify the critical role of membrane domains, caveolae, in mediating PCB-induced inflammation by studying the activation of TLR4-associated signaling (Figure 5.1).

5.3 Methods and Materials

Reagents and Materials

PCB 126 was obtained from AccuStandard (New Haven, CT). Western blotting reagents were obtained from BioExpress (Kaysville, UT). Reverse transcriptase reagents were purchased from Fisher Scientific (Waltham, MA). Reagents used for mRNA isolation and qPCR were purchased from Life Technologies (Grand Island, NY). Unless otherwise stated, chemicals were purchased from Sigma-Aldrich (St. Louis, MO).

Sucrose Gradient

Discontinuous sucrose gradients were performed to separate caveolae-rich lipid fractions[129]. Primary porcine endothelial cells (ECs) were grown to 90% confluence in 150 mm culture dishes. Cells were normalized overnight with 1% FBS M199 and treated for 30 min or 16 hr with 0.25 μM PCB 126, 0.1 ug/mL LPS, or DMSO (vehicle). Treated cells were harvested by scraping with morpholine ethanesulfonic acid (MES)-buffered saline (MBS), and fractions were separated by layering 45% (equal volume sample:90% sucrose/MBS solution), 35% and 5% sucrose/MBS solutions which were centrifuged at

39,000 rpm with a SW41 rotor. Western blotting was performed using equal volume protein fractions loaded on to 8% SDS-PAGE gels, and blots were probed using TLR4 (H-80) sc-10741 (1:500 primary and 1:4,000 secondary), Santa Cruz Biotechnology, Inc., Dallas, TX) and Cav-1 #3238S (1:10,000 primary and secondary, Cell Signaling Technology, Inc,, Danvers, MA), Anti-rabbit secondary antibody was from Cell Signaling.

Cholesterol Depletion Assay

M199 treatment media with 1% L-glutamine was prepared with 10 mM methyl-β-cyclodextrin (MβCD)[116, 290-292]. Confluent 150 mm culture dishes were conditioned with 1% FBS M199 overnight and were pre-treated with treatment media with or without 10 mM MβCD for 30 or 60 minutes at 37°C. Plates were washed three times with HANKS buffer and were given 0.5% M199 with 1% L-glutamine and 1% penicillin/streptomycin. Samples were treated with DMSO or 0.25 μM PCB 126 in DMSO for 8 hr and were co-treated with 0.1 μg/mL LPS for an additional 4 hr. Cultures were harvested and fractionated by sucrose gradient as described earlier. Sucrose gradient fractions were assessed by Western blot using 10% SDS-PAGE gels.

Inhibition Assays and MCP-1 ELISA

For the inhibition assays, ECs were grown in 12-well plates. Cardiolipin (CL) was suspended in PBS at 0.5 mg/mL stock concentration[293]. For treatment, CL was diluted from 10 to 1000 ng/mL in 1% FBS M199 treatment media. Cultures were treated with DMSO, 1000 ng/mL CL, 0.5 μM PCB 126, 10 ng/mL LPS, or co-treatment of PCB 126 or LPS with different concentrations of CL. CLI-095, also reported as TAK-242, (InvivoGen, San Diego, CA) was suspended in DMSO and working stocks were diluted to 200 μg/mL in 1% FBS M199[294]. Cultures were treated with DMSO, 1000 ng/mL CLI-095, 0.25 μM PCB 126, 10 ng/mL LPS, or co-treatment of PCB 126 or LPS with 10 to 1000 ng/mL CLI-095. After 24 hr incubation, supernatant was collected and centrifuged at 4°C and 7500 rpm for 5 min. An aliquot was removed and stored at -80°C until analysis by MCP-1 ELISA. Cell culture supernatants were diluted 1:1 and analyzed using the OptEIA Human MCP-1 ELISA Kit (BD Biosciences, San Diego, CA) according to manufacturer guidelines.

Real Time – PCR

ECs were grown to confluence using 6-well plates, and mRNA was isolated using the Trizol® method[125, 126]. Isolated mRNA was resuspended in RNAse/DNAse free water and quantified using UV-vis spectroscopy at 260 nM. cDNA was made using a reverse

transcriptase reaction. SYBR® Green reagent was used to perform the real time-PCR reactions, and absolute quantification was run using the7300 Real Time PCR Systems (Life Technologies, Grand Island, NY). The housekeeping gene, β-actin, was used to normalize VCAM1, and data are presented as a ratio of VCAM1/ β-actin.

Western Blot

Western blots were performed as described previously[140]. ECs were grown to confluence in 6-well plates and treated with 0.025%v/v DMSO (vehicle), 0.25 μM PCB 126, and/or 0.01-1.0 μg/mL LPS for 8 hr. Protein was collected using 1X RIPA buffer, sonicated for 10 s, incubated on ice for 30 min, and centrifuged at 4°C and12, 000 rpm for 15 min. Supernatants were collected and quantified using the Bradford method. Aliquots containing 30 μg of protein were made and run on 10% SDS-PAGE gels. Following semi-dry transfer, nitrocellulose membranes were incubated for 2 h in blocking buffer (5% non-fat milk in Tris-buffered saline containing 0.05% Tween 20). VCAM1(C-19)-R (Santa Cruz Biotechnology, Inc., Santa Cruz, CA) primary antibody was diluted 1:1000 in 5% milk and incubated overnight at 4°C . Anti-rabbit secondary was applied at 1:4000 dilution. β-actin primary and secondary antibodies were diluted 1:10,000 [125].

Statistical Analysis

Comparisons between treatments were made by one-way analysis of variance followed by Tukey's post-hoc test. Statistical probability of $P<0.05$ was considered significant. SigmaPlot version 12.0 software (Systat Software, San Jose, CA) was used to perform the data analysis. When letters are used to indicate differences in significance, shared marker letters between treatments indicate no statistical difference. Values are reported as the mean +SEM.

5.4 Results

To investigate the interactions of PCBs with TLR4, EC cultures were treated with PCB 126 or LPS for 30 minutes (Figure 5.2) or 16 hours (Figure 5.3). Using sucrose gradients to separate cellular domains by density, we found that PCB 126 and LPS, the primary ligand of TLR4 and positive control, both shifted to a more buoyant lipid raft fraction for Cav-1 (Figure 5.2A) and TLR4 (Figure 5.2B) suggesting interaction by both ligands with these domains at 30 minutes. After 16 hr of treatment, both Cav-1 (Figure 5.3A) and TLR4 (Figure 5.3B) proteins were distributed throughout the gradient implicating association with other proteins either to promote signaling or because of migration into the cytoplasm. Looking at endothelial dysfunction markers, cells treated with PCB 126 or

LPS showed an increase in VCAM-1 mRNA expression (Figure 5.4). Previous work in our laboratory demonstrated that PCBs increase caveolae endocytosis (as does activation of TLR4[278]) and that treatment with PCBs increases the co-immunoprecipitation of AhR with Cav-1 linking the activation of Cav-1 with the downstream consequences of AhR stimulation[124]. Caveolae activation and trafficking provide a link between the diverse NFκB activation pathways of TLR4 and AhR.

Several groups have explored the protective role of certain long-chain fatty acids, phospholipids, and their oxidized products. In one study, the phospholipid cardiolipin (CL) was shown to inhibit activation of TLR4 via chaperone protein binding[293]; we utilized CL as an inhibitor of TLR4 activation to determine if downstream inflammatory markers were modulated similarly for both PCB and LPS. When cells were co-treated with CL and PCB or LPS, monocyte chemoattractant protein-1 (MCP-1) protein, a chemokine indicative of endothelial cell activation, was decreased (Figure 5.5). To confirm the activity of TLR4 in PCB-induced inflammation, TAK-242, a TLR4-specific inhibitor, was tested[294]. PCB 126 treated groups displayed a significant increase of MCP-1 over TAK-242 alone (brand name CLI-095, InvivoGen, San Diego, CA) except for the 250 ng/mL CLI-095 treated group, which had a $p_{value} = 0.055$ (Figure 5.6A). In contrast, the LPS treated groups displayed only a significant increase for MCP-1 protein over inhibitor alone with 10 and 50 ng/mL CLI-095, which were also significantly increased over the 1000 ng/mL and LPS co-treated group (Figure 5.6B). The 1000 ng/mL CLI-095 (TAK-242) showed the greatest inhibition of MCP-1 protein expression in the presence of LPS treatment which was not replicated with PCB 126 treatment.

Though the TLR4-specific inhibitor assay indicates that PCB 126 (at the dose and time points studied) does not activate the TLR4 signaling mechanism, similarities exist between LPS and PCB-induced Cav-1 localization in the sucrose gradient data and inflammatory endpoint expression. We, therefore, focused on caveolae and Cav-1 to confirm shared activity. Using a cholesterol depletion assay, we observed changes in the localization of Cav-1 following treatment with PCB 126 and/or LPS. Previously, work with mRNA indicated that LPS stimulated an increase in VCAM1 expression in half the time of PCB 126 (see for example, Figure 5.4); for this reason cultures were treated for 4 hr with LPS and 8 hr with PCB 126 and were harvested and subjected to sucrose gradient fractionation. In the vehicle treated gradient, Cav-1 had a broad presence including the most buoyant fractions to fraction 10 with the highest protein density in fractions 4-6

(Figure 5.7A). PCB 126 treatment stimulated a shift from the most buoyant fractions to fractions 5-12 (Figure 5.7B); similarly, LPS treatment caused a shift away from fractions 1-3 (Figure 5.7C). Cholesterol depletion with MβCD reduced the total Cav-1 and forced Cav-1 out of the buoyant lipid raft fractions into fractions 5-10 regardless of treatment (Figure 5.7). Interestingly, co-stimulation with both PCB 126 and LPS caused a shift in Cav-1 localization to fractions 5-11 and was sufficient to overcome the effects of cholesterol depletion on Cav-1 expression (Figure 5.7D). To further assess the inflammatory response to PCB 126, LPS, or LPS/PCB 126 co-treatment, we probed for Cav-1 and VCAM1 protein in the sucrose gradient fractions. All treatments demonstrated a shift of Cav-1 away the most buoyant fractions when compared to vehicle, but PCB 126 and the PCB 126/LPS co-treatment caused tighter grouping of Cav-1 in the less buoyant fractions. For VCAM1, vehicle and PCB 126 treated fractions only displayed non-specific binding above the protein ladder at fractions 10-13. LPS and the co-treated gradients also displayed this non-specific binding. The LPS treated group had a faint VCAM1 band around fraction 7, outside of the buoyant membrane fractions; in contrast, the LPS/PCB 126 co-treated fractions clearly presented VCAM1 in lipid raft fraction 4 (Figure 5.8B). To confirm the observation that PCB 126 and LPS strengthened the expression of inflammatory markers, we assessed VCAM1 expression following treatment with PCB 126 with co-treatment using different concentrations of LPS. Co-treatment with LPS increased VCAM1 expression in mRNA when compared to control, PCB 126 alone, and LPS alone (Figure 5.9), and a similar trend was observed in protein expression (Figure 5.10).

5.5 Discussion

The data presented here seem to suggest a similar phenomenon, in which PCB 126 stimulates a TLR4 interaction with the Cav-1 fractions, but we were unable to substantiate a clear link between this interaction and an inflammatory response. There are multiple explanations for this observation; the following will be discussed (a) differences in coplanar PCB structure, (b) differences in signaling pathways with overlapping endpoints, and (c) loss of key chaperone proteins. The final discussion points will highlight the aspects of this research that are important for future studies of protective omega-3 fatty acids.

Previous work with PCB 77 and here with PCB 126 demonstrates coplanar PCB-induced Cav-1 activity. PCB 77 promotes Cav-1:AhR interaction [124] and activates endothelial nitric oxide synthase (eNOS) through PI3K/Akt signaling[164]. MCP-1 expression is induced by PCB 77 in a Cav-1-dependent manner through p38 and JNK signaling [125]. Because of their similar structure and AhR binding activity, both PCB 77 and PCB 126 are thought to have similar modes of action. However, in this study, PCB 126 did not mimic the typically robust inflammation that PCB 77 induces, despite having a higher TEF[167]. PCB 77 is metabolized and excreted; in one study, approximately 85% of the original dose was excreted after five days[295, 296]. In a similar five day excretion and metabolism study, only low levels of a single PCB 126 metabolite were detected, and this metabolite was associated with detoxification for excretion rather than toxicity[176]. The resistance of PCB 126 to cellular metabolism may also alter the development of the inflammatory response following AhR activation.

Modulation of the inflammatory response is becoming a field of intense study[297, 298]. Researchers are investigating the immune response and intensity following multiple exposures and/or doses of LPS. Environmental pollutants present another set of potential stimuli and in concert with other factors such as stress, infection, and diet, are likely modulators of body's ability to cope, protect, and recover from injury. In this study, co-stimulation by both PCB 126 and LPS elicited expression of the inflammatory marker, VCAM1. Others have demonstrated that LPS treatment of ECs promotes Cav-1 and adhesion molecule co-localization in caveolae[299], and our work suggests that PCB treatment also enhances VCAM1 and MCP-1 expression in a caveolae-dependent manner[125, 126]. Similar endpoints do not mandate a common signaling pathway. As reviewed in the introduction of this chapter, TLR4 stimulation utilizes multiple sets of adapter molecules that initiate different signaling pathways. The research presented here was unable to substantiate a productive interaction between TLR4 and PCB 126, meaning we could not directly link the membrane interaction observed in the sucrose gradients with the cytokine or adhesion molecule response. However, TLR4 is sensitive to ligands other than LPS. For example, hemin, an iron-containing porphyrin with a chlorine ligand, also promotes TLR4/Cav-1 binding, but when compared to LPS, different signaling pathways are initiated through this interaction[123]. In addition, caveolae are promiscuous domains that harbor multiple receptors and are sensitive to disruptions to the lipid balance in the plasma membrane[268, 300, 301]. These realities further promote the

idea of caveolae as a common signaling platform for both LPS and PCB 126 and help explain the enhanced suppression of MCP-1 following exposure to lipophilic inhibitors in the ELISA assays. We propose that different molecular pathways are activated in response to LPS and PCB 126 but both utilize caveolae as a common base for signal initiation and both culminate with NFκB-directed inflammation.

Another puzzling aspect of this study is the relative insensitivity of the ECs to LPS stimulation. Multiple forms of LPS were tested, but no differences were observed (data not shown). Others have reported that TLR4 is expressed primarily in the cytosol of endothelial cells rather than at the cells surface and that membrane and external chaperone proteins are required for the internalization of LPS[302]. For example, CD14, a critical chaperone for LPS trafficking and TLR4 activation/migration, can be lost in primary cell lines following passaging[303, 304]. Further the presence of soluble and membrane bound forms of CD14 contribute to the sensitivity of the endothelial response; however, very high doses of LPS, 1000 ng/mL, activated TLR4 signaling without CD14[305]. Here we report that TLR4 is present in the caveolae rich fraction, and LPS or PCB 126 stimulation of ECs is sufficient to see TLR4 migration with Cav-1, but it is not sufficient to produce a consistent inflammatory response. Therefore, it is possible that the necessary chaperone proteins were not expressed in our cell line. Combined stimulation of PCB 126 and LPS may have overcome the lack of chaperones; in other words, the two stimuli may have promoted sufficient caveolar internalization to initiate the inflammatory response without the assistance of chaperone proteins.

Caveolae are important regulatory platforms that are sensitive to nutritional modulation, such as omega-3 lipids[105]. The phospholipid cardiolipin was effective in disrupting caveolae-based chemokine response in the inhibition assay (Figure 5.5). Others have reported that incorporation of omega-3 fatty acids into the plasma membrane alters the lipid raft microdomain composition[97]. For this reason, we are interested in signaling changes caused by omega-3 fatty acid incorporation into caveolae. This localized change in lipid content also alters the amount of Cav-1, eNOS, and certain Ras protein in the caveolae[97]. Our laboratory has observed changes in PCB-induced signaling following treatment with differing ratios of omega-3 and omega-6 fatty acids[16]. Similarly, TLR4 signaling is disrupted by omega-3 fatty acids, such as DHA, through inhibition of the PI3K/Akt signaling pathway [106]. We have demonstrated that PI3K/Akt signaling is also critical to the inflammatory signaling induced by the omega-6, linoleic acid, in

vascular endothelial cells[199]. Together both our work with PCBs and the work with TLR4 indicate polyunsaturated fatty acids, primarily omega-3 fatty acids, as a promising nutritional intervention[96]. Future work should continue to explore caveolae-based signaling mechanisms that are sensitive to nutritional modulation.

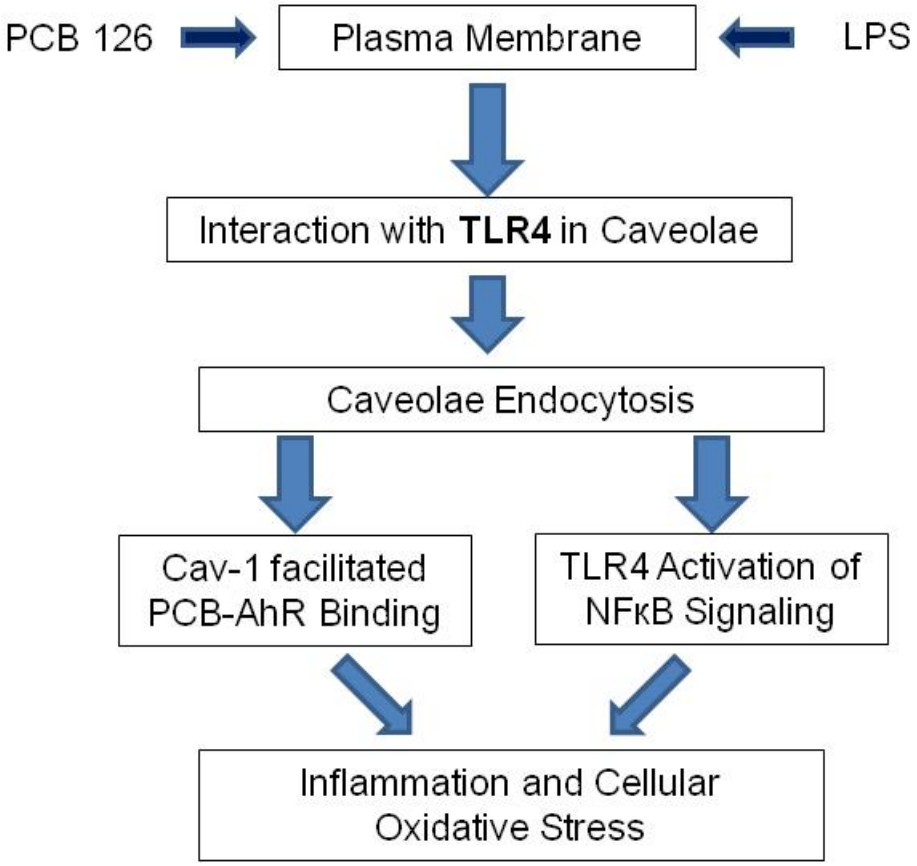

Figure 5.1 Summary of the proposed mechanism of action. Similar to LPS, PCB interaction with TLR4 in caveolae initiates endocytosis. PCB-activated TLR4 causes NFκB-induced inflammation, which contributes to AhR-mediated inflammation and oxidative stress.

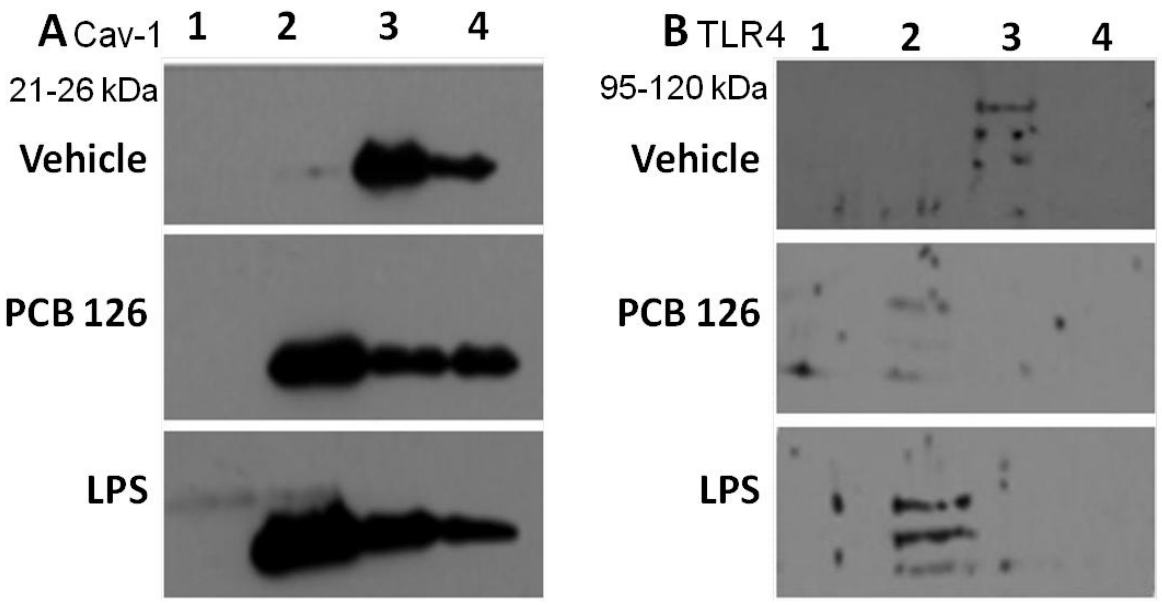

Figure 5.2 PCB 126 and LPS treatments stimulate a localization shift in caveolae fractions. Sucrose gradient lipid fractions 1-4 of 12 fractions showing localization of Cav-1 (A), and TLR4 (B) in lipid raft fractions after 30 minute treatment with DMSO vehicle (0.005%), PCB 126 (<1ppm), or LPS (0.1 μg/mL). (Higher molecular weight TLR4 bands are glycosylated proteins.)

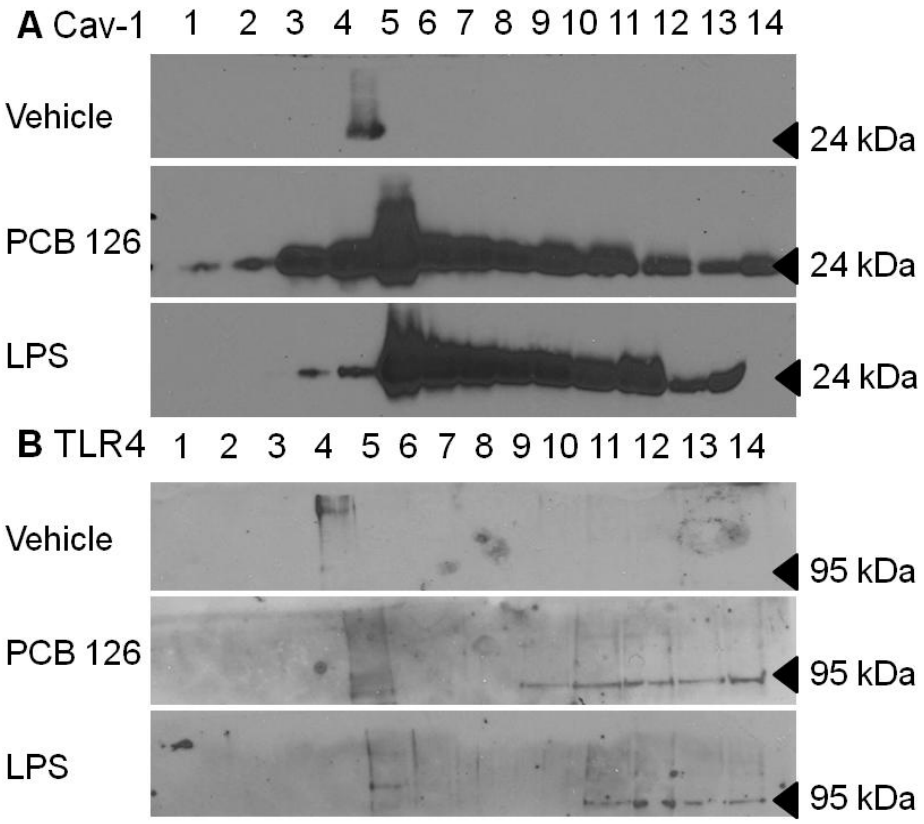

Figure 5.3 PCB 126 and LPS treatments promote Cav-1 and TLR4 migration within cellular fractions. Sucrose gradient fractions showing density localization of Cav-1 (A), and TLR4 (B) in lipid raft and non-raft fractions after 16 hr treatment with DMSO vehicle (0.005%), PCB 126 (<1ppm), or LPS (0.1 µg/mL). Fractions range from most (1) to least (14) buoyant.

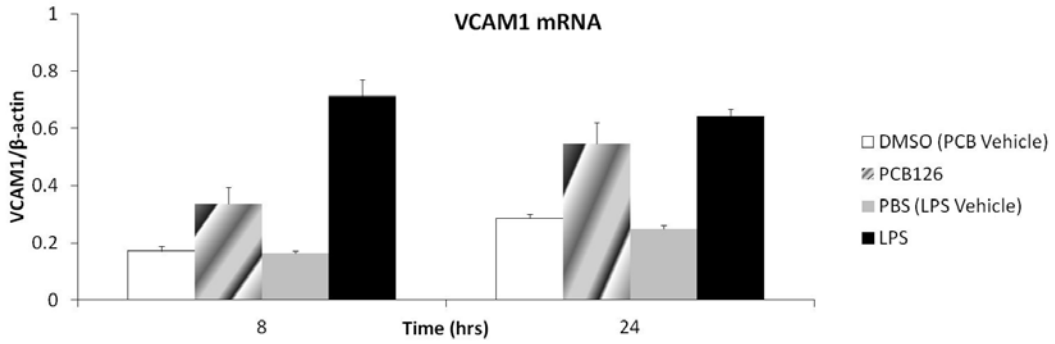

Figure 5.4 PCB 126 and LPS treatments significantly increase adhesion molecule expression. VCAM1 mRNA expression of primary porcine vascular ECs treated with PCB 126 (~ 1 ppm) with DMSO, vehicle control, and LPS (0.1 µg/mL) with PBS, vehicle control at 8 and 24 hours. Results are the mean + SEM, n=3. Significantly different compared with vehicle control at * P≤0.002 and significantly different from PCB 126 at $^{+}$ P≤0.05.

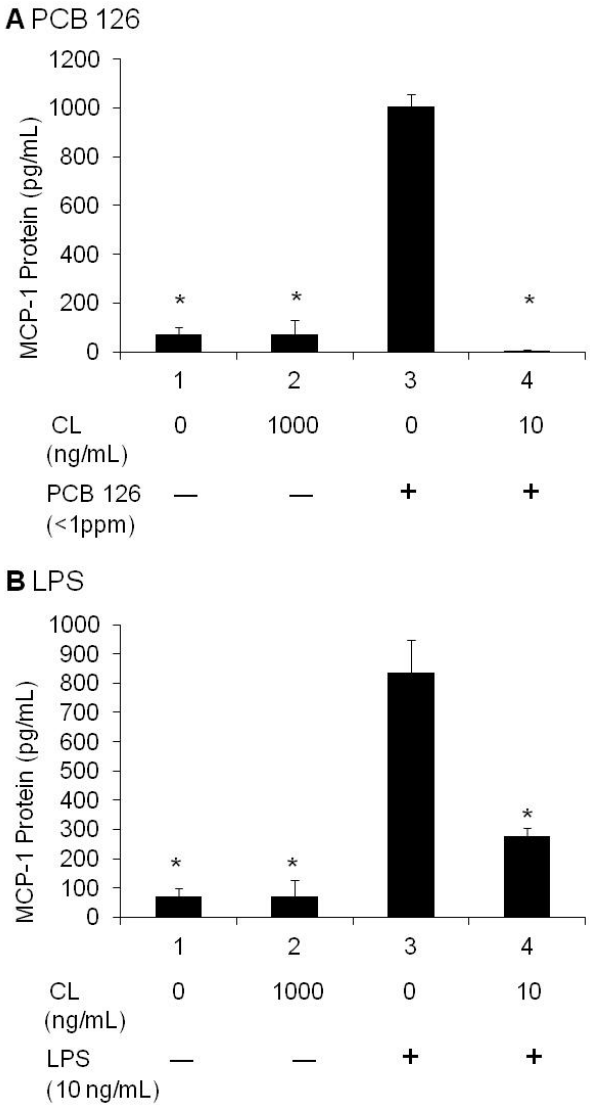

Figure 5.5 MCP-1 protein expression is attenuated by cardiolipin (CL) in (A) PCB 126 and (B) LPS treated cells. ELISA of MCP-1 protein expression in cell culture media collected from ECs treated with DMSO, vehicle control, (A) PCB 126 (<1ppm), or (B) LPS (10 ng/mL) and co-treated with 10 ng/mL cardiolipin (CL) for 24 hours. Significantly different compared with PCB or LPS, respectively at * P≤0.002.

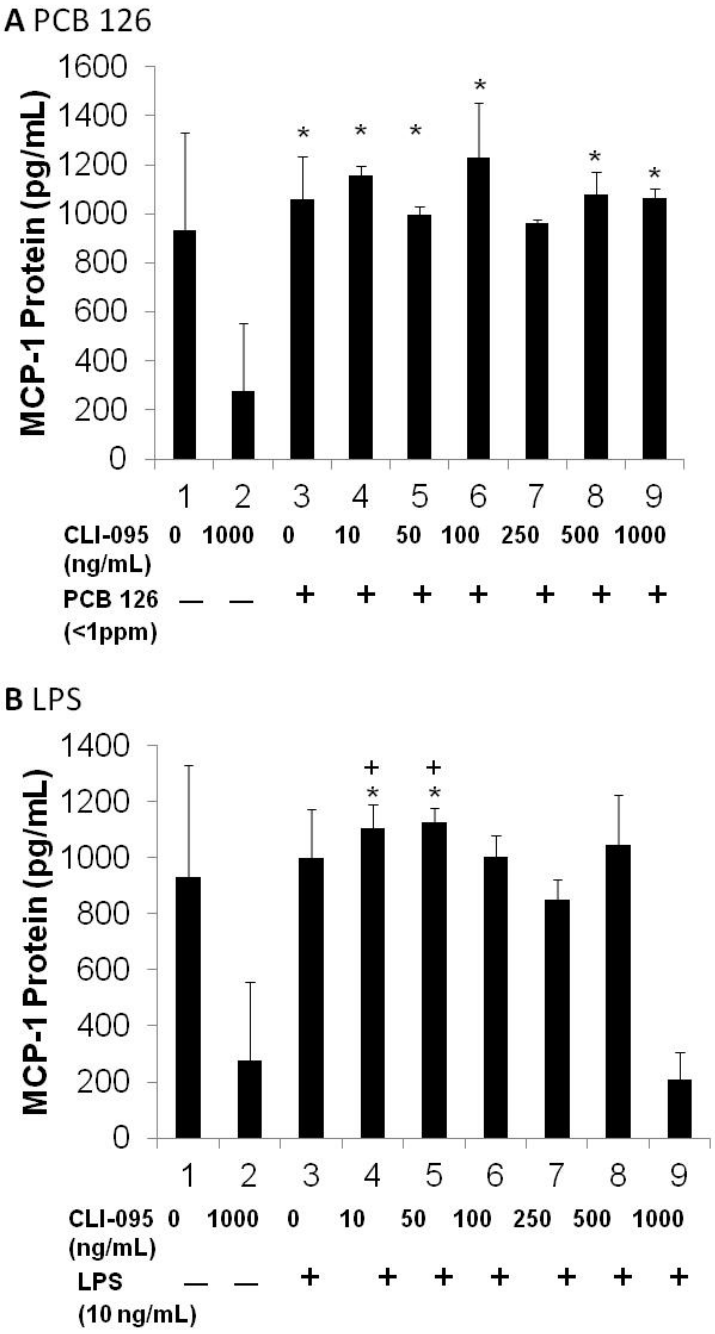

Figure 5.6 MCP-1 protein expression is not attenuated by CLI-095 in (A) PCB 126 but is attenuated in (B) LPS treated cells. ELISA of MCP-1 protein expression in cell culture media collected from ECs treated with DMSO, vehicle control, (A) PCB 126 (<1ppm), or (B) LPS (10 ng/mL) and co-treated with 10 ng/mL CLI-095 (TAK-242) for 24 hours. Significantly different from untreated 1000 ng/mL CLI-095, at * $P \leq 0.05$, and significantly different from 1000 ng/mL CLI-095 with LPS treatment, $^{+}$ $P \leq 0.05$.

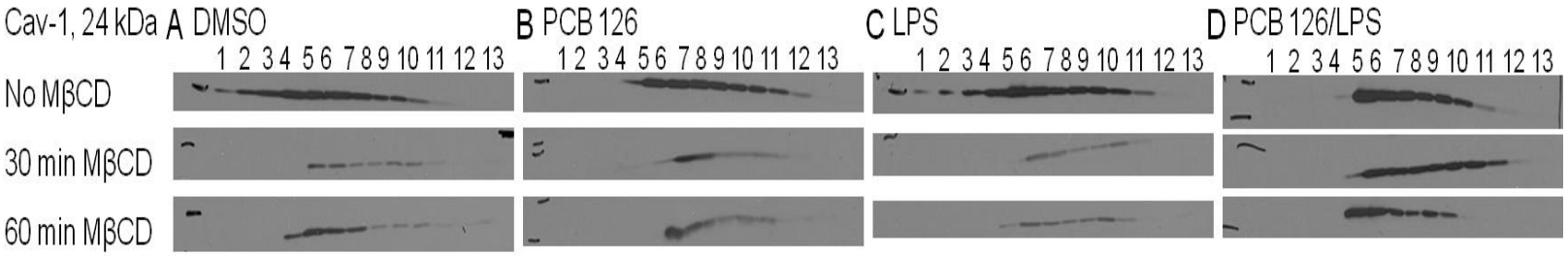

Figure 5.7 Membrane cholesterol depletion mitigates PCB 126 and LPS induced redistribution of Cav-1. Sucrose gradient fractions with no cholesterol depletion by MβCD, 30 min 10 mM MβCD or 60 min 10 mM MβCD and treatment with either (A) DMSO (vehicle control), (B) 0.25 μM PCB 126, (C) 0.10 μg/mL LPS or (D) 0.25 μM PCB 126 with 0.10 μg/mL LPS co-treatment.

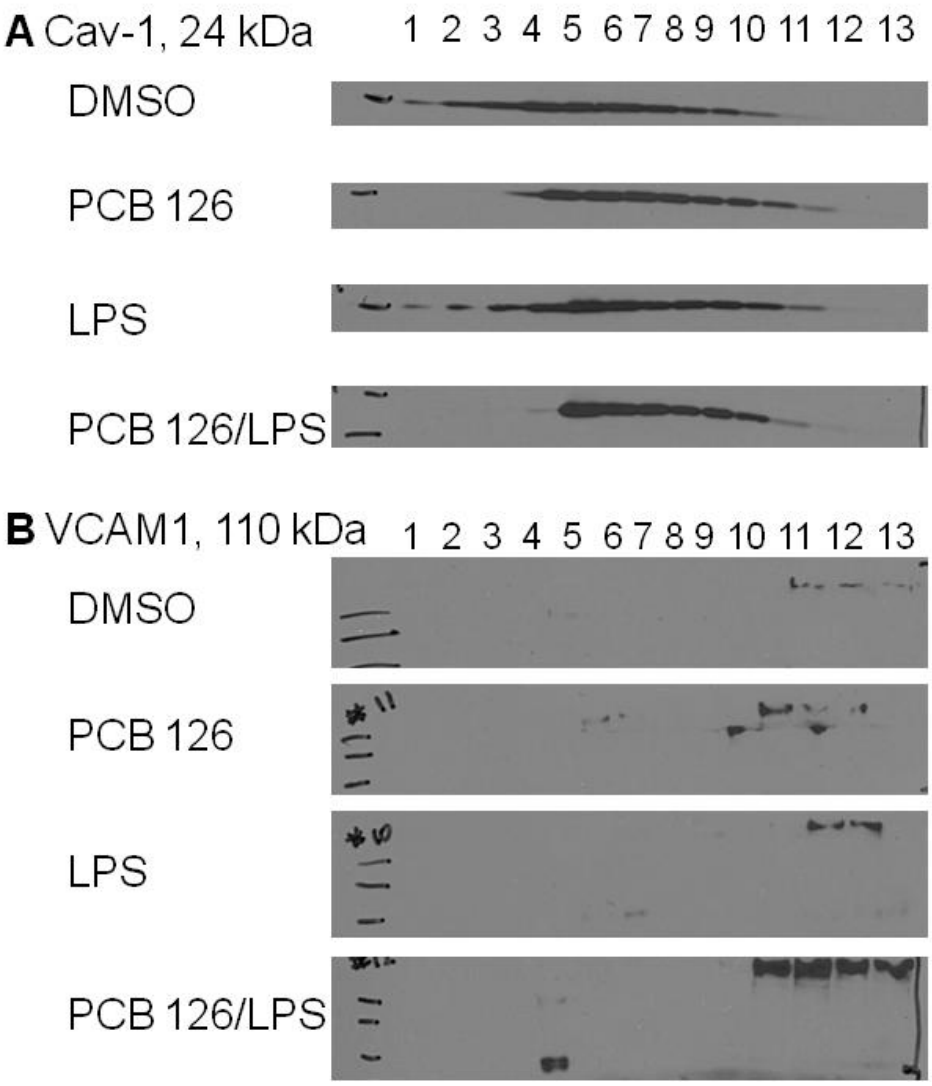

Figure 5.8 PCB 126, LPS and PCB126/LPS co-treated cells exhibit different patterns of (A) Cav-1 and (B) VCAM1 protein expression. DMSO (vehicle control), PCB 126 (0.25 μM), LPS (0.10 μg/mL) or PCB 126/LPS co-treated cell cultures produced different sucrose gradient fractionation patterns.

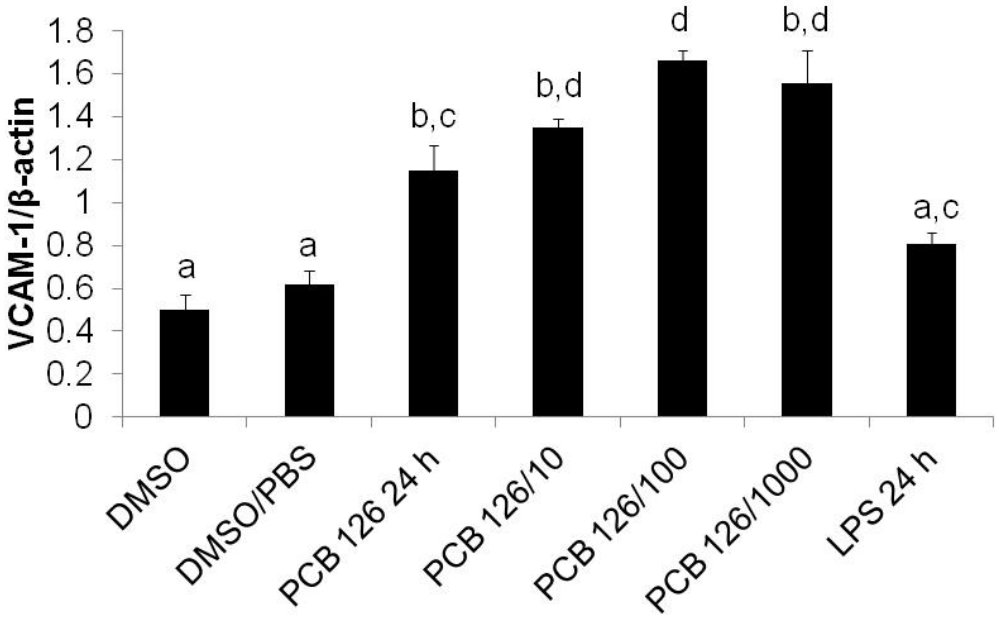

Figure 5.9 PCB 126 co-treatment with varying concentrations of LPS promotes different patterns of VCAM1 mRNA expression. Cell cultures were treated with PCB 126 for 16 hr and co-treated with LPS at 10, 100 or 1000 ng/mL for an additional 8 hr, and LPS treated for 24 hr at 1000 ng/mL. Statistical differences at p_{value} <0.05 is indicated by different letters; shared letters indicate no statistical difference between treatments.

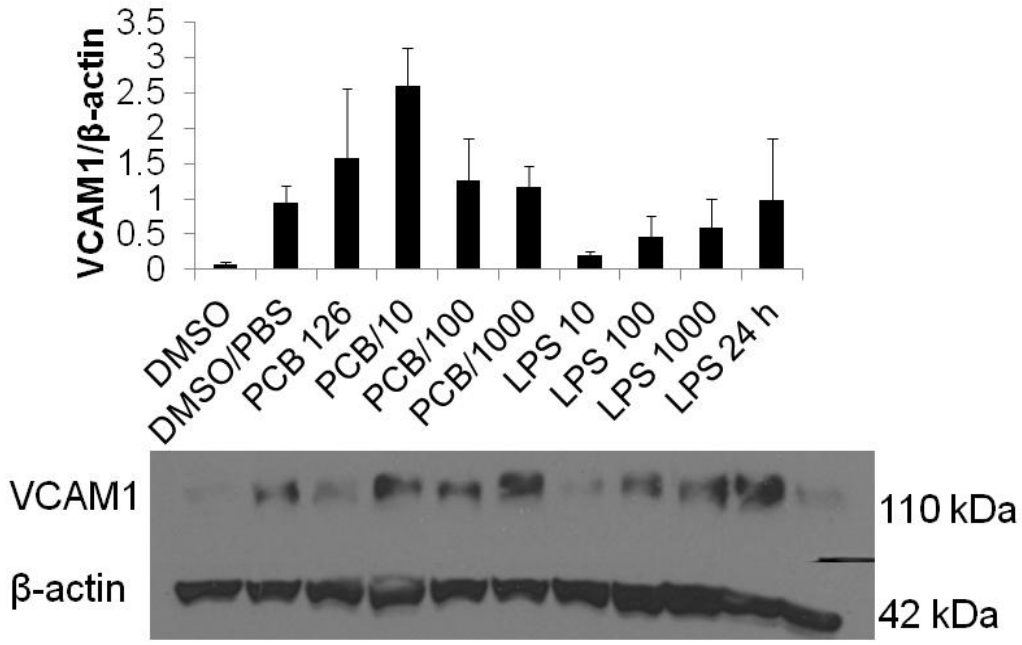

Figure 5.10 PCB 126, co-treated with varying concentrations of LPS exhibit different patterns of VCAM1 protein expression. Cell cultures were treated with PCB 126 for 16 h and co-treated with LPS at 10, 100 or 1000 ng/mL for an additional 8 hr. Western blot includes samples a and b of LPS 24 h treatment at 1000 ng/mL.

Chapter Six: Final Discussion – coplanar PCB-induced inflammation and nutritional modulation

6.1 Synopsis

Inflammation links multiple disease processes[58]. As persistent environmental pollutants, coplanar PCBs accumulate in human adipose[6, 173], and this toxic body burden promotes oxidative stress and endothelial dysfunction[73, 306]. PCB 77 and its dechlorination products are pro-inflammatory and promote oxidative stress in a primary endothelial cell model[307]. The persistence of coplanar PCB 126 in human tissues presents it as a more representative model for PCB-induced toxicity. We identified 5 µmol PCB 126/kg body weight as a pro-inflammatory but not overtly toxic dose in mice. Mitigating the effects of PCB-induced inflammation through nutrition is the most pro-active means of responding to environmental stressors. Omega-3 fatty acids and their neuroprostane metabolites have effectively attenuated PCB-induced oxidative stress in primary endothelial cells[16, 92]. We, therefore, fed mice a DHA-enriched diet and challenged them with PCB 126 to observe the metabolic and anti-oxidant response. At the same time, we pursued the caveolae based-TLR4 inflammatory signaling mechanism as a potential platform for better understanding the modulation of PCB-induced signaling through lipid rafts. Coplanar PCBs represents one class of many environmental stressors that promote inflammation. The anti-oxidant response mediated by Nrf2 and PPARγ and caveolae-based signaling are both mechanism which are sensitive to nutritional modulation by omega-3 fatty acids and as such present viable options for future investigation.

6.2 Dechlorination and inflammation

Remediation of persistent organic pollutants has been a significant portion of the response to environmental pollution. Our ability to assess the outcome of the remediation techniques is critical to verifying the effectiveness of emerging remediation strategies. In addition, the field of environmental toxicology needs to develop sensitive, high- throughput *in vitro* models that may be used to test dose, pharmacokinetic and toxicological implications of environmental toxins[308]. The products of dechlorination that were assessed in chapter two reveal the necessity of complete remediation[307].

6.2.2 Limitations and Future work

The inflammatory capacity of PCB 77 and its remediation products necessitated complete dechlorination. Biphenyl, though not toxic to our primary endothelial cell model, exhibits toxicity in the renal and neurological systems[309, 310]. In response to this challenge, the Chloro-Organic Degradation Project Research Team at the University of

Kentucky, College of Engineering has developed a more complete system that remediates the PCBs to biphenyl and biphenyl to mono- and di-hydroxybipheyls and benzoic acid[311].

Studying mixture toxicity has been one of the challenges for environmental toxicology. Thus, cell models which can be used to assess the total toxicity of a mixture rather than select or known constituents are beneficial. One system that is being tested to detect polycyclic aromatic hydrocarbons (PAHs), which are AhR agonists, utilizes a reporter assay that has an AhR sensitive promoter coupled to luciferase enzyme[312]. The assay, which is based in a mammalian cell line and utilizes benzo[a]pyrene as the reference molecule, is reported to produce a more meaningful assessment of complex mixtures than current assays which assess only known constituents. An alternative approach to the mixture problem is to define calculations that can combine toxicological data from individual toxicants and produce an accurate toxicity value for the mixture. In a model testing sex hormone synthesis, a generalized concentration addition model was most successful in predicting the testosterone effects of a mixture[313]. Together these approaches represent the next generation of toxicity assessment.

6.2.3 Contribution to our knowledge as a whole

The inflammatory potential of coplanar PCB 77 was sufficient to induce inflammation in our endothelial cell model, and the dechlorination products had reduced inflammatory potential but were not inert[307]. The human environment is saturated with chemical mixtures that activate an array of receptors and biological processes. Our work as well as the work of others focuses primarily on a specific toxicant or family of toxicants; as a result, many chemical stressors are not included in traditional risk assessment[314]. For this reason, a proactive response to environmental stress requires the identification of nutritional or lifestyle modulators of toxicological response and inflammatory stress[315].

6.3 PCB 126 as a model toxicant

PCB 126 distributes throughout the body but is primarily sequestered in liver and adipose. The highest doses of PCB 126 (50 and 150 µmol PCB 126/kg body weight) promoted wasting syndrome, increased expression of Bax protein, a key regulator of apoptosis, and increased VCAM1 protein expression. In contrast, the lowest dose (0 and 0.5 µmol PCB 126/kg body weight) did not contribute to weight change, increased expression of inflammatory endpoints, or indications of cellular apoptosis. Only the 5 µmol PCB 126/kg body weight dose produced a significant change in liver to body

weight ratio without significant weight lose, promoted the expression of MCP-1 and did not initiate Bax protein.

6.3.2 Limitations and Future work

As with any study, we had to limit the number of parameters that we examined. We choose a wide dose range which included 150 µmol/kg, a concentration that is equivalent to the dose of PCB 77 that was utilized in our previous animal work and is expected to be overtly toxic for PCB 126[91, 125]. The acute time point provides a limited view of the inflammatory response, and unlike studies of atherosclerosis this window was not sufficient to determine vascular outcomes in our animals. Previous work with PCB 77, indicates that vessel inflammation and lesion development are increased in animals challenged with PCB[91, 151]. The overview of this study would have been improved by some additional measurement. For example, an assessment of oxidative stress could have been made using tissue or urinary measures of 8-iso-prostaglandin $F_{2\alpha}$. Measurements of PCB 126 hydroxylated metabolites in the tissues and feces would have provided an indication of PCB 126 metabolism. Future optimization of this model should include collection of urine and feces for measures of oxidative stress and PCB 126 hydroxylated metabolites and include later time points to determine the progression of inflammation following acute exposure.

In fact, PCB 126 is very persistent in human tissues. A review of the general population revealed that levels of PCB 126 remained relatively static from 1989-2008 which is in contrast to decreased population levels of polychlorinated dibenzofurans (PCDFs) and polychlorinated dibenzo-para-dioxins (PCDDs)[316]. One possible explanation for the stable levels of PCB 126 in the human population is a species difference in rodent and human CYP1A1 binding pockets that prevents proper orientation of PCB 126 with the human heme for hydroxyl- metabolite formation[317]. The authors do not comment on whether this ineffective binding promotes CYP1A1 enzyme uncoupling and reactive oxygen species formation which would promotes cellular oxidative stress and inflammation. In a study of human intake, PCB 126 was not one the top congeners consumed but did contribute 67% of the TEF value, yet for all the toxicants consumed, the subjects did not exceed the current threshold set for allowable human consumption[318].

6.3.3 Contribution to our knowledge as a whole

As an acute exposure model, two doses of 5 µmol PCB 126/kg body weight are sufficient to elicit moderate inflammation. The long-term consequences of this exposure level have not been identified.

6.4 Omega-3 fatty acids and PCB 126-induced inflammation

Inflammation resolution is a major topic emerging in the omega-3 fatty acid literature. At present, there has not been a consensus on the inflammatory profile representing the changes expected from omega-3 immunomodulation. In some studies, the data include decreases in inflammatory cytokines like tumor necrosis factor alpha (TNFα), IL-6, and IL-8[101, 127]. Alternatively, others have reported sustained cytokine levels but reductions in F_2-isoprostanes[99]. The oxidized products and enzymatic metabolites of omega-3 fatty acids are active in inflammation resolution by promoting phagocytosis and class switching in leukoctyes and in cellular anti-oxidant and anti-inflammatory response processes that utilize nuclear receptors, i.e. Nrf2 and PPAR[102, 207, 319].

Organic pollutants, such as polychlorinated biphenyls, contribute to sustained systemic inflammation and promote diseases such as atherosclerosis[73, 320]. Dietary changes present a means of mitigating the inflammatory effects of pollutant exposure[92, 320]. The introduction of polyphenols, such as quercetin from vegetables and epigallocatechin gallate (EGCG) from green tea, and omega-3 fatty acids, such as α-linolenic acid from flax and DHA from fish oil, promote the expression of anti-oxidant enzymes and counteract PCB promotion of NFκB-induced inflammation[16, 92, 128, 130]. Nutritional modulation of Nrf2 and the PPARs is critical to the attenuation of PCB-induced inflammation[92, 130, 255].

6.4.2 Limitations and Future work

The DHA diet was developed following a literature search of diets in which feeding of diets with 2%-4% DHA from 4 to 12 weeks improved molecular and inflammatory outcomes[99, 210-212, 321]. In one feeding study, changes in plasma, eye, spleen, brain, and liver fatty acid composition were detected in Balb/c mice as early as three weeks of dietary feeding[230]; similarly, in a 10 week feeding study, they observed arachidonic acid decreases in lung at 2 weeks and by 3 weeks omega-3 fatty acid levels had reached a steady state[99]. PCB 126 is a persistent organic pollutant which promotes the development of inflammatory diseases over time; therefore, future studies might assess the interaction of PCB-induced inflammation and dietary DHA over a broader time range

which will allow us to assess when DHA modulates acute inflammation and inflammation resolution. Example time points may include submandibular blood collection 24 h and 4 days after the initial gavage and takedowns 24 h, 2 weeks, and 4 weeks after the final gavage. These time points are inferred from a study of impaired glucose tolerance which observed glucose intolerance in mice receiving coplanar PCB 77 beginning after the second gavage on week 2 through the duration of the 12 week study[322]. The tissue levels of coplanar PCB 77 were decreased well below 50% by week 4 of the study, yet the metabolic disturbance and TNFα levels in the adipose persisted[322]. From these observations, we may imply that the inflammatory actions of coplanar PCBs are sustained and thus extended observation would be advised. The investigation of PCB 77-induced glucose tolerance revealed an interesting role for dietary fat which indicates that modulation of the PCB-77 induced insulin disturbance and TNFα tissue levels may be influenced by dietary fat composition[70]. Those mice receiving a high fat diet (60% kcal from fat) did not experience PCB-induced differences in glucose tolerance; however, after weight loss on low fat (10% kcal from fat), the mice experienced coplanar PCB-induced decreases in glucose and insulin tolerance. The recommended human consumption of fat is 30% kcal or less, which makes this diet of 25% kcal from fat a moderate representative of human consumption[323], yet a recommended rodent diet contains only 10% kcal from fat[324]. The present study of dietary DHA as intervention for PCB 126-induced inflammation may be limited by the moderate fat content of 25% kcal from fat, which may promote storage rather than metabolism of PCB 126. Future studies of dietary DHA as a modulator of PCB-induced inflammation should consider the use of both low and high fat diets and multiple ratios of omega-3 fatty acid to determine the most effective intervention[252].

A significant portion of the omega-3 fatty acid literature assesses the changes in leukocyte behavior following an inflammatory stimulus[85, 207, 225, 325]. Continued investigation into the role of omega-3 fatty acids in mitigating coplanar PCB-induced inflammation should include and assessment of inflammatory capacity, e.g. cytokine response/profile, and phagocytic ability in macrophages and natural killer cells. In addition, a follow-up DHA feeding study designed to include atherosclerotic lesion assessment would enable us to visualize changes in both inflammatory markers, such as MCP-1 and VCAM1, and macrophage accumulation. We would expect that the improved cellular anti-oxidant environment of DHA-fed mice would reduce lesion

formation to model baseline. DHA feeding promotes the expression of PPARγ, which is protective against atherosclerotic lesion development[326].

The changes in cholesterol and glucose tolerance are indicative of underlying metabolic changes, which may be driven by novel DHA oxidation products[103]. Identification of the novel lipid mediators could be accomplished through a comparison study of the lipid mediators produced in mice challenged by PCB 126 or LPS. Our present assessment was limited primarily to monohydroxy- metabolites and did not investigate potential oxidized DHA metabolites[92, 204, 205, 249]. Investigation into novel lipid mediators should also include nitro fatty acids. Polyunsaturated fatty acid-derived nitro fatty acids are potential modulators of PPARγ, Nrf2, and the NFκB subunit p65[327-330]. The activities of these novel lipid mediators involve interactions with PPARγ and Nrf2 nuclear receptors. For this reason, subsequent *in vitro* studies should begin by exploring the interactions of Nrf2 and the PPARs with novel lipid mediators following coplanar PCB stimulation.

6.4.3 Contribution to our knowledge as a whole

The 25% kcal from fat content of the diet may have mitigated the overall response to DHA-enriched diet as was indicated by others in a different model of inflammation[252]. The dietary fat content could also moderate the metabolic and inflammatory response to PCB 126 exposure. In a study of coplanar PCB-induced metabolic dysregulation after weight loss, the authors demonstrated that mice fed a high fat diet did not experience the negative changes in glucose and insulin tolerance that affected mice who underwent weight loss and mobilization of PCBs from the adipose depots[70]. Together dietary fat content greater than 10%, low fat, may dampen the effects of both PCBs and omega-3 fatty acids by promoting storage rather than metabolism.

The literature emphasizes the role of enzymatic and oxidized metabolites in the regulation of inflammation resolution and metabolism[205, 207, 331]. Research from our laboratory has demonstrated the anti-inflammatory potential of oxidized DHA in the activation of Nrf2 inflammatory response[92]. In a similar study, activation of Nrf2 was observed with oxidized eicosapentaenoic acid (EPA) neuroprostanes[205]. 15-deoxy-$\Delta^{12,14}$-PGJ_3, an EPA cyclooxygenase dehydration product, also activates PPAR to induce adiponectin, which promotes insulin sensitivity[243, 331]. Our work supports the activity of arachidonic acid-derived,15-deoxy-$\Delta^{12,14}$-PGJ_2, which activates Nrf2[227]. These observations alter the previous paradigm which focused on the pro-inflammatory effects of arachidonic acid metabolism, LDL oxidation and lipid peroxidation[332, 333]. The

activation of pro-resolving, anti-inflammatory and metabolism stabilizing lipid mediators requires dietary supplementation to proactively modulate the inflammatory response[334].

6.5 Synergy of innate immunity and PCB-induced inflammation

One of the mechanisms by which DHA and other omega-3 FAs provide protection involve interactions with lipid domains and may be similar to that of the signaling changes induced by the phospholipid cardiolipin[267, 293]. Lipid rafts, like caveolae, are sensitive to changes in membrane lipid homeostasis and are responsive to dietary modulation which alters the functional role of lipid rafts in disease[335]. Caveolae host critical signaling domains, which include the LPS receptor toll-like receptor 4 (TLR4)[278, 336]. Caveolae are sensitive to lipophilic pollutants and facilitate the inflammatory cascade which leads to NFκB activation[124-126].

Caveolae have been established as critical inflammatory mediators[105]. In our research, response to stimulation from PCBs and LPS required the presence of caveolin-1 in the plasma membrane. Activation of caveolin-1 by PCBs displaced TLR4 from the lipid raft fractions. The response was not linked to direct TLR4 activation by PCBs but signaling changes occurring within the caveolae domain. In this context, we were able to observe the additive effect of PCB and LPS co-stimulation.

6.5.2 Limitations and Future work

Primary endothelial cells are caveolin-1 (Cav-1) rich, and provide a sensitive model for the study of endothelial dysfunction and inflammation[126, 276]. A comparison of immortalized endothelial cell lines and human umbilical vein endothelial cells (HUVECs) indicates that certain inflammatory and immunological signaling factors, such as VCAM1 and MHC class II antigens, are not mutually expressed[337]. The primary pulmonary porcine endothelial cells used for the experiments in chapters two and five have inducible expression of key inflammatory markers including VCAM1 and MCP-1[125, 126]. However, primary cell lines may not consistently express certain markers after passaging as is the case with CD14, a TLR4 chaperone protein[304]. Future studies should include an immortalized endothelial cell line, such as the EAhy926 cells, which would serve as a control for potential loss of key signaling proteins. In our experience, the EAhy926 cells produced similar but less robust MCP-1 protein expression in response to PCB 126 or LPS in the cardiolipin inhibition assay when compared to the primary endothelial cells (data not shown).

Caveolae are critical to the signaling of cellular stressors such as LPS and PCBs, and these domains are also necessary for the protective signaling response that comes from interaction with certain phytochemicals such as quercetin and EGCG[128, 129]. The signaling controls which modulate the differences between response to environmental pollutants and nutritional interventions are not well understood, and thus, the role and function of caveolae domains remain an important aspect of future studies.

The additive nature of PCB 126 and LPS co-stimulation presents an interesting dynamic for future study. Others have published that PCBs promote barrier dysfunction and PCB/LPS co-stimulation enhances PCB-induced dysfunction of the blood brain barrier[67]. One avenue through which TLR4/MyD88 and TLR4/TRIF signaling are initiated is the PI3K/Akt pathway[338]. LPS induction of TLR4/PI3K has been modulated by the saturated fatty acid, lauric acid, which promotes transient Akt phosphorylation; in contrast, the polyunsaturated fatty acid, DHA, suppresses NFκB activation in a TLR4/PI3K-dependent manner[339]. Further, investigation of TLR4/PI3K signaling suggests that PI3K functions as a regulator that limits TLR4 signaling through modification of the local phospholipid composition[340]. Our research has also demonstrated both PI3K-associated signaling and fatty acid-dependent modulation of PCB-induced inflammatory response, providing PI3K as a potential link between the membrane-based TLR4 signaling in caveolae and the downstream activities of PCBs. Further lipid rafts are known to be critical modulators of Src activated PI3K/Akt signaling[341]. We established that PCBs modulate the phosphorylation of endothelial nitric oxide synthase (eNOS) through Src mediated PI3K/Akt activation[164]. Akt is a critical initiator of many cellular processes and is therefore is a potential regulator of PCB/LPS co-stimulatory events.

The cellular inflammatory response is sensitive to different stimuli and combination of stimuli. Emerging research suggests that low level exposure to an inflammatory stimulus disengages negative feedback mechanism and prolongs the inflammatory response[297]. When applied to our work, low level chronic exposure to PCBs has the potential to disrupt the negative feedback response to inflammatory stimuli and promote chronic inflammation that leads to atherosclerosis and other chronic disorders. Further, the “deprogramming” of low dose inflammatory stimuli establishes a condition in which a higher secondary stimulus initiates a hyperactive response due to insufficient negative feedback[342]. As of yet, the role of environmental pollutants in this mechanism have not

been studied, but PI3K and Akt are key regulators of this pathway, the actions of which warrant further study in our model.

6.5.3 Contribution to our knowledge as a whole

This work substantiates previous research which has indicated the role of caveolin-1 as being critical to the inflammatory response to lipophilic environmental stresses, such as coplanar PCBs[124, 126]. Caveolae have the capacity to respond to multiple stressors. The strength or specificity of the inflammatory stimuli activates different receptors and signaling pathways to culminate in an inflammatory response, yet caveolae are sensitive to modulation by omega-3 fatty acids and phytochemicals which activate anti-oxidant pathways[97, 128].

6.6 Implications

The environment that we live in contains a mixture of pollutants that includes legacy chemicals like PCBs and newly synthesized toxicants that have not yet been recognized as health hazards[343]. The risk for heart disease, diabetes, liver disease, and other inflammation- related disorders increase with exposure to PCBs and other persistent organic pollutants[59, 62, 64, 66, 71]. When studying subjects who have high dietary fish intake and as a result have both increased pollutant exposure and increased omega-3 intake, the increased pollutant exposure has negative outcomes such as increased arterial stiffness, but the vascular inflammation is reduced in response to a high intake of omega-3 fatty acids[203]. Our observations suggest that even low exposures to coplanar PCBs, such as PCB 77 and its dechlorination products, promote inflammation in vascular endothelial cells. PCB 77 promotes endothelial dysfunction and vascular inflammation, by for example, increasing the expression of VCAM1 in the artery wall[14, 91]. Lipid exposure regulates the extent of the PCB 77-induced inflammatory response with omega-6 linoleic acid promoting inflammation while omega-3 α-linoleic acid and high oleic acid-olive oil counter regulate the inflammation, respectively[15, 16, 91].

As a coplanar PCB, PCB 126 is an AhR ligand, and the pro-inflammatory potential of PCB 126 is demonstrated by the induction of IL-8 and MCP-1 in pre-adipocytes and differentiated adipocytes[344]. These findings implicate that PCB 126 promotes inflammatory markers which are generally associated with obesity and diabetes[345, 346]. PCB 126 affects cardiovascular outcomes as well. For example, in the 1999-2002 NHANES (National Health and Nutrition Examination Survey) data, heightened serum PCB 126 was strongly associated with a risk for hypertension[347], and animal models

suggest an association between PCB 126 and the development of vascular lesions[168]. PCB 126 is a very stable dioxin-like congener which is detectable in human blood samples and is consumed through the human diet [316, 318]. These studies substantiate human exposure through dietary sources, but implicate a limited human capacity to metabolize and excrete PCB 126. The literature does not define whether the toxicity of PCB 126 is primarily derived from the parent compound or the hydroxylated metabolites. In our *in vivo* exposure model, PCB 126 activates a moderate inflammatory response including the upregulation of CYP1A1 and MCP-1, which we attribute to the activity of the parent PCB and the AhR. The epidemiological literature suggests that PCB 126 contributes to inflammatory disease states, but the human experience includes exposure to mixtures of PCBs and other toxicants. In a comparison of persistent organic pollutants (POPs) and plastic-associated chemicals (PACs), such as bisphenol A and phthalates, there was more evidence supporting the role of POPs in cardiovascular disease, yet sufficient literature supports a link between the PACs and vascular disease that it could not be excluded from consideration[348]. In conclusion, avoiding a single toxicant over another does not eliminate disease risk.

For this reason, nutrition and other healthy lifestyle choices are the best option for maintaining health. Omega-3 fatty acids and the metabolites resolvin E1 and protectin D1 promote insulin sensitization in an ob/ob mouse model[239]. The protectins and resolvins promote inflammation resolution by directing leukocyte class switching which promotes cytokine expression patterns that drive wound healing[334]. The oxidized DHA neuroprostanes promote Nrf2 mediated protection against coplanar-PCB induced inflammation[92], and EGCG, a green tea catechin, provides protection against TNFα-induced inflammation via a similar mechanism[129, 349]. Omega-3 fatty acids and phytochemicals both inhibit LPS-induced inflammation through TLR4[107, 350]. The former inhibits dimer formation and migration into lipid rafts[107], and the latter alters phosphorylation patterns of the TLR4 cysteine residues; thus, altering dimer formation, which is required for associated inflammatory signaling[350]. Our data suggest that the presence of DHA or its metabolites promote the anti-oxidant activities of PPARγ and Nrf2, which increase HO-1 and NQO1 expression to mitigate PCB-induced inflammation. Together these studies substantiate the hypothesis that modulation of diet promotes an anti-inflammatory environment within a living organism.

Appendix

Electrophoretic Mobility Shift Assay (EMSA)

Harvesting cells for nuclear extraction:

1) Aspirate media from 10 cm plates.
2) Rinse 2X with 10 mL cold 1X PBS.
3) Add 2 mL of PBS and scrap plates.
4) Transfer to 15 mL conical tubes (on ice) and pelleted cells at 500 x g for 5 min at 4°C.
5) Remove the supernatant leaving the cell pellet as dry as possible.
6) Premade buffers for 10-15 ul cell volume for a 100 mm plate (keep on ice):
    a. Reagent volumes per sample for the NE-PER Nuclear and Cytoplasmic Extraction Reagents kit (Thermo Scientific):

Packed Cell Volume (µL)	CER I (µL)	CER II (µL)	NER (µL)
10	100	5.5	50
20	200	11	100
50	500	27.5	250
100	1000	55	500
Protease Inhibitor (Halt) Required	Yes		Yes

7) Add ice-cold CER I buffer and vortex on high for 15 s to suspend the pellet.
8) Let stand on ice for 10 min.
9) Add ice-cold CER II to the tube.
10) Vortex for 5 s on the highest setting and incubate on ice for 1 min.
11) Vortex for 5 s on the highest setting. Centrifuge the tube for 5 min at max speed in a microcentrifuge. (16, 000 x g, 4°C, 5 min)
12) Immediately transfer the supernatant (**cytoplasmic extract**) to a clean pre-chilled tube. Hold tube on ice to assess protein concentration or for storage. (Measure the protein concentration by BCA or store at -80°C.)
13) Suspend the nuclear pellet in ice-cold NER.
14) Vortex on high for 15 s. Place the samples on ice and vortex for 15 s every 10 minutes, for a total of 40 min.
15) Centrifuge tubes at 16, 000 x g, 4°C for 10 min.
16) Immediately transfer the supernatant (**nuclear extract**) to a clean pre-chilled tube. Place on ice.
17) Perform BCA or Bradford to determine protein concentration and store at - 80°C.

Prepare and run EMSA:

1) Set up gel cassette molds.
2) Prepare 6% (or 4.5%) Acrylamide Gel (EMSA does not require a stacking gel):

Reagent	6% gel	6% gel	4.5% gel	4.5% gel
diH_2O (mL)	14.1	28.2		
10X TBE buffer	2.5	5.0		
40% bis-acrylamide	3.125	6.25		
10% APS (uL)	250	500		
TEMED	20	40		
Total	20 mL	40 mL	20 mL	80 mL

3) Fill the cassette to just over the edge and insert comb.
4) Allow gel to set until solidified and wells are well-formed. (1h-1.5hrs)
5) Pre-run the gel with 0.5X TBE buffer for 30 min. or more at 60V, RT.
6) Meanwhile, prepare samples for gel electrophoresis:

    a. Set up EMSA reactions in order with a 5 min incubation before adding the biotin labeled probe:

Reagents	1	2	3	4	5	cold	no extract
Ultrapure Water	11.0	11.4	11.5	11.6	11.6	10.0	15.0
10X Binding Buffer	2.0	2.0	2.0	2.0	2.0	2.0	2.0
1 ug/ul Poly(dI*dC)	1.0	1.0	1.0	1.0	1.0	1.0	1.0
cold (10 µM) or bio-mutant (100 nM)						2.0	
Nuclear Ext (5 µg)	4.0	3.6	3.5	3.4	3.4	3.0	0.0
Incubate 5 minutes.							
Biotin-Probe (100 nM)	2.0	2.0	2.0	2.0	2.0	2.0	2.0
Total Volume	20	20	20	20	20	20	20

    b. Incubate for 20 min at RT.

7) Add 4 µL of 6X orange/blue loading dye with triturating to each sample.
8) Check wells; if not well formed, flush with 0.5X TBE buffer to clear.
9) Load samples into gel and run at 70 V at RT for ~ 1 h.
10) Pre-soak the pads and nylon membrane for a minimum of 10 min in 0.5X TBE buffer.
11) Rinse gels in 0.5X TBE buffer and assemble for semi-dry transfer.
12) Transfer via semi-dry transfer at 300 mA for 30 min at RT.
13) Remove membrans and allow to dry face up on a Kim wipe. (2-5 min)
14) Cross-link for ~ 45 s (use automatic setting) at 120 mJ/cm^3 using a commercial UV cross-linker.

Detection of the biotin binding

1) Block the nylon membrane for 30 min in blocking buffer with shaking on an orbital shaker.
2) Prep the Conjugate/blocking buffer cocktail (66.7 µL stabilized streptavidine-horseradish peroxidase conjugate to 20 mL blocking buffer (1:300 dilution)).
3) Decant blocking buffer and replace with the Conjugate/blocking buffer cocktail for 15 min on orbital shaker.
4) Prepare 1X wash solution 30 mL 4X wash solution to 90 mL H_2O.
5) In fresh boxes, wash membranes for 4X at 5 min each with wash solution.
6) Prepare the substrate working solution. (Start with the following dilution and incrementally increase as necessary):
   1 mL each Luminol Enhancer Solution and Stable Peroxide Solution plus 8 mL dH_2O for a total of 10 mL.
7) In a fresh box, cover nylon membranes with substrate working solution for 5 min, and gently rock by hand to maintain coverage of the membranes.
8) In a cassette, place membranes in a plastic sheath and photograph in the dark room starting with 1 min.
9) Store nylon membranes in dH_2O, if necessary.

Ordering probe from IDT

1) Determine probe sequence from literature. If a porcine sequence is not available, use a validated human sequence.
2) On the IDT website select “Custom DNA Oligos.”
3) Select duplex, and a space will appear for the insertion of a second sequence.
4) Name the sequence.
5) Paste the sequence and press the complement button. (The complement should appear in the alternate space.)
6) No additional purification required. Select amount based on needed; generally the lowest is sufficient for us.
7) For each sequence, go to the bottom and select “5’ modification”.
8) Select /5Biosg/, 5’ Biotin.
9) To order cold probe, do the same set-up, but do not add the biotin tag.

Preparing probe for EMSA

1) Reconstitute the lyophilized stock based on nmol of product, e.g., 94.8 nmol make Stock 1: 100 µM with 948 µL of diH_2O.
2) To make Stock 2 for the biotin labeled probe, dilute Stock 1 - 1:1000 to 100 nM (for the ChemiEMSA).
3) To make Stock 2 for the cold probe, dilute Stock 1 - 1:10 to 10 µM (for the ChemiEMSA).

Protein Isolation from Cells

1) Aspirate media.
2) Rinse 2X with 2mL cold 1X PBS.
3) Carefully, remove residual PBS by pipette.

4) Apply premade lysis buffer, 200 ul for a 35mm plate (keep on ice); 100-150 uL per 6 -well:
    a. Lysis buffer Option A:

Reagent	1 mL	2.5 mL	5 mL	10 mL
diH_2O (mL)	0.780	1.95	3.90	7.8
10X RIPA buffer	0.100	0.25	0.50	1.0
10% SDS	0.100	0.25	0.50	1.0
100X EDTA (uL)	10	25	50	100
Protease Inhibitor (Halt)	10	25	50	100

    b. Lysis buffer Option B:

Reagent	1 mL	2.5 mL	5 mL	10 mL
diH_2O (mL)	0.750	2.00	3.92	7.84
10X RIPA buffer	0.125	0.25	0.50	1.0
10% SDS	0.125	0.25	0.50	1.0
Aprotinin (uL)	0.25	0.50	1.0	2.0
Pepstatin A	1.25	2.50	5.0	10.0
PMSF	12.5	25	50	100
NaF	6.25	12.5	25	50

    c. Lysis buffer Option C:

	1 mL	1.5 mL	2 mL	3 mL	4 mL	5 mL	6 mL
Lysis (-) (mL)	0.974	1.464	1.948	2.922	3.896	4.87	5.84
NP-40 (uL)	5	7.5	10	15	20	25	30
PMSF	10	15	20	30	40	50	60
Na_3VO_4	1	1.5	2	3	4	5	6
Protease Inhib. Cocktail	10	15	20	30	40	50	60

5) Scrap plates, pipette up and down 10-20X, and transfer lysate to 1.5 Eppendorf tubes.
6) Sonicate for 10 sec. with the sonicator set at 20 and 4.
7) Let stand on ice for 30 min.
8) Centrifuge for 15 min. @ 13,000rpm and 4°C.
9) Transfer supernatant to chilled Eppies and freeze on dry ice.
10) Store at -80°C.
11) Measure the protein concentration by BCA.

Protein Isolation from Tissues

Equipment: forceps, scalpel, weigh boats, autoclaved mortar and pestle, power drill, labeled 1.5mL tubes on ice, 1X RIPA buffer (no SDS) on ice, 2 mL serological pipettes and pipette aid, diH_2O & 70% EtOH for cleaning/sterilization

1) Make 1X RIPA buffer and set on ice. Label tubes and set on ice.

Reagent	1 mL	2.5 mL	5 mL	10 mL
diH_2O (mL)	0.880	2.25	4.40	8.8
10X RIPA buffer	0.100	0.25	0.50	1.0
100X EDTA (uL)	10	25	50	100
Protease Inhibitor (Halt)	10	25	50	100

2) Tare weigh boat on analytical balance. Quickly open frozen tissue sample and remove a piece of tissue with the scalpel using forceps to transfer to weigh boat. (Tissue should weigh between 0.04-0.08g.)
3) Insert mortar into power drill. Add 300uL of 1X RIPA buffer to the pestle and insert the tissue sample. Homogenize the sample using the mortar/power drill, moving mortar up and down as necessary to homogenize the entire sample.
4) Carefully, remove the homogenized sample by pipette and place in chilled 1.5mL tubes.
5) Sterilize the equipment with EtOH and remove residual sample matter with diH_2O after each sample.
6) Once sample have been collected, sonicate for 10 sec. with the sonicator set at 20 and 4.
7) Let stand on ice for 30 min.
8) Centrifuge for 15 min. @ 13,000rpm and 4°C.
9) Transfer supernatant to chilled Eppies and add 600uL of DN/RNase free H_2O to dilute.
10) Freeze on dry ice, and store at -80°C. Or, proceed to BCA.
11) Measure the protein concentration by BCA. In the BCA plate, dilute each sample 1:5 (1uL sample: 4uL diH_2O).

Sucrose Gradient Procedure

Harvesting

1. Cells grown on 150mm x25mm plate/treatment were washed with 1X PBS twice (around 5 ml a time), then lysed with 2 mL of ice-cold MES buffered saline (MBS; 25mM MES (morpholineethanesulfonic acid, pH 6.5) 150 NaCl) containing 500 mM Na_2CO_3. Scrape plates.
    a. Prepare:
        i. 25mM MES: 2.4405g (MEShydride, Sigma # M2933-100g) in 500 ml water. Adjust PH to 6.5.
        ii. Then add 4.383 NaCl into MES to make MBS.
        iii. For lysis buffer, take 50mL MBS, add 2.65g Na_2Co_3, get 500mM.
2. Homogenization was carried out with 10 strokes of a loose-fitting Dounce homogenizer (7mL) (aka the adapter homogenizing tips fitted to the power drill, 10 strokes with samples in the special glass tubes [volume 2mL lower part]). Make sure to wash adapters and tubes with DI water and 70% ethanol between

samples. After homogenizing, pour into 15ml conical tubes for sonication: 15 strokes set at 4.
3. After sonication, centrifuge at 3000rpm for 10 min at 4°C.
4. Collect supernatant into centrifuge tubes (14x89mm), if it's not exactly 2ml, add more MBS to reach 2ml.

Ultracentrifugation

1. Make your sucrose solutions
    a. 90% Sucrose: 45g sucrose and make final volume to 50ml using MBS solution. Heat in water bath and/or sonicator to dissolve.
    b. 35% Sucrose: 17.5g sucrose and final volume 50 ml.
    c. 5% Sucrose: 2.5g sucrose and final volume 50 ml.
2. In Ultraclear Centrifuge tubes (14x89 mm Cat#344059, Beckman Coulter, Inc, Brea, CA) , combine 2 fractions of lysate sample with 2 fractions of 90% sucrose in the bottom of an ultracentrifuge tube. A fraction is 800µl. Be sure to cut the tip larger for the thicker 90% sucrose solution. Vortex for 5 seconds on medium speed. Volume should now be 3.2 ml.
3. Carefully layer on 5 fractions of 35% sucrose. The first two fractions should be done drop by drop, down the inside side of the tube. Be sure to check for a layer for the first 2 fractions, then addition can be faster, but still along the side to keep mixing from occurring. Volume should be around 7.2 ml.
4. Carefully layer on 3 fractions of 5% sucrose in same manner.
5. Make sure to cool down ultra-centrifuge. Set to program of 39k m/s, 18 hours + 2 hours at 0 m/s, Max Accel, no brake, 4°C. Should be under "Hennig Sucrose Gradient" program name.
6. Change gloves, wipe outside of tubes with DI water and chemwipes, and slide tubes into the swinging buckets (should be cleaned before with DI water and 70% ethanol). This is to insure there are no sugar grains on the outside of the tubes.
7. Place your first sample on the scale, then add a final fraction of 5% sucrose. Rotate through the other tubes, adding the final fraction to all to the point that they are within 0.01g of each other.
8. Place vacuum grease on the threads of all the bucket caps before screwing them into place.
9. Carry out and load onto rotor & into ultracentrifuge. Initiate program. Make sure to check back in 30 min or so to assure no problems have occurred.

Fraction collection

1. After removing the buckets, remove the first fraction while tube is still in the bucket. Fractions are same as before, 800 µl.
2. Then, remove tube from bucket and place in holder.
3. Gently remove the remaining fractions. Make sure to keep the tip of the pipette just below the surface. There will be a total of 13 fractions.
    a. There is usually a floating mass near the bottom of the 4^{th} fraction. Be sure to collect it only in the 4^{th} fraction until it actually seems to be lower,

in the 5th fraction. Be careful, because as you collect, the mass may try to shift downward.

4. Aliquot fractions a couple times (7µl sample buffer+ 42µl fraction sample).
5. Store samples in -80 until ready to use.

Western blotting for sucrose gradients

1. For TLR4 and other difficult antibodies, use 8% SDS gels. Run gels as normal. Transfer using semi-dry.
2. During blocking, block the normal 4 hours in 5% milk, then 1 hour at room temperature for the primary. Afterwards, place in cold room overnight.
3. Wash for one 8 minute and two 5 minute session. Then apply secondary and sit for 2 hours.
4. When washing after secondary, wash for two 8 minute and two 5 minute sessions before applying ECL. Let rock for at least 1 minute with ECL before positioning in cassettes and developing.

Western Protocol

1) Make acrylamide gels:
   a. Separating gel

Reagent	10 mL	20 mL
diH_2O (mL)	4.8	9.6
1.5 M Tris-HCl pH 8.8	2.5	5.0
40% Acryl:Bis	2.5	5.0
10% SDS (uL)	100	200
10% APS	50	100
TEMED	10	20

   b. Stacking gel

Reagent	5 mL	10 mL	20 mL
diH_2O (mL)	3.05	6.1	12.2
0.5 M Tris-HCl pH 6.8	1.35	2.5	5.0
40% Acryl:Bis	0.65	1.3	2.6
10% SDS (uL)	50	100	200
10% APS	25	50	100
TEMED	5	10	20

2) Combine protein samples (30ug) with 6X loading dye as per BCA results.
3) Heat samples for 5min. at 100°C.
4) Set-up the Western apparatus and fill inner chamber with 1X Running Buffer until it just overflows. Fill bottom of the chamber until it passes the wire.
5) Load samples into gel(s) with gel loading tips avoiding the flanking wells when possible. Use 6uL of Rainbow Ladder for each gel.
6) Run for approx. 80min. at 130V.
7) Prepare the dry transfer blot system:

a. Submerge the pads, nitrocellulose membrane, and the Western gel in transfer buffer.
b. Pour a small amount of transfer buffer on the apparatus.
c. Using a forceps, place the “sandwich,” pad, membrane, gel, and pad on the apparatus. After each layer use a plastic wedge, test tube, etc. to gently remove bubbles.
d. Pour a little more transfer buffer over the sandwich and secure both lids.
e. Run the transfer at 350 mAmps for 1 hour.

8) Remove the nitrocellulose gel and rinse with TBST.
9) Cover with Ponceau stain, remove excess, wash 1-2x with TBST to view banding, cut as needed. (May store ON at 4°C in TBST if unable to continue.)
10) Cover membrane with 5% milk (5g + 100mL TBST) and incubate with shaking for 1-3hr at RT.
11) Remove milk and wash while shaking in TBST for 10 min.
12) Remove TBST and apply 4mL of 5% milk or appropriate volume and add primary antibody. For most antibodies, add 1:1000 dilution (i.e. 4uL to 4mL, 8uL to 8mL) except β-actin antibody add a minimum of 1:10,000 to a max of 1:4000 dilution.
13) Either store in primary antibody ON at 4°C with shaking or incubate at RT with shaking for 3hrs.
14) Wash 3x with TBST for 5-10min. each (on shaker).
15) Add secondary antibody in 5% milk to a 1:4000 dilution. Incubate at RT for 1-2hrs on shaker.
16) Wash 4x with TBST for 5-10min. each (on shaker). (May store at 4°C in TBST.)
17) Combine equal amounts of “black” and “white” ECL reagents making enough to apply 2-4mL to each membrane depending on size. Incubate with shaking for 1 min.
18) Cut appropriately sized plastic sheath for each membrane and tape into a cassette.
19) Dab the edge of the membrane on some Kim wipes and place in the plastic sheath.
20) In the dark room, bend the upper right corner of the film for orientation and place on the membrane for an appropriate length of time.
21) Develop film and mark rainbow ladder bands.
22) Label appropriately.
23) Membranes may be stripped or stored in TBST.

Bibliography

1. Carson R, Darling L, Darling L. *Silent spring*. Boston Cambridge, Mass.: Houghton Mifflin ; Riverside Press; 1962.
2. Friis RH. *Essentials of environmental health*. Sudbury, MA: Jones & Bartlett Learning; 2012.
3. Robertson LW, Hansen LG. *Pcbs: Recent advances in environmental toxicology and health effects*. University Press of Kentucky; 2001.
4. Fiedler H. Polychlorinated biphenyls (pcbs): Uses and environmental releases. 2004
5. Safe S, Bandiera S, Sawyer T, Robertson L, Safe L, Parkinson A, Thomas PE, Ryan DE, Reik LM, Levin W, et al. Pcbs: Structure-function relationships and mechanism of action. *Environ Health Perspect*. 1985;60:47-56
6. Tanabe S, Kannan N, Subramanian A, Watanabe S, Tatsukawa R. Highly toxic coplanar pcbs: Occurrence, source, persistency and toxic implications to wildlife and humans. *Environ Pollut*. 1987;47:147-163
7. Kannan N, Tanabe S, Tatsukawa R. Potentially hazardous residues of non-ortho chlorine substituted coplanar pcbs in human adipose tissue. *Archives of environmental health*. 1988;43:11-14
8. Leece B, Denomme MA, Towner R, Li SM, Safe S. Polychlorinated biphenyls: Correlation between in vivo and in vitro quantitative structure-activity relationships (qsars). *Journal of toxicology and environmental health*. 1985;16:379-388
9. Gahrs M, Roos R, Andersson PL, Schrenk D. Role of the nuclear xenobiotic receptors car and pxr in induction of cytochromes p450 by non-dioxinlike polychlorinated biphenyls in cultured rat hepatocytes. *Toxicol Appl Pharmacol*. 2013
10. Wong PW, Brackney WR, Pessah IN. Ortho-substituted polychlorinated biphenyls alter microsomal calcium transport by direct interaction with ryanodine receptors of mammalian brain. *J Biol Chem*. 1997;272:15145-15153
11. Wahlang B, Falkner KC, Gregory B, Ansert D, Young D, Conklin DJ, Bhatnagar A, McClain CJ, Cave M. Polychlorinated biphenyl 153 is a diet-dependent obesogen that worsens nonalcoholic fatty liver disease in male c57bl6/j mice. *J Nutr Biochem*. 2013
12. Rignell-Hydbom A, Rylander L, Hagmar L. Exposure to persistent organochlorine pollutants and type 2 diabetes mellitus. *Human & experimental toxicology*. 2007;26:447-452
13. McFarland VA, Clarke JU. Environmental occurrence, abundance, and potential toxicity of polychlorinated biphenyl congeners: Considerations for a congener-specific analysis. *Environ Health Perspect*. 1989;81:225-239
14. Toborek M, Barger SW, Mattson MP, Espandiari P, Robertson LW, Hennig B. Exposure to polychlorinated biphenyls causes endothelial cell dysfunction. *Journal of biochemical toxicology*. 1995;10:219-226
15. Hennig B, Slim R, Toborek M, Robertson LW. Linoleic acid amplifies polychlorinated biphenyl-mediated dysfunction of endothelial cells. *Journal of biochemical and molecular toxicology*. 1999;13:83-91
16. Wang L, Reiterer G, Toborek M, Hennig B. Changing ratios of omega-6 to omega-3 fatty acids can differentially modulate polychlorinated biphenyl toxicity in endothelial cells. *Chem Biol Interact*. 2008;172:27-38
17. Van den Berg M, Birnbaum L, Bosveld AT, Brunstrom B, Cook P, Feeley M, Giesy JP, Hanberg A, Hasegawa R, Kennedy SW, Kubiak T, Larsen JC, van Leeuwen FX, Liem AK, Nolt C, Peterson RE, Poellinger L, Safe S, Schrenk D,

Tillitt D, Tysklind M, Younes M, Waern F, Zacharewski T. Toxic equivalency factors (tefs) for pcbs, pcdds, pcdfs for humans and wildlife. *Environ Health Perspect*. 1998;106:775-792
18. Van den Berg M, Birnbaum LS, Denison M, De Vito M, Farland W, Feeley M, Fiedler H, Hakansson H, Hanberg A, Haws L, Rose M, Safe S, Schrenk D, Tohyama C, Tritscher A, Tuomisto J, Tysklind M, Walker N, Peterson RE. The 2005 world health organization reevaluation of human and mammalian toxic equivalency factors for dioxins and dioxin-like compounds. *Toxicol Sci*. 2006;93:223-241
19. Geyer H, Scheunert I, Korte F. Bioconcentration potential of organic environmental chemicals in humans. *Regulatory toxicology and pharmacology : RTP*. 1986;6:313-347
20. Yu GW, Laseter J, Mylander C. Persistent organic pollutants in serum and several different fat compartments in humans. *Journal of environmental and public health*. 2011;2011:417980
21. Jandacek RJ, Genuis SJ. An assessment of the intestinal lumen as a site for intervention in reducing body burdens of organochlorine compounds. *TheScientificWorldJournal*. 2013;2013:205621
22. Jandacek RJ, Rider T, Yang Q, Woollett LA, Tso P. Lymphatic and portal vein absorption of organochlorine compounds in rats. *Am J Physiol Gastrointest Liver Physiol*. 2009;296:G226-234
23. Mohammed A, Eklund A, Ostlund-Lindqvist AM, Slanina P. Distribution of toxaphene, ddt, and pcb among lipoprotein fractions in rat and human plasma. *Arch Toxicol*. 1990;64:567-571
24. Borlakoglu JT, Welch VA, Wilkins JPG, Dils RR. Transport and cellular uptake of polychlorinated biphenyls (pcbs)—i: Association of individual pcb isomers and congeners with plasma lipoproteins and proteins in the pigeon. *Biochemical Pharmacology*. 1990;40:265-272
25. Mannetje A, Coakley J, Mueller JF, Harden F, Toms LM, Douwes J. Partitioning of persistent organic pollutants (pops) between human serum and breast milk: A literature review. *Chemosphere*. 2012;89:911-918
26. Kim D, Ryu HY, Lee JH, Lee JH, Lee YJ, Kim HK, Jang DD, Kim HS, Yoon HS. Organochlorine pesticides and polychlorinated biphenyls in korean human milk: Contamination levels and infant risk assessment. *Journal of environmental science and health. Part. B, Pesticides, food contaminants, and agricultural wastes*. 2013;48:243-250
27. Crinnion WJ. Polychlorinated biphenyls: Persistent pollutants with immunological, neurological, and endocrinological consequences. *Alternative medicine review : a journal of clinical therapeutic*. 2011;16:5-13
28. Birnbaum LS, Tuomisto J. Non-carcinogenic effects of tcdd in animals. *Food Addit Contam*. 2000;17:275-288
29. White SS, Birnbaum LS. An overview of the effects of dioxins and dioxin-like compounds on vertebrates, as documented in human and ecological epidemiology. *Journal of environmental science and health. Part C, Environmental carcinogenesis & ecotoxicology reviews*. 2009;27:197-211
30. Carlson DB, Perdew GH. A dynamic role for the ah receptor in cell signaling? Insights from a diverse group of ah receptor interacting proteins. *Journal of biochemical and molecular toxicology*. 2002;16:317-325
31. Wilson CL, Safe S. Mechanisms of ligand-induced aryl hydrocarbon receptor-mediated biochemical and toxic responses. *Toxicol Pathol*. 1998;26:657-671

32. Kobayashi A, Sogawa K, Fujii-Kuriyama Y. Cooperative interaction between ahr.Arnt and sp1 for the drug-inducible expression of cyp1a1 gene. *J Biol Chem*. 1996;271:12310-12316
33. Nguyen LP, Bradfield CA. The search for endogenous activators of the aryl hydrocarbon receptor. *Chemical research in toxicology*. 2008;21:102-116
34. Guyot E, Chevallier A, Barouki R, Coumoul X. The ahr twist: Ligand-dependent ahr signaling and pharmaco-toxicological implications. *Drug Discovery Today*. 2013;18:479-486
35. Kohle C, Bock KW. Coordinate regulation of phase i and ii xenobiotic metabolisms by the ah receptor and nrf2. *Biochem Pharmacol*. 2007;73:1853-1862
36. Stegeman JJ, Hahn ME, Weisbrod R, Woodin BR, Joy JS, Najibi S, Cohen RA. Induction of cytochrome p4501a1 by aryl hydrocarbon receptor agonists in porcine aorta endothelial cells in culture and cytochrome p4501a1 activity in intact cells. *Mol Pharmacol*. 1995;47:296-306
37. Schlezinger JJ, Stegeman JJ. Induction and suppression of cytochrome p450 1a by 3,3',4,4',5-pentachlorobiphenyl and its relationship to oxidative stress in the marine fish scup (stenotomus chrysops). *Aquat Toxicol*. 2001;52:101-115
38. Schlezinger JJ, Struntz WD, Goldstone JV, Stegeman JJ. Uncoupling of cytochrome p450 1a and stimulation of reactive oxygen species production by co-planar polychlorinated biphenyl congeners. *Aquat Toxicol*. 2006;77:422-432
39. Shertzer HG, Clay CD, Genter MB, Chames MC, Schneider SN, Oakley GG, Nebert DW, Dalton TP. Uncoupling-mediated generation of reactive oxygen by halogenated aromatic hydrocarbons in mouse liver microsomes. *Free Radic Biol Med*. 2004;36:618-631
40. Nebert DW, Roe AL, Dieter MZ, Solis WA, Yang Y, Dalton TP. Role of the aromatic hydrocarbon receptor and [ah] gene battery in the oxidative stress response, cell cycle control, and apoptosis. *Biochem Pharmacol*. 2000;59:65-85
41. Kabe Y, Ando K, Hirao S, Yoshida M, Handa H. Redox regulation of nf-kappab activation: Distinct redox regulation between the cytoplasm and the nucleus. *Antioxidants & redox signaling*. 2005;7:395-403
42. Rollins BJ. Monocyte chemoattractant protein 1: A potential regulator of monocyte recruitment in inflammatory disease. *Molecular medicine today*. 1996;2:198-204
43. Shin WS, Szuba A, Rockson SG. The role of chemokines in human cardiovascular pathology: Enhanced biological insights. *Atherosclerosis*. 2002;160:91-102
44. Cybulsky MI, Iiyama K, Li H, Zhu S, Chen M, Iiyama M, Davis V, Gutierrez-Ramos J-C, Connelly PW, Milstone DS. A major role for vcam-1, but not icam-1, in early atherosclerosis. *The Journal of Clinical Investigation*. 2001;107:1255-1262
45. Dansky HM, Barlow CB, Lominska C, Sikes JL, Kao C, Weinsaft J, Cybulsky MI, Smith JD. Adhesion of monocytes to arterial endothelium and initiation of atherosclerosis are critically dependent on vascular cell adhesion molecule-1 gene dosage. *Arteriosclerosis, Thrombosis, and Vascular Biology*. 2001;21:1662-1667
46. Sturgill MG, Lambert GH. Xenobiotic-induced hepatotoxicity: Mechanisms of liver injury and methods of monitoring hepatic function. *Clinical Chemistry*. 1997;43:1512-1526
47. Klaassen CD. *Casarett and doull's toxicology: The basic science of poisons*. McGraw-Hill; 2008.

48. Aleksunes LM, Klaassen CD. Coordinated regulation of hepatic phase i and ii drug-metabolizing genes and transporters using ahr-, car-, pxr-, pparα-, and nrf2-null mice. *Drug Metabolism and Disposition*. 2012;40:1366-1379
49. Ross R. Atherosclerosis--an inflammatory disease. *N Engl J Med*. 1999;340:115-126
50. Ichihara S. The pathological roles of environmental and redox stresses in cardiovascular diseases. *Environmental health and preventive medicine*. 2013;18:177-184
51. Hennig B, Ettinger AS, Jandacek RJ, Koo S, McClain C, Seifried H, Silverstone A, Watkins B, Suk WA. Using nutrition for intervention and prevention against environmental chemical toxicity and associated diseases. *Environ Health Perspect*. 2007;115:493-495
52. Madamanchi NR, Vendrov A, Runge MS. Oxidative stress and vascular disease. *Arterioscler Thromb Vasc Biol*. 2005;25:29-38
53. Liao JK. Linking endothelial dysfunction with endothelial cell activation. *J Clin Invest*. 2013;123:540-541
54. Li H, Cybulsky MI, Gimbrone MA, Jr., Libby P. An atherogenic diet rapidly induces vcam-1, a cytokine-regulatable mononuclear leukocyte adhesion molecule, in rabbit aortic endothelium. *Arteriosclerosis and thrombosis : a journal of vascular biology / American Heart Association*. 1993;13:197-204
55. Karimi S, Dadvar M, Modarress H, Dabir B. A new correlation for inclusion of leaky junctions in macroscopic modeling of atherosclerotic lesion initiation. *Journal of theoretical biology*. 2013;329:94-100
56. Roifman I, Beck PL, Anderson TJ, Eisenberg MJ, Genest J. Chronic inflammatory diseases and cardiovascular risk: A systematic review. *The Canadian journal of cardiology*. 2011;27:174-182
57. Wilson PW. Evidence of systemic inflammation and estimation of coronary artery disease risk: A population perspective. *The American journal of medicine*. 2008;121:S15-20
58. Libby P. Inflammatory mechanisms: The molecular basis of inflammation and disease. *Nutr Rev*. 2007;65:S140-146
59. Codru N, Schymura MJ, Negoita S, Rej R, Carpenter DO. Diabetes in relation to serum levels of polychlorinated biphenyls and chlorinated pesticides in adult native americans. *Environ Health Perspect*. 2007;115:1442-1447
60. Silverstone AE, Rosenbaum PF, Weinstock RS, Bartell SM, Foushee HR, Shelton C, Pavuk M. Polychlorinated biphenyl (pcb) exposure and diabetes: Results from the anniston community health survey. *Environ Health Perspect*. 2012;120:727-732
61. Uemura H, Arisawa K, Hiyoshi M, Kitayama A, Takami H, Sawachika F, Dakeshita S, Nii K, Satoh H, Sumiyoshi Y, Morinaga K, Kodama K, Suzuki T, Nagai M, Suzuki T. Prevalence of metabolic syndrome associated with body burden levels of dioxin and related compounds among japan's general population. *Environ Health Perspect*. 2009;117:568-573
62. Cave M, Appana S, Patel M, Falkner KC, McClain CJ, Brock G. Polychlorinated biphenyls, lead, and mercury are associated with liver disease in american adults: Nhanes 2003-2004. *Environ Health Perspect*. 2010;118:1735-1742
63. Wahlang B, Beier JI, Clair HB, Bellis-Jones HJ, Falkner KC, McClain CJ, Cave MC. Toxicant-associated steatohepatitis. *Toxicologic Pathology*. 2012
64. Lind PM, van Bavel B, Salihovic S, Lind L. Circulating levels of persistent organic pollutants (pops) and carotid atherosclerosis in the elderly. *Environ Health Perspect*. 2012;120:38-43

65. Lind PM, Orberg J, Edlund UB, Sjoblom L, Lind L. The dioxin-like pollutant pcb 126 (3,3',4,4',5-pentachlorobiphenyl) affects risk factors for cardiovascular disease in female rats. *Toxicol Lett*. 2004;150:293-299
66. Gustavsson P, Hogstedt C. A cohort study of swedish capacitor manufacturing workers exposed to polychlorinated biphenyls (pcbs). *Am J Ind Med*. 1997;32:234-239
67. Choi JJ, Choi YJ, Chen L, Zhang B, Eum SY, Abreu MT, Toborek M. Lipopolysaccharide potentiates polychlorinated biphenyl-induced disruption of the blood–brain barrier via tlr4/irf-3 signaling. *Toxicology*. 2012
68. Fontes JD, Yamamoto JF, Larson MG, Wang N, Dallmeier D, Rienstra M, Schnabel RB, Vasan RS, Keaney JF, Jr., Benjamin EJ. Clinical correlates of change in inflammatory biomarkers: The framingham heart study. *Atherosclerosis*. 2013;228:217-223
69. Kressel G, Trunz B, Bub A, Hulsmann O, Wolters M, Lichtinghagen R, Stichtenoth DO, Hahn A. Systemic and vascular markers of inflammation in relation to metabolic syndrome and insulin resistance in adults with elevated atherosclerosis risk. *Atherosclerosis*. 2009;202:263-271
70. Baker NA, Karounos M, English V, Fang J, Wei Y, Stromberg A, Sunkara M, Morris AJ, Swanson HI, Cassis LA. Coplanar polychlorinated biphenyls impair glucose homeostasis in lean c57bl/6 mice and mitigate beneficial effects of weight loss on glucose homeostasis in obese mice. *Environ Health Perspect*. 2013;121:105-110
71. Nakamoto M, Arisawa K, Uemura H, Katsuura S, Takami H, Sawachika F, Yamaguchi M, Juta T, Sakai T, Toda E, Mori K, Hasegawa M, Tanto M, Shima M, Sumiyoshi Y, Morinaga K, Kodama K, Suzuki T, Nagai M, Satoh H. Association between blood levels of pcdds/pcdfs/dioxin-like pcbs and history of allergic and other diseases in the japanese population. *Int Arch Occup Environ Health*. 2012
72. Taylor KW, Novak RF, Anderson HA, Birnbaum LS, Blystone C, Devito M, Jacobs D, Jr., Kohrle J, Lee DH, Rylander L, Rignell-Hydbom A, Tornero-Velez R, Turyk ME, Boyles A, Thayer KA, Lind L. Evaluation of the association between persistent organic pollutants (pops) and diabetes in epidemiological studies: A national toxicology program workshop review. *Environ Health Perspect*. 2013
73. Hennig B, Meerarani P, Slim R, Toborek M, Daugherty A, Silverstone AE, Robertson LW. Proinflammatory properties of coplanar pcbs: In vitro and in vivo evidence. *Toxicol Appl Pharmacol*. 2002;181:174-183
74. Whitney EN, Rolfes SR. *Understanding nutrition*. Wadsworth Group; 2002.
75. Hall WL. Dietary saturated and unsaturated fats as determinants of blood pressure and vascular function. *Nutrition research reviews*. 2009;22:18-38
76. Huang S, Rutkowsky JM, Snodgrass RG, Ono-Moore KD, Schneider DA, Newman JW, Adams SH, Hwang DH. Saturated fatty acids activate tlr-mediated pro-inflammatory signaling pathways. *J Lipid Res*. 2012
77. Enos RT, Davis JM, Velazquez KT, McClellan JL, Day SD, Carnevale KA, Murphy EA. Influence of dietary saturated fat content on adiposity, macrophage behavior, inflammation, and metabolism: Composition matters. *J Lipid Res*. 2013;54:152-163
78. Edfeldt K, Swedenborg J, Hansson GK, Yan ZQ. Expression of toll-like receptors in human atherosclerotic lesions: A possible pathway for plaque activation. *Circulation*. 2002;105:1158-1161
79. Ding Y, Subramanian S, Montes VN, Goodspeed L, Wang S, Han C, Teresa AS, 3rd, Kim J, O'Brien KD, Chait A. Toll-like receptor 4 deficiency decreases

atherosclerosis but does not protect against inflammation in obese low-density lipoprotein receptor-deficient mice. *Arterioscler Thromb Vasc Biol*. 2012;32:1596-1604
80. Hu FB, Stampfer MJ, Manson JE, Rimm E, Colditz GA, Rosner BA, Hennekens CH, Willett WC. Dietary fat intake and the risk of coronary heart disease in women. *New England Journal of Medicine*. 1997;337:1491-1499
81. Mozaffarian D, Micha R, Wallace S. Effects on coronary heart disease of increasing polyunsaturated fat in place of saturated fat: A systematic review and meta-analysis of randomized controlled trials. *PLoS medicine*. 2010;7:e1000252
82. Simopoulos AP. The importance of the omega-6/omega-3 fatty acid ratio in cardiovascular disease and other chronic diseases. *Experimental Biology and Medicine*. 2008;233:674-688
83. Gorjão R, Azevedo-Martins AK, Rodrigues HG, Abdulkader F, Arcisio-Miranda M, Procopio J, Curi R. Comparative effects of dha and epa on cell function. *Pharmacology & Therapeutics*. 2009;122:56-64
84. Calder PC. Fatty acids and inflammation: The cutting edge between food and pharma. *European Journal of Pharmacology*. 2011;668, Supplement 1:S50-S58
85. Massaro M, Scoditti E, Carluccio MA, De Caterina R. Basic mechanisms behind the effects of n-3 fatty acids on cardiovascular disease. *Prostaglandins Leukot Essent Fatty Acids*. 2008;79:109-115
86. Massaro M, Habib A, Lubrano L, Turco SD, Lazzerini G, Bourcier T, Weksler BB, De Caterina R. The omega-3 fatty acid docosahexaenoate attenuates endothelial cyclooxygenase-2 induction through both nadp(h) oxidase and pkcε inhibition. *Proceedings of the National Academy of Sciences*. 2006;103:15184-15189
87. Panigrahy D, Kaipainen A, Greene ER, Huang S. Cytochrome p450-derived eicosanoids: The neglected pathway in cancer. *Cancer metastasis reviews*. 2010;29:723-735
88. Arnold C, Konkel A, Fischer R, Schunck WH. Cytochrome p450-dependent metabolism of omega-6 and omega-3 long-chain polyunsaturated fatty acids. *Pharmacological reports : PR*. 2010;62:536-547
89. James MJ, Gibson RA, Cleland LG. Dietary polyunsaturated fatty acids and inflammatory mediator production. *Am J Clin Nutr*. 2000;71:343S-348S
90. Milne GL, Musiek ES, Morrow JD. F2-isoprostanes as markers of oxidative stress in vivo: An overview. *Biomarkers : biochemical indicators of exposure, response, and susceptibility to chemicals*. 2005;10 Suppl 1:S10-23
91. Hennig B, Reiterer G, Toborek M, Matveev SV, Daugherty A, Smart E, Robertson LW. Dietary fat interacts with pcbs to induce changes in lipid metabolism in mice deficient in low-density lipoprotein receptor. *Environ Health Perspect*. 2005;113:83-87
92. Majkova Z, Layne J, Sunkara M, Morris AJ, Toborek M, Hennig B. Omega-3 fatty acid oxidation products prevent vascular endothelial cell activation by coplanar polychlorinated biphenyls. *Toxicol Appl Pharmacol*. 2011;251:41-49
93. Kromhout D, Giltay EJ, Geleijnse JM, Alpha Omega Trial G. N-3 fatty acids and cardiovascular events after myocardial infarction. *N Engl J Med*. 2010;363:2015-2026
94. Marik PE, Varon J. Omega-3 dietary supplements and the risk of cardiovascular events: A systematic review. *Clin Cardiol*. 2009;32:365-372
95. Grenon SM, Aguado-Zuniga J, Hatton JP, Owens CD, Conte MS, Hughes-Fulford M. Effects of fatty acids on endothelial cells: Inflammation and monocyte adhesion. *Journal of Surgical Research*. 2012

96. Chapkin RS, Kim W, Lupton JR, McMurray DN. Dietary docosahexaenoic and eicosapentaenoic acid: Emerging mediators of inflammation. *Prostaglandins Leukot Essent Fatty Acids*. 2009;81:187-191
97. Ma DW, Seo J, Davidson LA, Callaway ES, Fan YY, Lupton JR, Chapkin RS. N-3 pufa alter caveolae lipid composition and resident protein localization in mouse colon. *FASEB J*. 2004;18:1040-1042
98. Li Q, Zhang Q, Wang M, Liu F, Zhao S, Ma J, Luo N, Li N, Li Y, Xu G, Li J. Docosahexaenoic acid affects endothelial nitric oxide synthase in caveolae. *Arch Biochem Biophys*. 2007;466:250-259
99. Yin H, Liu W, Goleniewska K, Porter NA, Morrow JD, Peebles RS, Jr. Dietary supplementation of omega-3 fatty acid-containing fish oil suppresses f2-isoprostanes but enhances inflammatory cytokine response in a mouse model of ovalbumin-induced allergic lung inflammation. *Free Radic Biol Med*. 2009;47:622-628
100. Kong W, Yen JH, Vassiliou E, Adhikary S, Toscano MG, Ganea D. Docosahexaenoic acid prevents dendritic cell maturation and in vitro and in vivo expression of the il-12 cytokine family. *Lipids Health Dis*. 2010;9:12
101. Bento AF, Claudino RF, Dutra RC, Marcon R, Calixto JB. Omega-3 fatty acid-derived mediators 17(r)-hydroxy docosahexaenoic acid, aspirin-triggered resolvin d1 and resolvin d2 prevent experimental colitis in mice. *The Journal of Immunology*. 2011;187:1957-1969
102. Zhang MJ, Spite M. Resolvins: Anti-inflammatory and proresolving mediators derived from omega-3 polyunsaturated fatty acids. *Annual review of nutrition*. 2012;32:203-227
103. Itoh T, Yamamoto K. Peroxisome proliferator activated receptor gamma and oxidized docosahexaenoic acids as new class of ligand. *Naunyn-Schmiedeberg's archives of pharmacology*. 2008;377:541-547
104. Kusunoki C, Yang L, Yoshizaki T, Nakagawa F, Ishikado A, Kondo M, Morino K, Sekine O, Ugi S, Nishio Y, Kashiwagi A, Maegawa H. Omega-3 polyunsaturated fatty acid has an anti-oxidant effect via the nrf-2/ho-1 pathway in 3t3-l1 adipocytes. *Biochemical and biophysical research communications*. 2013;430:225-230
105. Layne J, Majkova Z, Smart EJ, Toborek M, Hennig B. Caveolae: A regulatory platform for nutritional modulation of inflammatory diseases. *J Nutr Biochem*. 2011;22:807-811
106. Lee JY, Plakidas A, Lee WH, Heikkinen A, Chanmugam P, Bray G, Hwang DH. Differential modulation of toll-like receptors by fatty acids: Preferential inhibition by n-3 polyunsaturated fatty acids. *J Lipid Res*. 2003;44:479-486
107. Wong SW, Kwon MJ, Choi AM, Kim HP, Nakahira K, Hwang DH. Fatty acids modulate toll-like receptor 4 activation through regulation of receptor dimerization and recruitment into lipid rafts in a reactive oxygen species-dependent manner. *J Biol Chem*. 2009;284:27384-27392
108. Pike LJ. Rafts defined: A report on the keystone symposium on lipid rafts and cell function. *J Lipid Res*. 2006;47:1597-1598
109. Cohen AW, Hnasko R, Schubert W, Lisanti MP. Role of caveolae and caveolins in health and disease. *Physiol Rev*. 2004;84:1341-1379
110. Hnasko R, Lisanti MP. The biology of caveolae: Lessons from caveolin knockout mice and implications for human disease. *Molecular interventions*. 2003;3:445-464

111. Schubert W, Frank PG, Razani B, Park DS, Chow CW, Lisanti MP. Caveolae-deficient endothelial cells show defects in the uptake and transport of albumin in vivo. *J Biol Chem*. 2001;276:48619-48622
112. Trigatti BL, Anderson RG, Gerber GE. Identification of caveolin-1 as a fatty acid binding protein. *Biochemical and biophysical research communications*. 1999;255:34-39
113. Frank PG, Lee H, Park DS, Tandon NN, Scherer PE, Lisanti MP. Genetic ablation of caveolin-1 confers protection against atherosclerosis. *Arterioscler Thromb Vasc Biol*. 2004;24:98-105
114. Mirza MK, Yuan J, Gao XP, Garrean S, Brovkovych V, Malik AB, Tiruppathi C, Zhao YY. Caveolin-1 deficiency dampens toll-like receptor 4 signaling through enos activation. *Am J Pathol*. 2010;176:2344-2351
115. Beutler B. Tlr4: Central component of the sole mammalian lps sensor. *Current opinion in immunology*. 2000;12:20-26
116. Triantafilou M, Miyake K, Golenbock DT, Triantafilou K. Mediators of innate immune recognition of bacteria concentrate in lipid rafts and facilitate lipopolysaccharide-induced cell activation. *J Cell Sci*. 2002;115:2603-2611
117. Triantafilou M, Morath S, Mackie A, Hartung T, Triantafilou K. Lateral diffusion of toll-like receptors reveals that they are transiently confined within lipid rafts on the plasma membrane. *J Cell Sci*. 2004;117:4007-4014
118. Zhu X, Owen JS, Wilson MD, Li H, Griffiths GL, Thomas MJ, Hiltbold EM, Fessler MB, Parks JS. Macrophage abca1 reduces myd88-dependent toll-like receptor trafficking to lipid rafts by reduction of lipid raft cholesterol. *J Lipid Res*. 2010;51:3196-3206
119. Lee JY, Zhao L, Youn HS, Weatherill AR, Tapping R, Feng L, Lee WH, Fitzgerald KA, Hwang DH. Saturated fatty acid activates but polyunsaturated fatty acid inhibits toll-like receptor 2 dimerized with toll-like receptor 6 or 1. *J Biol Chem*. 2004;279:16971-16979
120. HWANG D. Modulation of the expression of cyclooxygenase-2 by fatty acids mediated through toll-like receptor 4-derived signaling pathways. *The FASEB Journal*. 2001;15:2556-2564
121. Nakahira K, Kim HP, Geng XH, Nakao A, Wang X, Murase N, Drain PF, Wang X, Sasidhar M, Nabel EG, Takahashi T, Lukacs NW, Ryter SW, Morita K, Choi AM. Carbon monoxide differentially inhibits tlr signaling pathways by regulating ros-induced trafficking of tlrs to lipid rafts. *J Exp Med*. 2006;203:2377-2389
122. Ryter SW, Alam J, Choi AMK. Heme oxygenase-1/carbon monoxide: From basic science to therapeutic applications. *Physiological Reviews*. 2006;86:583-650
123. Wang XM, Kim HP, Nakahira K, Ryter SW, Choi AM. The heme oxygenase-1/carbon monoxide pathway suppresses tlr4 signaling by regulating the interaction of tlr4 with caveolin-1. *J Immunol*. 2009;182:3809-3818
124. Lim EJ, Majkova Z, Xu S, Bachas L, Arzuaga X, Smart E, Tseng MT, Toborek M, Hennig B. Coplanar polychlorinated biphenyl-induced cyp1a1 is regulated through caveolae signaling in vascular endothelial cells. *Chem Biol Interact*. 2008;176:71-78
125. Majkova Z, Smart E, Toborek M, Hennig B. Up-regulation of endothelial monocyte chemoattractant protein-1 by coplanar pcb77 is caveolin-1-dependent. *Toxicol Appl Pharmacol*. 2009;237:1-7
126. Han SG, Eum SY, Toborek M, Smart E, Hennig B. Polychlorinated biphenyl-induced vcam-1 expression is attenuated in aortic endothelial cells isolated from caveolin-1 deficient mice. *Toxicology and Applied Pharmacology*. 2010;246:74-82

127. Wang L, Lim E-J, Toborek M, Hennig B. The role of fatty acids and caveolin-1 in tumor necrosis factorα - induced endothelial cell activation. *Metabolism*. 2008;57:1328-1339
128. Choi YJ, Arzuaga X, Kluemper CT, Caraballo A, Toborek M, Hennig B. Quercetin blocks caveolae-dependent pro-inflammatory responses induced by co-planar pcbs. *Environment International*. 2010;36:931-934
129. Zheng Y, Morris A, Sunkara M, Layne J, Toborek M, Hennig B. Epigallocatechin-gallate stimulates nf-e2-related factor and heme oxygenase-1 via caveolin-1 displacement. *J Nutr Biochem*. 2012;23:163-168
130. Han SG, Han SS, Toborek M, Hennig B. Egcg protects endothelial cells against pcb 126-induced inflammation through inhibition of ahr and induction of nrf2-regulated genes. *Toxicol Appl Pharmacol*. 2012
131. Zheng Y, Lim EJ, Wang L, Smart EJ, Toborek M, Hennig B. Role of caveolin-1 in egcg-mediated protection against linoleic-acid-induced endothelial cell activation. *The Journal of Nutritional Biochemistry*. 2009;20:202-209
132. Rodenburg LA, Guo J, Du S, Cavallo GJ. Evidence for unique and ubiquitous environmental sources of 3,3'-dichlorobiphenyl (pcb 11). *Environ Sci Technol*. 2010;44:2816-2821
133. Hu D, Hornbuckle KC. Inadvertent polychlorinated biphenyls in commercial paint pigments. *Environ Sci Technol*. 2010;44:2822-2827
134. Brown JF, Feng H, Bedard DL, Brennan MJ, Carnahan JC, May RJ. Environmental dechlorination of pcbs. *Environmental Toxicology and Chemistry*. 1987;6:579-593
135. Rodenburg LA, Du S, Lui H, Guo J, Oseagulu N, Fennell DE. Evidence for dechlorination of polychlorinated biphenyls and polychlorinated dibenzo-p-dioxins and -furans in wastewater collection systems in the new york metropolitan area. *Environmental Science & Technology*. 2012;46:6612-6620
136. Ruzo LO, Zabik MJ, Schuetz RD. Photochemistry of bioactive compounds. Photoproducts and kinetics of polychorinated biphenyls. *Journal of agricultural and food chemistry*. 1974;22:199-202
137. Hawari J, Demeter A, Samson R. Sensitized photolysis of polychlorobiphenyls in alkaline 2-propanol: Dechlorination of aroclor 1254 in soil samples by solar radiation. *Environmental Science & Technology*. 1992;26:2022-2027
138. Doskey PV, Andren AW. Concentrations of airborne pcbs over lake michigan. *Journal of Great Lakes Research*. 1981;7:15-20
139. Zahran EM, Bhattacharyya D, Bachas LG. Development of reactive pd/fe bimetallic nanotubes for dechlorination reactions. *Journal of Materials Chemistry*. 2011;21:10454-10462
140. Venkatachalam K, Arzuaga X, Chopra N, Gavalas VG, Xu J, Bhattacharyya D, Hennig B, Bachas LG. Reductive dechlorination of 3,3',4,4'-tetrachlorobiphenyl (pcb77) using palladium or palladium/iron nanoparticles and assessment of the reduction in toxic potency in vascular endothelial cells. *Journal of hazardous materials*. 2008;159:483-491
141. Beyer A, Biziuk M. Environmental fate and global distribution of polychlorinated biphenyls. *Reviews of environmental contamination and toxicology*. 2009;201:137-158
142. Puga A, Sartor MA, Huang MY, Kerzee JK, Wei YD, Tomlinson CR, Baxter CS, Medvedovic M. Gene expression profiles of mouse aorta and cultured vascular smooth muscle cells differ widely, yet show common responses to dioxin exposure. *Cardiovasc Toxicol*. 2004;4:385-404

143. Hennig B, Oesterling E, Toborek M. Environmental toxicity, nutrition, and gene interactions in the development of atherosclerosis. *Nutr Metab Cardiovasc Dis*. 2007;17:162-169
144. Ganey PE, Boyd SA. An approach to evaluation of the effect of bioremediation on biological activity of environmental contaminants: Dechlorination of polychlorinated biphenyls. *Environ Health Perspect*. 2005;113:180-185
145. Hennig B, Shasby DM, Fulton AB, Spector AA. Exposure to free fatty acid increases the transfer of albumin across cultured endothelial monolayers. *Arteriosclerosis*. 1984;4:489-497
146. Lim EJ, Kim CW. Functional characterization of the promoter region of the chicken elongation factor-2 gene. *Gene*. 2007;386:183-190
147. Han SS, Yun H, Son DJ, Tompkins VS, Peng L, Chung ST, Kim JS, Park ES, Janz S. Nf-kappab/stat3/pi3k signaling crosstalk in imyc e mu b lymphoma. *Molecular cancer*. 2010;9:97
148. Environmental Protection Agency. Cleanup and disposal of polychlorinated biphenyls (pcbs). 2011;2012
149. Sergeev AV, Carpenter DO. Exposure to persistent organic pollutants increases hospitalization rates for myocardial infarction with comorbid hypertension. *Primary prevention insights*. 2010;2:1-9
150. Sergeev AV, Carpenter DO. Residential proximity to environmental sources of persistent organic pollutants and first-time hospitalizations for myocardial infarction with comorbid diabetes mellitus: A 12-year population-based study. *International journal of occupational medicine and environmental health*. 2010;23:5-13
151. Arsenescu V, Arsenescu R, Parulkar M, Karounos M, Zhang X, Baker N, Cassis LA. Polychlorinated biphenyl 77 augments angiotensin ii-induced atherosclerosis and abdominal aortic aneurysms in male apolipoprotein e deficient mice. *Toxicol Appl Pharmacol*. 2011;257:148-154
152. Kopf PG, Scott JA, Agbor LN, Boberg JR, Elased KM, Huwe JK, Walker MK. Cytochrome p4501a1 is required for vascular dysfunction and hypertension induced by 2,3,7,8-tetrachlorodibenzo-p-dioxin. *Toxicol Sci*. 2010;117:537-546
153. Kopf PG, Walker MK. 2,3,7,8-tetrachlorodibenzo-p-dioxin increases reactive oxygen species production in human endothelial cells via induction of cytochrome p4501a1. *Toxicol Appl Pharmacol*. 2010;245:91-99
154. Han SG, Eum SY, Toborek M, Smart E, Hennig B. Polychlorinated biphenyl-induced vcam-1 expression is attenuated in aortic endothelial cells isolated from caveolin-1 deficient mice. *Toxicol Appl Pharmacol*. 2010;246:74-82
155. Espandiari P, Glauert HP, Lehmler HJ, Lee EY, Srinivasan C, Robertson LW. Polychlorinated biphenyls as initiators in liver carcinogenesis: Resistant hepatocyte model. *Toxicol Appl Pharmacol*. 2003;186:55-62
156. Oakley GG, Robertson LW, Gupta RC. Analysis of polychlorinated biphenyl-DNA adducts by 32p-postlabeling. *Carcinogenesis*. 1996;17:109-114
157. Pereg D, Robertson LW, Gupta RC. DNA adduction by polychlorinated biphenyls: Adducts derived from hepatic microsomal activation and from synthetic metabolites. *Chem Biol Interact*. 2002;139:129-144
158. Hass JR, Jao LT, Wilson NK, Matthews HB. Metabolism of 4-chlorobiphenyl and 4,4'-dichlorobiphenyl in the rat: Qualitative and quantitative aspects. *Journal of agricultural and food chemistry*. 1977;25:1330-1333
159. de Winther MP, Kanters E, Kraal G, Hofker MH. Nuclear factor kappab signaling in atherogenesis. *Arterioscler Thromb Vasc Biol*. 2005;25:904-914

160. Goncharov A, Haase RF, Santiago-Rivera A, Morse G, McCaffrey RJ, Rej R, Carpenter DO. High serum pcbs are associated with elevation of serum lipids and cardiovascular disease in a native american population. *Environ Res*. 2008;106:226-239
161. Faroon O, Jones D, de Rosa C. Effects of polychlorinated biphenyls on the nervous system. *Toxicology and industrial health*. 2000;16:305-333
162. Newman J, Gallo MV, Schell LM, DeCaprio AP, Denham M, Deane GD, Akwesasne Task Force on E. Analysis of pcb congeners related to cognitive functioning in adolescents. *Neurotoxicology*. 2009;30:686-696
163. Mayura K, Spainhour CB, Howie L, Safe S, Phillips TD. Teratogenicity and immunotoxicity of 3,3',4,4',5-pentachlorobiphenyl in c57bl/6 mice. *Toxicology*. 1993;77:123-131
164. Lim EJ, Smart EJ, Toborek M, Hennig B. The role of caveolin-1 in pcb77-induced enos phosphorylation in human-derived endothelial cells. *American Journal of Physiology - Heart and Circulatory Physiology*. 2007;293:H3340-H3347
165. Ramadass P, Meerarani P, Toborek M, Robertson LW, Hennig B. Dietary flavonoids modulate pcb-induced oxidative stress, cyp1a1 induction, and ahr-DNA binding activity in vascular endothelial cells. *Toxicological Sciences*. 2003;76:212-219
166. White RD, Shea D, Schlezinger JJ, Hahn ME, Stegeman JJ. In vitro metabolism of polychlorinated biphenyl congeners by beluga whale (delphinapterus leucas) and pilot whale (globicephala melas) and relationship to cytochrome p450 expression. *Comparative biochemistry and physiology. Toxicology & pharmacology : CBP*. 2000;126:267-284
167. Alcock RE, Behnisch PA, Jones KC, Hagenmaier H. Dioxin-like pcbs in the environment - human exposure and the significance of sources. *Chemosphere*. 1998;37:1457-1472
168. Jokinen MP, Walker NJ, Brix AE, Sells DM, Haseman JK, Nyska A. Increase in cardiovascular pathology in female sprague-dawley rats following chronic treatment with 2,3,7,8-tetrachlorodibenzo-p-dioxin and 3,3',4,4',5-pentachlorobiphenyl. *Cardiovasc Toxicol*. 2003;3:299-310
169. Lai I, Chai Y, Simmons D, Luthe G, Coleman MC, Spitz D, Haschek WM, Ludewig G, Robertson LW. Acute toxicity of 3,3',4,4',5-pentachlorobiphenyl (pcb 126) in male sprague-dawley rats: Effects on hepatic oxidative stress, glutathione and metals status. *Environ Int*. 2010;36:918-923
170. Alkhouri N, Gornicka A, Berk MP, Thapaliya S, Dixon LJ, Kashyap S, Schauer PR, Feldstein AE. Adipocyte apoptosis, a link between obesity, insulin resistance, and hepatic steatosis. *J Biol Chem*. 2010;285:3428-3438
171. Malhi H, Gores GJ. Cellular and molecular mechanisms of liver injury. *Gastroenterology*. 2008;134:1641-1654
172. Forgacs AL, Kent MN, Makley MK, Mets B, DelRaso N, Jahns GL, Burgoon LD, Zacharewski TR, Reo NV. Comparative metabolomic and genomic analyses of tcdd-elicited metabolic disruption in mouse and rat liver. *Toxicol Sci*. 2012;125:41-55
173. National Toxicology P. Ntp toxicology and carcinogenesis studies of 3,3',4,4',5-pentachlorobiphenyl (pcb 126) (cas no. 57465-28-8) in female harlan sprague-dawley rats (gavage studies). *National Toxicology Program technical report series*. 2006:4-246
174. Fisher JW, Campbell J, Muralidhara S, Bruckner JV, Ferguson D, Mumtaz M, Harmon B, Hedge JM, Crofton KM, Kim H, Almekinder TL. Effect of pcb 126 on

hepatic metabolism of thyroxine and perturbations in the hypothalamic-pituitary-thyroid axis in the rat. *Toxicol Sci*. 2006;90:87-95
175. Kopec AK, Boverhof DR, Burgoon LD, Ibrahim-Aibo D, Harkema JR, Tashiro C, Chittim B, Zacharewski TR. Comparative toxicogenomic examination of the hepatic effects of pcb126 and tcdd in immature, ovariectomized c57bl/6 mice. *Toxicological Sciences*. 2008;102:61-75
176. Koga N, Beppu M, Yoshimura H. Metabolism in vivo of 3,4,5,3',4'-pentachlorobiphenyl and toxicological assessment of the metabolite in rats. *Journal of pharmacobio-dynamics*. 1990;13:497-506
177. Philip W. Harvey KCR, Andrew Cockburn. Endocrine and hormonal toxicology. 1999;3:596
178. Schecter A. *Dioxins and health*. Springer; 1994.
179. Baraona E, Leo M, Borowsky S, Lieber C. Alcoholic hepatomegaly: Accumulation of protein in the liver. *Science*. 1975;190:794-795
180. Castell JV, Gomez-Lechon MJ, David M, Fabra R, Trullenque R, Heinrich PC. Acute-phase response of human hepatocytes: Regulation of acute-phase protein synthesis by interleukin-6. *Hepatology*. 1990;12:1179-1186
181. Heinrich PC, Castell JV, Andus T. Interleukin-6 and the acute phase response. *The Biochemical journal*. 1990;265:621-636
182. Kopf M, Baumann H, Freer G, Freudenberg M, Lamers M, Kishimoto T, Zinkernagel R, Bluethmann H, Kohler G. Impaired immune and acute-phase responses in interleukin-6-deficient mice. *Nature*. 1994;368:339-342
183. Ichihara S, Yamada Y, Gonzalez FJ, Nakajima T, Murohara T, Ichihara G. Inhibition of ischemia-induced angiogenesis by benzo[a]pyrene in a manner dependent on the aryl hydrocarbon receptor. *Biochemical and biophysical research communications*. 2009;381:44-49
184. Jensen BA, Leeman RJ, Schlezinger JJ, Sherr DH. Aryl hydrocarbon receptor (ahr) agonists suppress interleukin-6 expression by bone marrow stromal cells: An immunotoxicology study. *Environmental health : a global access science source*. 2003;2:16
185. Puz P, Lasek-Bal A, Ziaja D, Kazibutowska Z, Ziaja K. Inflammatory markers in patients with internal carotid artery stenosis. *Archives of medical science : AMS*. 2013;9:254-260
186. McCarty MF. Interleukin-6 as a central mediator of cardiovascular risk associated with chronic inflammation, smoking, diabetes, and visceral obesity: Down-regulation with essential fatty acids, ethanol and pentoxifylline. *Medical hypotheses*. 1999;52:465-477
187. Siow RC, Sato H, Leake DS, Ishii T, Bannai S, Mann GE. Induction of antioxidant stress proteins in vascular endothelial and smooth muscle cells: Protective action of vitamin c against atherogenic lipoproteins. *Free radical research*. 1999;31:309-318
188. He M, Siow RC, Sugden D, Gao L, Cheng X, Mann GE. Induction of ho-1 and redox signaling in endothelial cells by advanced glycation end products: A role for nrf2 in vascular protection in diabetes. *Nutr Metab Cardiovasc Dis*. 2011;21:277-285
189. Speciale A, Chirafisi J, Saija A, Cimino F. Nutritional antioxidants and adaptive cell responses: An update. *Current molecular medicine*. 2011;11:770-789
190. Yang YC, Lii CK, Wei YL, Li CC, Lu CY, Liu KL, Chen HW. Docosahexaenoic acid inhibition of inflammation is partially via cross-talk between nrf2/heme oxygenase 1 and ikk/nf-kappab pathways. *J Nutr Biochem*. 2013;24:204-212

191. Kopec AK, Burgoon LD, Ibrahim-Aibo D, Burg AR, Lee AW, Tashiro C, Potter D, Sharratt B, Harkema JR, Rowlands JC, Budinsky RA, Zacharewski TR. Automated dose-response analysis and comparative toxicogenomic evaluation of the hepatic effects elicited by tcdd, tcdf, and pcb126 in c57bl/6 mice. *Toxicological Sciences*. 2010;118:286-297
192. Zheng JL, Parfett C, Williams A, Yagminas A, Zhou G, Douglas GR, Yauk CL. Assessment of subclinical, toxicant-induced hepatic gene expression profiles after low-dose, short-term exposures in mice. *Regulatory Toxicology and Pharmacology*. 2011;60:54-72
193. Burr ML, Fehily AM, Gilbert JF, Rogers S, Holliday RM, Sweetnam PM, Elwood PC, Deadman NM. Effects of changes in fat, fish, and fibre intakes on death and myocardial reinfarction: Diet and reinfarction trial (dart). *Lancet*. 1989;2:757-761
194. Wang C, Harris WS, Chung M, Lichtenstein AH, Balk EM, Kupelnick B, Jordan HS, Lau J. N-3 fatty acids from fish or fish-oil supplements, but not alpha-linolenic acid, benefit cardiovascular disease outcomes in primary- and secondary-prevention studies: A systematic review. *Am J Clin Nutr*. 2006;84:5-17
195. Duncan BB, Schmidt MI, Pankow JS, Ballantyne CM, Couper D, Vigo A, Hoogeveen R, Folsom AR, Heiss G. Low-grade systemic inflammation and the development of type 2 diabetes: The atherosclerosis risk in communities study. *Diabetes*. 2003;52:1799-1805
196. Yudkin JS, Stehouwer CD, Emeis JJ, Coppack SW. C-reactive protein in healthy subjects: Associations with obesity, insulin resistance, and endothelial dysfunction: A potential role for cytokines originating from adipose tissue? *Arterioscler Thromb Vasc Biol*. 1999;19:972-978
197. Hartge MM, Unger T, Kintscher U. The endothelium and vascular inflammation in diabetes. *Diabetes & vascular disease research : official journal of the International Society of Diabetes and Vascular Disease*. 2007;4:84-88
198. Wong ET, Tergaonkar V. Roles of nf-kappab in health and disease: Mechanisms and therapeutic potential. *Clin Sci (Lond)*. 2009;116:451-465
199. Hennig B, Lei W, Arzuaga X, Ghosh DD, Saraswathi V, Toborek M. Linoleic acid induces proinflammatory events in vascular endothelial cells via activation of pi3k/akt and erk1/2 signaling. *The Journal of Nutritional Biochemistry*. 2006;17:766-772
200. Toborek M, Blanc EM, Kaiser S, Mattson MP, Hennig B. Linoleic acid potentiates tnf-mediated oxidative stress, disruption of calcium homeostasis, and apoptosis of cultured vascular endothelial cells. *Journal of Lipid Research*. 1997;38:2155-2167
201. Ye S, Tan L, Ma J, Shi Q, Li J. Polyunsaturated docosahexaenoic acid suppresses oxidative stress induced endothelial cell calcium influx by altering lipid composition in membrane caveolar rafts. *Prostaglandins Leukot Essent Fatty Acids*. 2010;83:37-43
202. Iso H. Changes in coronary heart disease risk among japanese. *Circulation*. 2008;118:2725-2729
203. Turunen AW, Jula A, Suominen AL, Mannisto S, Marniemi J, Kiviranta H, Tiittanen P, Karanko H, Moilanen L, Nieminen MS, Kesaniemi YA, Kahonen M, Verkasalo PK. Fish consumption, omega-3 fatty acids, and environmental contaminants in relation to low-grade inflammation and early atherosclerosis. *Environ Res*. 2013;120:43-54
204. Musiek ES, Brooks JD, Joo M, Brunoldi E, Porta A, Zanoni G, Vidari G, Blackwell TS, Montine TJ, Milne GL, McLaughlin B, Morrow JD. Electrophilic cyclopentenone neuroprostanes are anti-inflammatory mediators formed from the

peroxidation of the omega-3 polyunsaturated fatty acid docosahexaenoic acid. *J Biol Chem*. 2008;283:19927-19935
205. Gao L, Wang J, Sekhar KR, Yin H, Yared NF, Schneider SN, Sasi S, Dalton TP, Anderson ME, Chan JY, Morrow JD, Freeman ML. Novel n-3 fatty acid oxidation products activate nrf2 by destabilizing the association between keap1 and cullin3. *J Biol Chem*. 2007;282:2529-2537
206. Roberts LJ, 2nd, Montine TJ, Markesbery WR, Tapper AR, Hardy P, Chemtob S, Dettbarn WD, Morrow JD. Formation of isoprostane-like compounds (neuroprostanes) in vivo from docosahexaenoic acid. *J Biol Chem*. 1998;273:13605-13612
207. Schwab JM, Chiang N, Arita M, Serhan CN. Resolvin e1 and protectin d1 activate inflammation-resolution programmes. *Nature*. 2007;447:869-874
208. Merched AJ, Ko K, Gotlinger KH, Serhan CN, Chan L. Atherosclerosis: Evidence for impairment of resolution of vascular inflammation governed by specific lipid mediators. *FASEB J*. 2008;22:3595-3606
209. Campbell EL, Louis NA, Tomassetti SE, Canny GO, Arita M, Serhan CN, Colgan SP. Resolvin e1 promotes mucosal surface clearance of neutrophils: A new paradigm for inflammatory resolution. *FASEB J*. 2007;21:3162-3170
210. Rogers LK, Valentine CJ, Pennell M, Velten M, Britt RD, Dingess K, Zhao X, Welty SE, Tipple TE. Maternal docosahexaenoic acid supplementation decreases lung inflammation in hyperoxia-exposed newborn mice. *The Journal of Nutrition*. 2011;141:214-222
211. Watkins BA, Li Y, Seifert MF. Dietary ratio of n-6/n-3 pufas and docosahexaenoic acid: Actions on bone mineral and serum biomarkers in ovariectomized rats. *J Nutr Biochem*. 2006;17:282-289
212. Chen YJ, Chen CC, Li TK, Wang PH, Liu LR, Chang FY, Wang YC, Yu YH, Lin SP, Mersmann HJ, Ding ST. Docosahexaenoic acid suppresses the expression of foxo and its target genes. *J Nutr Biochem*. 2012;23:1609-1616
213. Daugherty A, Manning MW, Cassis LA. Angiotensin ii promotes atherosclerotic lesions and aneurysms in apolipoprotein e–deficient mice. *The Journal of Clinical Investigation*. 2000;105:1605-1612
214. Jiao S, Cole TG, Kitchens RT, Pfleger B, Schonfeld G. Genetic heterogeneity of plasma lipoproteins in the mouse: Control of low density lipoprotein particle sizes by genetic factors. *J Lipid Res*. 1990;31:467-477
215. Yang WC, Adamec J, Regnier FE. Enhancement of the lc/ms analysis of fatty acids through derivatization and stable isotope coding. *Analytical chemistry*. 2007;79:5150-5157
216. Deems R, Buczynski MW, Bowers-Gentry R, Harkewicz R, Dennis EA. Detection and quantitation of eicosanoids via high performance liquid chromatography-electrospray ionization-mass spectrometry. *Methods Enzymol*. 2007;432:59-82
217. Gomolka B, Siegert E, Blossey K, Schunck WH, Rothe M, Weylandt KH. Analysis of omega-3 and omega-6 fatty acid-derived lipid metabolite formation in human and mouse blood samples. *Prostaglandins & other lipid mediators*. 2011;94:81-87
218. Masoodi M, Nicolaou A. Lipidomic analysis of twenty-seven prostanoids and isoprostanes by liquid chromatography/electrospray tandem mass spectrometry. *Rapid communications in mass spectrometry : RCM*. 2006;20:3023-3029
219. Delanty N, Reilly M, Pratico D, FitzGerald DJ, Lawson JA, FitzGerald GA. 8-epi pgf2 alpha: Specific analysis of an isoeicosanoid as an index of oxidant stress in vivo. *British journal of clinical pharmacology*. 1996;42:15-19

220. Basu S. Oxidative injury induced cyclooxygenase activation in experimental hepatotoxicity. *Biochemical and biophysical research communications*. 1999;254:764-767
221. Yoshida Y, Hayakawa M, Habuchi Y, Itoh N, Niki E. Evaluation of lipophilic antioxidant efficacy in vivo by the biomarkers hydroxyoctadecadienoic acid and isoprostane. *Lipids*. 2007;42:463-472
222. Claria J, Nguyen BT, Madenci AL, Ozaki CK, Serhan CN. Diversity of lipid mediators in human adipose tissue depots. *American journal of physiology. Cell physiology*. 2013;304:C1141-1149
223. Sapieha P, Stahl A, Chen J, Seaward MR, Willett KL, Krah NM, Dennison RJ, Connor KM, Aderman CM, Liclican E, Carughi A, Perelman D, Kanaoka Y, Sangiovanni JP, Gronert K, Smith LE. 5-lipoxygenase metabolite 4-hdha is a mediator of the antiangiogenic effect of omega-3 polyunsaturated fatty acids. *Science translational medicine*. 2011;3:69ra12
224. Stephensen CB, Armstrong P, Newman JW, Pedersen TL, Legault J, Schuster GU, Kelley D, Vikman S, Hartiala J, Nassir R, Seldin MF, Allayee H. Alox5 gene variants affect eicosanoid production and response to fish oil supplementation. *J Lipid Res*. 2011;52:991-1003
225. McDaniel JC, Massey K, Nicolaou A. Fish oil supplementation alters levels of lipid mediators of inflammation in microenvironment of acute human wounds. *Wound repair and regeneration : official publication of the Wound Healing Society [and] the European Tissue Repair Society*. 2011;19:189-200
226. Duttaroy AK, Spener F, Wiley J. *Cellular proteins and their fatty acids in health and disease*. Wiley Online Library; 2003.
227. Kansanen E, Kivela AM, Levonen AL. Regulation of nrf2-dependent gene expression by 15-deoxy-delta12,14-prostaglandin j2. *Free Radic Biol Med*. 2009;47:1310-1317
228. Rollins MD, Sudarshan S, Firpo MA, Etherington BH, Hart BJ, Jackson HH, Jackson JD, Emerson LL, Yang DT, Mulvihill SJ, Glasgow RE. Anti-inflammatory effects of ppar-gamma agonists directly correlate with ppar-gamma expression during acute pancreatitis. *Journal of gastrointestinal surgery : official journal of the Society for Surgery of the Alimentary Tract*. 2006;10:1120-1130
229. Huang da W, Sherman BT, Lempicki RA. Systematic and integrative analysis of large gene lists using david bioinformatics resources. *Nature protocols*. 2009;4:44-57
230. Sierra S, Lara-Villoslada F, Comalada Mn, Olivares Mn, Xaus J. Dietary eicosapentaenoic acid and docosahexaenoic acid equally incorporate as decosahexaenoic acid but differ in inflammatory effects. *Nutrition*. 2008;24:245-254
231. Arterburn LM, Boswell KD, Lawlor T, Cifone MA, Murli H, Kyle DJ. In vitro genotoxicity testing of arasco® and dhasco® oils. *Food and Chemical Toxicology*. 2000;38:971-976
232. Abuzaytoun R, Shahidi F. Oxidative stability of algal oils as affected by their minor components. *Journal of agricultural and food chemistry*. 2006;54:8253-8260
233. Beyer A, Biziuk M. Environmental fate and global distribution of polychlorinated biphenyls

reviews of environmental contamination and toxicology vol 201. In: Whitacre DM, ed.: Springer US; 2009:137-158.

234. Schuchardt JP, Schneider I, Meyer H, Neubronner J, von Schacky C, Hahn A. Incorporation of epa and dha into plasma phospholipids in response to different omega-3 fatty acid formulations--a comparative bioavailability study of fish oil vs. Krill oil. *Lipids Health Dis*. 2011;10:145
235. Plourde M, Chouinard-Watkins R, Vandal M, Zhang Y, Lawrence P, Brenna JT, Cunnane S. Plasma incorporation, apparent retroconversion and beta-oxidation of 13c-docosahexaenoic acid in the elderly. *Nutrition & Metabolism*. 2011;8:5
236. Gronn M, Christensen E, Hagve TA, Christophersen BO. Peroxisomal retroconversion of docosahexaenoic acid (22:6(n-3)) to eicosapentaenoic acid (20:5(n-3)) studied in isolated rat liver cells. *Biochimica et biophysica acta*. 1991;1081:85-91
237. Conquer JA, Holub BJ. Dietary docosahexaenoic acid as a source of eicosapentaenoic acid in vegetarians and omnivores. *Lipids*. 1997;32:341-345
238. Stark KD, Holub BJ. Differential eicosapentaenoic acid elevations and altered cardiovascular disease risk factor responses after supplementation with docosahexaenoic acid in postmenopausal women receiving and not receiving hormone replacement therapy. *The American Journal of Clinical Nutrition*. 2004;79:765-773
239. Gonzalez-Periz A, Horrillo R, Ferre N, Gronert K, Dong B, Moran-Salvador E, Titos E, Martinez-Clemente M, Lopez-Parra M, Arroyo V, Claria J. Obesity-induced insulin resistance and hepatic steatosis are alleviated by omega-3 fatty acids: A role for resolvins and protectins. *FASEB J*. 2009;23:1946-1957
240. Lehrke M, Lazar MA. Inflamed about obesity. *Nature medicine*. 2004;10:126-127
241. Berger J, Bailey P, Biswas C, Cullinan CA, Doebber TW, Hayes NS, Saperstein R, Smith RG, Leibowitz MD. Thiazolidinediones produce a conformational change in peroxisomal proliferator-activated receptor-gamma: Binding and activation correlate with antidiabetic actions in db/db mice. *Endocrinology*. 1996;137:4189-4195
242. Yu YH, Lin EC, Wu SC, Cheng WT, Mersmann HJ, Wang PH, Ding ST. Docosahexaenoic acid regulates adipogenic genes in myoblasts via porcine peroxisome proliferator-activated receptor gamma. *Journal of animal science*. 2008;86:3385-3392
243. Awazawa M, Ueki K, Inabe K, Yamauchi T, Kubota N, Kaneko K, Kobayashi M, Iwane A, Sasako T, Okazaki Y, Ohsugi M, Takamoto I, Yamashita S, Asahara H, Akira S, Kasuga M, Kadowaki T. Adiponectin enhances insulin sensitivity by increasing hepatic irs-2 expression via a macrophage-derived il-6-dependent pathway. *Cell metabolism*. 2011;13:401-412
244. CHU I, VILLENEUVE DC, YAGMINAS A, LECAVALIER P, POON R, FEELEY M, KENNEDY SW, SEEGAL RF, HÄKANSSON H, AHLBORG UG, VALLI VE. Subchronic toxicity of 3,3′,4,4′,5-pentachlorobiphenyl in the rat: I. Clinical, biochemical, hematological, and histopathological changes. *Toxicological Sciences*. 1994;22:457-468
245. Arzuaga X, Ren N, Stromberg A, Black EP, Arsenescu V, Cassis LA, Majkova Z, Toborek M, Hennig B. Induction of gene pattern changes associated with dysfunctional lipid metabolism induced by dietary fat and exposure to a persistent organic pollutant. *Toxicol Lett*. 2009;189:96-101
246. Masi LN, Rodrigues AC, Curi R. Fatty acids regulation of inflammatory and metabolic genes. *Current opinion in clinical nutrition and metabolic care*. 2013;16:418-424
247. Wang S, Matthan NR, Wu D, Reed DB, Bapat P, Yin X, Grammas P, Shen C-L, Lichtenstein AH. Lipid content in hepatic and gonadal adipose tissue parallel

aortic cholesterol accumulation in mice fed diets with different omega-6 pufa to epa plus dha ratios. *Clinical Nutrition*. 2013
248. Li H, Ruan XZ, Powis SH, Fernando R, Mon WY, Wheeler DC, Moorhead JF, Varghese Z. Epa and dha reduce lps-induced inflammation responses in hk-2 cells: Evidence for a ppar-[gamma]-dependent mechanism. *Kidney Int*. 2005;67:867-874
249. Mishra A, Chaudhary A, Sethi S. Oxidized omega-3 fatty acids inhibit nf-kappab activation via a pparalpha-dependent pathway. *Arterioscler Thromb Vasc Biol*. 2004;24:1621-1627
250. Trinchieri G. Interleukin-12: A proinflammatory cytokine with immunoregulatory functions that bridge innate resistance and antigen-specific adaptive immunity. *Annual Review of Immunology*. 1995;13:251-276
251. Matsumoto K, Morita I, Hibino H, Murota S. Inhibitory effect of docosahexaenoic acid-containing phospholipids on 5-lipoxygenase in rat basophilic leukemia cells. *Prostaglandins Leukot Essent Fatty Acids*. 1993;49:861-866
252. German JB, Lokesh B, Kinsella JE. The effect of dietary fish oils on eicosanoid biosynthesis in peritoneal macrophages is influenced by both dietary n-6 polyunsaturated fats and total dietary fat. *Prostaglandins, Leukotrienes and Essential Fatty Acids*. 1988;34:37-45
253. Touyz RM, Schiffrin EL. Peroxisome proliferator-activated receptors in vascular biology-molecular mechanisms and clinical implications. *Vascular pharmacology*. 2006;45:19-28
254. Arzuaga X, Reiterer G, Majkova Z, Toborek M, B H. Ppar-alpha agonists protect against pcb-induced vascular endothelial cell activation. *9th Annual Gill Heart Institute Cardiovascular Research Day*. 2006
255. Arzuaga X, Reiterer G, Majkova Z, Kilgore M, Toborek M, Hennig B. Pparî± ligands reduce pcb-induced endothelial activation: Possible interactions in inflammation and atherosclerosis. *Cardiovascular Toxicology*. 2007;7:264-272
256. Cho H-Y, Gladwell W, Wang X, Chorley B, Bell D, Reddy SP, Kleeberger SR. Nrf2-regulated pparγ expression is critical to protection against acute lung injury in mice. *American Journal of Respiratory and Critical Care Medicine*. 2010;182:170-182
257. Jover R, Hoffmann F, Scheffler-Koch V, Lindberg RLP. Limited heme synthesis in porphobilinogen deaminase-deficient mice impairs transcriptional activation of specific cytochrome p450 genes by phenobarbital. *European Journal of Biochemistry*. 2000;267:7128-7137
258. Gurusamy N, Goswami S, Malik G, Das DK. Oxidative injury induces selective rather than global inhibition of proteasomal activity. *Journal of Molecular and Cellular Cardiology*. 2008;44:419-428
259. Donohue TM, Zetterman RK, Zhang-Gouillon Z-Q, French SW. Peptidase activities of the multicatalytic protease in rat liver after voluntary and intragastric ethanol administration. *Hepatology*. 1998;28:486-491
260. French S. Mechanisms of alcoholic liver injury. *Canadian Journal of Gastroenterology*. 2000;14:327 - 332
261. Oliva J, French SW, Li J, Bardag-Gorce F. Proteasome inhibitor treatment reduced fatty acid, triacylglycerol and cholesterol synthesis. *Experimental and Molecular Pathology*. 2012;93:26-34
262. Welch CL, Xia YR, Shechter I, Farese R, Mehrabian M, Mehdizadeh S, Warden CH, Lusis AJ. Genetic regulation of cholesterol homeostasis: Chromosomal organization of candidate genes. *Journal of Lipid Research*. 1996;37:1406-1421

263. Lobo S, Wiczer BM, Bernlohr DA. Functional analysis of long-chain acyl-coa synthetase 1 in 3t3-l1 adipocytes. *J Biol Chem*. 2009;284:18347-18356
264. Monsalve FA, Pyarasani RD, Delgado-Lopez F, Moore-Carrasco R. Peroxisome proliferator-activated receptor targets for the treatment of metabolic diseases. *Mediators of inflammation*. 2013;2013:549627
265. Choudhary D, Jansson I, Schenkman JB, Sarfarazi M, Stoilov I. Comparative expression profiling of 40 mouse cytochrome p450 genes in embryonic and adult tissues. *Archives of Biochemistry and Biophysics*. 2003;414:91-100
266. Feng S, Cao Z, Wang X. Role of aryl hydrocarbon receptor in cancer. *Biochimica et biophysica acta*. 2013;1836:197-210
267. Rockett BD, Franklin A, Harris M, Teague H, Rockett A, Shaikh SR. Membrane raft organization is more sensitive to disruption by (n-3) pufa than nonraft organization in el4 and b cells. *J Nutr*. 2011;141:1041-1048
268. Fessler MB, Parks JS. Intracellular lipid flux and membrane microdomains as organizing principles in inflammatory cell signaling. *J Immunol*. 2011;187:1529-1535
269. Lee DH, Lee IK, Song K, Steffes M, Toscano W, Baker BA, Jacobs DR, Jr. A strong dose-response relation between serum concentrations of persistent organic pollutants and diabetes: Results from the national health and examination survey 1999-2002. *Diabetes Care*. 2006;29:1638-1644
270. Majkova Z, Toborek M, Hennig B. The role of caveolae in endothelial cell dysfunction with a focus on nutrition and environmental toxicants. *J Cell Mol Med*. 2010;14:2359-2370
271. Yorita Christensen KL, White P. A methodological approach to assessing the health impact of environmental chemical mixtures: Pcbs and hypertension in the national health and nutrition examination survey. *International journal of environmental research and public health*. 2011;8:4220-4237
272. Xu Y, Buikema H, van Gilst WH, Henning RH. Caveolae and endothelial dysfunction: Filling the caves in cardiovascular disease. *Eur J Pharmacol*. 2008;585:256-260
273. Parton RG, Joggerst B, Simons K. Regulated internalization of caveolae. *The Journal of cell biology*. 1994;127:1199-1215
274. Parton RG, Howes MT. Revisiting caveolin trafficking: The end of the caveosome. *The Journal of cell biology*. 2010;191:439-441
275. Hayer A, Stoeber M, Ritz D, Engel S, Meyer HH, Helenius A. Caveolin-1 is ubiquitinated and targeted to intralumenal vesicles in endolysosomes for degradation. *The Journal of cell biology*. 2010;191:615-629
276. Parton RG, del Pozo MA. Caveolae as plasma membrane sensors, protectors and organizers. *Nature reviews. Molecular cell biology*. 2013;14:98-112
277. Pelkmans L, Bürli T, Zerial M, Helenius A. Caveolin-stabilized membrane domains as multifunctional transport and sorting devices in endocytic membrane traffic. *Cell*. 2004;118:767-780
278. Blanco AM, Perez-Arago A, Fernandez-Lizarbe S, Guerri C. Ethanol mimics ligand-mediated activation and endocytosis of il-1ri/tlr4 receptors via lipid rafts caveolae in astroglial cells. *Journal of Neurochemistry*. 2008;106:625-639
279. Martin MU, Wesche H. Summary and comparison of the signaling mechanisms of the toll/interleukin-1 receptor family. *Biochimica et biophysica acta*. 2002;1592:265-280
280. Takeda K, Akira S. Tlr signaling pathways. *Seminars in immunology*. 2004;16:3-9

281. Yamamoto M, Sato S, Hemmi H, Hoshino K, Kaisho T, Sanjo H, Takeuchi O, Sugiyama M, Okabe M, Takeda K, Akira S. Role of adaptor trif in the myd88-independent toll-like receptor signaling pathway. *Science*. 2003;301:640-643
282. Hyun J, Kanagavelu S, Fukata M. A unique host defense pathway: Trif mediates both antiviral and antibacterial immune responses. *Microbes and infection / Institut Pasteur*. 2013;15:1-10
283. Pestka J, Zhou HR. Toll-like receptor priming sensitizes macrophages to proinflammatory cytokine gene induction by deoxynivalenol and other toxicants. *Toxicol Sci*. 2006;92:445-455
284. Doz E, Noulin N, Boichot E, Guenon I, Fick L, Le Bert M, Lagente V, Ryffel B, Schnyder B, Quesniaux VF, Couillin I. Cigarette smoke-induced pulmonary inflammation is tlr4/myd88 and il-1r1/myd88 signaling dependent. *J Immunol*. 2008;180:1169-1178
285. Curtiss LK, Tobias PS. Emerging role of toll-like receptors in atherosclerosis. *J Lipid Res*. 2009;50 Suppl:S340-345
286. Kiechl S, Lorenz E, Reindl M, Wiedermann CJ, Oberhollenzer F, Bonora E, Willeit J, Schwartz DA. Toll-like receptor 4 polymorphisms and atherogenesis. *N Engl J Med*. 2002;347:185-192
287. Michelsen KS, Wong MH, Shah PK, Zhang W, Yano J, Doherty TM, Akira S, Rajavashisth TB, Arditi M. Lack of toll-like receptor 4 or myeloid differentiation factor 88 reduces atherosclerosis and alters plaque phenotype in mice deficient in apolipoprotein e. *Proc Natl Acad Sci U S A*. 2004;101:10679-10684
288. Li H, Sun B. Toll-like receptor 4 in atherosclerosis. *J Cell Mol Med*. 2007;11:88-95
289. den Dekker WK, Cheng C, Pasterkamp G, Duckers HJ. Toll like receptor 4 in atherosclerosis and plaque destabilization. *Atherosclerosis*. 2010;209:314-320
290. Singh RD, Marks DL, Pagano RE. Using fluorescent sphingolipid analogs to study intracellular lipid trafficking. *Current protocols in cell biology*. John Wiley & Sons, Inc.; 2001.
291. Zidovetzki R, Levitan I. Use of cyclodextrins to manipulate plasma membrane cholesterol content: Evidence, misconceptions and control strategies. *Biochimica et Biophysica Acta (BBA) - Biomembranes*. 2007;1768:1311-1324
292. Levitan I, Christian AE, Tulenko TN, Rothblat GH. Membrane cholesterol content modulates activation of volume-regulated anion current in bovine endothelial cells. *The Journal of General Physiology*. 2000;115:405-416
293. Mueller M, Brandenburg K, Dedrick R, Schromm AB, Seydel U. Phospholipids inhibit lipopolysaccharide (lps)-induced cell activation: A role for lps-binding protein. *The Journal of Immunology*. 2005;174:1091-1096
294. Kawamoto T, Ii M, Kitazaki T, Iizawa Y, Kimura H. Tak-242 selectively suppresses toll-like receptor 4-signaling mediated by the intracellular domain. *Eur J Pharmacol*. 2008;584:40-48
295. Yoshimura H, Yonemoto Y, Yamada H, Koga N, Oguri K, Saeki S. Metabolism in vivo of 3,4,3',4'-tetrachlorobiphenyl and toxicological assessment of the metabolites in rats. *Xenobiotica; the fate of foreign compounds in biological systems*. 1987;17:897-910
296. Wehler EK, Bergman A, Brandt I, Darnerud PO, Wachtmeister CA. 3,3',4,4'-tetrachlorobiphenyl. Excretion and tissue retention of hydroxylated metabolites in the mouse. *Drug metabolism and disposition: the biological fate of chemicals*. 1989;17:441-448
297. Maitra U, Deng H, Glaros T, Baker B, Capelluto DG, Li Z, Li L. Molecular mechanisms responsible for the selective and low-grade induction of

proinflammatory mediators in murine macrophages by lipopolysaccharide. *J Immunol*. 2012;189:1014-1023
298. Murphey ED, Fang G, Varma TK, Sherwood ER. Improved bacterial clearance and decreased mortality can be induced by lps tolerance and is not dependent upon ifn-gamma. *Shock*. 2007;27:289-295
299. Fu C, He J, Li C, Shyy JYJ, Zhu Y. Cholesterol increases adhesion of monocytes to endothelium by moving adhesion molecules out of caveolae. *Biochimica et Biophysica Acta (BBA) - Molecular and Cell Biology of Lipids*. 2010;1801:702-710
300. Patel HH, Murray F, Insel PA. Caveolae as organizers of pharmacologically relevant signal transduction molecules. *Annual review of pharmacology and toxicology*. 2008;48:359-391
301. Huot PSP, Sarkar B, Ma DWL. Conjugated linoleic acid alters caveolae phospholipid fatty acid composition and decreases caveolin-1 expression in mcf-7 breast cancer cells. *Nutrition Research*. 2010;30:179-185
302. Dunzendorfer S, Lee H-K, Soldau K, Tobias PS. Toll-like receptor 4 functions intracellularly in human coronary artery endothelial cells: Roles of lbp and scd14 in mediating lps-responses. *The FASEB Journal*. 2004;18:1117-1119
303. Zanoni I, Ostuni R, Marek LR, Barresi S, Barbalat R, Barton GM, Granucci F, Kagan JC. Cd14 controls the lps-induced endocytosis of toll-like receptor 4. *Cell*. 2011;147:868-880
304. Lloyd KL, Kubes P. Gpi-linked endothelial cd14 contributes to the detection of lps. *American journal of physiology. Heart and circulatory physiology*. 2006;291:H473-481
305. Lloyd-Jones KL, Kelly MM, Kubes P. Varying importance of soluble and membrane cd14 in endothelial detection of lipopolysaccharide. *J Immunol*. 2008;181:1446-1453
306. Hennig B, Hammock BD, Slim R, Toborek M, Saraswathi V, Robertson LW. Pcb-induced oxidative stress in endothelial cells: Modulation by nutrients. *Int J Hyg Environ Health*. 2002;205:95-102
307. Eske K, Newsome B, Han SG, Murphy M, Bhattacharyya D, Hennig B. Pcb 77 dechlorination products modulate pro-inflammatory events in vascular endothelial cells. *Environmental science and pollution research international*. 2013
308. Collins FS, Gray GM, Bucher JR. Toxicology. Transforming environmental health protection. *Science*. 2008;319:906-907
309. Ambrose AM, Booth AN, Deeds F, Cox AJ. A toxicological study of biphenyl, a citrus fungistat. *Journal of Food Science*. 1960;25:328-336
310. EPA US. Health and environmental effects profile for 1,1'-biphenyl. 1984
311. Gui M, Ormsbee LE, Bhattacharyya D. Reactive functionalized membranes for polychlorinated biphenyl degradation. *Industrial & Engineering Chemistry Research*. 2013;52:10430-10440
312. Pieterse B, Felzel E, Winter RE, Van Der Burg B, Brouwer A. Pah-calux, an optimized bioassay for ahr-mediated hazard identification of polycyclic aromatic hydrocarbons (pahs) as individual compounds and in complex mixtures. *Environ Sci Technol*. 2013
313. Hadrup N, Taxvig C, Pedersen M, Nellemann C, Hass U, Vinggaard AM. Concentration addition, independent action and generalized concentration addition models for mixture effect prediction of sex hormone synthesis in vitro. *PloS one*. 2013;8:e70490

314. Daughton CG. The matthew effect and widely prescribed pharmaceuticals lacking environmental monitoring: Case study of an exposure-assessment vulnerability. *The Science of the total environment*. 2013;466-467C:315-325
315. Hennig B, Ormsbee L, Bachas L, Silverstone A, Milner J, Carpenter D, Thompson C, Suk WA. Introductory comments: Nutrition, environmental toxins and implications in prevention and intervention of human diseases. *J Nutr Biochem*. 2007;18:161-162
316. Consonni D, Sindaco R, Bertazzi PA. Blood levels of dioxins, furans, dioxin-like pcbs, and teqs in general populations: A review, 1989–2010. *Environment International*. 2012;44:151-162
317. Yamazaki K, Suzuki M, Itoh T, Yamamoto K, Kanemitsu M, Matsumura C, Nakano T, Sakaki T, Fukami Y, Imaishi H, Inui H. Structural basis of species differences between human and experimental animal cyp1a1s in metabolism of 3,3′,4,4′,5-pentachlorobiphenyl. *Journal of Biochemistry*. 2011;149:487-494
318. Fromme H, Albrecht M, Boehmer S, Büchner K, Mayer R, Liebl B, Wittsiepe J, Bolte G. Intake and body burden of dioxin-like compounds in germany: The ines study. *Chemosphere*. 2009;76:1457-1463
319. Deckelbaum RJ, Worgall TS, Seo T. N-3 fatty acids and gene expression. *Am J Clin Nutr*. 2006;83:1520S-1525S
320. Hennig B, Reiterer G, Majkova Z, Oesterling E, Meerarani P, Toborek M. Modification of environmental toxicity by nutrients: Implications in atherosclerosis. *Cardiovasc Toxicol*. 2005;5:153-160
321. Tiesset H, Pierre M, Desseyn JL, Guery B, Beermann C, Galabert C, Gottrand F, Husson MO. Dietary (n-3) polyunsaturated fatty acids affect the kinetics of pro- and antiinflammatory responses in mice with pseudomonas aeruginosa lung infection. *J Nutr*. 2009;139:82-89
322. Baker NA. Polychlorinated biphenyl ligands of the aryl hydrocarbon receptor promote adipocyte-mediated diabetes. *Nutritional Sciences*. 2013;Ph.D. of Nutritional Science
323. Lichtenstein AH, Kennedy E, Barrier P, Danford D, Ernst ND, Grundy SM, Leveille GA, Van Horn L, Williams CL, Booth SL. Dietary fat consumption and health. *Nutrition Reviews*. 1998;56:3-19
324. Reeves PG, Nielsen FH, Fahey GC, Jr. Ain-93 purified diets for laboratory rodents: Final report of the american institute of nutrition ad hoc writing committee on the reformulation of the ain-76a rodent diet. *J Nutr*. 1993;123:1939-1951
325. Sethi S, Ziouzenkova O, Ni H, Wagner DD, Plutzky J, Mayadas TN. Oxidized omega-3 fatty acids in fish oil inhibit leukocyte-endothelial interactions through activation of ppar alpha. *Blood*. 2002;100:1340-1346
326. Pelham CJ, Keen HL, Lentz SR, Sigmund CD. Dominant negative pparγ promotes atherosclerosis, vascular dysfunction, and hypertension through distinct effects in endothelium and vascular muscle. *American Journal of Physiology - Regulatory, Integrative and Comparative Physiology*. 2013;304:R690-R701
327. Schopfer FJ, Cole MP, Groeger AL, Chen CS, Khoo NK, Woodcock SR, Golin-Bisello F, Motanya UN, Li Y, Zhang J, Garcia-Barrio MT, Rudolph TK, Rudolph V, Bonacci G, Baker PR, Xu HE, Batthyany CI, Chen YE, Hallis TM, Freeman BA. Covalent peroxisome proliferator-activated receptor gamma adduction by nitro-fatty acids: Selective ligand activity and anti-diabetic signaling actions. *J Biol Chem*. 2010;285:12321-12333

328. Trostchansky A, Bonilla L, Gonzalez-Perilli L, Rubbo H. Nitro-fatty acids: Formation, redox signaling, and therapeutic potential. *Antioxidants & redox signaling*. 2012
329. Kansanen E, Bonacci G, Schopfer FJ, Kuosmanen SM, Tong KI, Leinonen H, Woodcock SR, Yamamoto M, Carlberg C, Yla-Herttuala S, Freeman BA, Levonen AL. Electrophilic nitro-fatty acids activate nrf2 by a keap1 cysteine 151-independent mechanism. *J Biol Chem*. 2011;286:14019-14027
330. Freeman BA, Baker PR, Schopfer FJ, Woodcock SR, Napolitano A, d'Ischia M. Nitro-fatty acid formation and signaling. *J Biol Chem*. 2008;283:15515-15519
331. Lefils-Lacourtablaise J, Socorro M, Geloen A, Daira P, Debard C, Loizon E, Guichardant M, Dominguez Z, Vidal H, Lagarde M, Bernoud-Hubac N. The eicosapentaenoic acid metabolite 15-deoxy-delta(12,14)-prostaglandin j3 increases adiponectin secretion by adipocytes partly via a ppargamma-dependent mechanism. *PloS one*. 2013;8:e63997
332. Leonarduzzi G, Gamba P, Gargiulo S, Biasi F, Poli G. Inflammation-related gene expression by lipid oxidation-derived products in the progression of atherosclerosis. *Free Radic Biol Med*. 2012;52:19-34
333. Mylonas C, Kouretas D. Lipid peroxidation and tissue damage. *In vivo*. 1999;13:295-309
334. Freire MO, Van Dyke TE. Natural resolution of inflammation. *Periodontology 2000*. 2013;63:149-164
335. Yaqoob P, Shaikh SR. The nutritional and clinical significance of lipid rafts. *Current opinion in clinical nutrition and metabolic care*. 2010;13:156-166
336. Walton KA, Cole AL, Yeh M, Subbanagounder G, Krutzik SR, Modlin RL, Lucas RM, Nakai J, Smart EJ, Vora DK, Berliner JA. Specific phospholipid oxidation products inhibit ligand activation of toll-like receptors 4 and 2. *Arteriosclerosis, Thrombosis, and Vascular Biology*. 2003;23:1197-1203
337. Lidington EA, Moyes DL, McCormack AM, Rose ML. A comparison of primary endothelial cells and endothelial cell lines for studies of immune interactions. *Transplant immunology*. 1999;7:239-246
338. Bauerfeld CP, Rastogi R, Pirockinaite G, Lee I, Huttemann M, Monks B, Birnbaum MJ, Franchi L, Nunez G, Samavati L. Tlr4-mediated akt activation is myd88/trif dependent and critical for induction of oxidative phosphorylation and mitochondrial transcription factor a in murine macrophages. *J Immunol*. 2012;188:2847-2857
339. Lee JY, Ye J, Gao Z, Youn HS, Lee WH, Zhao L, Sizemore N, Hwang DH. Reciprocal modulation of toll-like receptor-4 signaling pathways involving myd88 and phosphatidylinositol 3-kinase/akt by saturated and polyunsaturated fatty acids. *Journal of Biological Chemistry*. 2003;278:37041-37051
340. Laird MH, Rhee SH, Perkins DJ, Medvedev AE, Piao W, Fenton MJ, Vogel SN. Tlr4/myd88/pi3k interactions regulate tlr4 signaling. *Journal of leukocyte biology*. 2009;85:966-977
341. Arcaro A, Aubert M, Espinosa del Hierro ME, Khanzada UK, Angelidou S, Tetley TD, Bittermann AG, Frame MC, Seckl MJ. Critical role for lipid raft-associated src kinases in activation of pi3k-akt signalling. *Cellular signalling*. 2007;19:1081-1092
342. Deng H, Maitra U, Morris M, Li L. Molecular mechanism responsible for the priming of macrophage activation. *J Biol Chem*. 2013;288:3897-3906
343. Hutchinson TH, Lyons BP, Thain JE, Law RJ. Evaluating legacy contaminants and emerging chemicals in marine environments using adverse outcome pathways and biological effects-directed analysis. *Marine pollution bulletin*. 2013

344. Kim MJ, Pelloux V, Guyot E, Tordjman J, Bui L-C, Chevallier A, Forest C, Benelli C, Clément K, Barouki R. Inflammatory pathway genes belong to major targets of persistent organic pollutants in adipose cells. *Environ Health Perspect*. 2012;120
345. Rossmeislová L, Mališová L, Kračmerová J, Tencerová M, Kováčová Z, Koc M, Šiklová-Vítková M, Viquerie N, Langin D, Štich V. Weight loss improves the adipogenic capacity of human preadipocytes and modulates their secretory profile. *Diabetes*. 2013;62:1990-1995
346. Herder C, Baumert J, Thorand B, Koenig W, Jager W, Meisinger C, Illig T, Martin S, Kolb H. Chemokines as risk factors for type 2 diabetes: Results from the monica/kora augsburg study, 1984–2002. *Diabetologia*. 2006;49:921-929
347. Everett CJ, Mainous Iii AG, Frithsen IL, Player MS, Matheson EM. Association of polychlorinated biphenyls with hypertension in the 1999–2002 national health and nutrition examination survey. *Environmental Research*. 2008;108:94-97
348. Lind L, Lind PM. Can persistent organic pollutants and plastic-associated chemicals cause cardiovascular disease? *Journal of internal medicine*. 2012;271:537-553
349. Zheng Y, Toborek M, Hennig B. Epigallocatechin gallate-mediated protection against tumor necrosis factor-α - induced monocyte chemoattractant protein-1 expression is heme oxygenase-1 dependent. *Metabolism*. 2010;59:1528-1535
350. Zhao L, Lee JY, Hwang DH. Inhibition of pattern recognition receptor-mediated inflammation by bioactive phytochemicals. *Nutrition Reviews*. 2011;69:310-320

Vita

Katryn Elizabeth Eske Graduate Research Assistant, Doctoral Candidate

A. Education

Messiah College Grantham, PA	2002-2006	B.S. in Biochemistry	05/06
University of Kentucky Lexington, KY	2009-Present	Ph.D. in Nutritional Science	Candidate

B. Personal Statement

Nutrition as a modulator of environmentally induced disease is my key research interest. I have a broad background in basic science including nutritional science, environmental toxicology, and genomics. My research experience has included gene sequencing, genotyping, *in vitro* work with primary cell cultures, basic animal handling, animal diet formulation, Western blotting, real time-PCR, and ELISA. I am familiar with basic toxicological testing techniques and have tested remediation mixtures. My research has given me the opportunity to experience cross-disciplinary collaborations. I was mentored within the University of Kentucky Superfund Research Program (UK-SRP), which trained me to communicate scientific research to both scientific and lay audiences. Following this training, I have had opportunities to communicate our research to government officials and staff, members of the Kentucky Department of Environmental Protection and to teachers involved in secondary education. In addition, I have had the opportunity to mentor several undergraduate students and have found the mentorship process to be very rewarding. In the future, I intend to incorporate a cross-disciplinary focus in my research and plan to develop my ability to successfully mentor students. I have interests in expanding my research to the public health and international arenas. My background with the UK-SRP has provided me with a broad understanding of the environmental and physiological consequences of pollution, which will support future collaborative work.

C. Positions and Honors

<u>Positions and Employment</u>

Summer 2003	Laboratory Assistant, TestAmerica, Inc., Watertown, WI
Nov. 2002 – May 2005	Natural Sciences Team Leader, Water for the World (student group), Grantham, PA
Summer 2005	Laboratory Assistant, SMART Program of Baylor College of Medicine, Houston, TX
Aug. 2004 – May 2006	Supplemental Instruction Leader, Messiah College, Grantham, PA
Spring 2005 & 2006	Senior Research, Messiah College, Grantham, PA

Aug. 2006 – Ju*ne 2009 Research Technologist I, Medical College of Wisconsin, Milwaukee*, WI

July 2009 – Present Graduate Research Assistant, University of Kentucky, Lexington, KY

Other Experiences and Professional Memberships

Spring 2010 – Present Student/Postdoc/Alumni Network (SPAN) Committee, Superfund Research Program, Research Triangle Park, NC

Dec. 2011 – Present Society of Toxicology Student Member, Society of toxicology, Reston, VA

May 2012 – Present Nutritional Sciences Student Association Secretary, Graduate Center for Nutritional Sciences, Lexington, KY

Dec. 2012 – Present American Society for Nutrition Student Member, American Society for Nutrition, Bethesda, MD

Honors

Spring 2013 Pfizer Predoctoral Fellowship from the American Society for Nutrition

D. Peer Reviewed Publications

Eske K, Newsome B, Han SG, Murphy M, Bhattacharyya D, Hennig B (2013) PCB 77 dechlorination products modulate pro-inflammatory events in vascular endothelial cells. Environmental science and pollution research international. doi:10.1007/s11356-013-1591-3

E. Oral Presentations

Eske K: PCBs and Cardiovascular Disease – The Role of Fatty Acids. *Fighting with Foods Teacher's Training Workshop;* Middletown, OH, June 26, 2013.

Eske K: The Role of PCBs in inflammatory diseases. *Nutritional Sciences Seminar Series;* Lexington, KY, October 10, 2012.

Eske K: PCBs and Cardiovascular Disease – The Role of Fatty Acids. *Fighting with Foods Teacher's Training Workshop;* Middletown, OH, June 20, 2012.

Eske K: PCBs and Cardiovascular Disease: The Role of Fatty Acids. *Fighting with Foods Teacher's Training Workshop;* Cold Spring, KY, June 27, 2012.

Eske K: Therapeutic properties of omega-3 fatty acids against inflammatory stressors. *Nutritional Sciences Seminar Series;* Lexington, KY, March 23, 2011.

Eske K and Murphy M: PCBs and Cardiovascular Disease – Understanding the Risk and Implementing Interventions. Kentucky *Department of Environmental Protection Seminar Series*; Frankfort, KY, August 18, 2010.

F. Abstracts

Eske K, Murphy M, Petriello P, Newsome B, Han SG, Hennig B: Dietary DHA promotes an anti-oxidant response in mice exposed to environmental pollutants. *Experimental Biology 2013;* April 20-24, 2013; Boston, MA

Eske K, Murphy M, Petriello P, Newsome B, Han SG, Hennig B: Dietary DHA promotes an anti-oxidant response in mice exposed to environmental pollutants. *8th Annual Center for Clinical and Translational Science Spring Conference;* April 8, 2013; Lexington, KY

Eske K, Newsome B, Murphy M, Han SG, Bhattacharyya D, Hennig B: PCB77 dechlorination mixtures alter proinflammatory events in vascular endothelial cells. *25th Annual Superfund Basic Research Program Meeting*; October 21-24, 2012; Raleigh, NC

Eske K, Brock R, Layne J, Petriello M, Hennig B: TLR4 signaling and subsequent inflammation is modulated by 3,3',4,4',5-pentachlorobiphenyl (PCB 126) and LPS. *21st Annual South East Lipid Research Conference*; September 27-29, 2012; Pine Mountain, GA

Eske K and Murphy M: University of Kentucky Superfund Research Program. *Connecting Research and Practice: A Dialogue between ATSDR and the NIEHS Superfund Research Program Workshop*; August 7-8, 2012; Atlanta, GA

Eske K, Murphy M, Layne J, Han SG, Hennig B: Toxicity and inflammatory endpoints in C57BL/6 mice exposed to different doses of 3,3',4,4',5-pentachlorobiphenyl (PCB 126). *2012 Barnstable Brown Obesity & Diabetes Research Day*; May 14, 2012; Lexington, KY

Eske K, Murphy M, Layne J, Han SG, Hennig B: Toxicity and inflammatory endpoints in C57BL/6 mice exposed to different doses of 3,3',4,4',5-pentachlorobiphenyl (PCB 126). *51st Annual Meeting of the Society of Toxicology*; March 11-15, 2012; San Francisco, CA

Eske K, Murphy M, Layne J, Newsome B, Han SG, Hennig B: Dose response of 3,3',4,4',5-pentachlorobiphenyl (PCB 126) exposure on toxicity and inflammatory endpoints in C57BL/6 mice. *Superfund Research Program Annual Meeting 2011*; October 24-25, 2011; Lexington, KY

Eske K, Murphy M, Layne J, Han SG, Hennig B: Toxicity and inflammatory endpoints in C57BL/6 mice exposed to different doses of 3,3',4,4',5-pentachlorobiphenyl (PCB 126). *Gill Heart Institute Cardiovascular Research Day 2011*; October 21, 2011; Lexington, KY

Eske K, Murphy M, Layne J, Han SG, Barton, Hennig B: Dose response of 3,3',4,4',5-pentachlorobiphenyl (PCB 126) exposure on toxicity and inflammatory endpoints in C57BL/6 mice. *OVSOT 2011 Annual Fall Meeting*; September 23, 2011; Dayton, OH

Eske K, Han SG, Barton CR, Palumbo AN, Majkova Z, Zahran EM, Bachas DB, Toborek M, Hennig B: PCB77 dechlorination mixtures modulate pro-inflammatory events in vascular endothelial cells. *50th Annual Society of Toxicology Meeting*; March 6-10, 2011; Washington, D.C.

Eske K, Han SG, Barton CR, Palumbo AN, Majkova Z, Zahran EM, Bachas DB, Toborek M, Hennig B: PCB77 dechlorination mixtures modulate pro-inflammatory events in vascular endothelial cells. 2010 *John P. Wyatt Symposium on Environmental Health and Disease*; November 19, 2010; Lexington, KY

Eske K, Han SG, Barton CR, Palumbo AN, Majkova Z, Zahran EM, Bachas DB, Toborek M, Hennig B: PCB77 dechlorination mixtures modulate pro-inflammatory events in vascular endothelial cells. *23rd Annual Superfund Basic Research Program Meeting*; November 10-12, 2010; Portland, OR

G. Support

Pfizer Predoctoral Fellowship from the American Society for Nutrition
Spring 2013

The University of Kentucky Superfund Basic Research Program Interdisciplinary Training Grant
Spring 2011 – spring 2012